EXPERIMENTAL INVESTIGATIONS OF FLUID DYNAMIC AND THERMAL PERFORMANCE OF NANOFLUIDS

A

THESIS

Presented to the Faculty

of the University of Alaska Fairbanks

in Partial Fulfillment of the Requirements

for the Degree of

DOCTOR OF PHILOSOPHY

By

Devdatta Prakash Kulkarni, M.S.

Fairbanks, Alaska

August 2007

INFORMATION TO USERS

The quality of this reproduction is dependent upon the quality of the copy submitted. Broken or indistinct print, colored or poor quality illustrations and photographs, print bleed-through, substandard margins, and improper alignment can adversely affect reproduction.

In the unlikely event that the author did not send a complete manuscript and there are missing pages, these will be noted. Also, if unauthorized copyright material had to be removed, a note will indicate the deletion.

ProQuest Information and Learning Company
300 North Zeeb Road
P.O. Box 1346
Ann Arbor, MI 48106-1346

EXPERIMENTAL INVESTIGATIONS OF FLUID DYNAMIC AND THERMAL PERFORMANCE OF NANOFLUIDS

By

Devdatta Prakash Kulkarni

RECOMMENDED:

Advisory Committee Chair

Chair, Department of Mechanical Engineering

APPROVED:

Dean, College of Engineering and Mines

Dean of the Graduate School

July 2, 2007
Date

ABSTRACT

The goal of this research was to investigate the fluid dynamic and thermal performance of various nanofluids. Nanofluids are dispersions of metallic nanometer size particles (<100 nm) into the base fluids. The choice of base fluid is an ethylene or propylene glycol and water mixture in cold regions. Initially the rheological characterization of copper oxide (CuO) nanofluids in water and in propylene glycol was performed. Results revealed that higher concentrations of CuO nanoparticles (5 to 15%) in water exhibited time-independent pseudoplastic and shear-thinning behavior. Lower concentrations (1 to 6%) of CuO nanofluids in propylene glycol revealed that these nanofluids behaved as Newtonian fluids. Both nanofluids showed that viscosity decreased exponentially with increase in temperature. Subsequent correlations for viscosities as a function of volume concentration and temperature were developed.

Effects of different thermophysical properties on the Prandtl number of CuO, silicon dioxide (SiO_2) and aluminum oxide (Al_2O_3) nanofluids were investigated. Results showed that the Prandtl number increased with increasing volume concentrations, which in turn increased the heat transfer coefficients of the nanofluids.

Various nanofluids were compared for their heat transfer rates based on the Mouromtseff number, which is a Figure of Merit for heat transfer fluids. From this analysis, the optimal concentrations of nanoparticles in base fluids were found for CuO-water nanofluids.

Experiments were performed to investigate the convective heat transfer enhancement and pressure loss of CuO, SiO_2 and Al_2O_3 nanofluids in the turbulent regime. The increases in heat transfer coefficient by nanofluids for various volume concentrations compared to the base fluid were determined. Pressure loss was observed

to increase with nanoparticle volume concentration. It was observed that an increase in particle diameter increased the heat transfer coefficient.

Calculations showed that application of nanofluids in heat exchangers in buildings could result in volumetric flow reduction, reduction in the mass flow rate and size, and pumping power savings.

Experiments on a diesel electric generator with nanofluids showed a reduction of cogeneration efficiency due to the decrease in specific heat compared to the base fluids. However, it was found that the efficiency of the waste heat recovery heat exchanger increased for nanofluids.

TABLE OF CONTENTS

LIST OF FIGURES

LIST OF TABLES

LIST OF APPENDICES

ACKNOWLEDGEMENTS

After all those years, I remain with quite a list of people who contributed in some way to this thesis, for which I would like to express thanks.

My overwhelming thanks go to my advisor and committee chair Dr. Debendra K Das for the enthusiasm and inspiration. He has been available as a recourse in every way, be it socially, scholarly or administratively. I cannot overstate the importance of his involvement in my graduate career. I must also thank my committee members Dr. Douglas J. Goering, Dr. Vikas Sonwalkar and Dr. Chuen Sen-Lin for their valuable support and guidance throughout.

I would also like to thank Ms. Sandra Boatwright and Ms. Kala Hansen for grammatical corrections of all our manuscripts. Ms. Sarah Hall has always been a very helpful administrative assistant.

Finally, yet importantly, I wish to record my sincere appreciation to my wife Sayali who has been a great source of strength all through this work. My appreciation also goes to my family and friends for their support and encouragement throughout.

CHAPTER ONE
Introduction

1.1 Introduction of Nanofluids

Choi [1] at Argonne National Laboratory demonstrated the functionality of nanofluids by substantially augmenting the amount of heat transported by means of copper and aluminum nanoparticles suspended in water and other liquids. A nanofluid is a mixture of metallic particles (copper, copper oxide, aluminum oxide, silver etc.) having sizes of few nanometers (<100 nm), dispersed in a liquid like water or ethylene glycol. Nanofluid heat transport properties depend on the thermal properties, concentration, size and shape of the suspended particles. Many investigations have been performed in order to find more efficient heat transfer fluids to use in car engines and industrial equipment. Improved oils and coolants would allow more efficient engines, which are smaller and cheaper. According to Boutin [2] adding nano-spherical particles to a conventional fluid can improve heat transfer up to 40%. Choi envisions using these kinds of nanofluids to cool miniaturized high heat flux devices such as supercomputer circuits and high power microchips.

In the past, microparticles were used to enhance heat transfer, but these particles were so large that they quickly settled out of the fluid, and sank to the bottom of the pipe or tank. Additionally, as these particles flow through tubes they might damage the inner surface of the tubes. Because nanoparticles operate with Brownian motion, adding nanoparticles solved this problem. These particles are permanently suspended in Brownian motion and when they are in equilibrium with no flow, they are distributed in a balance between buoyant weight and thermal agitation (Figure 1.1). In fact this kind of equilibrium does not generate a uniform distribution; instead the concentration of small particles of radius 'a' will decrease exponentially with height according to the well known theory of Albert Einstein. This variation can be nearly uniform for very small

particles in devices of laboratory dimension. The balance between small fluctuations and buoyant weight can be expressed by gravitational height, l as follows:

$$l = \frac{kT}{(\rho_s - \rho_f)g\frac{4}{3}\pi a^3}. \tag{1}$$

Where k is Boltzmann's constant, T is temperature in Kelvin, ρ_s is particle density, ρ_f is fluid density and a is radius of particles. This quantity appears in the exponential distribution of equilibrium concentration

$$c(z) = \bar{c}\exp(-\frac{m}{l}z) \tag{2}$$

where m is the compressibility of the suspension. This expression shows that the concentration is nearly uniform when l is large. For nanoparticles, l is in 10's of meters even for copper density of about 8 gm/cc. Hence for all nanofluids the concentration is nearly uniform.

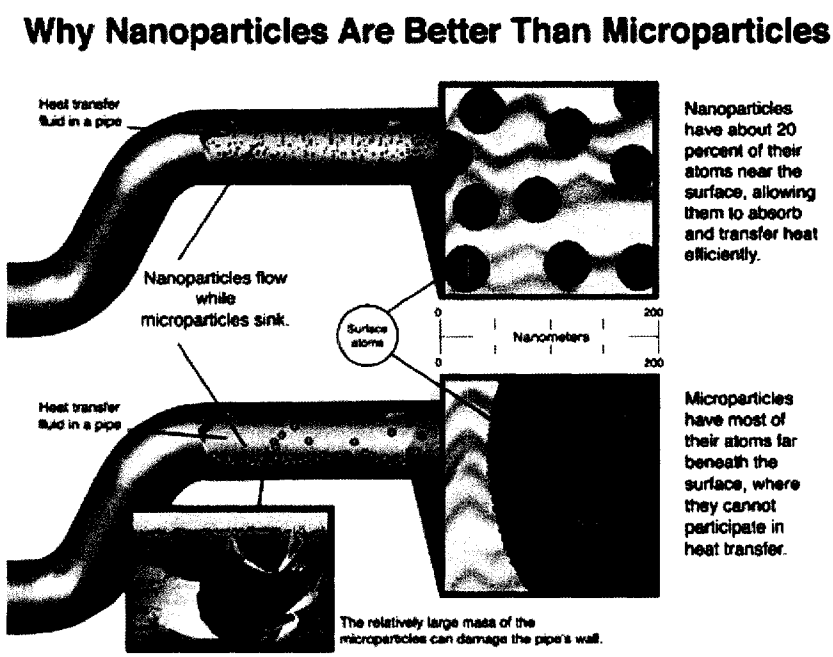

Figure 1.1 Comparisons of microparticles and nanoparticles to enhance heat transfer. (Source: Boutin [2])

Cooling is one of the most important technical challenges facing numerous industries such as electronics, automobiles and manufacturing. New technologies, with their increased thermal loads, are the driving mechanism behind the demand for faster and better cooling techniques. The conventional methods to increase the cooling rate such as fins and microchannels are stretched to their limits. Hence, there is an urgent need for new and innovative coolants to achieve this high performance cooling [3, 4]. Thermal conductivities of traditional heat transfer fluids, such as engine coolants and water, are very low. With increasing global competition, industries have a strong need to develop energy efficient heat transfer fluids with significantly higher thermal conductivities than the available fluids. Nanofluids offer us novel and truly innovative solutions; heat transfer fluids containing suspended nanoparticles, have been developed to meet such cooling challenges [5].

1.2 Outline of Research

The schematic outline of the overall research on fluid dynamics and thermal performance of various nanofluids is given below.

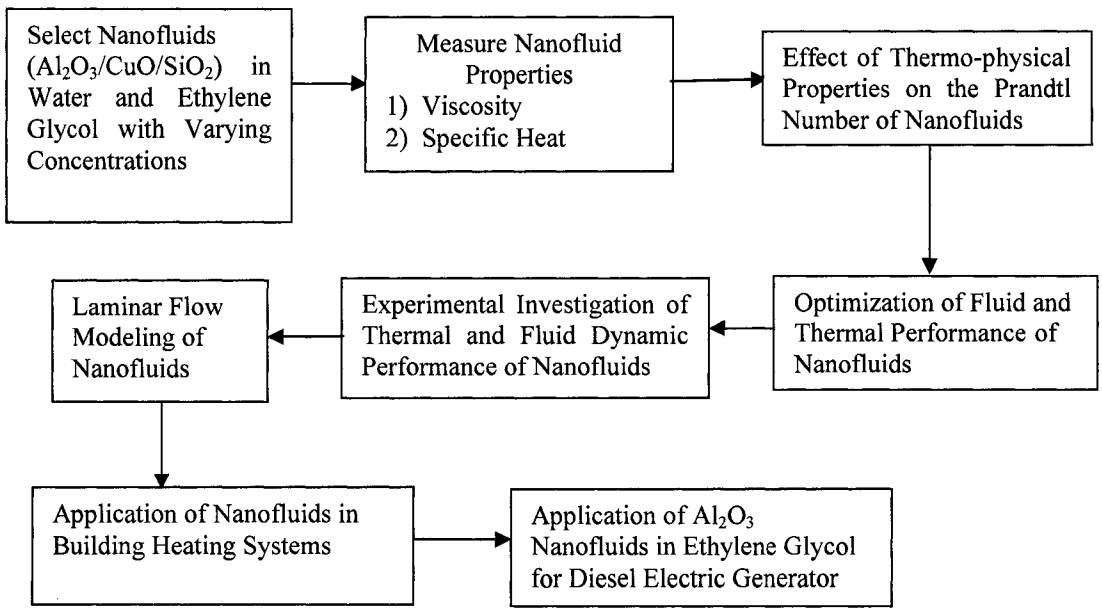

1.3 Objectives

The objectives of our research were as follows:

I) Determine the viscosity and rheological behavior of the nanofluids with varying nanoparticle concentrations as well as varying temperature.

II) Determine the specific heat of various nanofluids.

III) Determine the effect of different thermophysical properties on the Prandtl number.

IV) Determine the optimum volumetric concentration of various nanoparticles on the basis of Mouromtseff number.

V) Experimentally investigate the fluid dynamics and thermal performance of various nanofluids.

VI) Numerical modeling of nanofluids using the computational fluid dynamics code, FLUENT.

VII) Apply nanofluid technology in heating cold climate buildings.

VIII) Apply nanofluid technology in Diesel Electric Generators (DEG) as a jacket water coolant.

The detailed description of each objective is explained in the subsequent chapters.

1.4 Synthesis of Nanofluids

Various potentially useful combinations of nanoparticles such as nanoparticles of oxides, nitrides, metals, metal carbides and nonmetals can be dispersed into base fluids such as water, ethylene glycol or oils. Eastman et al. [3] described two methods to synthesize nanofluids: the two-step and single-step processes.

Initial experimental studies employed the two-step approach, in which nanoparticles are produced first in a dry powder form. This is typically done by inert gas condensation, which involves a vaporized material embedded in a vacuum chamber, and

subsequently, the condensation of the vapor into nanoparticles through collisions with controlled pressure of an inert gas such as helium. In the second step, the resulting nanoparticles are dispersed into the base fluid. In this process, a large degree of nanoparticle agglomeration occurs. This method is useful in dispersing oxide nanoparticles in deionized (DI) water and less successful producing nanofluids with heavier metallic nanoparticles. The advantage of this inert-gas condensation technique is that it can economically produce a large quantity of nanoparticles.

The second successful approach is through "direct evaporation". This is a single step process that produces nanofluids containing dispersed metallic nanoparticles. As with the inert-gas technique, this technique involves the vaporization of a source material in a vacuum. However, in this technique the condensation forms nanoparticles through direct contact between the vapor and the base fluid. The agglomeration of nanoparticles is minimized by continuously circulating the base fluid. The schematic of this direct evaporation technique is shown in Figure 1.2.

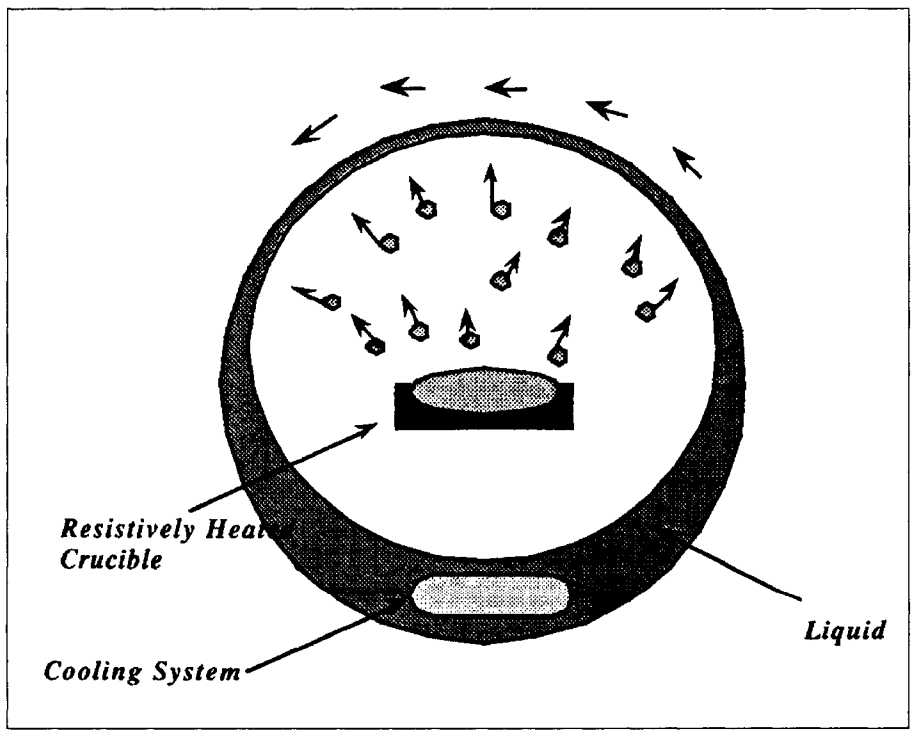

Figure 1.2 Schematic diagram of nanofluid production system for direct evaporation of materials into base fluids. (Source: Choi et al. [6])

A significant limitation of the direct evaporation technique is that the liquid must have a low vapor pressure, typically less than 1 torr. Higher vapor pressure leads to gas condensation and problems related to nanoparticle agglomeration. At present, the quantities of nanofluids produced by this technique are limited, but it is likely that this technique will be modified to economically produce large quantities of various nanofluids.

Other techniques such as the chemical vapor condensation technique are also finding application in nanofluids production. In this technique, nanoparticles are formed by thermal decomposition of a metal-organic precursor entrained in a carrier gas passing thorough a furnace. This process has been modified to synthesize and disperse non-agglomerated nanoparticles into the base fluid in one step. The advantage of this technique over the direct evaporation technique is that this technique offers control of particle size, ease of scalability and possibility of producing novel core-shell nanostructures.

1.5 Literature Review

Buongiorno [7] studied several slip mechanisms to investigate the dominant mechanisms responsible for the heat transfer enhancement of nanofluids. An increased heat transfer coefficient cannot be clearly assessed because of the high thermal conductivity of nanofluids. He has considered seven slip mechanisms to produce a relative velocity between the nanoparticles and the base fluid. These mechanisms are: inertia, Brownian diffusion, thermophoresis, diffusiophoresis, Magnus effect, fluid drainage and gravity. Buongiorno showed that the Knudsen number, Kn, the ratio of water molecule mean free path to the diameter of the nanoparticle, is relatively small and the continuum assumption is reasonable. He concluded that out of the seven mechanisms studied, only Brownian diffusion and thermophoresis are important slip mechanisms in

nanofluids. Convective heat transfer enhancement can be explained mainly by a reduction of viscosity within and consequent thinning of the laminar sublayer.

Li and Xuan [8] investigated the thermal and fluid dynamic performance of copper-water nanofluid in both laminar and turbulent regimes. They discussed the effects of nanoparticle volume concentration and Reynolds number on the heat transfer coefficient. They showed that a 2% volume concentration of copper nanoparticles in water increased the heat transfer coefficient of the base fluid by almost 60% at the same Reynolds number. They have also concluded that the friction factor of the same nanofluid with the low volume fraction of nanoparticles is almost unchanged.

Eastman et al. [9] investigated the effective thermal conductivity of copper nanoparticles dispersed in ethylene glycol. Thermal conductivity of ethylene glycol nanofluid increases up to 40% by adding 0.3% by volume copper nanoparticles with a diameter less than 10 nm. Maxwell's model [10] predicts that the effective thermal conductivity of solid suspensions increases with volume concentration of particles. Eastman et al. also showed that the thermal conductivity of an ethylene glycol nanofluid increases up to 20% by adding 4% volume copper oxide (CuO) nanoparticles. The thermal conductivity enhancement of various ethylene glycol nanofluids is shown in Figure 1.3. It was demonstrated that thermal conductivities predicted by theoretical models, such as that of Hamilton and Crosser [11] are much lower than the actual measured data for oxide nanofluids.

Gosselin and Silva [12] studied combined heat transfer and power dissipation optimization of laminar and turbulent nanofluid flows. As nanofluid effective thermal conductivity increases with concentration of nanoparticles, so does the effective viscosity of the fluid. This means that solid-liquid mixtures are more expensive to pump. This competition reveals a tradeoff opportunity for maximizing the heat transfer rate, at constant power, by selecting an appropriate amount of particles.

Too fuzzy scan higher resolution

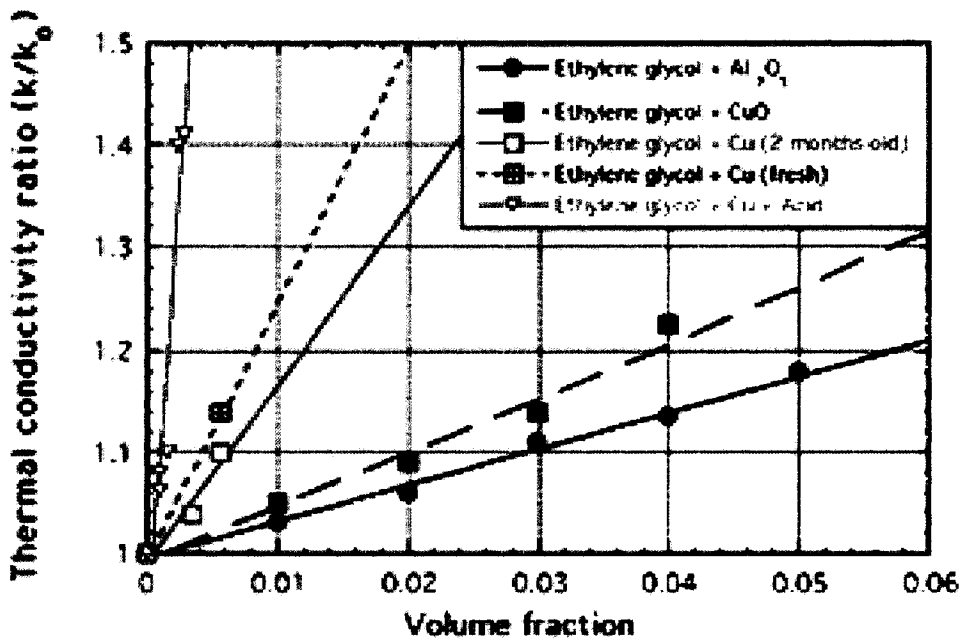

Figure 1.3 Improvement of thermal conductivity of ethylene glycol with suspensions of nanoparticles. (Source: Eastman et al. [9])

Ding et al. [13] investigated heat transfer of aqueous suspensions of carbon nanotube (CNT) nanofluids. CNTs have a very high thermal conductivity (~3000 W/mK for multi-walled and ~6000 W/mK for single walled CNTs) and hence have great potential for significant heat transfer enhancement. For nanofluids containing 0.5 weight % CNTs, the maximum heat transfer enhancement reaches over 350% at Re = 800.

Maiga et al. [14] have numerically investigated the heat transfer behaviors of nanofluids in a uniformly heated pipe. For this analysis, they have considered two nanofluids; water-γ Al_2O_3 and ethylene glycol-γ Al_2O_3. As a boundary condition, they have assumed the tube is heated with a uniform heat flux at the wall. They observed that including particles in a fluid, the heat transfer at the wall increased remarkably in both laminar and turbulent regimes. Also, results showed that glycol-γ Al_2O_3 gives a far better heat transfer enhancement than water-γ Al_2O_3.

Wen and Ding [15] have experimentally investigated the convective heat transfer of water-γ Al_2O_3 nanofluids flowing through a copper tube at the entrance region under laminar flow conditions. The results showed that there is considerable enhancement in convective heat transfer at the entrance region. A possible reason for this enhancement was attributed to a disturbance to the boundary layer due to migration of nanoparticles.

Xuan and Roetzel [16] numerically investigated the mechanism of nanofluid heat transfer enhancement. As a starting point, they assumed that the nanofluid behaves more like a single-phase fluid rather than conventional solid-liquid two-phase flow. To handle the thermal dispersion resulting from irregular movement of the nanoparticles, they used a dispersion model.

Xuan and Li [17] investigated the thermal conductivity enhancement of copper-water nanofluids. They discussed factors such as volume fraction, dimensions, shapes and properties of nanofluids. Also, they investigated [18] the effects of volume fraction and Reynolds number on convective heat transfer, and came up with a correlation, which is described in the Section 1.5.5.

Pak and Cho [19] investigated turbulent friction and heat transfer behaviors of water-γ Al_2O_3 and water-titanium dioxide (TiO_2) nanofluids. They measured the viscosities of those nanofluids and found that viscosity values were 200 and 3 times greater than pure water for 10% volumetric concentration of nanoparticles. Darcy friction factors for dispersed fluids matched closely with Kays and Crawford's [20] correlation for turbulent flow of a single-phase flow over a range of 1% to 3% volumetric concentration of nanoparticles. They have proposed a new correlation for the turbulent convective heat transfer for dilute dispersed fluids with submicron metallic oxide particles.

1.5.1 Thermal conductivity of nanofluids

The conductivity enhancement for both metallic and oxide nanofluids are approximately linear with particle volume percent. Hamilton and Crosser's [11] analysis which predicts the thermal conductivity of two component mixtures, can be given as

$$k_{nf} = k_f [\frac{k_p + (n-1)k_f - (n-1)\phi(k_f - k_p)}{k_p + (n-1)k_f + \phi(k_f - k_p)}]. \quad (3)$$

Where k_{nf} is the mixture thermal conductivity, k_f is the liquid thermal conductivity, k_p is the conductivity of solid particles, ϕ is the particle volume fraction and n is an empirical scaling factor, which takes into account the effect of different particle shapes on thermal conductivity. For spherical particles n = 3.

Pak and Cho [19] presented two thermal conductivity correlations for alumina (Al_2O_3) and titania (TiO_2) nanofluids as follows:

$$k_{nf} = k_f (1 + 7.47\phi) \quad \text{(for alumina particles)} \quad (4)$$

$$k_{nf} = k_f (1 + 2.92\phi - 11.99\phi^2). \quad \text{(for titania particles)} \quad (5)$$

Prasher et al. [21] showed that convection caused by the Brownian movement of these nanoparticles is primarily responsible for the enhancement in conductivity of these colloidal nanofluids. Taking the clue from the Nusselt correlation for particle to fluid heat transfer in fluidized beds, they proposed a general correlation of heat transfer coefficient, h of the form below, for the Brownian motion-induced convection from multiple nanoparticles.

$$h = k_f / a(1 + A\,\mathrm{Re}^m\,\mathrm{Pr}^{0.333}\,\phi). \quad (6)$$

where A and m are constants depending on the type of fluid, ϕ is the particle volume fraction, Re is Reynolds number and Pr is the Prandtl number.

From this correlation, the thermal conductivity of nanofluid can be found as:

$$k_{nf}/k_f = (1 + A\,\mathrm{Re}^m\,\mathrm{Pr}^{0.333}\,\phi)[\frac{(1+2\alpha)+2\phi(1-\alpha)}{(1+2\alpha)-\phi(1-\alpha)}]. \quad (7)$$

Where $\alpha = 2R_b k_m / d$; where R_b is interfacial resistance and d is the particle diameter.

Maiga et al. [14] presented two conductivity equations for two fluids:

$$k_{nf} = k_f(1 + 7.47\phi) \quad \text{(for water-}\gamma\,Al_2O_3\text{)} \quad (8)$$

$$k_{nf} = k_f(1 + 2.8273\phi + 28.905\phi^2). \quad \text{(for ethylene glycol-}\gamma\,Al_2O_3\text{)} \quad (9)$$

The transient hot wire (THW) method was used to measure fluid thermal conductivity [9]. A THW system involves a platinum wire suspended symmetrically in a liquid in a vertical cylindrical container. The THW technique works by measuring the temperature time response of the wire to an electrical pulse. This wire is used as both heater and thermometer. The thermal conductivity k is found from:

$$k = \frac{q}{4\pi(T_2 - T_1)}\ln(\frac{t_2}{t_1}). \quad (10)$$

Where q is the applied electric power and T_1 and T_2 are the temperatures at times, t_1 and t_2.

Chopkar et al. [22] developed a new method to measure the thermal conductivity of nanofluids. They characterized nanofluids by X-ray diffraction and transmission electron microscopy, and thermal conductivity of the nanofluid was measured using a modified thermal comparator.

1.5.2 Density of nanofluids

This section summarizes the theory for the calculations of the density of nanofluids. Pak & Cho [19] studied the hydrodynamic and heat transfer behavior of nanofluids where the volume concentration is defined as the fraction of space of the total

suspension occupied by the suspended material. This term is often used instead of mass concentration. The volume concentration is given by:

$$\phi = \frac{1}{(100/\phi_m)(\rho_s/\rho_f)+1} * 100(\%). \quad (11)$$

Where ρ_s and ρ_f are the densities of solid particles and fluid, respectively, and ϕ and ϕ_m are the volume and mass concentrations (%) of the dispersed fluid, respectively. The density of the dispersed nanofluid is given by Pak & Cho [19]:

$$\rho_{nf} = (1-\phi)\rho_f + \phi\rho_s. \quad (12)$$

Figure 1.4 clearly indicates that Equation (11) is accurate enough to match the calculated values of the density of nanofluids with the measured values.

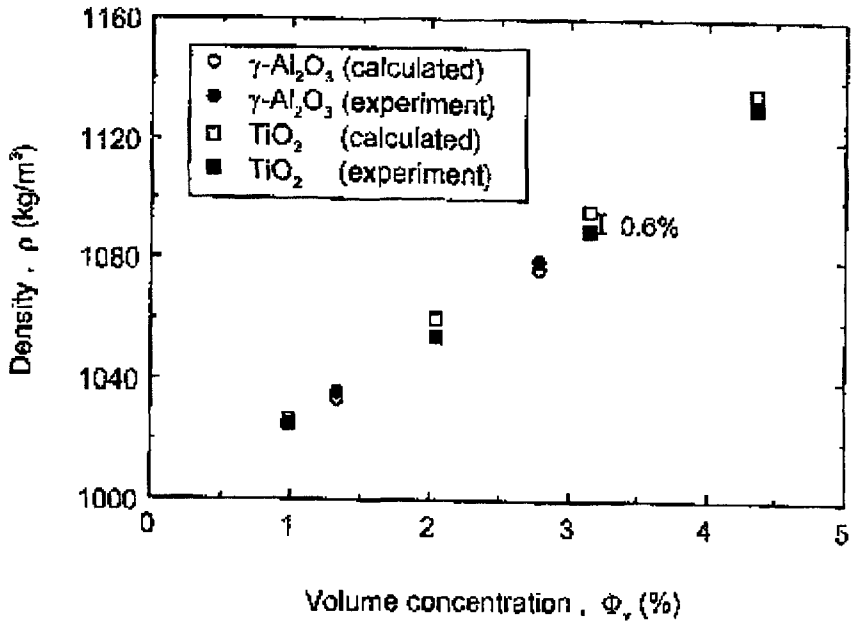

Figure 1.4. Comparison of theoretical and experimental densities of nanofluids versus volume concentration. (Source: Pak & Cho [19])

1.5.3 Viscosity of nanofluids

The viscosity of the nanofluid is determined from the relative viscosity, which is a function of volume concentration. It is defined as the ratio of the viscosity of a fluid with suspended nanoparticles to that of the fluid alone. The approximate analytical value of relative viscosity μ_r is given by Batchelor theory [23]:

$$\mu_r = 1 + 2.5\phi + 6.25\phi^2 . \tag{13}$$

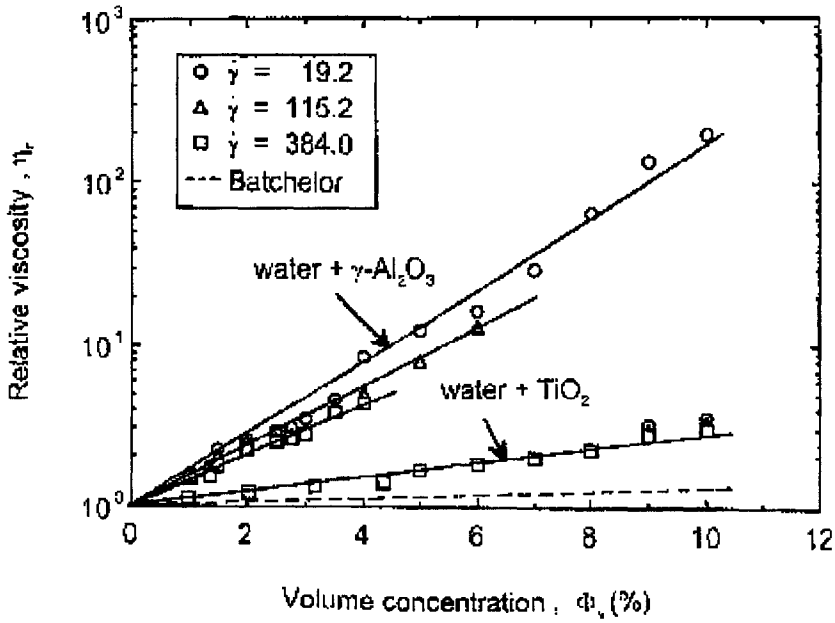

Figure 1.5. Relative viscosity of various nanofluids versus volume concentration of nanoparticles. (Source: Pak & Cho [19])

The uncertainty in Batchelor's equation is in the determination of the constant coefficient of the third term on the right hand side of equation (12).

Maiga et al. [14] presented two viscosity equations for two fluids:

$$\mu_{nf} = \mu_f (1 + 7.3\phi + 123\phi^2) \qquad \text{(for water-}\gamma\ Al_2O_3\text{)} \tag{14}$$

$$\mu_{nf} = \mu_f (1 - 0.19\phi + 306\phi^2) . \qquad \text{(for ethylene glycol-}\gamma\ Al_2O_3\text{)} \tag{15}$$

Research on viscosity measurement of submicron particles in a fluid medium started as far back as 1954 [24-26]. To date, various studies have investigated the viscosities of different nanofluids, including TiO_2 nanoparticles in water [27], carbon nanotubes and graphite nanofluids [28-29], Al_2O_3 nanofluids [30], aqueous silica suspensions [31], $BaTiO_3$ suspensions [32], copper oxide in ethylene glycol at room temperature [33] and nickel suspensions [34-35]. The rheology of aluminum nanoparticles suspended in paraffin oil was studied by Teipel and Forter-Barth [36]. Many correlations have been developed for nanofluid viscosity as a function of volume fraction [37]. A few of the most relevant include, Einstein [38], who proposed the correlation for the viscosity of a suspension as:

$$\mu_s = \mu_f (1 + \frac{5}{2}\phi). \tag{16}$$

Where μ_s = suspension viscosity, μ_f = viscosity of base fluid and ϕ is volume fraction. A similar kind of correlation is given by Bicerano et al. [39] as:

$$\mu_s = \mu_f (1 + \eta\phi + k_H\phi^2 + ...). \tag{17}$$

Where η is virial coefficient and k_H is the Huggins coefficient.

The most commonly used viscosity correlation was developed by Brinkman [40]:

$$\mu_s = \mu_f \frac{1}{(1-\phi)^{2.5}}. \tag{18}$$

To date, the literature offers no correlation for nanofluid viscosity as a function of both temperature and volume fraction. A rheological property like viscosity is a strong function of temperature; that is, viscosity near the freezing point of a fluid has a very high value and near the boiling temperature, a very low value. White [41] gave a temperature-dependent viscosity correlation for a single phase liquid as:

$$\ln\frac{\mu}{\mu_0} \approx a + b(\frac{T_0}{T}) + c(\frac{T_0}{T})^2. \tag{19}$$

Where (μ_0, T_0) are reference values and (a,b,c) are dimensionless curve fit values.

Many correlations have been developed for nanofluid viscosity as a function of volume fraction and temperature. Among these, an earlier study by Kulkarni et al. [42] showed the temperature dependency of copper oxide nanoparticles in water from 5°C to 50°C:

$$\ln \mu_s = A(\frac{1}{T}) - B \tag{20}$$

Where A & B are functions of volume percent ϕ.

Researching temperature dependency of viscosity is very important for cold climate regions like Alaska, Canada and circumpolar nations. Nanofluids are useful as new generation heat transfer fluids in automobiles, various heat exchangers and baseboard heaters in cold regions. In the arctic and subarctic climate, equipment employing nanofluids may encounter temperatures well below 0°C. It is a common practice to use ethylene or propylene glycol mixed with water in different proportions as a heat transfer fluid [43]. Inhibited ethylene glycol and propylene glycol are used as aqueous freezing point depressants and heat transfer media in heat transfer systems [44].

1.5.4 Specific heat of nanofluids

The specific heat of dispersed nanofluids C_{pnf} was calculated in the early stages using an equation based on the volume fraction [19]:

$$C_{pnf} = (1-\phi)C_{pf} + \phi C_{ps}. \tag{21}$$

Later, because the nanoparticles and the base fluid are in thermal equilibrium, the nanofluid specific heat equation was improved by Buongiorno [7]:

$$C_{pnf} = \frac{\phi \rho_s C_{ps} + (1-\phi)\rho_f C_{pf}}{\rho_{nf}}. \tag{22}$$

1.5.5. Heat transfer coefficient of nanofluids

Li and Xuan [8] investigated the correlation for the Nusselt number for copper-water nanofluid. They varied the Reynolds number from 800-25000. Figure 1.6 shows variation of heat transfer coefficient for different Reynolds number (laminar & turbulent).

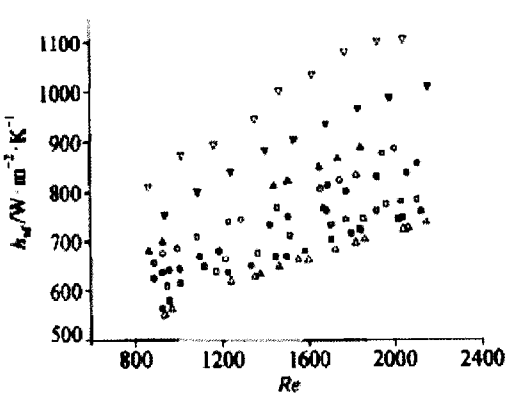

Fig. 3. The convective heat transfer coefficient of nanofluids for the laminar flow. △, Water (experimental values); ■, 0.3 vol%; □, 0.5 vol%; ●, 0.8 vol%; ○, 1.0 vol%; ▲, 1.2 vol%; ▼, 1.5 vol%; ▽, 2.0 vol%.

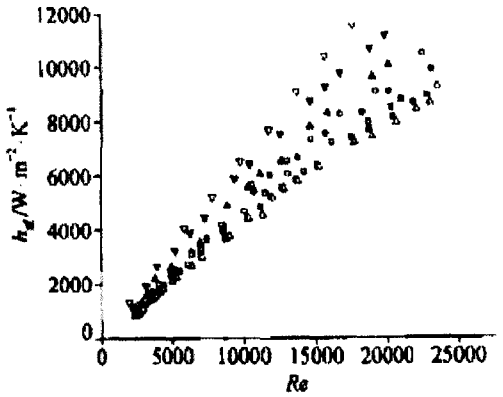

Fig. 4. The convective heat transfer coefficient of nanofluids for the turbulent flow. △, Water (experimental values); ■, 0.3 vol%; □, 0.5 vol%; ●, 0.8 vol%; ○, 1.0 vol%; 1.2 vol%; ▼, 1.5 vol%; ▽, 2.0 vol%.

Figure 1.6 Variation of heat transfer coefficient for different Reynolds number.

(Source: Li and Xuan [8])

In general, the Nusselt number (*Nu*) of a nanofluid may be expressed as follows:

$$Nu_{nf} = f(\mathrm{Re}_{nf}, \mathrm{Pr}_{nf}, k_s / k_f, (\rho C_p)_s / (\rho C_p)_f, \phi, diameter\ \&\ shape). \tag{23}$$

The following formula was proposed by Li & Xuan [8] to correlate the experimental data for copper oxide nanofluids.

$$Nu_{nf} = c_1(1.0 + c_2 \phi^{m_1} Pe_d^{m_2})\,\mathrm{Re}_{nf}^{m_3}\,\mathrm{Pr}_{nf}^{0.4}. \tag{24}$$

Where c_1, c_2, m_1, m_2, m_3 are the coefficients found from the experimental data for laminar or turbulent flows. The particle Peclet number is defined as:

$$Pe_d = \frac{u_m d_p}{\alpha_{nf}}. \tag{25}$$

Where u_m is the mean velocity, d_p is the mean diameter of nanoparticles and α_{nf} is the

thermal diffusivity of nanofluids. The Peclet number describes the effect of thermal dispersion caused by microconvective and microdiffusion of the suspended nanoparticles. From experimental data reduction, the Nusselt number for laminar and turbulent flow is given by Li & Xuan [8] as:

$$Nu_{nf} = 0.4328(1.0 + 11.285\phi^{0.754} Pe_d^{0.218}) \mathrm{Re}_{nf}^{0.333} \mathrm{Pr}_{nf}^{0.4} \quad \text{(For laminar flow) and (26)}$$

$$Nu_{nf} = 0.0059(1.0 + 7.6286\phi^{0.6886} Pe_d^{0.001}) \mathrm{Re}_{nf}^{0.9238} \mathrm{Pr}_{nf}^{0.4} \quad \text{(For turbulent flow). (27)}$$

The calculated values of the Nusselt number match with the experimental values. Figure 1.7 below shows the accuracy of the correlations developed.

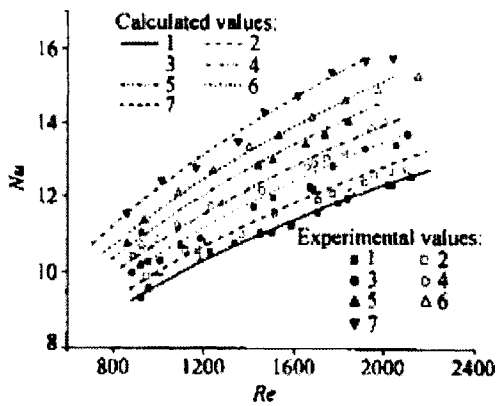

Fig. 6. Comparison between the measured data and the calculated values for laminar flow. Calculated values: 1, 0.3 vol%; 2, 0.5 vol%; 3, 08 vol%; 4, 1.0 vol%; 5, 1.2 vol%; 6, 1.5 vol%; 7, 2.0 vol%. Experimental values: 1, 0.3 vol%; 2, 0.5 vol%; 3, 0.8 vol%; 4, 1.0 vol%; 5, 1.2 vol%; 6, 1.5 vol%; 7, 2.0 vol%.

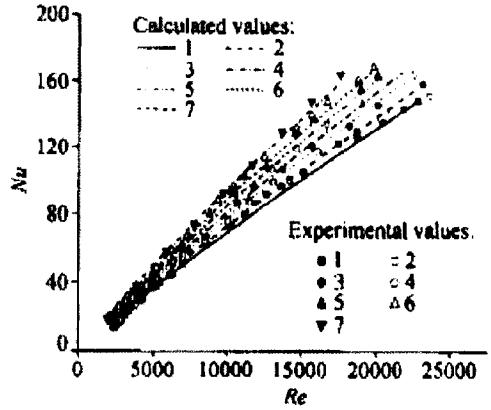

Fig. 7. Comparison between the measured data and the calculated values for turbulent flow. Calculated values: 1, 0.3 vol%; 2, 0.5 vol%; 3, 08 vol%; 4, 1.0 vol%; 5, 1.2 vol%; 6, 1.5 vol%; 7, 2.0 vol%. Experimental values: 1, 0.3 vol%; 2, 0.5 vol%; 3, 0.8 vol%; 4, 1.0 vol%; 5, 1.2 vol%; 6, 1.5 vol%; 7, 2.0 vol%.

Figure 1.7. Comparison of calculated and experimental values of Nusselt number.
(Source: Li and Xuan [8])

Yang et al. [45] have presented several different correlations for the Nusselt number for nanofluids. The Seider-Tate equation for convective heat transfer for laminar flow in tubes is given as [46]:

$$Nu = 1.86 \mathrm{Re}^{1/3} \mathrm{Pr}^{1/3} (\frac{D}{L})^{1/3} (\frac{\mu_b}{\mu_w})^{0.14} \quad (28)$$

In which $(\frac{\mu_b}{\mu_w})^{0.14}$ represents the radial variation of viscosity and the natural convection effect. D and L are the diameter and length of the pipe respectively.

The Oliver correlation [47] for horizontal flow in tubes is:

$$Nu(\frac{\mu_b}{\mu_w})^{0.14} = 1.75(Gz + 5.6E - 4(Gr \Pr L/D)^{0.7})^{1/3}. \quad (29)$$

In which Gz is the Graetz number, and Gr is the Grashoff number. μ_b and μ_w are viscosities of the fluid calculated at bulk and wall temperature respectively.

Xuan and Roetzel [16] have presented the equation for the Nusselt number of a nanofluid flowing through a pipe as:
From the above relation the heat transfer coefficient is found by:

$$h_{nf} = (Nu_{nf} k_{nf})/D. \quad (30)$$

From the above relation the heat transfer coefficient is found by:

$$h_{nf} = (Nu_{nf} k_{nf})/D. \quad (31)$$

Where D is the inside diameter of the tube.

Heris et al. [48, 49] experimentally studied the convective heat transfer of Al_2O_3 and water nanofluids in a circular tube for constant heat flux. They studied different concentrations of Al_2O_3 nanoparticles including 0.2%, 0.5%, 1%, 1.5 %, 2% and 2.5% volume fraction in water with Reynolds number varying from 700 to 2050 (laminar conditions). They found that the increase in heat transfer coefficient due to presence of nanoparticles is much higher than the prediction of single phase heat transfer correlations used with nanofluid properties. This increased heat transfer may be due to chaotic movement of nanoparticles, Brownian motion and nanoparticle migration.

Nguyen et al. [50] studied the performance of Al_2O_3-water nanofluids flowing inside a closed system that is designed to cool microprocessors and electronic

components. They found that for this particular fluid with a volume concentration of 6.8% of Al_2O_3 nanofluids, the heat transfer coefficient increased by 40% compared to the base fluid. Also, they have shown that a nanofluid with a 36 nm particle diameter provides higher heat transfer coefficients than that of a 47 nm particle diameter nanofluid. But in this analysis, they have considered a constant viscosity value for both nanofluids, i.e. nanofluids with 36 nm and 47 nm particle diameters.

Maiga et al. [51] studied laminar forced convection flow of nanofluids for two particular configurations: a uniformly heated tube and a system of parallel, coaxial and heated disks. Numerical results obtained for γ Al_2O_3- water and γ Al_2O_3- ethylene glycol nanofluids showed that inclusion of nanoparticles into the base fluid has produced considerable augmentation of the heat transfer coefficient, which increases as particle concentration increases. They have also shown that such nanoparticles induce drastic effects on the wall shear stress that increases with particle concentration as well.

Mansour et al. [52] showed that changes in thermophysical properties (specific heat and viscosity) change the pumping power in laminar and turbulent flows. Hence correlations used for specific heat and viscosity in this analysis reflect the change and it is essential to provide more data for thermophysical properties of various nanofluids.

Behzadmehr et al. [53] numerically studied turbulent-forced convection heat transfer in a tube. For this analysis, they have used the computational fluid dynamics solution technique called SIMPLE. They considered a nanofluid consisting of 1% by volume copper nanoparticles suspended in water and investigated the problem using a two-phase mixture model for numerical analysis. They also compared the results with frequently used single-phase nanofluid correlations and with experimental results. They showed the mixture model is more precise than the single-phase model for numerical analysis.

Akbarinia and Behzadmehr [54] numerically investigated the laminar mixed convection of nanofluids in a tube. They used three-dimensional elliptical governing equations with simultaneous effects of buoyancy force, centrifugal force and nanoparticle concentrations. They showed, for a given Reynolds number, that the buoyancy force has a negative impact on the Nusselt number and that the nanoparticle concentration has a positive impact on the Nusselt number.

In addition, He et al. [55] studied the convective heat transfer and flow behavior of nanofluids flowing upward through a vertical pipe. They found that the convective heat transfer coefficient increases with nanoparticle concentration, and the pressure drop of the nanofluid flows is very close to that of the base fluid flow for a given Reynolds number.

1.6 Applications of Nanofluids

Rapid development is taking place in warfare and armament electronic design and application. This phenomenon has led to dramatic increases in chip densities and power densities, as well as continuous decreases in the physical dimensions of electronic packages. Hence, thermal management continues to be one of the most critical areas in electronic product development. Advances in thermal management will significantly impact the cost, overall design, reliability and performance of the next generation of weapons technology that heavily uses microelectronic devices.

The US DoD has several research programs involving electric weapons or Directed Energy (DE) concepts, in which high-power lasers and high-power microwave systems are employed. Furthermore, associated power conditioning electronics for prime power generation are also being developed. Researchers expect that DE weapons will result in heat sources causing high heat flux, in excess of 500-1000 W/cm^2, and may require transport and rejection capability of 100 kW of heat. Utilizing nanofluids as

designer thermo-fluids, efficient thermal management can be achieved in Directed Energy weapons, as well as power conditioning electronics and high-power microwave devices.

Lee and Choi [56] used the application of nanofluids to cool crystal silicon mirrors used in high intensity X-ray sources such as Argonne's Advanced Photon Source. Because the X-ray beam creates tremendous heat as it strikes the mirror, cooling rates of 2000 – 3000 W/cm^2 must be achieved with the advanced technology. They analyzed the performance of microchannel heat exchangers with water, liquid nitrogen and nanofluids as working fluids. For the optimized configuration, the performance of a nanofluid-cooled microchannel heat exchanger has been compared with that of a water-cooled and liquid nitrogen cooled microchannel heat exchanger. The results show the superiority of a nanofluid-cooled microchannel heat exchanger. When nanofluids are used, the thermal resistances are reduced and higher power densities can be handled. For applications where overall cooling system size must be kept to minimum, nanofluids are a very attractive coolant. Furthermore, the possibility of thermal distortion and flow induced vibration will be eliminated by passing the nanofluids through the microchannels with the silicon mirror used in high intensity X-ray sources.

The advanced nanofluid cooling technology may be used in internal combustion engines, superconducting magnets and supercomputers where densely packed chips generate much more heat. It may also be beneficial in reducing the size of current industrial cooling equipment.

Koo and Kleinstreuer [57] simulated the performance of copper oxide nanoparticles at low volume concentration in water and ethylene glycol under a steady laminar flow in microchannels. Based upon their study, they recommended the following for improving the performance of a microscale heat sink: (i) use of high Prandtl number

carrier fluids; (ii) nanoparticles at volume concentrations of about 4% with higher thermal conductivities; and (iii) dielectric constant close to that of the carrier fluid.

Chein and Huang [58] analyzed the performance of a silicon microchannel heat sink using copper–water nanofluids. Because of the increased thermal conductivity and thermal dispersion effects, they found that the performance improved significantly for two specific geometries when nanofluids were used as coolants. Also, they concluded that the existence of nanoparticles in the fluid did not produce extra pressure drop because of small particle size and low particle volume concentration up to 2%.

Nguyen et al. [59] also studied heat transfer enhancement using nanofluids for the cooling of high heat output microprocessors. They numerically analyzed various volumetric concentrations of Al_2O_3–water nanofluids for various Reynolds numbers. The numerical results predict that the inclusion of nanoparticles within base liquid produced a noticeable effect on the heat sink cooling.

1.6.1 Vehicle thermal management

Choi et al. [6] showed that nanofluids have the potential of being recognized as a new generation of coolants for vehicle thermal management due to their significantly higher thermal conductivities than the base fluids. The heat rejection requirements of automobiles and trucks are continually increasing due to trends toward more power output.

Ollivier et al. [60] numerically investigated the possible application of nanofluids as a jacket water coolant in a gas spark ignition engine. They performed numerical simulations of unsteady heat transfer through the cylinder and inside the coolant flow. They have shown that because of higher thermal diffusivity of nanofluids, the thermal

signal variations for knock detection increased by 15% over that predicted using water alone.

Fuel cells are new developments in the power generation field which involve notable amounts of heat and mass exchange. Whenever the heat exchange phenomenon occurs within a fuel cell or in its auxiliary heat recovery systems, nanofluids can be employed to enhance heat transfer and raise the fuel cell efficiency [61].

1.6.2 Thermal management of advanced weapons and ships

The US DoD is developing new generations of pulsed power weapons, all electric warships and advanced electrical systems, all of which produce large amounts of heat. Waste heat from these systems may be of the order of megawatts, which can be transported by nanofluids to the hull of a ship. Therefore, the thermal management of weapons and hull heating can be accomplished simultaneously by circulating nanofluids to transport the heat from critical high heat flux components, in excess of 1000 W/cm^2 and deliver it to the ship hull. This heating of the ship hull will reduce the drag of the ship ultimately saving fuel costs.

1.6.3 Application in heating and cooling of buildings

Various nanofluids can be employed in conventional heat exchangers used in cold-region buildings. Analysis shows that nanofluid applications could result in volumetric flow reduction, reduction in the mass flow rate and pumping power savings. Nanofluids also require smaller heating systems in order to be capable of delivering the same amount of thermal energy, thus reducing the size and the initial cost of equipment. This will reduce the release of pollutants to the environment due to a reduction in power consumption and the waste produced at the end of the heat transfer system life-cycle. In

cooling systems nanofluids can be used in place of chilled water, which is commonly used in coils of air conditioning ducts. This application has not been explored extensively in the technical literature.

1.6.4 Application of nanofluids in thermal absorption systems

The thermally driven absorption system is an alternative to the vapor compression system, which may lead to environmental problems such as global warming and ozone layer depletion due to the use of certain refrigerants. The absorber is the most critical component in the absorption system. In order to improve the performance of the absorber, several studies have been carried out. Kim et al. [62] showed that by adding nanoparticles such as Cu, CuO and Al_2O_3 to a NH_3/H_2O solution improved the absorption performance by 5.32 times.

Whenever there are cooling baths using glycol water mixtures, methanol and silicon oil, exploratory studies should be performed on nanofluids to determine if any advantages may be gained.

1.7 Overview of the Papers Embedded in Thesis as Chapters 2 to 8

Chapter 2 addresses the rheology of copper oxide (CuO)-water nanofluids with varying concentrations (5%, 8%, 10%, 13% and 15%) and varying temperature (5°C to 50°C). The experiments showed that these nanofluids exhibited time-independent pseudoplastic and shear-thinning behavior. The suspension viscosity of nanofluids decreases exponentially with respect to the shear rate. Suspension viscosity follows the correlation in the form: $\ln(\mu_s) = A(\frac{1}{T}) - B$, where constants A and B are the functions of volumetric concentrations.

Chapter 3 shows the rheological behavior of copper oxide nanoparticles dispersed in a 60:40 propylene glycol and water mixture. The experiments were conducted over a temperature range of -35°C to 50°C to establish their behavior as a heat transfer fluid in cold climates. The experiments reveal that this nanofluid (in the range of particle volume percentage tested, 0 to 6%) exhibits Newtonian behavior. A new exponential correlation has been developed from the experimental data, which expresses the viscosity as a function of particle volume percent and the temperature of the nanofluid.

Chapter 4 illustrates how thermophysical properties affect the Prandtl number of various nanofluids (SiO_2, Al_2O_3 and CuO in ethylene glycol and water mixture). The increase in the heat transfer coefficient of the nanofluids is directly proportional to the increase in the Prandtl number. This analysis reveals that as the concentration of nanoparticles increased, the Prandtl number also increased. Also the effects of particle size and temperature variation on the Prandtl number of nanofluids were discussed in this chapter.

Chapter 5 presents the effectiveness of various liquid coolants (pure water, ethylene glycol, propylene glycol and various nanofluids) using the Mouromtseff number. The Mouromtseff number is a figure of merit (FOM) for heat transfer fluids. A higher value of FOM for a fluid indicates better heat transfer characteristics. This analysis is critical to choosing a particular coolant for a particular application.

Chapter 6 shows the experimental investigation of nanofluids comprised of silicon dioxide (SiO_2) nanoparticles suspended in a 60:40 (% by weight) ethylene glycol and water mixture for their heat transfer and fluid dynamic performance. The effects of particle diameter (20 nm, 50 nm, and 100 nm) on the viscosity of the fluid, heat transfer characteristics and pressure loss were investigated. It was found that an increase in particle diameter increased the heat transfer coefficient. Typical percentage increases of heat transfer coefficient and pressure loss at fixed Reynolds number are presented.

Chapter 7 shows the experimental analysis of heat transfer and fluid dynamic performance of various nanofluids (SiO_2, Al_2O_3 and CuO in ethylene glycol and water mixture). We have investigated the application of nanofluids in heating buildings in cold climates. Calculations have been carried out for a conventional heat exchanger used in a building. The analysis showed that application of nanofluids could result in volumetric flow reduction, reduction in the mass flow rate and pumping power savings. Nanofluids also require smaller heating systems capable of delivering the same amount of thermal energy, thus reducing the initial cost of the equipment.

Chapter 8 addresses Al_2O_3 nanofluid applications in a Diesel Electric Generator (DEG) as the jacket fluid coolant. Specific heat measurement results of various concentrations of Al_2O_3 nanofluids show that as the concentration of nanoparticles increases the specific heat decreases. Also, the specific heat increases as temperature increases similar to the data in ASHRAE [44] for base fluids. This is an important analysis in calculating thermal performance of nanofluids in the future. The study on cogeneration efficiency of a diesel engine using nanofluids shows that cogeneration efficiency decreases mainly due to decrease in their specific heat values.

1.8 References

1. Choi, U.S., Enhancing Thermal Conductivity of Fluids with Nanoparticles, Developments and Applications of Non-Newtonian Flows, FED-Vol. 231/MD-Vol. 66, ASME, New York, pp. 99-105, 1995.

2. Boutin, C., Taking the Heat Off: Nanofluids Promise Efficient Heat Transfer, logos, Vol. 19, No. 2, 2001.

3. Eastman, J.A., Phillpot, S.R., Choi, S.U.S. and Keblinski, P.K., Thermal Transport in Nanofluids, Annual Review of Material Research, vol. 34, pp. 219-246, 2004.

4. Choi, S.U.S., Zhang, Z.G. and Keblinski, P., Nanofluids, Encyclopedia of Nanoscience and Nanotechnology, vol. 6, pp. 757-773, 2004.

5. Wang, X.Q., Mujumdar, A.S., Heat Transfer Characteristics of Nanofluids: A Review, International Journal of Thermal Sciences, Vol. 46, pp. 1-19, 2007.

6. Choi, S.U.S., Yu, W., Hull, J.R., Zhang, Z.G., Lockwood, F.E., Nanofluids for Vehicle Thermal Management, Society of Automotive Engineers, SAE 2001-01-1706, pp. 139-144, 2001.

7. Buongiorno, J., Convective Transport in Nanofluids, ASME Journal of Heat Transfer, Vol. 128, p. 240-250, 2006.

8. Li, Q., Xuan, Y., Convective Heat Transfer and Flow Characteristics of Cu-water Nanofluid, Science in China (Series E), Vol. 45, No. 4, pp. 408-416, 2002.

9. Eastman, J.A., Choi, S.U.S., Li, S., Yu, W. and Thompson, L.J., Anomalously Increased Effective Thermal Conductivities of Ethylene Glycol-based Nanofluids Containing Copper Nanoparticles, Applied Physics Letters, Vol. 78, No. 6, pp. 718-720, 2001.

10. Maxwell J.C., A Treatise on Electricity and Magnetism, 2nd edition, Oxford University Press, Cambridge, pp. 435-441, 1904.

11. Hamilton, R.L., Crosser, O.K., Thermal Conductivity of Heterogeneous Two Component Systems, I & EC Fundamentals, Vol. 1, No. 3, pp. 187-191, 1962.

12. Gosselin, L., Silva, A.K.D., Combined Heat Transfer and Power Dissipation Optimization of Nanofluid Flows, Applied Physics Letters, Vol. 85, No. 18, pp. 4160-4162, 2004.

13. Ding, Y., Alias, H., Wen, D., Williams, R.A., Heat Transfer of Aqueous Suspensions of Carbon Nanotubes (CNT Nanofluids), International Journal of Heat and Mass Transfer, Vol. 49, pp. 240-250, 2006.

14. Maiga, S.E.B., Nguyen, C.T., Galanis, N. and Roy, G., Heat Transfer Behaviors of Nanofluids in a Uniformly Heated Tube, Superlattices and Microstructures, Vol. 35, pp. 543-557, 2004.

15. Wen, D. and Ding, Y., Experimental Investigation into Convective Heat Transfer of Nanofluids at the Entrance Region Under laminar Flow Conditions, International Journal of Heat and Mass Transfer, Vol. 48, pp. 5181-5188, 2004.

16. Xuan, Y., Roetzel, W., Conceptions of Heat Transfer Correlation of Nanofluids, International Journal of Heat and Mass Transfer, Vol. 43, pp. 3701-3707, 2000.

17. Xuan Y., Li, Q., Heat Transfer Enhancement of Nanofluids, International Journal of Heat and Fluid Flow, Vol. 21, pp. 58-64, 2000.

18. Xuan Y., Li, Q., Investigation on Convective Heat Transfer and Flow Features of Nanofluids, ASME Journal of Heat Transfer, Vol. 125, pp. 151-155, 2003.

19. Pak, B.C., Cho, Y.I., Hydrodynamic and Heat Transfer Study of Dispersed Fluids with Submicron Metallic Oxide Particles, Experimental Heat Transfer, Vol. 11, pp. 151-170, 1998.

20. Kays, W.M., Crawford, M.E., Convective Heat and Mass Transfer, 3rd Edition, pp. 244-249, 1993.

21. Prasher, R., Bhattacharya, P., Phelan, P.E., Thermal Conductivity of Nanoscale Colloidal Solutions (Nanofluids), Physical Review Letters, Vol. 94, pp. 025901-1 – 025901-5, 2005.

22. Chopkar, M., Das, P.K., Manna, I., Synthesis and Characterization of Nanofluid for Advanced Heat Transfer Applications, Scripta Materialia, Vol. 55, pp. 549-552, 2006.

23. Batchelor, G.K., The Effect of Brownian Motion on the Bulk Stress in a Suspension of Spherical Particles, Journal of Fluid Mechanics, Vol. 83, No.1, pp. 97-117, 1977.

24. Quinn, R.G. and Bauman, J., Heat Transfer Characteristics of non-Newtonian Suspension, M.S. Thesis, Newark College of Engineering, Newark, NJ, 1954.

25. Gullett, D.and Curtis, E., Viscosity of Non-Newtonian Suspensions, M.S. Thesis, Newark College of Engineering, Newark, NJ, 1955.

26. Wisla, I.S. and Kukowski, J.L., Correlation of Curtis and Gullett Equation for Viscosity of Non-Newtonian Suspensions and Franks and Rinaldi Equation for Heat Transfer Coefficients, M.S. Thesis, Newark College of Engineering, Newark, NJ, 1956.

27. Tseng, W.J. and Lin, K.C., Rheology and Colloidal Structure of Aqueous TiO_2 Nanoparticle Suspensions, Material Science and Engineering, A355, pp. 186-192, 2003.

28. Yang, Y., Grulke, E.A., Zhang, Z.G. and Wu, G., J. Rheological Behavior of Carbon Nanotube and Graphite Nanoparticle Dispersions, Journal of Nanoscience and Nanotechnology, Vol. 5, pp. 571-579, 2005.

29. Hilding, J., Grulke, E.A., Zhang, Z.G. and Lockwood, F., Dispersion of Carbon Nanotubes in Liquids, Journal of Dispersion Science and Technology, Vol. 24, No.1, pp. 1-41, 2003.

30. Tseng, W. and Wu, C.H., Aggregation, Rheology and Electrophoretic Packing Structure of Aqueous Al_2O_3 Nanoparticle Suspensions, Acta Materialia, Vol. 50, pp. 3757-3766, 2002.

31. Savarmand, S., Carreau, P.J., Betrand, F., Vidal, D.J. and Moan, M., Rheological Properties of Concentrated Aqueous Silica Suspensions: Effects of pH and Ions Content, Journal of Rheology, Vol. 47, No. 5, pp. 1133-1149, 2003.

32. Tseng, W. and Lin, C.L., Effect of Dispersants on Rheological Behavior of $BaTiO_3$ Powders in Ethanol-Isopropanol Mixtures, Materials Chemistry and Physics, Vol. 80, pp. 232-238, 2003.

33. Kwak, K., Kim, C., Viscosity and Thermal Conductivity of Copper Oxide Nanofluid Dispersed in ethylene Glycol, Korea-Australia Rheology Journal, Vol. 17, No. 2, pp. 35-40, 2005.

34. Tseng, W. and Chen, C.N., Effect of Polymeric Dispersant on Rheological Behavior of Nickel-Terpineol Suspensions, Materials Science and Engineering, A 347, pp. 145- 153, 2003.

35. Tseng, W. and Chen, C.N., Determination of Maximum Solids Concentration in Nickel Nanoparticle Suspensions, Journal of Materials Science Letters, Vol. 21, pp. 419-422, 2002.

36. Teipel, U., Forter-Barth, U., Rheology of Nano-Scale Aluminum Suspensions, Propellants, Explosives, Pyrotechnics, Vol. 26, pp. 268-272, 2001.

37. Drew, D.A., Passman, S.L., Theory of Multi Component Fluids, Springer Publications, Berlin, 1999.

38. A. Einstein, Investigations on the Theory of the Brownian Movement, Dover, New York, 1906.

39. Bicerano, J., Douglas, J.F. and Brune, D.A., Model for the Viscosity of Particle Dispersions, Journal of Macromolecular Science – Review Macromolecular Chemistry & Physics, C 39, (4), pp. 561-642, 1999.

40. Brinkman, H.C., The Viscosity of Concentrated Suspensions and Solutions, The Journal of Chemical Physics, Vol. 20, No.4, pp. 571, 1952.

41. White, F.M., Viscous Fluid Flow, McGraw Hill Publication, NY, 1991.

42. Kulkarni, D.P., Das, D.K., Chukwu, G. A., Temperature Dependent Rheological Property of Copper Oxide Nanoparticles Suspension (Nanofluid), Journal of Nanoscience and Nanotechnology, Vol. 6, pp. 1150-1154, 2006.

43. Mcquiston, F.C., Parker, J. D., Spitler, J. D., Heating, Ventilating, and Air Conditioning, John Wiley & Sons Inc., New York, 2000.

44. ASHRAE Handbook 1985 Fundamentals, American Society of Heating, Refrigerating and Air-Conditioning Engineers Inc., Atlanta, 1985.

45. Yang, Y., Zhang, G., Grulke, E.A., Anderson, W.B., Wu, G., Heat Transfer Properties of Nanoparticle-in-fluid Dispersions (Nanofluids) in Laminar Flow, International Journal of Heat and Mass Transfer, Vol. 48, pp. 1107-1116, 2005.

46. Sieder, E.N., Tate, G.E., Heat Transfer and Pressure Drop of Liquids in Tubes, Ind. Eng. Chem., Vol. 28, pp. 1429-1435, 1936.

47. Oliver, D.R., Effect of Natural Convection on Viscous Flow Heat Transfer In Horizontal Tubes, Chemical Engineering Science, Vol. 17, pp. 335-350, 1962.

48. Heris, Z. S., Esfahany, M.N., Etemad, S.Gh., Experimental Investigation of Convective Heat Transfer of Al_2O_3/water Nanofluid in Circular Tube, International Journal of Heat and Fluid Flow, Vol. 28, pp. 203-210, 2007.

49. Heris, Z. S., Etemad, S.Gh., Esfahany, M.N., Experimental Investigation of Oxide Nanofluids Laminar Flow Convection Heat Transfer, International Communications in Heat and Mass Transfer, Vol. 33, pp. 529-535, 2006.

50. Nguyen, C.T., Roy, G., Gauthier, C., Galanis, N., Heat Transfer Enhancement Using Al_2O_3-water Nanofluid for an Electronic Liquid Cooling System, Applied Thermal Engineering, Vol. 27, pp. 1501-1506, 2007.

51. Maiga, S.E.B., Palm, J., Nguyen, C.T., Roy, G., Galanis, N., Heat Transfer Enhancement by Using Nanofluids in Forced Convection Flows, International Journal of Heat and Fluid Flow, Vol. 26, pp. 530-546, 2005.

52. Mansour, R.B., Galanis, N., Nguyen, C.T., Effect of Uncertainties in Physical Properties on Forced Convection Heat Transfer with Nanofluids, Applied Thermal Engineering, Vol. 27, pp. 240-249, 2007.

53. Behzadmehr, A., Saffar-Avval, M., Galanis, N., Prediction of Turbulent Forced Convection of a Nanofluid In a Tube with Uniform Heat Flux Using a Two Phase Approach, International Journal of Heat and Fluid Flow, Vol. 28, pp. 211-219, 2007.

54. Akbarinia, A., Behzadmehr, A., Numerical Study of Laminar Mixed Convection of a Nanofluid in Horizontal Curved Tubes, Applied Thermal Engineering, Vol. 27, pp. 1327-1337, 2007.

55. He, Y., Chen, H., Ding, Y., Cang, D., Lu, H., Heat Transfer and Flow Behavior of Aqueous Suspensions of TiO_2 Nanoparticles (Nanofluids) Flowing Upward Through a Vertical Pipe, International Journal of Heat and Mass Transfer, Vol. 50, pp. 2272-2281, 2007.

56. Lee, S., Choi, S.U.S., Application of Metallic Nanoparticle Suspensions in Advanced Cooling Systems, Recent Advances in Solids / Structures and application of Metallic Materials, ASME PVP-Vol. 342 / MD-Vol. 72, pp. 227- 234, 1996.

57. Koo, J., Kleinstreuer, C., Laminar Nanofluid Flow in Microheat Sinks, International Journal of Heat and Mass Transfer, Vol. 48, pp. 2652-2661, 2005.

58. Chein, R., Huang, G., Analysis of Microchannel Heat Sink Performance Using Nanofluids, Applied Thermal Engineering, Vol. 25, pp. 3104-3114, 2005.

59. Nguyen, C.T., Roy, G., Maiga, S.E.B., Lajole, P.R., Heat Transfer Enhancement by Using Nanofluids for Cooling of High Heat Output Microprocessor, Electronics Cooling, 2004.

60. Ollivier, E., Bellettre, J., Tazerout, M., Roy, G.C., Detection of Knock Occurrence In a Gas SI Engine From a Heat Transfer Analysis, Energy Conservation and Management, Vol. 47, pp. 879-893, 2006.

61. Anonymous Nanofluids Improve Thermal Management, Fuel Cell Technology News, Business Communications Company Inc., Vol. 4, Issue 2, 2001.

62. Kim, J.K., Jung, J.Y., Kang, Y.T., Absorption Performance Enhancement by Nano-particles and Chemical Surfactants in Binary Nanofluids, International Journal of Refrigeration, Vol. 30, pp. 50-57, 2007.

CHAPTER TWO

Temperature Dependent Rheological Property of Copper Oxide Nanoparticles Suspension (Nanofluid)

Devdatta P. Kulkarni[1], Debendra K. Das[2*], Godwin A. Chukwu[3]

[1, 2] Department of Mechanical Engineering

[3] Department of Petroleum Engineering

University of Alaska Fairbanks

P.O. Box 755905, Fairbanks, AK, 99775-5905, USA.

Abstract

A nanofluid is the dispersion of metallic solid particles of nanometer size in a base fluid such as water or ethylene glycol. The presence of these nanoparticles affects the physical properties of a nanofluid via various factors, including shear stress, particle loading and temperature. In this paper the rheological behavior of copper oxide (CuO) nanoparticles of 29 nm average diameter dispersed in deionized (DI) water is investigated over a range of volumetric solids concentrations of 5 to 15% and various temperatures varying from 278-323°K. These experiments showed that these nanofluids exhibited time-independent pseudoplastic and shear-thinning behavior. The suspension viscosities of nanofluids decrease exponentially with respect to the shear rate. Suspension viscosity follows the correlation in the form $\ln(\mu_s) = A(\frac{1}{T}) - B$, where constants A and B are the functions of volumetric concentrations. The calculated viscosities from the developed correlations and experimental values were found to be within ± 10% of their values.

Journal of Nanoscience and Nanotechnology, Vol. 6, pp. 1150-1154, 2006

Key words:
Rheology, Viscosity, Copper Oxide Nanoparticles, Temperature Dependency

* Corresponding Author; Tel: (907) 474-6094; Email: ffdkd @uaf.edu

2.1 Introduction

In recent years nanofluids have grown in importance; they are seen as a new generation of cooling medium due to their tremendous potential in heat transfer processes. Nanofluids are much more important than conventional base fluids, such as water and ethylene glycol, because of the presence of suspended metallic nanoparticles, which increase the thermal conductivity of the mixture and thus enhance their energy exchange capability. Eastman et al.[1] showed an increase of 40% in thermal conductivity with 0.3 vol % of Cu nanoparticles in ethylene glycol. Thus far, many correlations have been developed for heat transfer coefficients of these nanofluids.[2-8] Due to this increase in heat transfer coefficients, these nanofluids are now being applied in areas like thermal management of microelectronics[10] and fuel cells.[11] Various theoretical and experimental analyses[4,7] have been conducted for heat transfer coefficients; and these assume that viscosity is a function of volume fraction and is constant over a range of temperatures.

Research on viscosity measurement of submicron particles in a fluid medium started as far back as 1954.[12-14] To date, various studies have investigated the viscosities of different nanofluids, including TiO_2 nanoparticles in water[15], carbon nanotubes and graphite nanofluids[16-17], Al_2O_3 nanofluids[18], aqueous silica suspensions[19], $BaTiO_3$ suspensions[20] and Nickel suspensions[21-22]. Many correlations have been developed for viscosity of nanofluids as a function of volume fraction. A few of the most relevant include, Einstein[23], who proposed the correlation for viscosity of suspension as:

$$\mu_s = \mu_f (1 + \frac{5}{2}\phi) \tag{1}$$

where μ_s = suspension viscosity, μ_f = viscosity of base fluid and ϕ is volume fraction. A similar kind of correlation is given by Bicerano et al.[24] as

$$\mu_s = \mu_f (1 + \eta\phi + k_H\phi^2 + ...) \tag{2}$$

where η is virial coefficient and k_H is Huggins coefficient.

The most commonly used viscosity correlation was developed by Brinkman[2, 4]:

$$\mu_s = \mu_f \frac{1}{(1-\phi)^{2.5}}. \tag{3}$$

To date, the literature offers no correlation for viscosity of nanofluids as is a function of both temperature and volume fraction. A rheological property like viscosity is a strong function of temperature; that is, viscosity near the freezing point of a fluid has a very high value and near the boiling temperature, a very low value. White[25] gave a temperature-dependent viscosity correlation as:

$$\ln\frac{\mu}{\mu_0} \approx a + b(\frac{T_0}{T}) + c(\frac{T_0}{T})^2 \tag{4}$$

where (μ_0, T_0) are reference values and (a,b,c) are dimensionless curve fit values.

Researching temperature dependency on viscosity is very important for cold climate regions like Alaska, Canada and circumpolar regions. Nanofluids are useful as the new generation coolant for automobiles, various heat exchangers and baseboard heaters in Alaskan houses. In the arctic and subarctic climate, equipment employing nanofluids may encounter temperatures well below 0°C.

2.2 Experimental Procedure to Measure the Viscosity

CuO nanofluid with 15% volume (49.9% by weight) of CuO nanoparticles with an average diameter of 29nm, and a particle density of 6.3 gm/cc (Nanophase, Inc.[26]) was used as a starting material for viscosity measurement. Subsequently, different concentrations of CuO nanofluids (5%, 8%, 10%, 13% & 15% by volume) were prepared by adding calculated amounts of deionized (DI) water. After adding DI water the mixture was thoroughly stirred and ultrasonically agitated for half an hour to achieve uniform mixing of nanoparticles in water.

Viscosity measurement of this CuO nanofluid was carried out using a LV DV-II+ Brookfield viscometer. The viscosity measurement range of the LV DV-II model is 1 to 2 $x10^6$ m.Pa.s [9], which exactly matches with requirements. The experimental set up is shown in Figure 2.1.

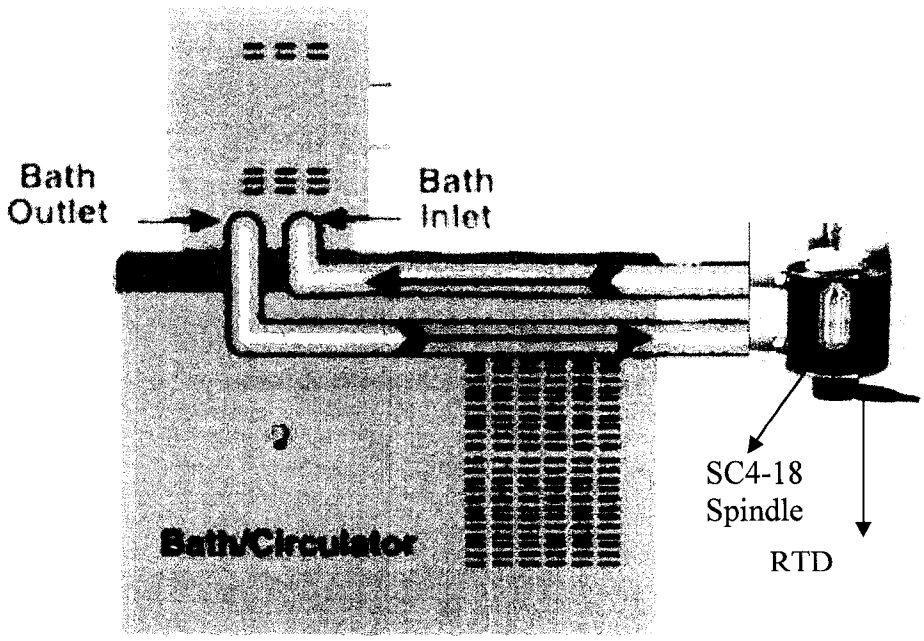

Figure 2.1. Experimental set-up for measuring temperature dependency on the viscosity of nanofluids.

This set-up also included a SC4-18 spindle, which has a viscosity range of 1.5 to 30K m.Pa.s. First, the viscometer with SC4-18 spindle assembly was calibrated using Brookfield's Silicone Viscosity Standard fluids (viscosity values of 9.7 and 97 m.Pas at 25°C). The equipment accuracy was found to be ± 2% of these standard viscosity values. The viscometer has a small sample chamber surrounded by a water jacket. Sample temperature is maintained by a Julabo temperature-controlled bath. A RTD temperature sensor embedded in the sample chamber provides accurate monitoring of sample temperatures during viscosity measurement. For this nanofluid experiment, the sample temperature was raised to 50°C, then gradually decreased to 5°C in increments of 5°C. Viscosity was measured at every 5°C interval. The accuracy of temperature control was ± 0.1°C. The control panel for temperature setting is shown in Figure 2.2 which clearly displays the step variation of 5°C. Freezing of nanofluid was found to occur at about 0°C, and hence 5°C was chosen as the lowest temperature for viscosity measurement.

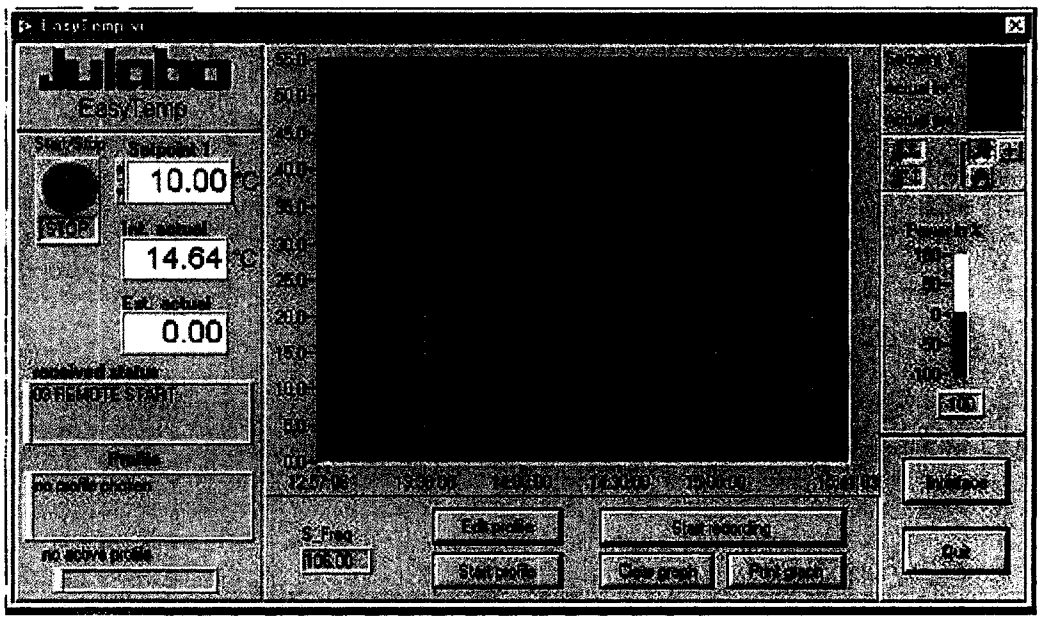

Figure 2.2. Temperature control panel for Julabo temperature control bath.

Viscosity was measured at various shear rates at specific temperatures. The shear rate range was 2 sec^{-1} to 265 sec^{-1}. Researchers took care to ensure that all readings were taken under steady state conditions (3-5 minutes for each reading).

2.3 Results and Discussion

The viscosity readings were taken at low shear rates (2 sec^{-1} to 265 sec^{-1}). The flow curve of CuO suspensions decreased according to a power law, with a correlation factor R^2 greater than 0.9 for all the curves shown in Figure 2.3. The viscosity readings were recorded from low to high RPM of the spindle, then back to low RPM, these readings were in the range of $\pm 0.1\%$ of torque. The viscosity correlations for the LV DV-II+ viscometer model are given by the Brookfield manual[9]:

Viscosity (m.Pa.s) = 100/RPM *TK * SMC * Torque (5)

Shear Rate (1/sec) = RPM * SRC (6)

Shear Stress (N/m2) = TK * SMC * SRC * Torque/10 (7)

Where, RPM = Viscometer spindle speed in revolution per minute

TK = Viscometer torque constant (0.09373)

SMC = Spindle multiplier constant (3.2 for SC4-18)

SRC = Spindle shear rate constant (1.32 for SC4-18)

Torque = Viscometer torque (%) expressed in numbers between 0 & 100

These results confirmed that the 15% volumetric CuO suspension was time–independent, pseudoplastic, and shear thinning. This behavior is shown in Figures 2.3 & 2.4. Following this, similar studies were performed for volume concentrations of 5%, 8%, 10% & 13%, and all showed similar trends of viscosity. The experimental data points curve-fitted with correlation factor R^2 are shown in Table 2.1.

experimental data points are available due to limitations for torque for this particular viscometer and spindle.

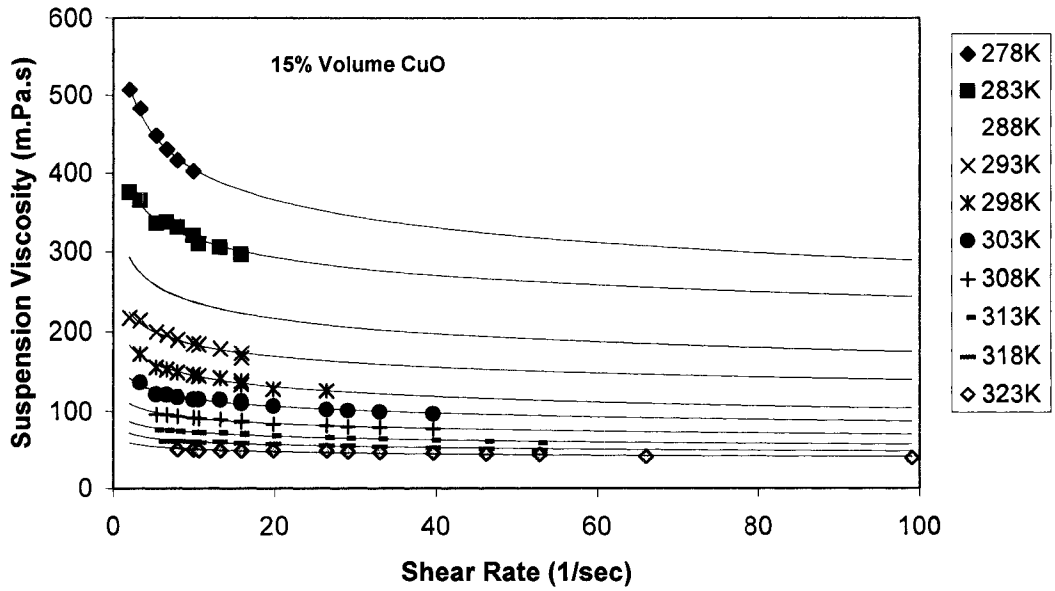

Figure 2.4. The viscosity (μ_s) – strain rate (γ) dependence of 15% volume CuO suspension at different temperatures (T).

The viscosity of nanofluids decreases in exponential form with correlation factor R^2, as shown in Table 2.2. These results are comparable with results obtained by Pak & Cho.[5]

Table 2.2. Correlation factors R^2 at different temperatures for 15% volume CuO.

Temp Deg K	278	283	288	293	298	303	308	313	318	323
R^2	0.99	0.96	0.96	0.95	0.97	0.97	0.98	0.96	0.91	0.91

As the concentration of nanoparticles within a fluid increases, the suspension viscosity increases exponentially. Figure 2.5 shows this exponential behavior with respect

to temperature. The viscosity increases more rapidly at lower temperatures than higher ones. This viscosity behavior trend is similar to results obtained by Tseng et al[15] for TiO_2 nano-suspensions.

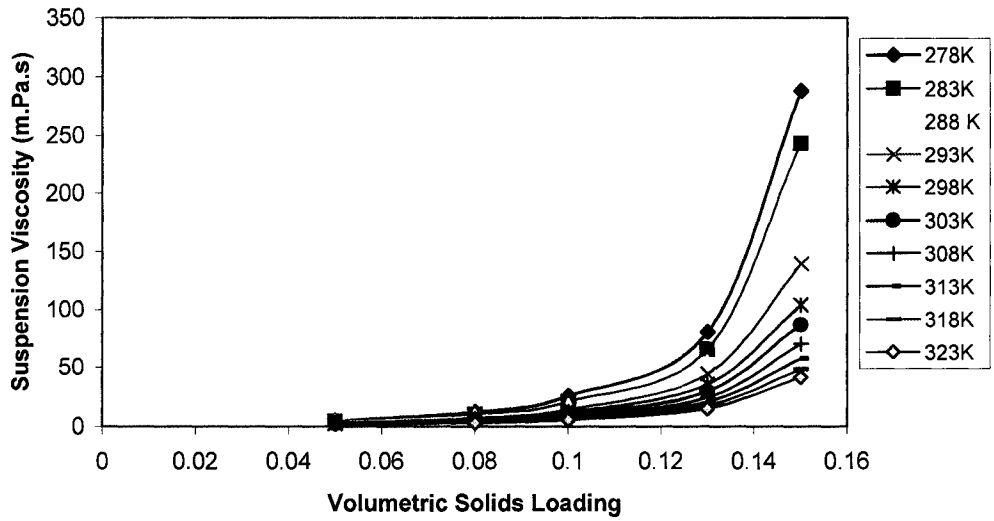

Figure 2.5. The experimental dependence of suspension viscosity (μ_s) with volume fraction (ϕ) at varied temperatures and at a constant shear rate of 100 s^{-1}.

A well-developed generalized correlation for liquid viscosity such as that given by Equation (4) was followed for further investigation. The assumed form of the equation is:

$$\ln \mu_s = A(\frac{1}{T}) - B \tag{9}$$

where μ_s is the suspension viscosity in m.Pa.s (cP), T is the temperature in Kelvin, A & B are polynomials which are functions of volumetric concentrations ϕ. These factors are given as

$$A = 20587\phi^2 + 15857\phi + 1078.3 \text{ with } R^2 = 0.99$$

$$B = -107.12\phi^2 + 53.548\phi + 2.8715 \text{ with } R^2 = 0.97$$

where ϕ is the volume fraction ranging from 0.05 to 0.15.

The comparison of calculated values from the above equation and the experimental values were plotted in Figure 2.6. These values are within ± 10%, except for two data points at temperatures 278 & 283 K, for a 15% CuO suspension. If we exclude these 2 experimental data points from the original 50, a generalized correlation for viscosity, with volume fraction and temperature as variables, presented via Equation (9), is valid.

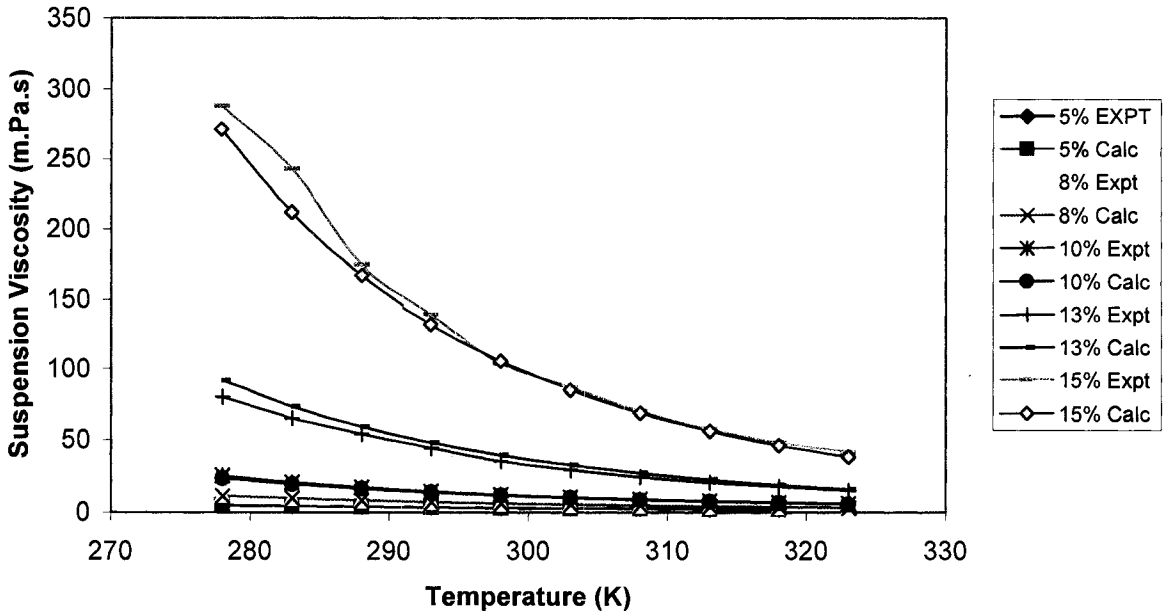

Figure 2.6. Comparisons of experimental and calculated suspension viscosity (μ_s) with varying volume fraction (%) at different temperatures and at constant shear rate of 100 s^{-1}

2. 4 Conclusions

The experiments on nanofluids using CuO suspension, varying in volume concentration for 5% to 15% showed that these fluids behave as time-independent, shear thinning, pseudoplastic fluids. The viscosity was found to be a strong function of temperature and the volumetric concentration. A new correlation for viscosity of these nanofluids as a function of temperature and volumetric concentration was developed. A special feature of this correlation is that the coefficients are functions of volumetric

concentration. The curve fit correlation of viscosity verses temperature agrees within ± 10% of the experimental measurements.

2.5 Acknowledgement

The authors would like to thank the Arctic Region Super Computing Center (ARSC) at University of Alaska Fairbanks for providing a graduate assistantship.

2.6 References

1. J.A. Eastman, S.U.S. Choi, S. Li, W. Yu and L.J. Thompson, Applied Physics Letters, 78:6, 718 (2001).
2. Y. Xuan and W. Roetzel, International J. of Heat and Mass Transfer, 43, 3701 (2000).
3. Y. Yang, Z.G. Zhang, E.A. Grulke, W.B. Anderson and G. Wu, International J. Heat and Mass Transfer, 48, 1107 (2005).
4. L. Gosselin and A.K. Silva, Applied Physics Letters, 85:18, 4160 (2004).
5. B.C. Pak and Y.I. Cho, Experimental Heat Transfer, 11, 151 (1998).
6. S.E.B. Maiga, C.T. Nguyen, N. Galanis and G. Roy, Superlattices and Microstructures, 35, 543 (2004).
7. G. Roy, C.T. Nguyen and P.R. Lajoie, Superlattices and Microstructures, 35, 497 (2004).
8. Y. Xuan and Q. Li, International J. Heat and Fluid Flow, 21, 58 (2000).
9. *Brookfield DV-II+ Programmable Viscometer Manual No. M/97-164-D1000,* Brookfield Engineering Laboratories Inc, MA, USA.
10. S. Lee and S.U.S. Choi, *Recent Advances in Solids/Structures and Application of Metallic Materials,* ASME Press, PVP-Vol. 342/MD-Vol. 72, 227 (1996).
11. Nanofluids improve thermal management (Brief Article), Nov. 2001, *Fuel Cell TechnologyNews,* Business Communications Company Inc., Vol. 4, Issue 2.
12. R.G. Quinn and J. Bauman, *Heat transfer characteristics of non-Newtonian*

suspension, (1954), M.S. Thesis, Newark College of Engineering, Newark, NJ.

13. D. Gullett and E. Curtis, *Viscosity of non-Newtonian suspensions,* (1955), M.S. Thesis, Newark College of Engineering, Newark, NJ.
14. I.S. Wisla and J.L. Kukowski, *Correlation of Curtis and Gullett equation for viscosity of non-Newtonian suspensions and Franks and Rinaldi equation for heat transfer coefficients,* (1956), M.S. Thesis, Newark College of Engineering, Newark, NJ.
15. W.J. Tseng and K.C. Lin, Material Science and Engineering, A355, 186 (2003).
16. Y. Yang, E.A. Grulke, Z.G. Zhang and G. Wu, J. Nanosci. Nanotech. 5, 571 (2005).
17. J. Hilding, E.A. Grulke, Z.G. Zhang and F. Lockwood, J. Dispersion Sci. and Tech. 24:1, 1 (2003).
18. W. Tseng and C.H. Wu, Acta Materialia, 50, 3757 (2002).
19. S. Savarmand, P.J. Carreau, F. Betrand, D.J. Vidal and M. Moan, J. Rheology 47:5, 1133 (2003).
20. W. Tseng and C.L. Lin, Materials Chemistry and Physics 80, 232 (2003).
21. W. Tseng and C.N. Chen, Materials Science and Engineering, A347, 145 (2003).
22. W. Tseng and C.N. Chen, J. of Materials Science Letters 21, 419 (2002).
23. D.A. Drew and S.L. Passman, *Theory of Multicomponent Fluids*, Springer-Verlag Publication, NY (1999).
24. J. Bicerano, J.F. Douglas and D.A. Brune, J.M.S. – Rev. Macromol. Chem. Phys., C 39, (4), 561 (1999).
25. F.M. White, *Viscous Fluid Flow,* McGraw Hill Publication, NY (1991).
26. Nanophase Technologies, Romeoville, IL, USA. http://www.nanophase.com

CHAPTER THREE

Effect of Temperature on Rheological Properties of Copper Oxide Nanoparticles Dispersed in Propylene Glycol and Water Mixture

Devdatta P. Kulkarni[1], Debendra K. Das[2*], Shirish L. Patil[3]

[1,2] Department of Mechanical Engineering

[3] Department of Petroleum Engineering

University of Alaska Fairbanks

P.O. Box 755905, Fairbanks, AK, 99775-5905, USA.

Abstract

This paper reports on experimental investigation of the rheological behavior of copper oxide nanoparticles dispersed in a 60:40 propylene glycol and water mixture. Nanofluids of a particle volume concentration from 0 to 6% have been tested in this study. The experiments were conducted over a temperature range of -35°C to 50°C to establish their behavior for use as a heat transfer fluid in cold climates. The experiments reveal that this nanofluid in the range of particle volume percentage tested exhibits a Newtonian behavior. A new exponential correlation has been developed from the experimental data, which expresses the viscosity as a function of particle volume percent and the temperature of the nanofluid. The slope of relative viscosity curve was found to be higher at lower temperatures.

Journal of Nanoscience and Nanotechnology, Accepted for Publication in October, 2006

Key Words

Rheology, Viscosity, Temperature Dependency, Nanofluid, Propylene Glycol

* Corresponding Author: ffdkd@uaf.edu, Ph. 907-474-6094.

3.1 Introduction

Nanofluids are the dispersions of nanometer-sized particles in a base fluid such as water, ethylene glycol or propylene glycol. In the last decade, nanofluids have attracted more attention as a new generation of coolant for various industrial and automotive applications. Use of high thermal conductivity metallic nanoparticles (e.g., copper, aluminum, silver, gold, etc.), has the effect of increasing the thermal conductivity of such mixtures, thus enhancing their overall energy transport capability[1, 2]. Eastman et al.[3] showed an increase of 40% in thermal conductivity with 0.3 volume percent of copper nanoparticles in ethylene glycol.

In cold climates like those found in Alaska, Canada and circumpolar regions, heat transfer fluids regularly encounter very low temperatures, on the order of -40°C. It is a common practice to use ethylene or propylene glycol mixed with water in different proportions as a heat transfer fluid[4] for automobiles, heat exchangers and baseboard heaters in Alaskan houses. Inhibited ethylene glycol and propylene glycol are used as aqueous freezing point depressants and heat transfer media in cooling systems[5]. Their main attributes are the ability to lower the freezing point of water, low volatility and relatively low corrosivity. Ethylene glycol solutions have better heat transfer properties than propylene glycol solutions, especially at low temperatures. However, because propylene glycol mixtures exhibit lower toxicity, they are preferred in many applications. The commonly used mixture in cold climates is 60% by weight propylene glycol and 40% water. This mixture's thermal performance could be enhanced by adding copper oxide (CuO) nanoparticles. The addition of these particles would affect the rheology of this mixture. No rheological data are currently available in the literature for such

nanofluids at lower temperatures. Investigating and reporting on the rheology of this nanofluid is very important to expanding its application in cold regions. In the present paper, the viscosity of propylene glycol and water with different volumetric percentages of CuO nanoparticles has been investigated over a range of temperatures, from –35°C to 50°C.

Early research on viscosity correlations for use in calculating the heat transfer coefficient and pressure drop relied on viscosity equations, which are a function of volume percentage only[6].

The most commonly used viscosity correlation was developed by Brinkman[7-8],

$$\mu_s = \mu_f \frac{1}{(1-\phi)^{2.5}} \tag{1}$$

where μ_s is the suspension viscosity of the nanofluid, μ_f is the viscosity of the base fluid, and ϕ is volume percent of the nanoparticles.

The viscosity-volume fraction relationship for stable dispersions is given as[9]:

$$\mu_s = \mu_f (1 + \eta\phi + k_H \phi^2 + O\phi^3) \tag{2}$$

where the intrinsic viscosity η was calculated to be 2.5 for uncharged spheres by Einstein[10], and k_H , the coefficient accounting for the interaction between two colliding particles, was shown to be 6.2 by Batchelor[11]. This equation is valid until a volume concentration of 15% is reached. Equations (1) and (2) do not contain the temperature dependency. White[12] reports that generally the viscosity of liquids decreases rapidly with temperature. In the present paper, the temperature dependence is included in a new viscosity correlation.

Research on measuring the viscosity of submicron particles in a fluid medium started as far back as 1954[13-14]. To date, various studies have investigated the viscosities of different nanofluids, including TiO_2 nanoparticles in water[15], carbon nanotubes and graphite nanofluids[16-17], Al_2O_3 nanofluids[18], aqueous silica suspensions[19], $BaTiO_3$ suspensions[20], Nickel suspensions[21-22] and also copper oxide in ethylene glycol at room

temperature[23]. The rheology of aluminum nanoparticle suspension in paraffin oil was studied by Teipel and Forter-Barth[24]. Many correlations have been developed for viscosity of nanofluids as a function of volume fraction. Among these, an earlier study by Kulkarni et al.[25] showed the temperature dependency of copper oxide nanofluid in water from 5°C to 50°C:

$$\ln \mu_s = A(\frac{1}{T}) - B \tag{3}$$

where A & B are functions of volume percent ϕ. The present study deals with a different base fluid and a much lower temperature range. In the discussion below, a new correlation has been developed to represent the nanofluid under study (CuO).

3.2 Experimental Procedure

As a starting solution, a CuO nanofluid (15% by volume, 49.9% by weight of CuO nanoparticles with an average diameter of 29 nm, and a particle density of 6.3 gm/cc [26]) was used for preparing the propylene glycol and water mixture for viscosity measurement. The base fluid was 60% propylene glycol and 40% water by weight. Subsequently, different concentrations of CuO nanofluids (5.9%, 5%, 4%, 3%, 2% & 1% by volume) were prepared by adding calculated amounts of propylene glycol/water solution. The addition of nanoparticles to maintain proper volume concentration was carefully performed by using a sensitive mass balance instrument (Mettler AE 160), with an accuracy of 0.1 mg. After adding the propylene glycol/water solution, the mixture was thoroughly stirred and ultrasonically agitated for half an hour to achieve uniform suspension of nanoparticles.

The experimental set up for measuring the viscosity of this CuO nanoparticle in propylene glycol was carried out using a LV DV-II+ Brookfield viscometer described by Kulkarni et al.[25] This setup also possessed the temperature control bath that allowed variation of the sample temperature from -35°C to 50°C for this experiment. The viscosity

measurement range of the LV DV-II model is 1 to 2 x10^6 m.Pa.s [27], which agrees with the values expected in this experiment's temperature range.

This experiment used a SC4-18 spindle, which has a viscosity range of 1.5 to 30,000 m.Pa.s. First, the viscometer with SC4-18 spindle assembly was calibrated using Brookfield's Silicone Viscosity Standard fluids (viscosity values of 9.7 and 97 m.Pa.s at 25°C). The equipment accuracy was tested to be ± 2% of these standard viscosity values. The viscometer has a small sample chamber surrounded by a liquid jacket. Sample temperature is maintained by a Julabo[27] temperature-controlled bath. A RTD temperature sensor placed in the sample chamber provides accurate monitoring of sample temperatures during viscosity measurements. At higher temperatures, the spindle speed was maintained over a broader range (0-200 RPM). At lower temperatures, the spindle speed was maintained in a narrow range (0-1 RPM). Speed selection is dependent upon the viscosities of propylene glycol or the base fluid and the concentration of nanoparticles: the higher the concentration, the lower the spindle RPM range.

Viscosity measurement began with the sample temperature at 50°C; then the temperature was decreased to -35°C in steps. Viscosity was measured at every 10°C interval with the last one being taken at a 5°C decrement. The accuracy of temperature control for this instrument is ± 0.1°C. The freezing temperature of the propylene glycol and water mixture (60:40) is about -45°C[3]. Therefore, as a precaution, the lowest temperature used in the experiment was -35°C, to avoid any freezing condition in the sample chamber.

About eight to fourteen viscosity measurements were recorded at various shear rates at specific temperatures for each volume concentration of nanofluid. Caution was taken to ensure that all readings were taken under steady state conditions by giving samples ample time (2-3 minutes for each reading) to stabilize the readings.

3.3 Results and Discussion

Figure 3.1 shows that a CuO nanoparticle suspension of 5.9% by volume in propylene glycol and water exhibits Newtonian behavior, as shear stress is directly proportional to shear rate and follows the constitutive equation of Newtonian fluid:

$$\tau = \mu \dot{\gamma} \tag{4}$$

This Newtonian behavior is found for all levels of CuO nanoparticle loading (0 to 5.9%) in 60:40 propylene glycol and water mixture at all temperatures within the test range of –35°C to 50°C. Prior experiments with higher concentrations of CuO particles in water have shown that adding nanoparticles into the base fluid influences the fluid rheology toward non-Newtonian behavior[24].

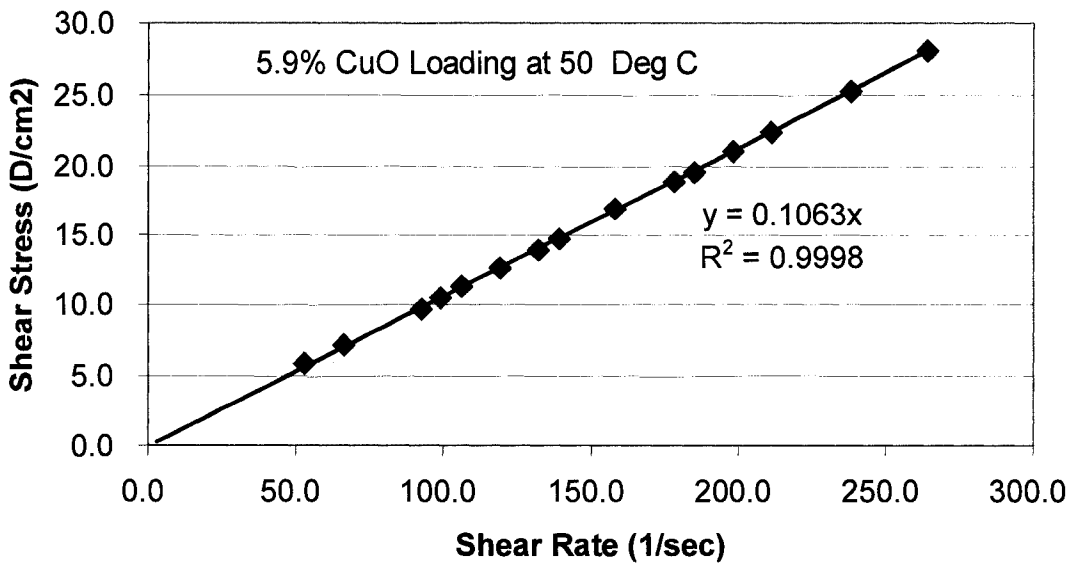

Figure 3.1. Shear stress (dyne/cm^2) versus shear rate of 5.9% volume CuO loading in propylene glycol/water mixture at 50°C.

However, in this research all the volume percentages tested up to 5.9% of copper oxide nanoparticle suspensions in propylene glycol and water mixture exhibited Newtonian behavior. This may be due to the fact that pure propylene glycol exhibits

Newtonian behavior, and its presence in the mixture dominates the rheological properties of these kinds of nanofluids. Also, at higher nanoparticle concentrations (>5.9%), this behavior may shift to non-Newtonian. Therefore further research is necessary at higher concentrations to explore this unknown behavior.

As a benchmark test case, the rheological properties of 60:40 propylene glycol and water mixture were observed without adding any copper oxide nanoparticles. These experimental results were compared to the values given in American Society of Heating Refrigeration and Air Conditioning Engineers (ASHRAE) handbook[5]. Figure 3.2 shows that the experimental values and ASHRAE values are in good agreement (maximum difference $\pm$ 2%) in a temperature range of -35°C to 50°C. Figure 3.3 shows the rheological characteristics of shear stress versus shear rate of propylene glycol/water behavior without nanoparticles. It clearly exhibits Newtonian behavior.

After this confirmation by the benchmark experiment, we carried out rheological experiments of fluids with CuO nanoparticles in different volumetric concentrations and of varying temperatures.

Figure 3.4 shows the viscosity of nanofluids at various concentrations as a function of temperature. Each data point in Figure 3.4 was derived from the slope of a line similar to Figure 3.3, which represents the viscosity according to Equation 4. As the particle concentration in a mixture increases, the fluid viscosity increases exponentially (see Equation 5). The viscosity of these nanofluids increases more rapidly at lower temperatures than at the higher temperatures. This viscosity behavior is similar to results obtained in other types of nanofluids[21, 25]. Figure 3.4 also suggests that the trends of the viscosity curves of all particle loadings are similar with varying temperatures.

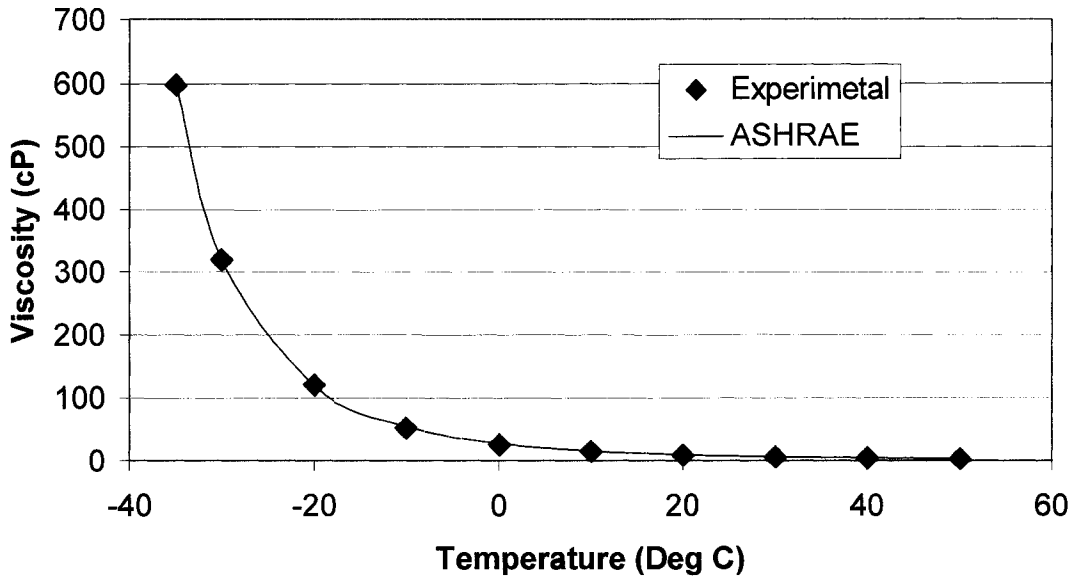

Figure 3.2. Comparison of experimental and ASHRAE viscosity values of 60:40 (by weight) propylene glycol and water mixture.

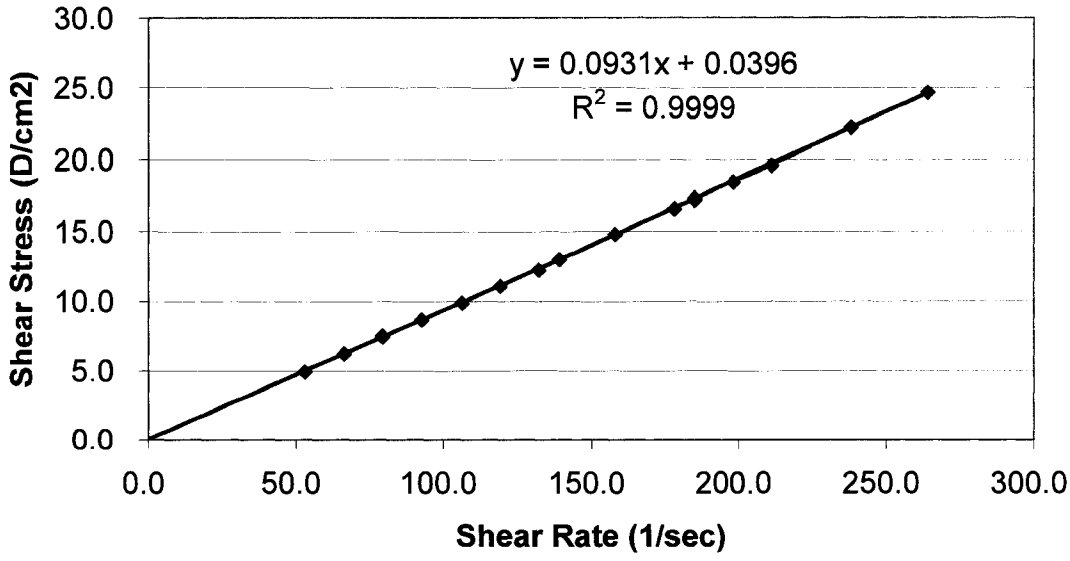

Figure 3.3. Shear stress versus shear rate of 60:40 propylene glycol and water mixture at 20°C.

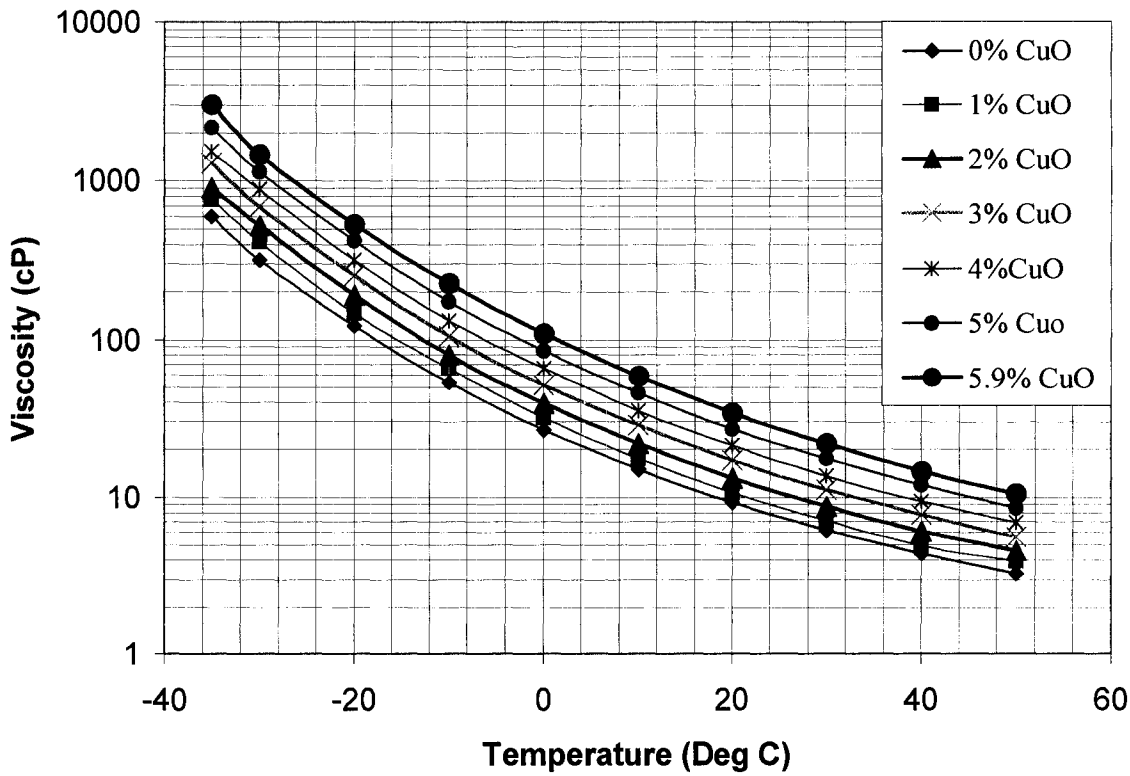

Figure 3.4. Nanofluid viscosity μ_s versus temperature for 60:40 propylene glycol & water mixture with varying volume percent of CuO loading.

Figure 3.5 presents the relative viscosity μ_r versus temperature as a function of volumetric particle loading. The relative viscosity μ_r is defined as the ratio of the viscosity of a nanofluid with suspended particles μ_s to that of the base fluid alone μ_f; Figure 3.5 depicts that as the volume concentration increases, the relative viscosity increases at a specific temperature; it also drops gradually with respect to increasing temperature for a particular concentration. At high volumetric percentage (5.9%), the slope of the relative viscosity μ_r curve is higher at low temperatures. At low volume percentage (1 & 2%) the slope of the μ_r curve is very small.

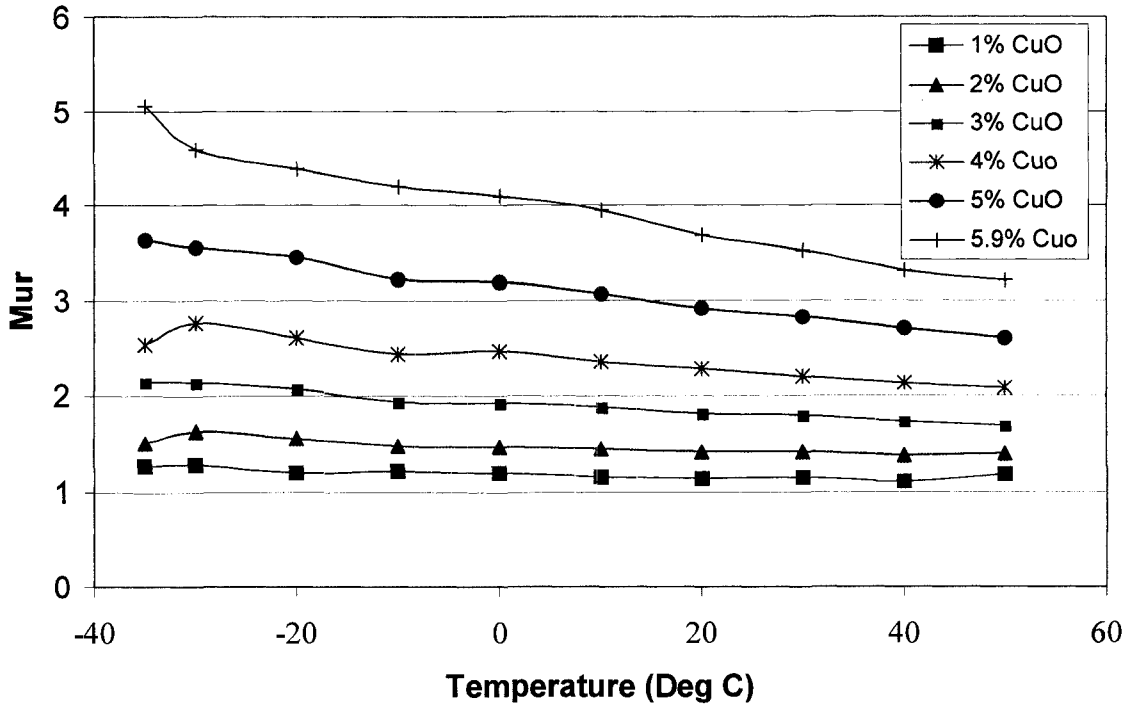

Figure 3.5. Relative viscosity μ_r (Mur) versus temperature for varying concentration of CuO.

Present experimental results were compared to the values obtained from Batchelor's[11] analytical theory and presented in Figure 3.6. These values show a large deviation of experimental data from Batchelor's theory as it appears in Equation (2). Similar deviations were shown by Pak & Cho[28] for TiO_2 and Al_2O_3 nanofluids.

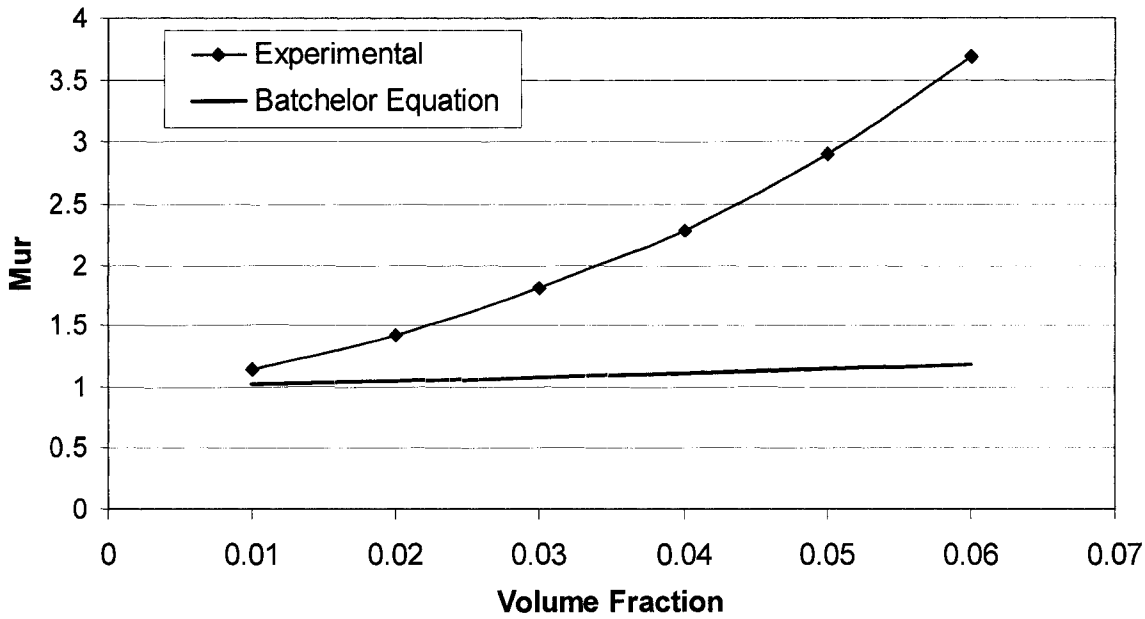

Figure 3.6. Comparison of relative viscosity μ_r (Mur) of 60:40 propylene glycol & water mixture and Batchelor's equation versus volume fraction of CuO nanoparticles at 298 K.

The experimental data points for viscosity as a function of temperature and volume percentage from Figure 4 were curve-fitted with correlation factor $R^2 > 0.99$. The assumed form of correlation for the curve fit is:

$$\mu_s = Ae^{B\phi} \tag{5}$$

where μ_s is the suspension viscosity in m.Pa.s (cP), ϕ is volumetric concentration (ranging from 0-0.06), and A & B are functions of temperature (T) in Kelvin. The curve fit values of A & B appear in Table 3.1.

Table 3.1. Curve fit values of A and B with correlation factor $R^2 > 0.98$.

Temp(K)	238	243	253	263	273	283	293	303	313	323
A	569.3	317.4	117.0	51.5	25.4	14.1	8.76	5.85	4.17	3.21
B	26.9	25.7	25.5	24.27	24.16	23.62	22.55	21.7	20.87	19.68

The factors A & B are correlated as

$$\ln(A) = 736.9e^{-0.0199T} \text{ with } R^2 = 0.99. \quad (6)$$

$$B = 44.794 - 0.0765T \text{ with } R^2 = 0.98. \quad (7)$$

The comparison of experimental values and the values obtained from the proposed correlation (Equations 5,6 & 7) are plotted in Figure 3.7. In these plots, E≡ Experimental values, C ≡ Correlation Values, and the volume percentage is in the parenthesis. These values are within ± 10% excepting a few at very low temperature (-35°C = 238K). The temperature-dependent rheological equation developed by Kulkarni et al.[25] for copper oxide nanoparticles in pure water followed a different correlation. Hence, we further concluded that within the range of volume percentage tested, the temperature-dependent rheological behavior of nanofluids varies with the nature of the base fluids, and therefore the correlation for one particular nanofluid cannot be generalized for all nanofluids at this stage.

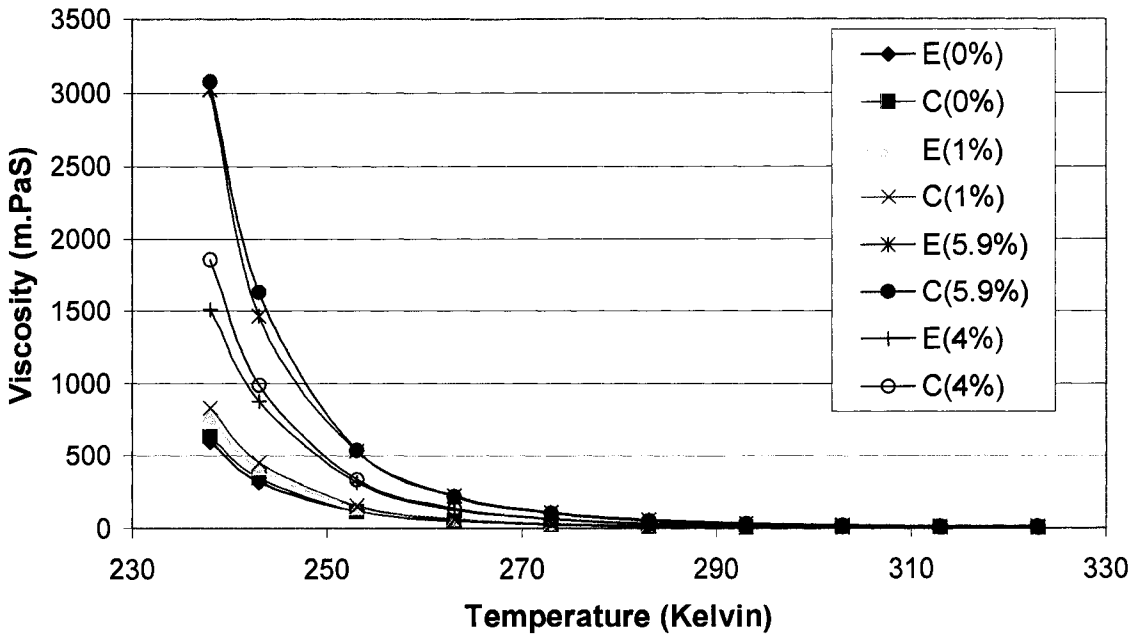

Figure 3.7 Comparison of experimental values 'E' and proposed correlation values 'C' for nanofluid viscosity μ_s with varying volume concentrations of 0,1,4 and 5.9%.

3.4 Conclusions

Viscosity measurement for a 60:40 propylene glycol/water mixture without any nanoparticle suspension shows excellent agreement with the ASHRAE data. The viscosity of a CuO nanofluid in propylene glycol and water solution is an exponential function of volume percentage and temperature. The behavior of this nanofluid up to a volume percentage of 5.9% is Newtonian in nature. The deviation from Batchelor's classical equation is observed to be substantial for nanofluids. Relative viscosity curves display higher slopes at low temperatures. A new correlation has been developed for this type of nanofluid and is presented as Equation 5. The deviation between experimental data and values given by this correlation is within ± 10%.

3.5 Acknowledgement

Financial assistance from the Arctic Region Supercomputing Center and the Dean of the Graduate School at University of Alaska Fairbanks is gratefully acknowledged. Authors are thankful to the Petroleum Development Laboratory for providing the experimental facilities to measure viscosity.

3.6 References

1. L. Qiang. X. Yimin, *Sci. in China (Series E)*, 45: 5, 408 (2002).
2. X. Yimin, L. Qiang, *ASME J. of Heat Transfer*, 125, 151 (2003).
3. J.A. Eastman, S.U.S. Choi, S. Li, W. Yu and L.J. Thompson, *Appl. Phys. Lett.*, 78:6, 718 (2001).
4. F.C., Mcquiston, J. D. Parker, J. D., Spitler, Heating, Ventilating, and Air Conditioning, John Wiley & Sons Inc., New York (2000).
5. ASHRAE Handbook 1985 Fundamentals, American Society of Heating, Refrigerating and Air-Conditioning Engineers Inc., Atlanta (1985).
6. Maiga, S.E., Nguyen, C.T., Galanis, N., Roy, G., *Superlattice Microst*, 35, 543-557 (2004).

7. Y. Xuan and W. Roetzel, *Int. J. of Heat and Mass Transfer*, 43, 3701 (2000).

8. L. Gosselin and A.K. Silva, *Appl. Phys. Lett.*, 85:18, 4160 (2004).

9. T.F. Tadros, Solid/Liquid Dispersions, Harcourt Brace Jovanovich Publishers, Academic Press, New York (1987).

10. A. Einstein, Investigations on the Theory of the Brownian Movement, Dover, New York (1906).

11. G.K., Batchelor, *J. Fluid Mech.*, 83 (1997).

12. F.M.White, Viscous Fluid Flow, McGraw Hill, New York (1991).

13. R.G. Quinn and J. Bauman, Heat transfer characteristics of non-Newtonian suspension, (1954), M.S. Thesis, Newark College of Engineering, Newark, NJ.

14. D. Gullett and E. Curtis, Viscosity of non-Newtonian suspensions, (1955), M.S. Thesis, Newark College of Engineering, Newark, NJ.

15. W.J. Tseng and K.C. Lin, *Mater. Sci. Eng.*, A355, 186 (2003).

16. Y. Yang, E.A. Grulke, Z.G. Zhang and G. Wu, *J. Nanosci. Nanotechnol.* 5, 571 (2005).

17. J. Hilding, E.A. Grulke, Z.G. Zhang and F. Lockwood, *J. Dispersion Sci. and Tech.* 24:1, 1 (2003).

18. W. Tseng and C.H. Wu, *Acta Materialia*, 50, 3757 (2002).

19. S. Savarmand, P.J. Carreau, F. Betrand, D.J. Vidal and M. Moan, *J. Rheology* 47:5, 1133 (2003).

20. W. Tseng and C.L. Lin, *Mater. Chem. and Phys.* 80, 232 (2003).

21. W. Tseng and C.N. Chen, *Mater. Sci. Eng.*, A347, 145 (2003).

22. W. Tseng and C.N. Chen, *J. of Mater. Sci. Lett.* 21, 419 (2002).

23. K. Kwak, C. Kim, *Korea-Australia Rheology J.*, 17:2, 35 (2005).

24. U. Teipel, U. Forter-Barth, *Propellants, Explosives, Pyrotechnics*, 26, 268-272 (2001).

25. D.P. Kulkarni, D.K., Das, G. A. Chukwu, *J. Nanosci. and Nanotechnol.*, 6, 1150 (2006).

26. Nanophase Technologies, Romeoville, IL, USA. http://www.nanophase.com

27. Brookfield DV-II+ Programmable Viscometer Manual No. M/97-164-D1000, Brookfield Engineering Laboratories Inc, MA, USA.
28. B.C. Pak, Y.L. Cho, *Exp Heat Transfer*, 11, 151, (1998).

CHAPTER FOUR

Effect of Thermophysical Properties on the Prandtl Number of Nanofluids

Devdatta P. Kulkarni, Praveen K. Namburu, Dr. Debendra K. Das*
University of Alaska Fairbanks
P.O. Box 755905, Fairbanks, AK, 99775-5905, USA.

Abstract

The Prandtl number, *Pr* is a function of the thermophysical properties of nanofluids, and it strongly influences the convective heat transfer coefficient of nanofluids. Therefore, an analysis has been undertaken to evaluate the effects of variation of density, specific heat, thermal conductivity and viscosity of nanofluids as a function of nanoparticle volume concentration and temperature. Three nanofluids SiO_2, Al_2O_3 and CuO in an ethylene glycol and water mixture have been considered for their application at subzero temperatures in cold regions. Results conclude that viscosity variation plays a dominant role because it is a strong function of temperature. For example, *Pr* increases nearly 8 times when nanofluid operating in a heat transfer device goes from 0°C to -35°C in an ethylene glycol and water (60:40 by weight) mixture. As volume concentration of nanoparticles increases, the Prandtl number dramatically increases. As an example, adding 6% volume concentration of CuO increases *Pr* by 123%, thus increasing the heat transfer coefficient *h* by 38%. For a given nanofluid at a given volume concentration the *Pr* increases as the particle size decreases.

Under Review, Material Science and Engineering, February 2007

Key Words:
Prandtl Number, Thermophysical Properties, Nanofluids

* Corresponding Author: ffdkd@uaf.edu, Ph. 907-474-6094.

4.1 Introduction

Nanofluids are created by dispersing nanometer-sized particles (<100 nm) in a base fluid such as water, ethylene glycol or propylene glycol. Using high thermal conductivity metallic nanoparticles (e.g., copper, aluminum, silver, silicon) increases the thermal conductivity of such mixtures, thus enhancing their overall energy transport capability [1]. Eastman et al. [2] showed an increase of 40% in thermal conductivity with 0.3% (vol.) of copper nanoparticles in ethylene glycol. Recently, Prasher et al. [3] demonstrated that this increase in thermal conductivity of nanofluids is primarily from the convection caused by the Brownian movement of nanoparticles. Various applicatory benefits of nanofluids include: improved heat transfer, minimal clogging, microchannel cooling and miniaturization of systems, savings in energy and reduced pumping power [4]. These results indicate that nanofluids are good candidates for future generation coolants.

Not much investigation has appeared in literature discussing how changing thermophysical properties affect heat transfer coefficients of nanofluids. In this paper, we present a comprehensive analysis on how changing nanofluids' properties, such as concentration and particle size, affect the Prandtl number and subsequently, the heat transfer coefficient, h.

4.2 Theory

The heat transfer coefficient of any fluid is directly proportional to the Nusselt number. A generalized correlation for Nusselt number, *Nu* for nanofluids is given as [1]:

$$Nu = f(\mathrm{Re}, \mathrm{Pr}) \tag{1}$$

where *Re* is the Reynolds number and *Pr* is the Prandtl number.

Li and Xuan [5] present two equations for Nusselt number of copper-water nanofluids by adding the Peclet number influence of particles, Pe_d.

$$Nu_{nf} = 0.4328(1.0 + 11.285\phi^{0.754} Pe_d^{0.218})\,\mathrm{Re}_{nf}^{0.333}\,\mathrm{Pr}_{nf}^{0.4} \quad \text{(For laminar flow)} \tag{2}$$

$$Nu_{nf} = 0.0059(1.0 + 7.6286\phi^{0.6886} Pe_d^{0.001})\,\mathrm{Re}_{nf}^{0.9238}\,\mathrm{Pr}_{nf}^{0.4} \text{ (For turbulent flow)} \tag{3}$$

where $Pe_d = \dfrac{u_m d_p}{\alpha_{nf}}$; $\mathrm{Re}_{nf} = \dfrac{u_m d}{\nu_{nf}}$; $\mathrm{Pr}_{nf} = \dfrac{\nu_{nf}}{\alpha_{nf}}$; $\alpha_{nf} = k_{nf}/(\rho_{nf}.C_{pnf})$

Heat transfer coefficient is given by $h_{nf} = (Nu_{nf} k_{nf})/d$. (4)

The Prandtl number for any fluid is given by:

$$\mathrm{Pr} = \frac{\mu C_p}{k}. \tag{5}$$

Previous research by Xuan and Li [6] on copper-oxide nanoparticles in water has revealed that a 60% increase in the thermal conductivity can be achieved at a particle concentration of only 5% by volume. The effective thermal conductivity equation for a nanofluid presented by Xuan and Li:

$$k_{nf} = k_f\left[\frac{k_p + (n-1)k_f - (n-1)\phi(k_f - k_p)}{k_p + (n-1)k_f + \phi(k_f - k_p)}\right] \tag{6}$$

where n is a function of shape; for spherical particles n is 3.

Pak and Cho [7] list the following correlations for various properties of nanofluids. The effective density of nanofluids is given by:

$$\rho_{nf} = (1-\phi)\rho_f + \phi\rho_p \tag{7}$$

where the volumetric concentration is given by:

$$\phi = \frac{1}{(100/\phi_m)(\rho_p/\rho_f)+1}(100\%)\text{; where } \phi_m \text{ is mass fraction.} \tag{8}$$

The effective specific heat of nanofluids is given by [7]:

$$C_{pnf} = (1-\phi)C_{pf} + \phi C_{ps}. \tag{9}$$

However, according to Buongiorno [8], the specific heat of a nanofluid should be calculated assuming the nanoparticles and base fluid is in thermal equilibrium. He presented the equation as:

$$C_{pnf} = \frac{\phi\rho_s C_{ps} + (1-\phi)\rho_f C_{pf}}{\rho_{nf}}. \tag{10}$$

For our investigation of the Prandtl number of nanofluids in the present paper, the correlation given by Buongiorno for specific heat of nanofluids is used.

The relative viscosity of nanofluids is given by Pak and Cho[7]

$$\mu_r = \frac{\mu_{nf}}{\mu_f} = 1 + 2.5\phi + 6.2\phi^2. \tag{11}$$

The viscosity increases by 100 times for γ-Al_2O_3 nanofluids with a particle volume of 10 % in water as shown by Pak and Cho. However, this equation does not reflect the temperature dependence of viscosity. The experiments conducted on rheological properties of copper-oxide nanofluids by Kulkarni et al. [9] yields the following equation, which includes both the temperature and concentration dependence.

$$\ln \mu_{nf} = A\left(\frac{1}{T}\right) - B \tag{12}$$

A and B are polynomials, which are functions of volumetric concentrationsϕ. These factors are given as

$$A = 20587\phi^2 + 15857\phi + 1078.3 \text{ with } R^2 = 0.99$$

$$B = -107.12\phi^2 + 53.548\phi + 2.8715 \text{ with } R^2 = 0.97$$

where ϕ is the volume fraction ranging from 0.05 to 0.15.

4.3 Effects of Different Properties

In cold regions like Alaska, Canada and the circumpolar north, the heat transfer fluid most commonly used is ethylene glycol and water mixture. Therefore, our study is focused on this as the base fluid.

4.3.1 Density

By considering various metallic nanoparticles in a base fluid (ethylene glycol/water mixture 60:40), we were able to investigate the resultant effect on density. Using equation (7), densities of various nanofluids have been plotted as shown in Figure 4.1. By increasing the nanoparticle concentration in a base fluid, the effective density of the nanofluid increases, due to higher density of particles. CuO nanofluid has higher density than Al_2O_3 and SiO_2 because of the higher density of the CuO nanoparticles. As typical numbers, by addition of 10% SiO_2 nanoparticles, density of the nanofluid increases by 10.9%; by addition of 10% Al_2O_3 nanoparticles, density the of nanofluid increases by 24% and by addition of 6% CuO nanoparticles, density the of nanofluid increases by 30.8% in comparison to the base fluid.

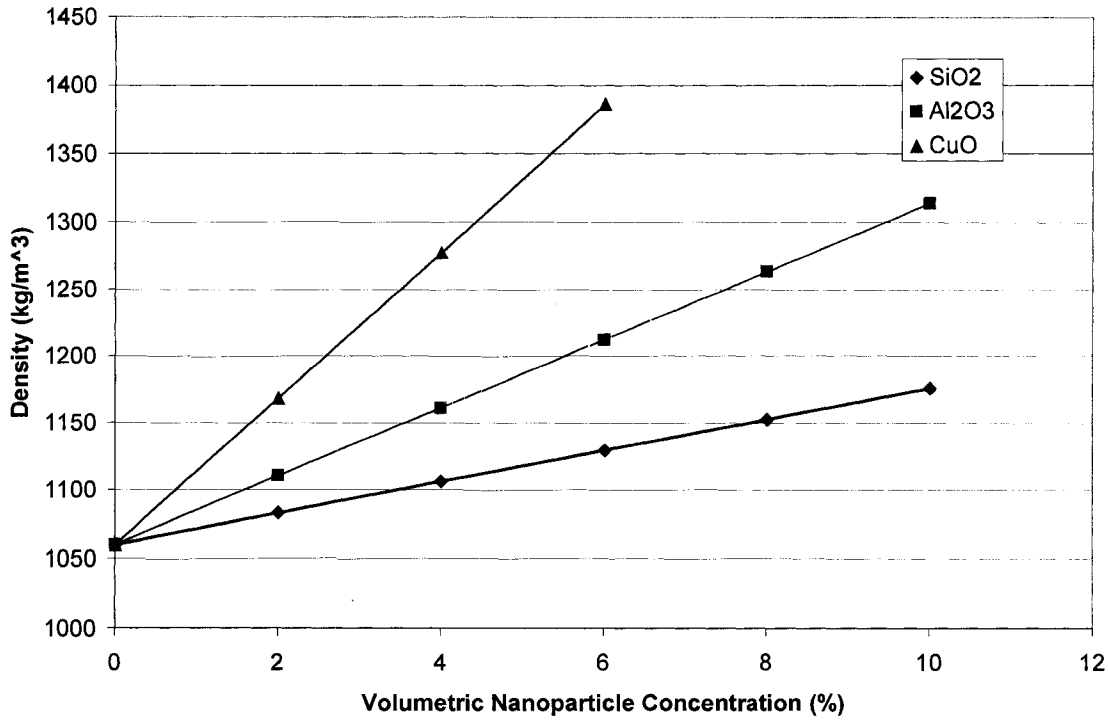

Figure 4.1. Effect of addition of various metallic nanoparticles on the density of nanofluid.

4.3.2 Thermal conductivity

From equation (6), the effective thermal conductivity of various nanofluids is computed for spherical particles and plotted as shown in Fig 4.2. As the nanoparticle concentration increases, thermal conductivity of fluid increases due to higher thermal conductivity of metallic particles. As typical numbers, by addition of 10% SiO_2 nanoparticles, thermal conductivity of the nanofluid increases by 32.7%; by addition of 10% Al_2O_3 nanoparticles, thermal conductivity of the nanofluid increases by 33% and by addition of 6% CuO nanoparticles, thermal conductivity of the nanofluid increases by 19.1%. Interestingly, adding any metallic particles i.e. SiO_2, Al_2O_3 or CuO, results in a very similar increase in thermal conductivity of the nanofluid. For example, with 6% SiO_2 the increase in conductivity is 18.8%, with 6% Al_2O_3 19.04% and with 6% CuO,

19.1%. Hence from the point of view just thermal conductivity enhancement, it is not important to add higher thermal conductivity particles. This invariant behavior of thermal conductivity with different materials requires further experimental investigation. The inconclusive results for this problem have been elaborately discussed by Bahrami et al. [10].

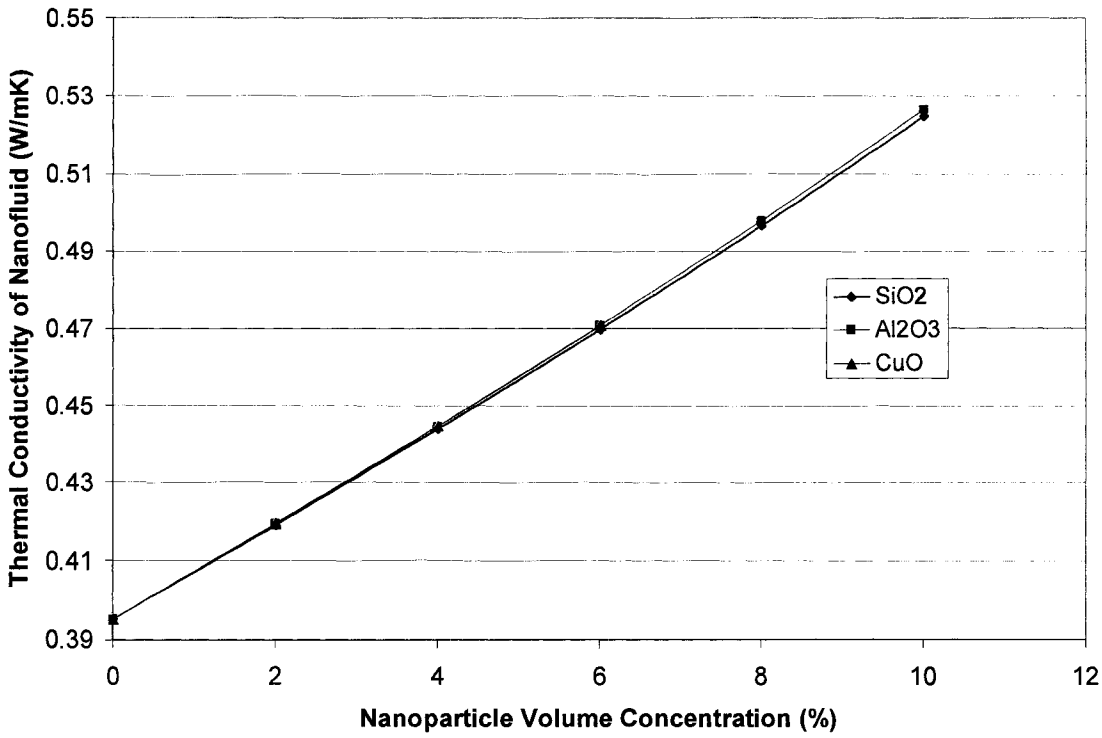

Figure 4.2. Effect on thermal conductivity of nanofluids by addition of metallic nanoparticles.

4.3.3 Specific heat

Using the correlation between particle concentration and temperature for specific heat of nanofluids (Equation 10) given by Buongiorno [8], the specific heats of SiO_2, Al_2O_3 and CuO nanofluids have been determined and plotted as shown in Fig. 4.3. It is clear from the plot that, as the concentration of metallic nanoparticles in base fluid increases, the effective specific heat of nanofluid decreases. This is mainly due to the

lower specific heat of metals compared to liquids. As typical numbers, by adding 10% SiO_2 nanoparticles, the nanofluid specific heat decreases by 14.4%; by adding 10% Al_2O_3 nanoparticles, the nanofluid specific heat decreases by 19.6 % and by adding 6% CuO nanoparticles, the nanofluid specific heat decreases by 24.7 % in comparison to the base fluid.

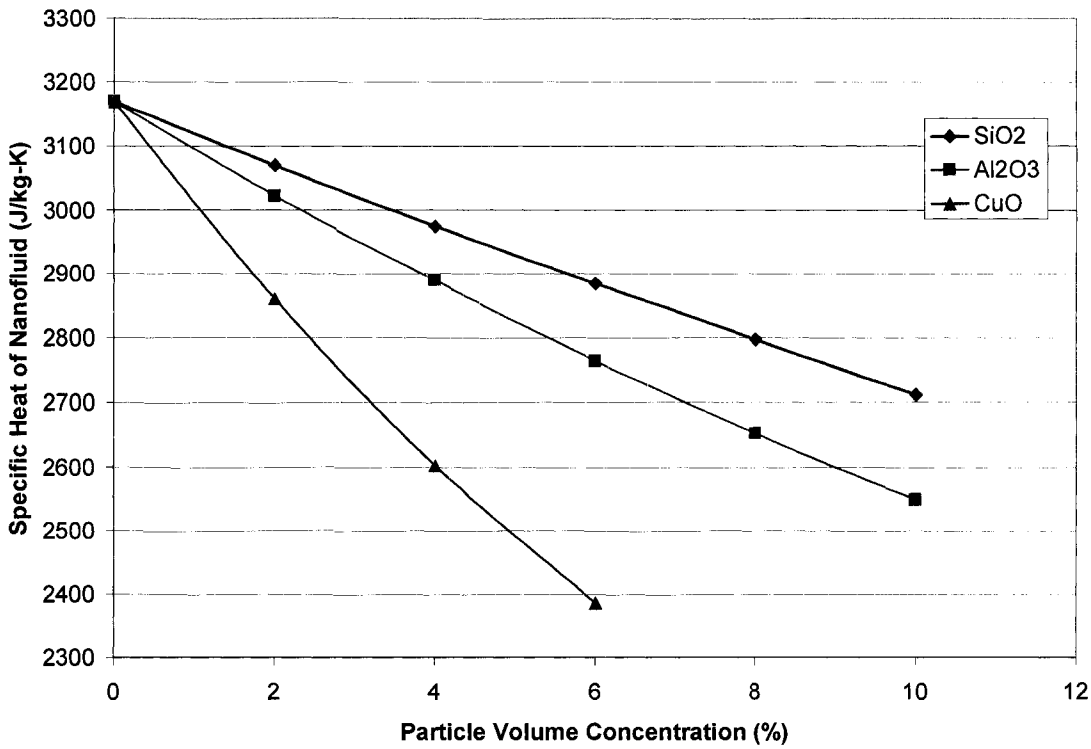

Figure 4.3. Specific heat of various nanofluids at different concentrations of metallic nanoparticles.

4.3.4 Viscosity

The viscosity values of SiO_2, Al_2O_3, CuO nanoparticles suspended in an ethylene glycol-water mixture were measured experimentally. The experimental set up consisted of an LV DV-II+ Brookfield programmable viscometer and a Julabo temperature control bath with a computer to control temperature. Temperature dependency of viscosity values was also determined. Viscosity measurements were started at 50°C and temperature was

gradually reduced to -30°C in 10°C intervals, with the last reading taken at -35°C. Because the base fluid freezes at about -45°C, the experiments were continued down to a minimum temperature of -35°C. As a typical example, Figure 4.4 illustrates the viscosity variation with temperature at different concentrations of CuO nanoparticles. Similarly, viscosity values were measured in similar fashion for SiO_2 and Al_2O_3. The equation for viscosity variation of nanofluids has already been presented in Equation (12).

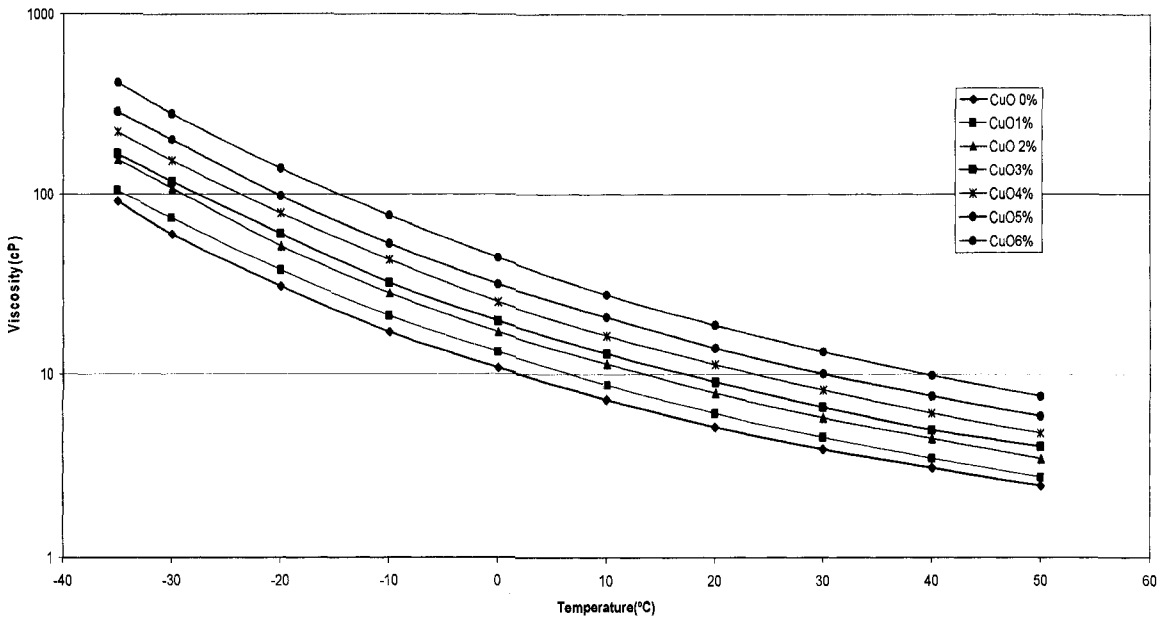

Figure 4.4. Experimental values of viscosity at varying volume concentrations of CuO nanoparticles with respect to temperature.

4.3.5 Effect on the Prandtl number

After investigating all thermophysical properties for SiO_2, Al_2O_3 and CuO nanoparticle suspensions in an ethylene glycol and water mixture, the Prandtl number was determined for each nanofluid. Since Prandtl numbers are functions of temperature, we have presented a first case at room temperature of 20° C. Figure 4.5 shows how adding various metallic particles affect the nanofluid Prandtl number. As the volume

concentration of particle increases, the Prandtl number increases more rapidly for CuO. For Example, by adding 10% SiO_2 nanoparticles, the nanofluid Prandtl number increases by 20.2%; by adding 10% Al_2O_3 nanoparticles, the Prandtl number increases by 88% and by adding 6% CuO nanoparticles, the Prandtl number increases by 123.5%. As Nusselt number (and heat transfer coefficient, h) is proportional to $(Pr)^{0.4}$, for 6% CuO nanofluid, a 123.5% increase in Pr results in an increase of 38% in convective heat transfer coefficient, h.

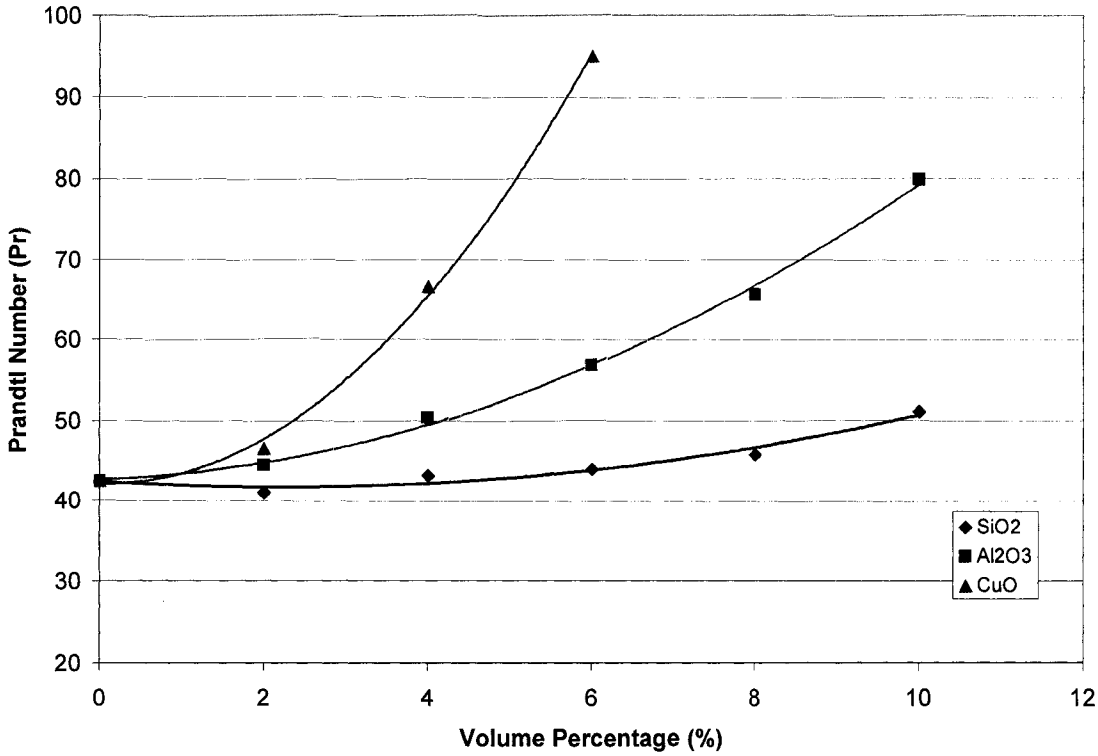

Figure 4.5. Effect of addition of metallic nanoparticles on Prandtl number of various nanofluids.

4.3.6 Particle size effect

Furthermore, in this study particle diameter's affect on the nanofluid Prandtl number has been investigated. Until now, very limited study has been reported for thermophysical properties of nanofluids with respect to particle size. We have measured

the viscosity of SiO_2 nanofluid in ethylene glycol and water mixture with varying particle diameter (i.e. 20 nm, 50 nm and 100 nm). All other properties are assumed to be constant with varying diameter. Figure 4.6 displays the effect of particle diameter on the Prandtl number. It is observed that the smaller the diameter, the higher the Prandtl number. This is mainly attributed to higher viscosity at smaller diameters. As the particle diameter decreases (for the same volume concentration), the total surface area of particles increases; giving rise to more drag and simultaneously more viscosity [11].

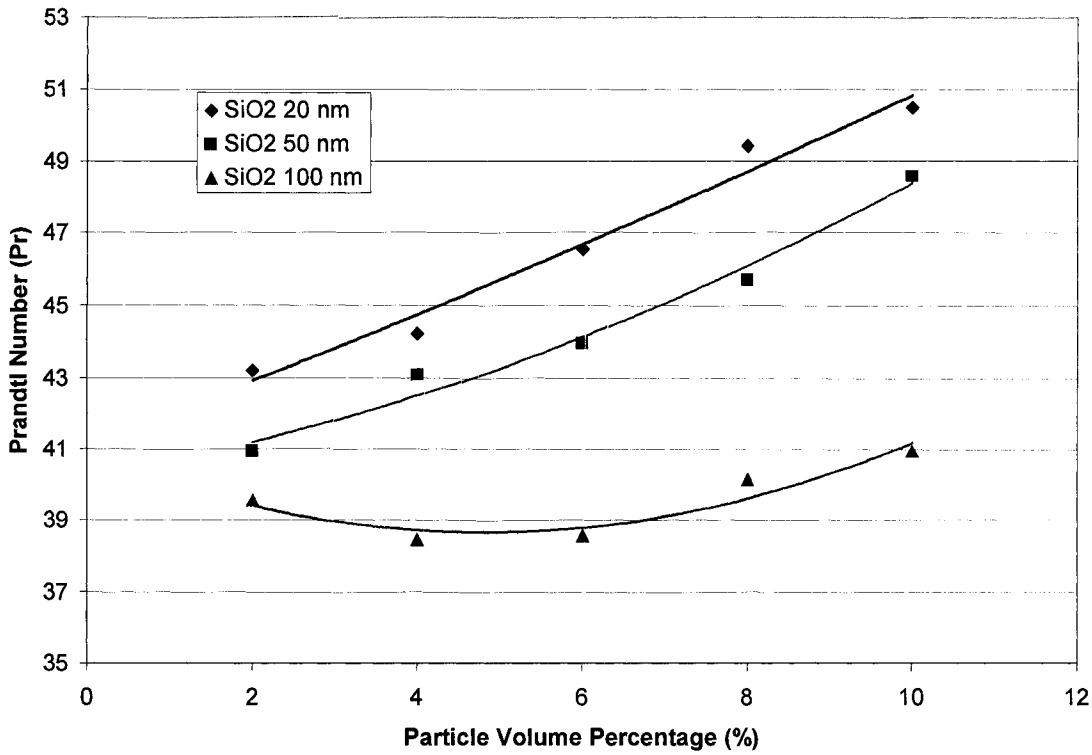

Figure 4.6. Effect of particle diameter on Prandtl number of various nanofluids.

4.3.7 Temperature dependence of the Prandtl number

Studying how varying temperature affects the Prandtl number for various nanofluids was also investigated. In literature, practically no data are available for temperature dependent thermophysical properties of nanofluids. However, it is well

known that viscosity varies more than other properties vary with varying temperatures. Therefore, ρ, C_P and k are taken as constant. We measured the viscosity of SiO_2, Al_2O_3 and CuO nanofluids with temperature variation from -35°C to 50°C and with varying concentration. At lower temperatures, the viscosity value increases exponentially. The increase in viscosity accompanies an increase in Prandtl number. Figure 4.7 illustrates the exponential increase in Prandtl number at sub zero temperatures for 50 nm SiO_2 nanofluids. Similar trends have been obtained from our experiment with Al_2O_3 and CuO nanofluids.

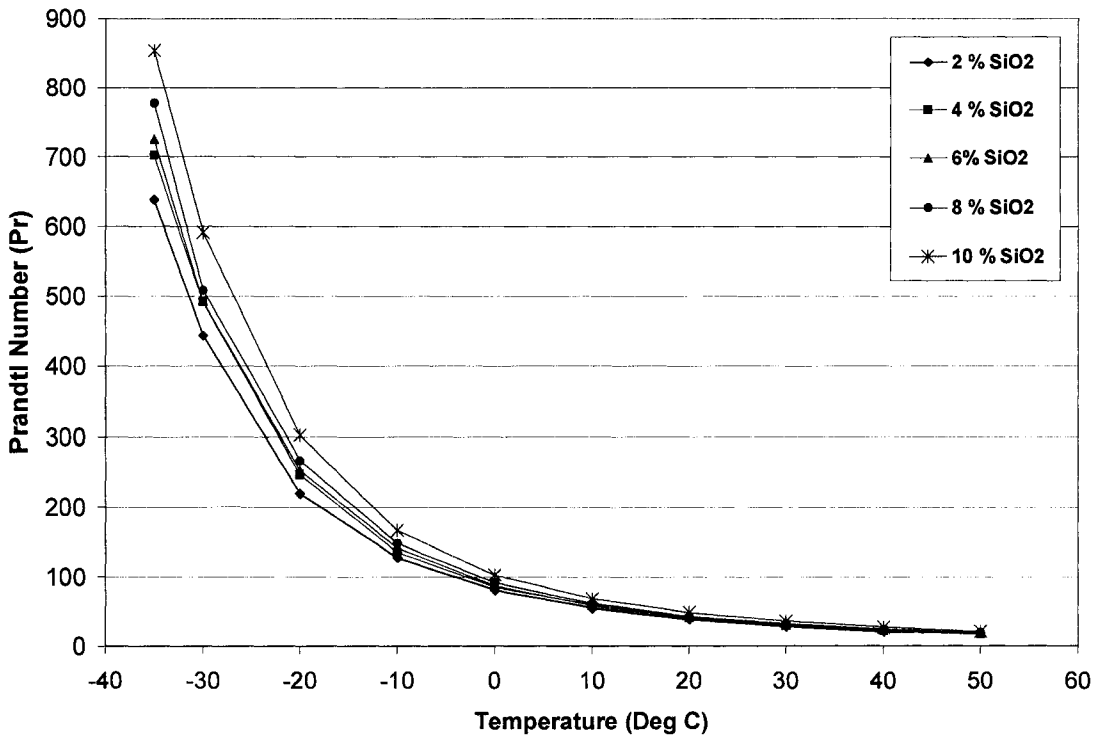

Figure 4.7. Effect of varying temperature on Prandtl number for 50 nm SiO_2 nanofluid.

4.4. Nanofluids Versus Conventional Fluids

For the same velocity in a pipe, an increase in viscosity will decrease the Reynolds number for nanofluids. The density will increase and specific heat will decrease for nanofluids. However it is not in the same proportion as the increase in viscosity. The

Prandtl number increases substantially for the nanofluids, and it overcomes the reduction in the Reynolds number. Hence, the Nusselt number increases as the Prandtl number increases. Heat transfer coefficient is a product of Nusselt number and thermal conductivity. So as the Prandtl number and thermal conductivity increase, the heat transfer coefficient increases. Therefore, the Prandtl number, Pr and thermal conductivity k_{nf} are the key factors in increasing the heat transfer coefficient, h in nanofluids.

4.5 Conclusions

From this study the following conclusions are drawn:

1. Nanofluid density increases as volume concentration increases. It increases rapidly for higher density particles.
2. Effective thermal conductivity of nanofluid is enhanced by adding metallic nanoparticles. The presented correlation shows that, regardless of which metallic nanoparticles were added, enhancement in thermal conductivity is practically the same. This topic needs more experimental studies.
3. Adding nanoparticles to a base fluid reduces the specific heat of the nanofluid. This is because of lower specific heat of metals compared to fluids.
4. Viscosity is a strong function of volume concentration, temperature and particle diameter of nanoparticles. As concentration increases, viscosity increases. As the diameter of nanoparticles decreases, the viscosity of the nanofluid increases. Also, as temperature decreases, viscosity of nanofluids increases exponentially.
5. Prandtl number increases rapidly as particle volume concentration increases. Among the three fluids analyzed, it is highest for copper oxide nanofluids and lowest for silicon dioxide nanofluids.
6. The Prandtl number also changes with particle diameter. The smaller the diameter, the higher is the Prandtl number.

7. The Prandtl number increases exponentially as the nanofluid is cooled below sub zero temperatures.

4.6 Nomenclature

C_p	Specific heat, J/kg K
d	Inner diameter of the tube, m
d_p	Particle diameter, m
h	Convective heat transfer coefficient, W/m^2 K
k	Thermal conductivity, W/m K
Nu	Nusselt number
Pe_d	Peclet number for particle
Pr	Prandtl number
Re	Reynolds number
u_m	Mean velocity, m/s
Greek Letters:	
α	Thermal diffusivity
μ	Coefficient of dynamic viscosity of the fluid, kg/m s
ν	Kinematic viscosity of fluid
ϕ	Particle volume concentration
ρ	Density of the fluid, kg/m^3
Subscripts	
f	Fluid
nf	Nanofluid
p	Particle /Solid

4.7 References

1. Xuan, Y. and Li, Q., Investigation on Convective Heat Transfer and Flow Features of Nanofluids, *ASME Journal of Heat Transfer*, vol. 125, pp. 151-155, 2003.

2. Eastman, J.A., Choi, S.U.S., Li, S., Yu, W. and Thompson, L.J., Anomalously Increased Effective Thermal Conductivities of Ethylene Glycol-based Nanofluids Containing Copper Nanoparticles, *Applied Physics Letters*, vol. 78, no. 6, pp. 718-720, 2001.

3. Prasher, R., Bhattacharya, P. and Phelan, P.E., Thermal Conductivity of Nanoscale Colloidal Solutions (Nanofluids), *Physical Review Letters*, PRL 94, 025901, 2005.

4. Choi, S.U.S., Zhang, Z.G. and Keblinski, P., Nanofluids, *Encyclopedia of Nanoscience and Nanotechnology*, vol. 6, pp. 757-773, 2004.

5. Li, Q., Xuan, Y., Convective Heat Transfer and Flow Characteristics of Cu-water Nanofluid, Science in China (Series E), Vol. 45, No. 4, 2002, pp. 408-416.

5. Xuan, Y., Li, Q., Heat Transfer Enhancement of Nanofluids., International Journal of Heat and Fluid Flow. Vol 21., 2000, pp. 58-64.

7. Pak, B. C., Cho, Y.I., Hydrodynamic and Heat Transfer Study of Dispersed Fluids with Submicron Particles., Experimental Heat Transfer. Vol. 11, 1998, pp. 151-170.

8. Buongiorno, J., Convective Transport in Nanofluids, ASME Journal of Heat Transfer, Vol. 128, p. 240-250, 2006.

9. Kulkarni, D.P., Das, D.K., Chukwu, G.A., Temperature Dependent Rheological Property of Copper Oxide Nanoparticles Suspension (Nanofluid), Journal of Nanoscience and Nanotechnolgy, Vol. 6, 2006, pp 1150-1154.

10. Bahrami, M., Yovanovich. M.M., Culham, J.R., Assessment of Relevant Physical Phenomenon Controlling Thermal Performance of Nanofluids, Proceedings of IMECE 2006-13417, ASME International Mechanical Engineering Congress, Chicago, IL, USA.

11. Cheremisinoff, N.P., Encyclopedia of Fluid Mechanics, Vol. 7, Rheology and Non-Newtonian Flows, Gulf publishing Company, Houston, 1988.

CHAPTER FIVE

Comparison of Heat Transfer Rates of Different Nanofluids on the Basis of the Mouromtseff Number

Devdatta P. Kulkarni, Praveen K. Namburu, Dr. Debendra K. Das*
University of Alaska Fairbanks
P.O. Box 755905, Fairbanks, AK, 99775-5905, USA.

Abstract

This paper presents the comparison of heat transfer rates for copper oxide (CuO) nanofluids based on Mouromtseff number. The Mouromtseff number is a Figure of Merit (FOM) for heat transfer fluids. A higher value of FOM for a fluid indicates better heat transfer characteristics. The Mouromtseff number was determined considering the thermophysical properties of CuO nanofluids, which in turn are functions of volume concentration of nanoparticles. Investigation revealed that for internal laminar flow, the FOM of water-based copper oxide nanofluids was much superior to that of pure water. For the same nanofluid, the optimal volume percentage appeared to be 5% in internal turbulent flows. Ethylene glycol based nanofluids had better FOM than propylene glycol based nanofluids.

Accepted for Publication, Electronics Cooling, December 2006, * Corresponding Author: ffdkd@uaf.edu, Ph. 907-474-6094.

5.1 Introduction

Nanofluids are the dispersion of nanometer-sized particles in a base fluid such as water, ethylene glycol or propylene glycol. In the last decade, nanofluids have attracted increasing attention as a new generation of coolant for various industrial and automotive applications. Use of high thermal conductivity metallic nanoparticles (e.g., copper, aluminum, silver, gold, etc.) effectively increases the thermal conductivity of such mixtures, thus enhancing their overall energy transport capability [1,2]. Eastman et al. [3] showed a 40% increase in thermal conductivity with 0.3 volume percent of copper nanoparticles in ethylene glycol.

Electronic designs for application in innovative products that use higher power levels in miniature systems are rapidly developing. This phenomenon has led to dramatic increase in chip densities and power densities, as well as a continuous decrease in physical dimensions of electronic packages. Hence, thermal management continues to be one of the most critical areas in electronic product development. Similarly, advances in thermal management will significantly impact the cost, overall design, reliability and performance of the next generation of weapons technology, which heavily uses microelectronic devices. In electronic cooling, as Azar [4] forecasted heat flux of 1000 W/cm^2 would become a reality in the foreseeable future. Therefore, air may become impractical as a coolant; hence innovative liquid cooling ideas are receiving more attention.

In the world's cold regions, such as Alaska, nanofluids may be very effective in such roles as household baseboard heating fluids and as coolants for automobiles and industries. Normally in these regions a 60:40 ethylene glycol/water or a propylene glycol/water solution are common choices due to their low freezing points. Therefore, for our analysis we investigated these fluids.

Simons [5] presented the effectiveness of various liquid coolants using the Mouromtseff number. The Mouromtseff number [6] is a Figure of Merit (FOM) for heat transfer fluids. The approach of Simons was further extended by Ellsworth [7]. A higher value of FOM for a fluid indicates better heat transfer characteristics. In electronic cooling, nanofluid flow through microchannels shows promise in removing high-density heat flux. In the present article we have extended the analysis of Simons to different nanofluids, which hold promise as next generation liquid coolants.

The Mouromtseff number is given by:

$$Mo = \frac{k^a \rho^b c_p{}^d}{\mu^e} \tag{1}$$

where k, ρ, c_p and μ are thermal conductivity, density, specific heat and dynamic viscosity of the fluid, respectively. The exponents a, b, d, and e take on values appropriate to the heat transfer mode of interest and the corresponding heat transfer correlation. For a specific nanofluid, these thermo-physical properties depend on the nanoparticle material, base fluid and the nanoparticle volumetric concentration. Simons [5] showed the comparison of heat transfer rates for various typically used coolants with respect to water.

The thermal conductivity of a nanofluid is given by [3]:

$$k_{nf} = k_f \left[\frac{k_p + (n-1)k_f - (n-1)\phi(k_f - k_p)}{k_p + (n-1)k_f + \phi(k_f - k_p)}\right] \tag{2}$$

where k_{nf} is the nanofluid thermal conductivity; k_f, base fluid thermal conductivity; k_p, bulk solid particle thermal conductivity; ϕ, particle volume fraction; and n is an empirical scaling factor that takes into account how different particle shapes affect thermal conductivity. We used spherical nanoparticles in our experiments for which n =3.

The effective density of nanofluids is given by [8],

$$\rho_{nf} = (1-\phi)\rho_f + \phi\rho_s \tag{3}$$

where ρ_{nf} is the nanofluid density and ρ_s & ρ_f are the densities of the solid particles and base fluid, respectively.

The specific heat of nanofluids C_{pnf} can be calculated using the standard equation based on the volume fraction [9], since no other correlation is currently available in the literature.

$$C_{pnf} = \phi C_{ps} + (1-\phi)C_{pf} \tag{4}$$

where C_{ps} is the specific heat of solid particles and C_{pf} is the specific heat of the base fluid.

Various researchers have measured viscosities of several nanofluids. Kulkarni et al. [10] presented a correlation for the temperature dependency of viscosity for copper oxide nanoparticles in water using a Brookfield Viscometer at different volume concentrations. The correlation is:

$$\ln \mu_s = A(\frac{1}{T}) - B \tag{5}$$

where μ_s is the suspension viscosity in m.Pa.s (cP), T is the temperature in Kelvin, A & B are polynomials which are functions of volumetric concentrations ϕ. These factors are given as

$$A = 20587\phi^2 + 15857\phi + 1078.3 \text{ with } R^2 = 0.99$$

$$B = -107.12\phi^2 + 53.548\phi + 2.8715 \text{ with } R^2 = 0.97$$

where ϕ is the volume fraction ranging from 0.05 to 0.15.

Researchers should note that each nanofluid exhibits different rheological properties; therefore different viscosity correlations for ethylene glycol / water and propylene glycol / water with CuO nanoparticles have been developed.

Qiang and Yimin [1] investigated the correlation for Nusselt number for copper-water nanofluid. From experimental data reduction, the Nusselt number for laminar and turbulent flow is given by

$$Nu_{nf} = 0.4328(1.0 + 11.285\phi^{0.754} Pe_d^{0.218}) \mathrm{Re}_{nf}^{0.333} \mathrm{Pr}_{nf}^{0.4} \quad \text{(laminar flow; Re} \le 2300) \qquad (6)$$

$$Nu_{nf} = 0.0059(1.0 + 7.6286\phi^{0.6886} Pe_d^{0.001}) \mathrm{Re}_{nf}^{0.9238} \mathrm{Pr}_{nf}^{0.4} \quad \text{(turbulent flow; } 2300 < \mathrm{Re} \le 25{,}000) \qquad (7)$$

where Peclet number: $Pe_d = \frac{u_m d_p}{\alpha_{nf}}$; Reynolds number: $\mathrm{Re}_{nf} = \frac{u_m d}{\nu_{nf}}$;

Prandtl number: $\mathrm{Pr}_{nf} = \frac{\nu_{nf}}{\alpha_{nf}}$; thermal diffusivity: $\alpha_{nf} = k_{nf} / (\rho_{nf} C_{pnf})$

u_m is the mean velocity; d_p is average particle diameter (d_p < 100nm); α_{nf} is nanofluid diffusivity; and ν_{nf} is nanofluid kinematic viscosity.

The Mouromtseff numbers derived from equations (6) & (7) for fully developed internal laminar and turbulent flow at a specific velocity of 1 m/s are given as:

$$Mo = [1 + (11.285\phi^{0.754} (\frac{d_p}{\alpha_{nf}})^{0.218})] \frac{\rho_{nf}^{0.333} C_{pnf}^{0.4} k_{nf}^{0.6}}{\mu_{nf}^{-0.07}} \quad \text{(laminar flow; Re} \le 2300) \qquad (8)$$

$$Mo = [1 + (7.6286\phi^{0.6886} (\frac{d_p}{\alpha_{nf}})^{0.001})] \frac{\rho_{nf}^{0.9238} C_{pnf}^{0.4} k_{nf}^{0.6}}{\mu_{nf}^{0.5238}} \quad \text{(turbulent flow; } 2300 < \mathrm{Re} \le 25{,}000) \qquad (9)$$

5.2 Results and Discussion

The following results (Figures 5.1 through 5.3) are based on an average particle diameter of 50 nm and a mean velocity of 1 m/s. Further analyses for velocities of 5 m/s and 10 m/s and a particle diameter of 100 nm indicate that similar trends are preserved for all nanofluids. The properties of various nanofluids used for further analysis are given in Table 5.1.

Table 5.1. Properties of various nanofluids with varying concentrations

Fluid	Density kg/m3	Specific Heat J/kg.K	Thermal Conductivity W/m.K	Viscosity mPa.s
[redacted]	997.8	4183.2	0.602	0.96
	1394.8	3993.3	0.694	3.12
	1632.8	3879.3	0.756	6.37
	1791.5	3803.4	0.799	12.30
	2029.6	3689.4	0.868	35.40
	2188.3	3613.5	0.916	104.01
	1066.2	3094.0	0.390	5.20
	1144.9	3066.9	0.401	6.15
	1223.5	3039.8	0.413	6.83
	1302.2	3012.7	0.426	9.08
	1380.9	2985.6	0.438	11.38
	1459.5	2958.6	0.451	14.00
	1538.2	2931.5	0.464	18.75
	1021.7	3161.9	0.300	9.31
	1100.8	3134.1	0.309	10.66
	1179.9	3106.3	0.318	13.27
	1259.0	3078.6	0.328	16.93
	1338.1	3050.8	0.337	21.26
	1417.2	3023.0	0.347	27.11
	1496.3	2995.3	0.357	34.29

Figure 5.1 shows the relative heat transfer rate (Mo_{nf}/Mo_{w}) versus volume percent of copper oxide nanoparticles in water. For internal laminar flow, the nanofluids show a continuous increase in thermal performance with increasing particle concentration. However for turbulent flow, the relative heat transfer peaks at around 5% volume concentration and gradually diminishes after 8% volume concentration. This

phenomenon is due to the increase in the viscosity of nanofluids at higher concentrations, which is inversely proportional to the Mo number (see Equation 9). This analysis suggests that for turbulent internal flow a 5 % volume concentration may be optimal. It must be emphasized that the heat transfer coefficient for turbulent flow is still much higher than that of laminar flow.

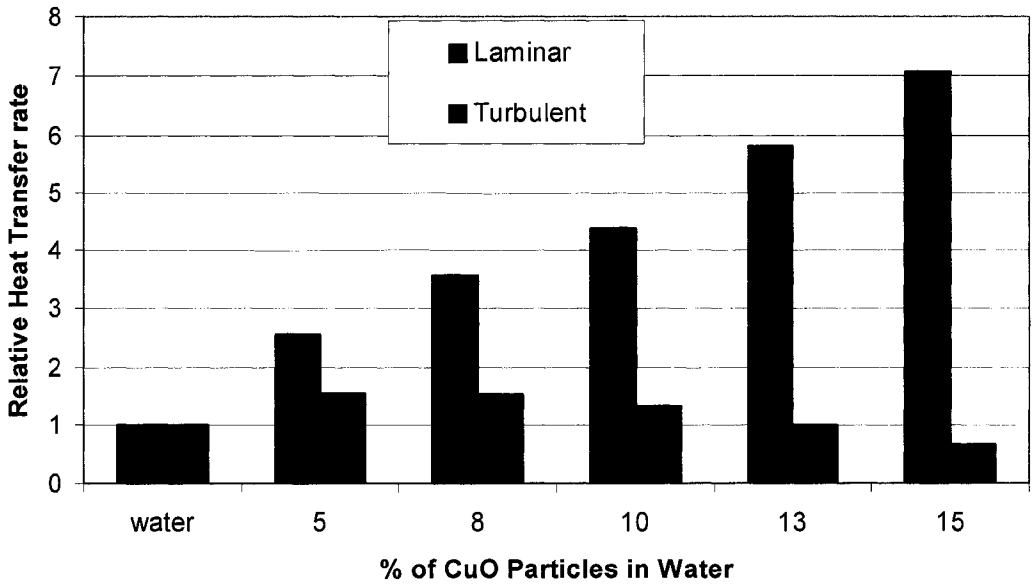

Figure 5.1. Comparative heat transfer rates (relative to water) for various concentrations of copper oxide (CuO) nanoparticles in water (at 20°C) for fully developed internal flow.

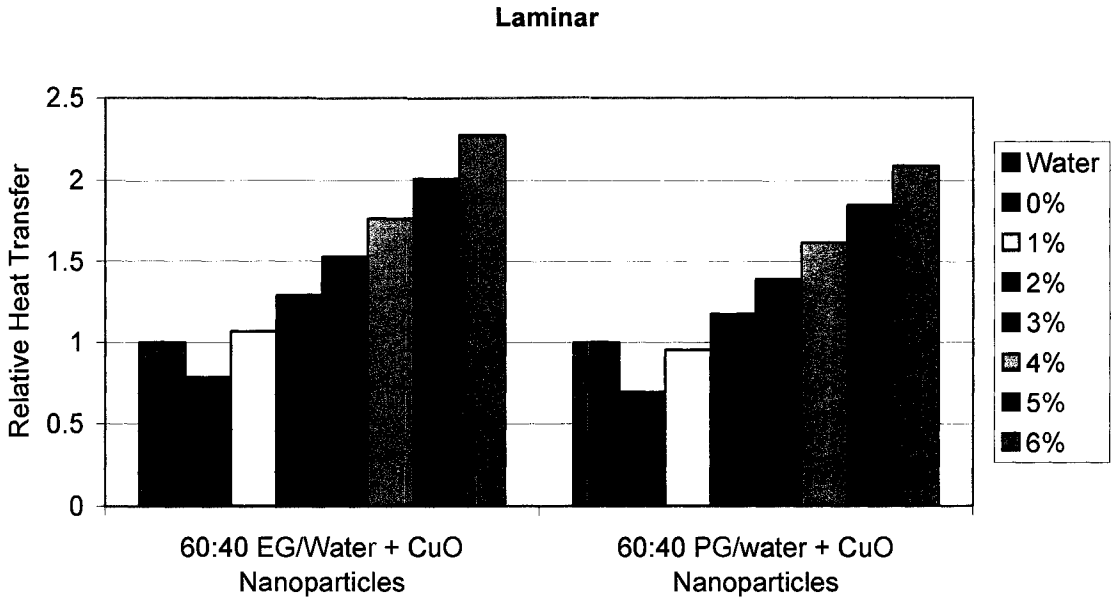

Figure 5.2. Comparative heat transfer rates (relative to water) for various percentages of copper oxide (CuO) nanoparticles (at 20°C) for fully developed internal laminar flow.

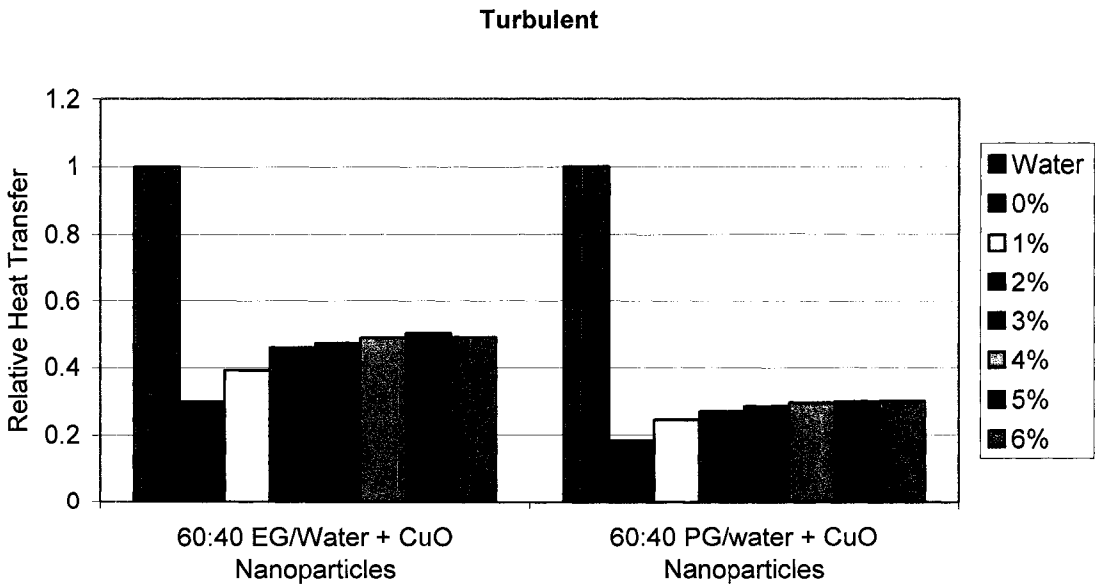

Figure 5.3. Comparative heat transfer rates (relative to water) for various percentages of copper oxide (CuO) nanoparticles (at 20°C) for fully developed internal turbulent flow.

Figure 5.2 shows the comparative heat transfer rate for 60:40 ethylene glycol/water and 60:40 propylene glycol/water with different concentrations of copper oxide nanoparticles for laminar flow. As in Figure 1, the relative heat transfer increases with the increase in nanoparticle concentration. Ethylene glycol performs better than the propylene glycol (see Figure 5.2); this effect is due to the variation of several thermal properties. Ethylene glycol has higher thermal conductivity and density, and lower specific heat and viscosity, than propylene glycol.

Figure 5.3 shows the comparative heat transfer rate for 60:40 ethylene glycol/water and 60:40 propylene glycol/water with different concentrations of copper oxide nanoparticles for turbulent flow. Although these results show that pure water has a better FOM than these nanofluids under turbulent conditions, in cold regions where fluid freezing is a serious problem, glycol solutions must be used. A concentration of 5% appears optimal for both these nanofluids; and these findings agree with the characteristics exhibited in Figure 5.1. It is also worth noting that the FOM of ethylene glycol is much better than that of propylene glycol.

Researchers are working on finding the compatibility of nanoparticles with pumps, valves and plumbing fittings. However, no definitive results have been published yet, because of the long-term experiments. It is generally thought that due to the small size of nanoparticles, wear on the surfaces will be minimal. We bought ready-to-use

nanofluids from Alfa Aesar, Inc. During the period of experiments conducted on the nanofluids, which lasted over several months, no agglomeration was observed. Cost of ready-to-use nanofluids is much higher than that of the traditional heat transfer fluids.

5.3 Conclusions

In conclusion, for internal laminar flow, the FOM of water-based copper oxide nanofluids is much superior to that of pure water. For the same nanofluid, the optimal volume percentage appears to be 5% in internal turbulent flows. Ethylene glycol based nanofluids have a better FOM than propylene glycol based nanofluids.

5.4 References

1. L. Qiang. X. Yimin, "Convective Heat Transfer and Flow Characteristics of Cu-water Nanofluid," Science in China (Series E), 45: 5, 408, 2002.

2. X. Yimin, L. Qiang, "Investigation on Convective Heat Transfer and Flow Features of Nanofluids," ASME Journal of Heat Transfer, 125, 151, 2003.

3. J.A. Eastman, S.U.S. Choi, S. Li, W. Yu and L.J. Thompson, "Anomalously Increased Effective Thermal Conductivities of Ethylene Glycol Based Nanofluids Containing Copper Nanoparticles," Applied Physics Letters, 78:6, 718, 2001.

4. Azar, K., "High Capacity or Not-do-it Up Front" Electronics Cooling, Vol. 12, No. 2, May 2006.

5. Simons, R.E., "Comparing Heat Transfer Rates of Liquid Coolants using the Mouromtseff Number," Electronics Cooling, Vol. 12, No. 2, May 2006.

6. Bar-Cohen, A.V., Kraus, A.D., "Advances in Thermal Modeling of Electronics Components and Systems," Vol. 2, ASME Press, 1990.

7. Ellswoth, M.J., "Comparing Liquid Coolants from Both A Thermal and Hydraulic Perspective," Electronics Cooling, Vol. 12, No.3, August 2006.

8. Pak, B.C., Cho, Y.I., "Hydrodynamic and Heat Transfer Study of Dispersed Fluids with Submicron Metallic Oxide Particles," Experimental Heat Transfer, Vol. 11, pp. 151-170, 1998.

9. Buongiorno, J., "Convective Transport in Nanofluids," ASME Journal of Heat Transfer, Vol. 128, p. 240-250, 2006.

10. Kulkarni, D.P., Das, D.K., Chukwu, G.A., "Temperature Dependent Rheological Property of Copper Oxide Nanoparticles Suspension (Nanofluid)," Journal of Nanoscience and Nanotechnology, Vol. 6, No.4, 2006.

CHAPTER SIX

Convective Heat Transfer and Fluid Dynamic Characteristics of SiO_2 – Ethylene Glycol/Water Nanofluid

Devdatta P. Kulkarni, Praveen K. Namburu, Harold E. Bargar, Debendra K. Das*
Department of Mechanical Engineering
University of Alaska Fairbanks
P.O. Box 755905, Fairbanks, AK, 99775-5905, USA.

Abstract

Nanofluids comprised of silicon dioxide (SiO_2) nanoparticles suspended in a 60:40 (% by weight) ethylene glycol and water (EG/water) mixture were investigated for their heat transfer and fluid dynamic performance. First, the rheological properties of different volume percents of SiO_2 in nanofluids were investigated at varying temperatures. The effect of particle diameter (20 nm, 50 nm, 100 nm) on the viscosity of the fluid was investigated. Subsequent experiments were performed to investigate the convective heat transfer enhancement of nanofluids in the turbulent regime by using the viscosity values measured. The experimental system was first tested with EG/water mixture to establish agreement with the Dittus-Boelter equation for Nusselt number and with the Blasius equation for friction factor. The increase in heat transfer coefficient due to nanofluids for various volume concentrations has been presented. Pressure loss was observed to increase with nanoparticle volume concentration. It was observed that an increase in particle diameter increased the heat transfer coefficient. Typical percentage increases of heat transfer coefficient and pressure loss at fixed Reynolds number are presented.

Under review, Heat Transfer Engineering, December 2006

Keywords:
SiO_2, Nanofluid, Heat Transfer Coefficient, Viscosity, Friction Factor, Ethylene Glycol

*Corresponding Author:ffdkd@uaf.edu,Ph:907-474-6094, Fax: 907-474-6141.

6.1 Introduction

In the last decade, as energy costs have escalated rapidly, there is a tremendous need for new kinds of heating/cooling fluid which will increase the thermal efficiency of the system and thus reduce overall energy consumption. Nanofluids have attracted attention as a new generation of coolant for various industrial and automotive applications because of their excellent thermal performance [1]. Nanofluids are the dispersions of nanometer-sized particles (<100 nm) in a base fluid such as water, ethylene glycol or propylene glycol. Use of high thermal conductivity metallic nanoparticles (e.g., copper, aluminum, silver, silicon) has the effect of increasing the thermal conductivity of such mixtures, thus enhancing their overall energy transport capability [2]. Eastman et al. [3] showed an increase of 40% in thermal conductivity with 0.3% (vol.) of copper nanoparticles in ethylene glycol. Recently, Prasher et al. [4] has demonstrated that this increase in thermal conductivity of nanofluids is primarily due to the convection caused by Brownian movement of nanoparticles. Various benefits of the application of nanofluids include: improved heat transfer, minimal clogging, microchannel cooling & miniaturization of systems, savings in energy, and reduced pumping power [5]. These benefits make nanofluids a future generation coolant.

In cold climates like those found in Alaska, Canada and the circumpolar regions, heat transfer fluids regularly encounter very low temperatures (on the order of -40°C). It is a common practice to use ethylene or propylene glycol mixed with water as a heat transfer fluid [6,7] for automobiles, heat exchangers in industry and baseboard heaters in houses. Inhibited ethylene glycol and propylene glycol are used as aqueous freezing point

depressants and heat transfer media in heating/cooling systems [8]. Their main attributes are the ability to lower the freezing point of water and low volatility. The commonly used mixture in cold climates is 60% glycol and 40% water by weight (EG/water mixture).

A major goal of this study is to assess the effect of particle diameter and concentration on the thermal and hydraulic characteristics of SiO_2 nanofluids, on which very few data are available in the current literature. We selected SiO_2 nanofluid because it is one of the least expensive nanofluids and a small increase in heat transfer will justify its use. The addition of these metallic particles would affect the rheology of this mixture. However, no rheological characteristics data are currently available in the literature for SiO_2 nanofluids at low temperatures. Investigating and reporting on the rheology and thermal characteristics of this nanofluid is very important to expanding its application in cold regions.

In the first part of the present paper, the viscosity of ethylene glycol and water with different volumetric percentages of SiO_2 nanoparticles has been investigated over a range of temperatures from $-35^{\circ}C$ to $50^{\circ}C$. In the second part, the investigation of heat transfer characteristics has been performed.

Earlier experimental investigations have demonstrated the enhancement of heat transfer coefficients of nanofluids over that of the pure base fluids [9-11]. Pak and Cho [12] studied the friction factor and heat transfer behavior of Al_2O_3 and TiO_2 nanofluids. They proposed a new correlation for Nusselt number for nanofluids. Also, nanofluids are finding their applications in electronics cooling where there is a high demand for removing a large amount of heat flux [12,13]. Yang et al. [14] studied several nanofluids under laminar conditions in a horizontal tube heat exchanger. Various numerical analyses have been conducted to demonstrate the better performance of nanofluids in macro [15] and microscale heat exchangers [16]. Kulkarni & Das [17] have studied two dimensional nanofluid flows using the well-known computational fluid dynamics software Fluent in

the laminar range and demonstrated that the heat transfer coefficient increased over that of the conventional base fluid. Wen and Ding [18] investigated the heat transfer of Al_2O_3 nanoparticles suspended in deionized water (DI) water in the entrance region under laminar conditions. Ding et al. [19] studied the heat transfer characteristics of multiwalled carbon nanotube (CNT) nanofluids. They demonstrated that with a small weight percent (0.5%), CNTs enhanced heat transfer by 350% at a Reynolds number of 800. Maiga et al. [20] numerically investigated the heat transfer behaviors of water-Al_2O_3 and ethylene glycol-Al_2O_3 nanofluids in a uniformly heated tube subjected to constant heat flux.

For rheological studies of different types of nanofluids, Tseng and Wu [21] have studied the effect of aqueous Al_2O_3 nanoparticle suspensions with an average diameter of 37 nm. They found these nanofluids exhibited a transition from pseudoplastic to dilatant flow. Tseng & Lin [22] have investigated the rheological properties of TiO_2 nanofluids over a volumetric concentration range of 5 to 12%. They came up with a correlation for relative viscosity (ratio of viscosity of nanofluid and the viscosity of the base fluid), which followed an exponential form with volume concentration. In recent years, other researchers have investigated the viscosities of different nanofluids, including carbon nanotubes and graphite nanofluids [23, 24], aqueous silica suspensions [25], $BaTiO_3$ suspensions [26] and also nickel suspensions [27,28]. Recently, Kulkarni et al. [29] investigated the temperature dependent viscosity of copper oxide nanoparticle suspension in water.

6.2 Theory

The effective thermal conductivity equation for a nanofluid presented by Hamilton and Crosser [38] is:

$$k_{nf} = k_f\left[\frac{k_s + (n-1)k_f - (n-1)\phi(k_f - k_s)}{k_s + (n-1)k_f + \phi(k_f - k_s)}\right] \quad (1)$$

Pak and Cho [9] list the following correlations for various properties of nanofluids.

The effective density of nanofluids is given by:

$$\rho_{nf} = (1-\phi)\rho_f + \phi\rho_s \tag{2}$$

where the volumetric concentration is given by:

$$\phi = \frac{1}{(100/\phi_m)(\rho_s/\rho_f)+1}(100\%). \tag{3}$$

The relative viscosity of nanofluids is given by Batchelor [39]:

$$\mu_r = \frac{\mu_{nf}}{\mu_f} = 1 + 2.5\phi + 6.25\phi^2. \tag{4}$$

The effective specific heat of nanofluids is given by Buongiorno [30]:

$$C_{pnf} = \frac{\phi\rho_s C_{ps} + (1-\phi)\rho_f C_{pf}}{\rho_{nf}} \quad . \tag{5}$$

The viscosity increases by 100 times for a particle volume of 10 % for γ-Al_2O_3 nanoparticles in water as shown by Pak and Cho [9]. The experiments conducted on rheological properties of copper oxide nanofluids by Kulkarni et al. [29] show that the viscosity of nanofluid is about 100 cP for a 15% particle volume concentration, whereas for pure water the value is around 1-2 cP at 298 K.

In heat transfer studies Li and Xuan [10] present two equations for the Nusselt number of nanofluids.

$$Nu_{nf} = 0.4328(1.0 + 11.285\phi^{0.754} Pe_d^{0.218})\,\mathrm{Re}_{nf}^{0.333}\,\mathrm{Pr}_{nf}^{0.4} \quad \text{(For laminar flow)} \tag{6}$$

$$Nu_{nf} = 0.0059(1.0 + 7.6286\phi^{0.6886} Pe_d^{0.001})\,\mathrm{Re}_{nf}^{0.9238}\,\mathrm{Pr}_{nf}^{0.4} \quad \text{(For turbulent flow)} \tag{7}$$

where $Pe_d = \frac{u_m d_p}{\alpha_{nf}}$; $\mathrm{Re}_{nf} = \frac{u_m d}{\nu_{nf}}$; $\mathrm{Pr}_{nf} = \frac{\nu_{nf}}{\alpha_{nf}}$; $\alpha_{nf} = k_{nf}/(\rho_{nf}.C_{pnf})$

The convective heat transfer coefficient: $h_{nf} = (Nu_{nf}.k_{nf})/d$ (8)

6.3 Experimental setup for measurement of viscosity

The experimental setup for measuring the viscosity of SiO_2 nanoparticles in ethylene glycol/water mixture was carried out using an LV DV-II+ Brookfield viscometer as shown in Fig. 6.1. This setup includes the temperature control bath that allows variation of the sample temperature from -35°C to 50°C for this experiment. The experimental procedure is described by Kulkarni et al. [29]. The viscosity measurement range of the LV DV-II model is 1 m.Pa.s to 2 $x10^6$ m.Pa.s [31], which encompasses the values expected in this experiment's temperature range.

The accuracy of the temperature control for this instrument is ± 0.1°C. The freezing temperature of the ethylene glycol and water mixture (60:40) is about -45°C [8]. Therefore, as a precaution, the lowest temperature used in the experiment was -35°C, to avoid any freezing condition in the sample chamber.

A benchmark test for viscosity was conducted to verify the accuracy of the experiments. The results are shown in Fig. 6.2 confirming that the experimental data for ethylene glycol/water mixture agreed well with American Society of Heating Refrigerating and Air Conditioning Engineers (ASHRAE) values. About eight to fourteen viscosity measurements were recorded at various shear rates at specific temperatures for each volume concentration of nanofluid. From these results the viscosity plot was generated and is shown in Fig. 6.3.

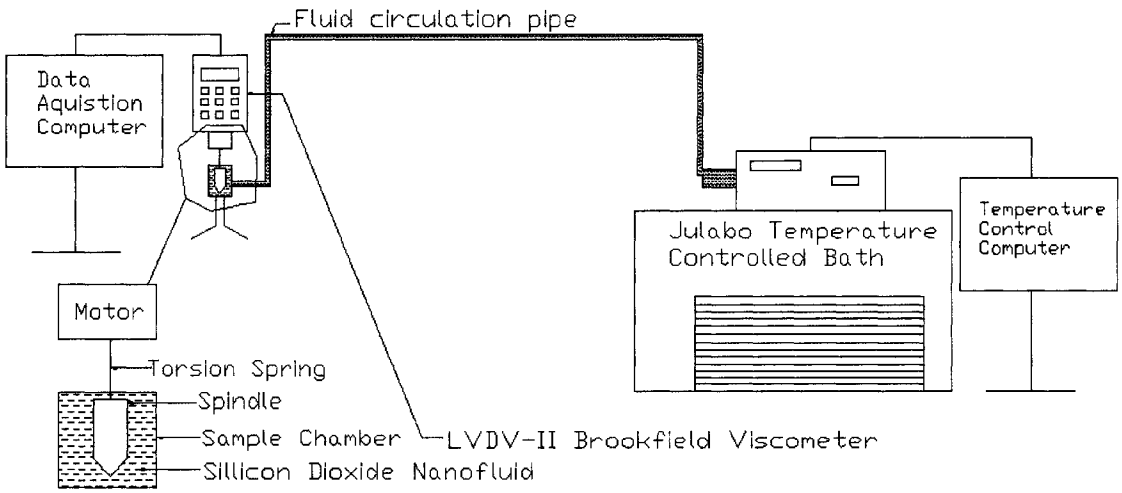

Figure 6.1. Experimental setup for viscosity measurement of nanofluids.

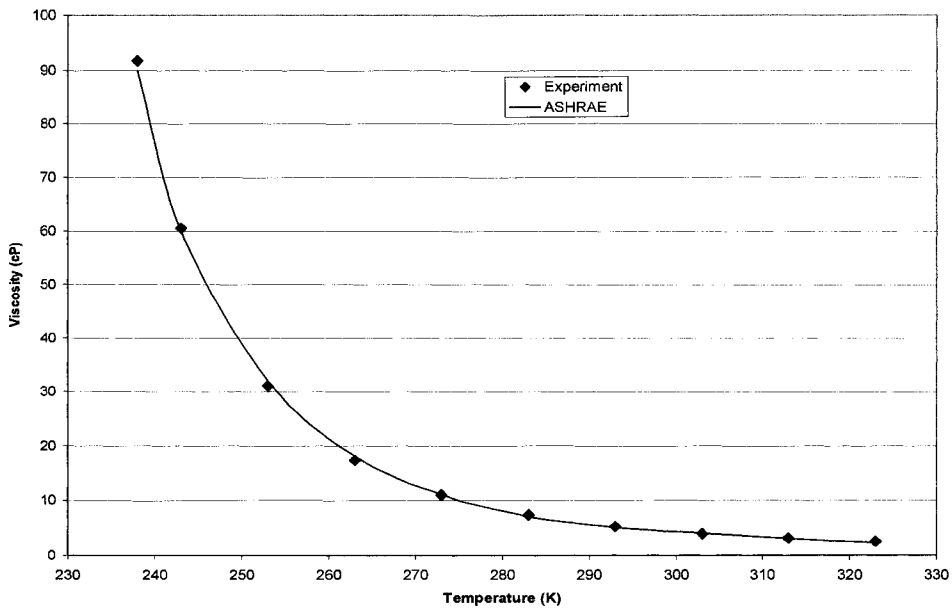

Figure 6.2. Comparison of ASHRAE viscosity values of 60:40 ethylene glycol and water mixture (by weight) and experimental data. 1 cP(centipoise) = 1 mPa.s.

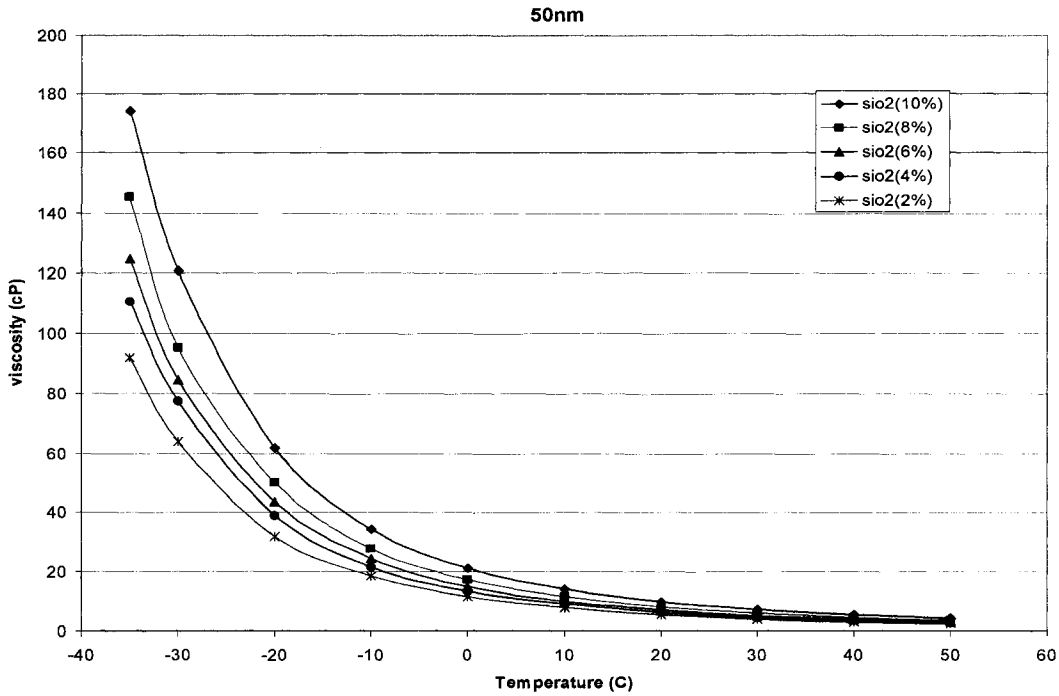

Figure 6.3. Experimental values of viscosity at varying volume concentrations of 50 nm SiO_2 nanofluids with respect to temperature.

From these experiments an exponential correlation was developed for viscosity of SiO_2 nanofluids. It is given as:

$$\log(\mu_{nf}) = Ae^{-BT} \tag{9}$$

where A & B are functions of volume percent ϕ ranging from 2 to 10 and T is in Kelvin.

$$A = 0.2339\phi^3 - 3.8943\phi^2 + 7.1232\phi + 155.06 \quad \text{with } R^2 = 0.9904$$

$$B = -7x10^{-6}\phi^2 - 0.0004\phi + 0.0192 \quad \text{with } R^2 = 0.9925$$

This correlation follows a logarithmic expression presented for viscosities of many liquids by Yaws [32]. This correlation was used in our subsequent calculations for Reynolds number and Prandtl number.

6.4 Experimental setup for measurement of heat transfer coefficient

An experimental apparatus was built to study the heat transfer and flow characteristics of various nanofluids flowing through a tube. The experimental setup is shown in Fig. 6.4. It consists of a turbine pump, heat transfer test section, a counterflow cooling heat exchanger, flowmeter, differential pressure transducer, bypass valve, reservoir and a datalogger.

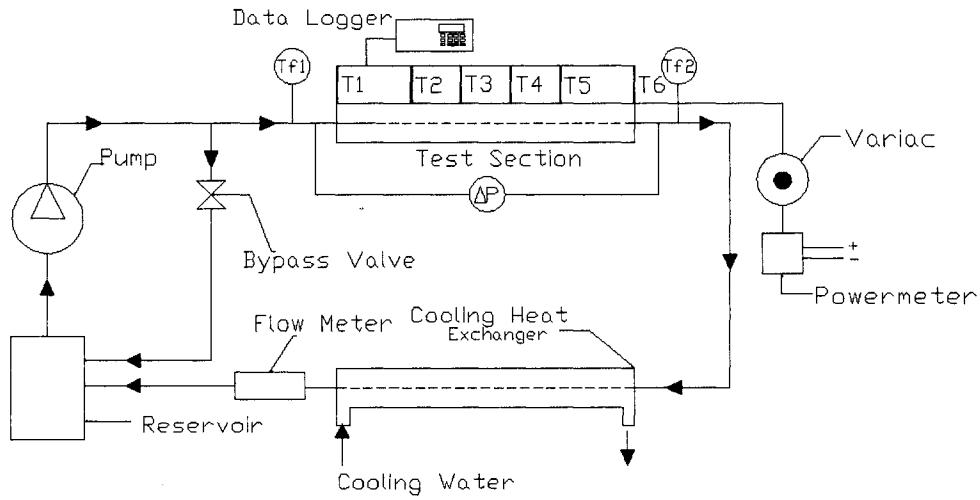

Figure 6.4. A schematic diagram of the nanofluids experimental apparatus, T = Thermocouples, ΔP = Differential pressure transducer.

The test system is designed in such a way that a small volume of nanofluid (approx. 2 litres) will be sufficient to investigate the heat transfer performance of nanofluids to hold down costs. The heat transfer test section is a straight copper tube with outside diameter of 4.76 mm (3/16 inch) and a length of 1 m (3.28 ft). Six type-T (copper-constantan) thermocouples mounted on the tube surface along the length measure the wall temperature. Two thermowells at the inlet and outlet of the test section measure the inlet and outlet temperature of the nanofluid. Two plastic fittings at inlet and outlet section of the copper tube provide a thermal barrier to axial heat conduction. For

turbulent flow, the hydrodynamic and thermal entry length in a tube is X/D = 10 [33]. In our experimental setup, this length is 4.76 cm beyond which all measurements are taken to ensure that the measurements are in the fully developed regions. To attain the constant heat flux boundary condition, the test section is heated electrically by four strip heaters capable of delivering 1 kW each. To measure the power input accurately, four power meters are used which are connected to four variacs. To minimize the heat loss from the heat transfer test section to ambient air, the test system is insulated by 10 cm of fiber glass. A four-pass shell and tube counterflow heat exchanger cools the nanofluids to keep the inlet fluid temperature constant using shop water. A bypass valve controls the nanofluid circulation rate.

During experiments, the tube wall temperatures, fluid inlet and outlet temperatures, volumetric flow rate of the fluid and power supplied are measured. Using this data, the convective heat transfer coefficient of the nanofluid (h_{nf}) is determined as:

$$h_{nf} = \frac{q''}{T_w - T_f} \tag{10}$$

where T_w is the average wall temperature and T_f is average of fluid inlet and outlet temperatures; q is the heat flux supplied to the test section. The heat flux provided can be equated to heat gained by fluid flowing through the test section. It is given as:

$$q = \dot{m} C_p \Delta T_f \tag{11}$$

where $\dot{m}$ is the mass flow rate, C_p is specific heat of nanofluid and ΔT_f is the difference between inlet and outlet temperature of the nanofluid.

Checks between equations (10) and (11) were performed and agreement was found to be within 5%. Part of this difference was attributed to the heat loss to the environment. A finite element analysis by Das et al. [34] estimated the heat loss through insulation to be about 2%.

Before determining the convective heat transfer coefficient of a nanofluid, the apparatus was calibrated using EG/water mixture. The experimental results were compared with the Dittus-Boelter equation [33] given below for fully developed turbulent flow.

$$Nu = 0.023\,\mathrm{Re}^{0.8}\,\mathrm{Pr}^{0.4}. \qquad (12)$$

Fig. 6.5 shows that the experimental results and values obtained by the Dittus-Boelter equation are comparable. To ensure consistency, the test runs were repeated and the results were reproduced with similar accuracy.

The nanofluid samples were prepared by mixing EG/water mixture and concentrated solutions of SiO_2 nanoparticles obtained from Alfa Aesar Inc.[35] suspended in ethylene glycol. Different nanoparticle volume concentrations (10%, 8%, 6%, 4% & 2%) were prepared by adding a calculated mass of nanofluid with a precision mass balance. Particle diameters of 20 nm, 50 nm and 100 nm were used to determine the effect of particle size on the heat transfer and pressure drop characteristics. In the present study, the Reynolds number was varied from 3,000 to 12,000.

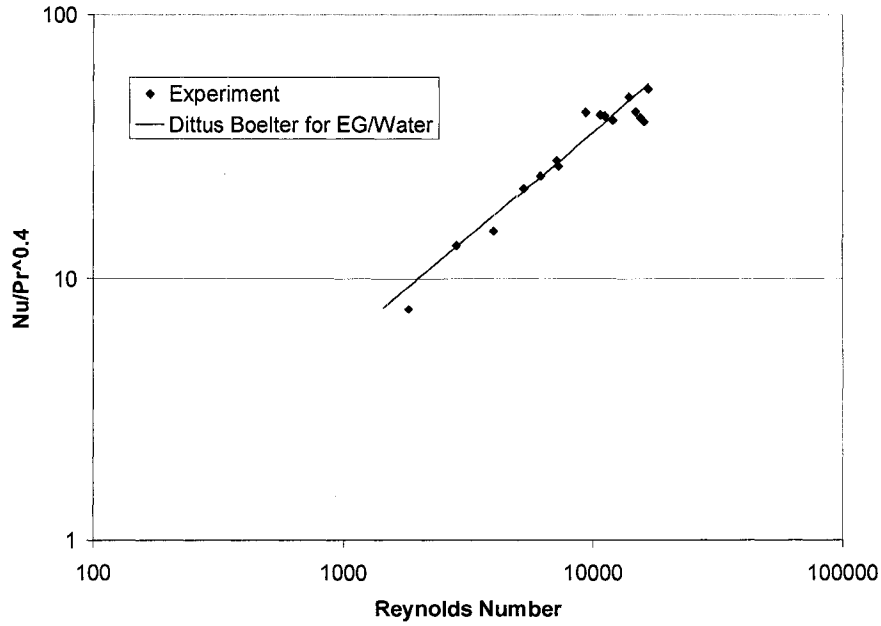

Figure 6.5. Comparison between the experimental results and the Dittus–Boelter equation for the ethylene glycol/water mixture.

6.5 Uncertainty in Experimental Data

In this experiment, uncertainty of experimental data results from measuring errors of parameters such as volume flow rate, viscosity and temperature, as decreased by Xuan and Li [2]. For the heat transfer experiment; h was calculated from readings of the volume flow meter and thermocouples.

$$\frac{\delta h}{h} = \sqrt{\left(\frac{\Delta T}{T}\right)^2 + \left(\frac{\Delta \dot{v}}{\dot{v}}\right)^2} \tag{13}$$

Precision of the thermocouples was $\pm 0.5^0 C$. Precision of the volumetric flow meter was $\pm 2\%$. Therefore, the uncertainty of the heat transfer experiment is less than 3 percent.

The Reynolds numbers were calculated from measurements of the volumetric flow meter and the viscometer. For viscosity measurements, the instrument was calibrated using standard Brookefield silicone fluids of known viscosity and an error of ± 2% was obtained.

$$\frac{\delta(\mathrm{Re})}{\mathrm{Re}} = \sqrt{\left(\frac{\Delta\mu}{\mu}\right)^2 + \left(\frac{\Delta \dot{v}}{\dot{v}}\right)^2 + \left(\frac{\Delta T}{T}\right)^2} \tag{14}$$

Therefore, the uncertainty in Reynolds number is less than 3 percent. The pressure loss was measured directly with a Omega differential pressure transducer. The accuracy of this transducer is ± 0.25%.

6. 6 Results for Heat Transfer Measurement

Fig. 6.6 shows the convective heat transfer coefficient of 20 nm SiO_2 nanofluid dispersed in an ethylene glycol/water mixture for various Reynolds numbers in the turbulent regime. The experimental results indicate that there is an increase in heat transfer coefficient of the base fluid with the addition of nanoparticles. For example, the convective heat transfer coefficient is increased by 16% by adding nanoparticles to a 10% SiO_2 concentration at Re = 10,200.

Figures 6.7, 6.8 and 6.9 show that the heat transfer coefficient increases with the particle size. A similar observation was presented by Li & Xuan [10]. For larger diameter particles viscosity decreases causing the Reynolds number to increase. At the same time for larger particles the Peclet number increases. The combined effects of this increase cause the heat transfer coefficient to be higher for larger particles. The enhancement caused by Reynolds and Peclet numbers in heat transfer is of much greater magnitude than the increased surface area effect of smaller particles.

From Fig. 6.7, we determine that for a 6% concentration, the nanofluid, with 100 nm particle diameter, is capable of increasing h by 12% at a Reynolds number of 10,000.

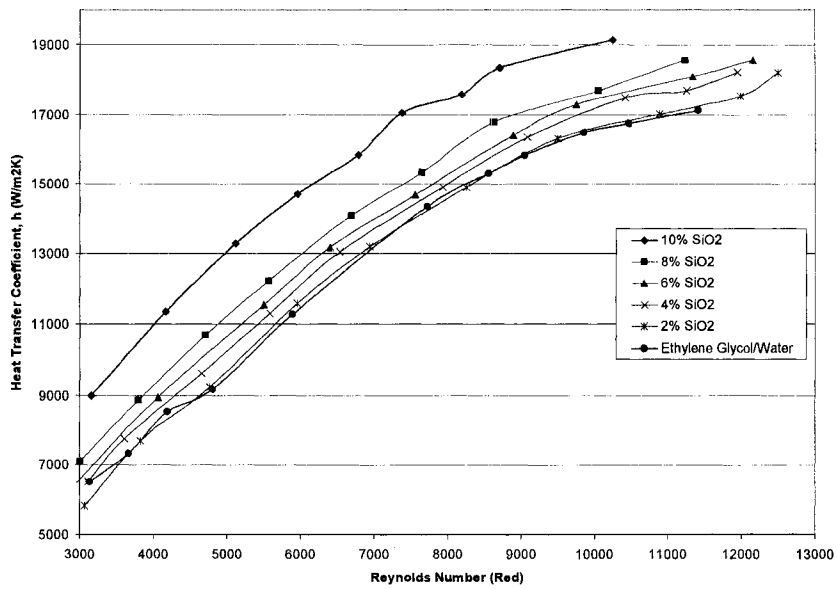

Figure 6.6. The convective heat transfer coefficient of SiO_2 nanofluids (20 nm dia) in ethlylene glycol/water mixture.

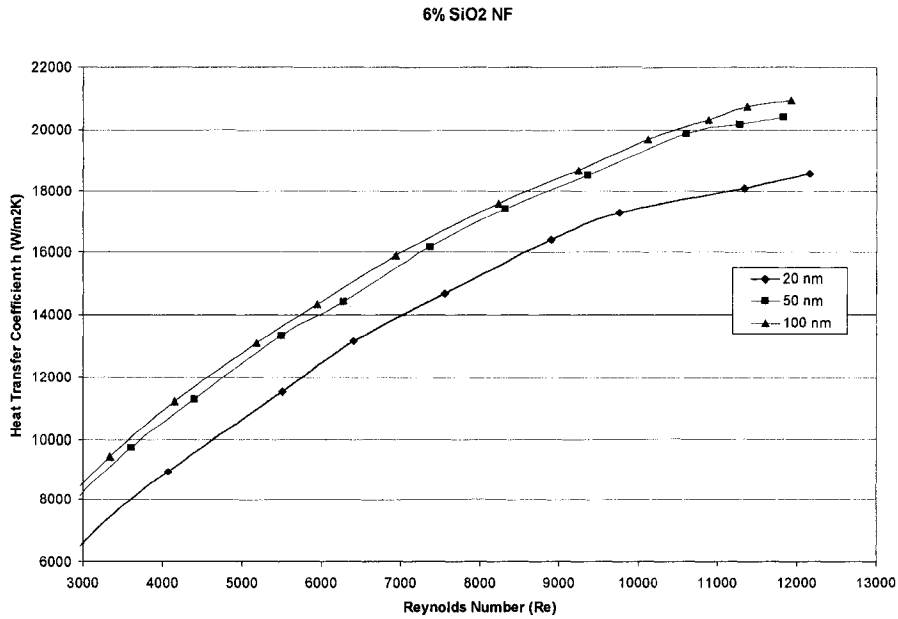

Figure 6.7. Effect of particle diameter on heat transfer characteristics of 6% SiO_2 nanoparticles in ethylene glycol/water mixture

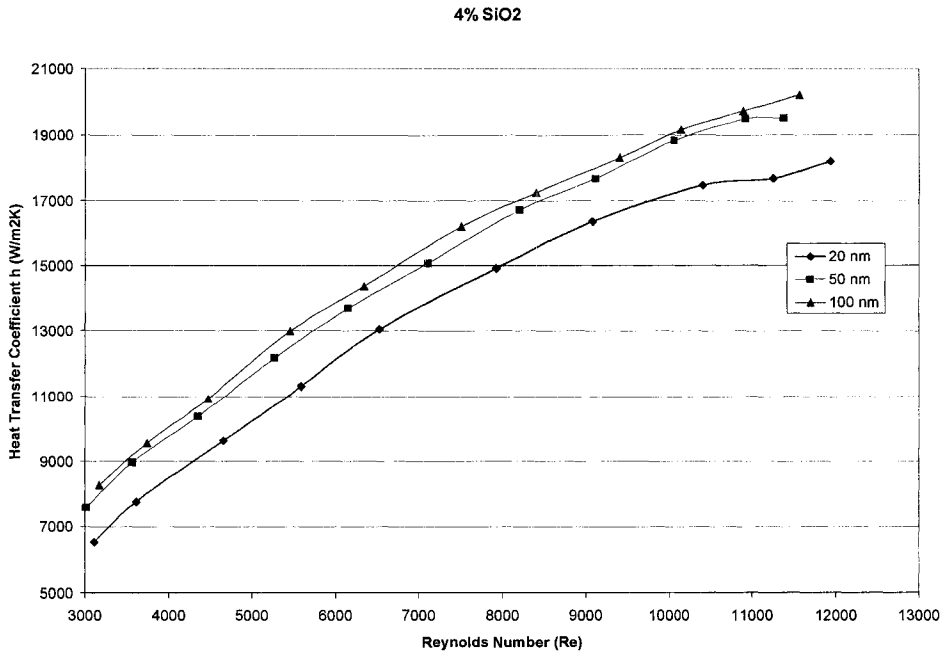

Figure 6.8. Effect of particle diameter on heat transfer characteristics of 4% SiO_2 nanoparticles in ethylene glycol/water mixture

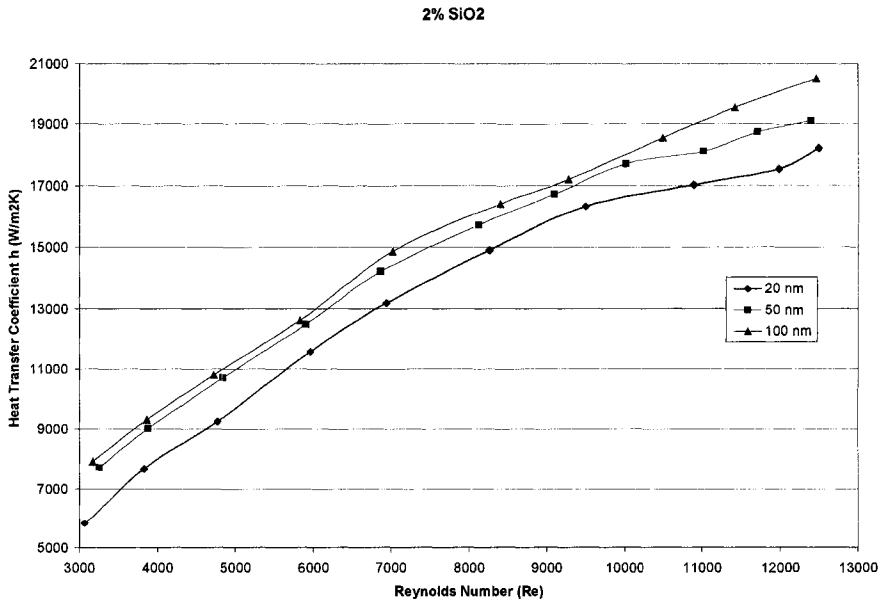

Figure 6.9. Effect of particle diameter on heat transfer characteristics of 2% SiO_2 nanoparticles in ethylene glycol/water mixture

6.7 Pressure Drop Measurement

A benchmark test was conducted with EG/water mixture for pressure loss measurements. Fig. 6.10 shows good agreement of this experimental data with the Darcy friction factor expressed via the Blasius equation presented by White [36] as

$$f = 4C_f = 4(0.0791\mathrm{Re}^{-1/4}) \tag{15}$$

From rheological measurements presented in Fig. 6.11, it was observed that the viscosity decreases with increased particle size. Although not much information is available in the literature on the size effect of nanoparticles, it has been reported for micro-particle suspensions. In Cheremisinoff [37], it is reported that the viscosity decreases as the particle diameter increases in coal-oil mixtures. For example, the viscosity values for 6% SiO_2 nanofluid (50 nm) at 32°C is 4.7 mPa.s and at 56°C it is 2.75 mPa.s. Therefore, the decrease in viscosity is 71% of the value of viscosity at 56°C. As viscosity decreases, the Reynolds number increases. This results in a lower friction factor and reduced pressure drop. Therefore, larger diameter nanoparticles are recommended for increased heat transfer. However, the maximum size should be limited to 100 nm to remain a nanofluid.

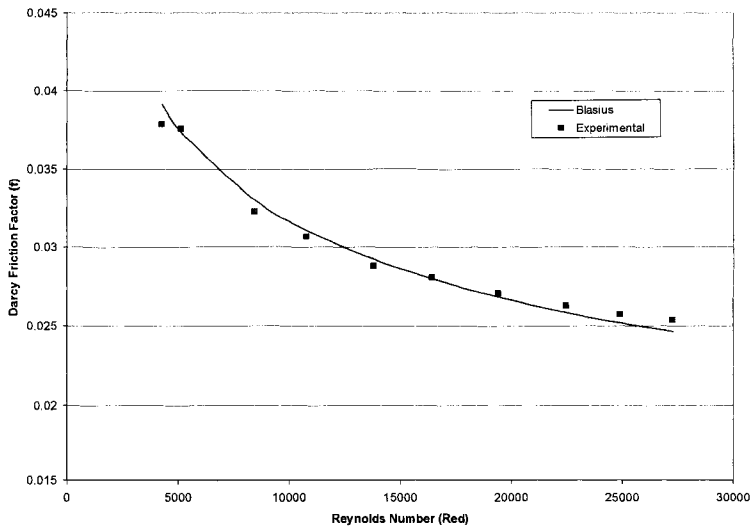

Figure 6.10. Comparison of Darcy friction factor calculated by using the Blasius equation and the experimental values for ethylene glycol/water mixture in turbulent regime.

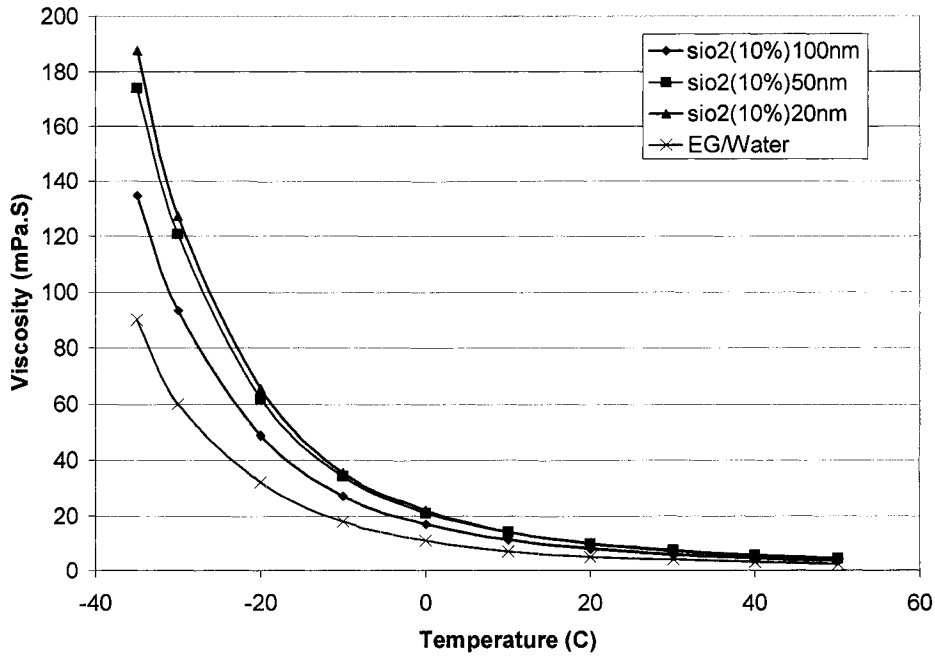

Figure 6.11. Effect of particle diameter on viscosity for 10% SiO_2 nanofluids.

Figure 6.12 displays the pressure loss measurement across the test section. The measurements show that as the concentration of the nanofluid increases, the pressure loss is increased. This is consistent with the increase in viscosity shown in Fig. 6.3. At a Reynolds number of 10,000, the pressure loss is higher for the 6% concentration nanofluid than the base fluid (0% nanoparticle concentration).

Figure 6.13 displays the variation of the nondimensional Darcy friction factor, f, with Reynolds number. The variation of f with concentration must be viewed through Eq. (16). The friction factor correlation from White [36] is:

$$f = \frac{\Delta P(2d)}{\rho L V^2} \tag{16}$$

From Fig. 6.3, it is seen that μ increases with concentration. When the concentration is higher, the pressure loss is higher. Therefore, from Eq. (16) f is higher for higher concentration as observed in Fig. 6.13.

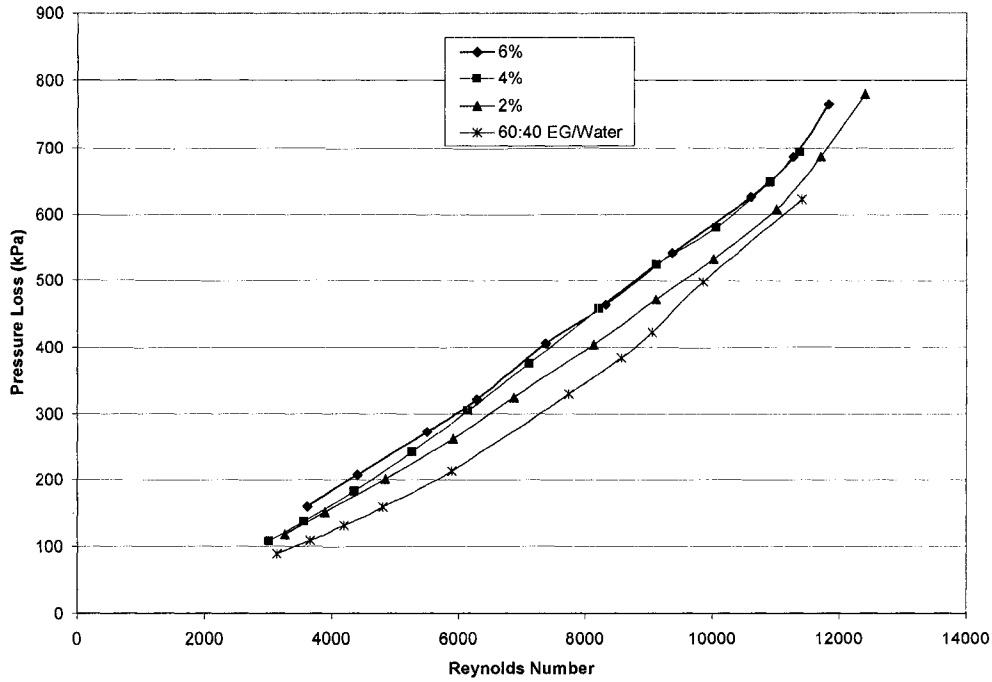

Fig. 6.12 Pressure loss of nanofluids with different concentrations of 50 nm SiO_2 nanoparticles

Figure 6.14 shows the effect of pressure loss versus velocity for different particle diameters. The lines are theoretical values derived from Blasius equation 'B' and the symbols with legend 'E' represent experimental values. It was observed that no appreciable change in pressure loss occurred for different diameter nanoparticles. This is due to the minor viscosity change with respect to particle diameters. The viscosity is affected much more by particle concentration than the particle diameters. Furthermore, this observation was for a test section of 1 m length and at a higher temperature range. Viscosity change from 20 nm to 100 nm is small and its effect on the Blasius equation, equation (15) is small showing that the three curves for 20, 50 and 100 nm practically coincide with each other. However, because the 6% concentration nanofluid has higher viscosity than the pure ethylene glycol/water mixture, this curve and experimental data points fall above the pure base fluid line.

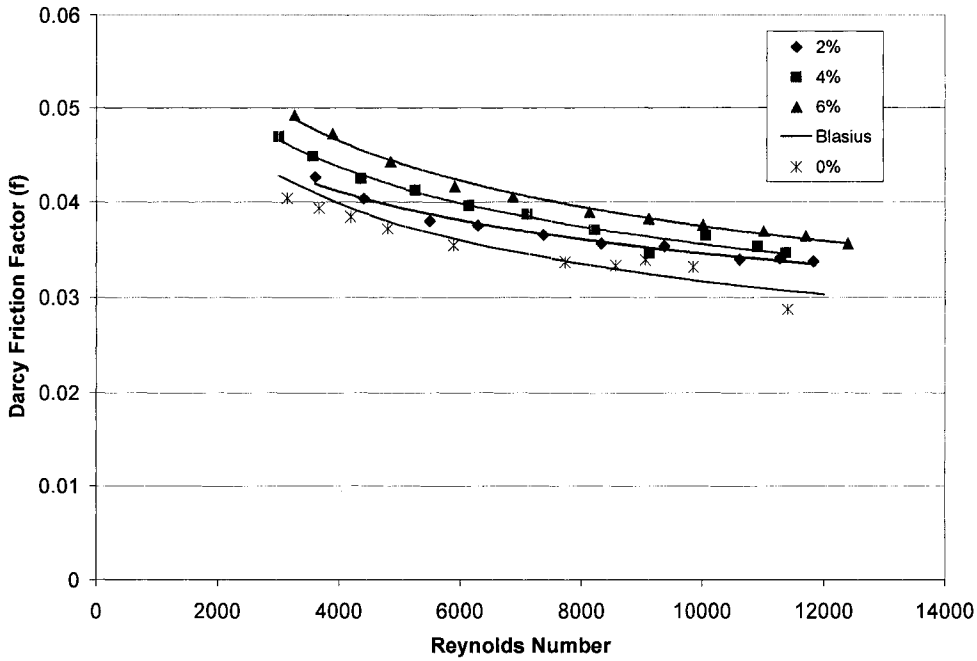

Fig. 6.13 Comparison of Darcy friction factor of different concentrations of 50 nm SiO_2 nanofluids

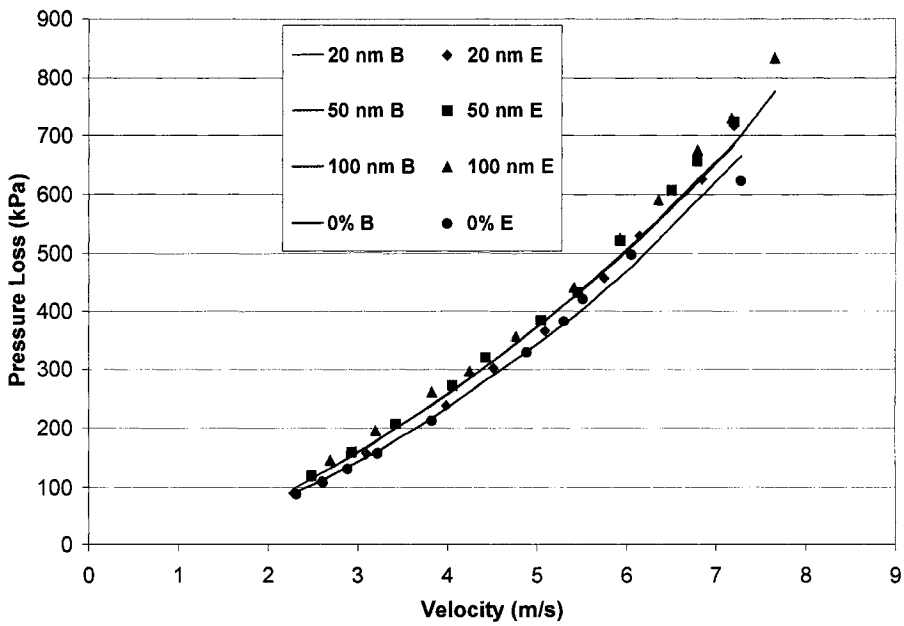

Fig. 6.14 Effect of particle size on pressure loss of 6% SiO_2 nanofluids (Note: B = Blasius equation and E = Experiment).

6.8 Conclusions

1. Viscosity of a nanofluid is a function of nanoparticle concentration, increasing as the concentration increases. This effect is more pronounced at sub-zero temperatures.
2. As particle size increases, the viscosity of nanofluids decreases.
3. Heat transfer coefficients of nanofluids increase with volume concentration. A typical enhancement of heat transfer coefficient is about 16% at a concentration of 10% with 20 nm particle diameter at Re = 10,000.
4. Particle size influences the heat transfer coefficient. The larger the diameter, the higher the heat transfer coefficient at a fixed Reynolds number.
5. Pressure loss is a function of the concentration, increasing with increasing concentration. This is because the viscosity increases with concentration.
6. No appreciable change in pressure loss was observed for different diameter nanoparticles within the range of experiment.

6.9 Acknowledgements

Financial assistance from the Arctic Region Supercomputing Center and the Dean of the Graduate School at the University of Alaska Fairbanks is gratefully acknowledged. Authors are thankful to the Mechanical Engineering Department and Petroleum Development Laboratory for providing the experimental facilities to measure heat transfer and viscosity.

6.10 Nomenclature

C_p Specific heat (J/kg K)

C_f Skin friction coefficient

d Inside diameter of tube (m)

d_p Diameter of particle (m)

f	Darcy friction factor
h	Heat transfer coefficient (W/m^2K)
k	Thermal conductivity (W/mK)
L	Length of tube (m)
$\dot{m}$	Mass flow rate (kg/s)
n	Sphericity of particle (For spherical particle: n =3)
Nu	Nusselt number
Pe_d	Particle Peclet number
Pr	Prandtl number
q	Heat Supplied (W)
q''	Heat flux, (W/m^2)
Re	Reynolds number
T	Temperature (^0C)
u_m	Mean fluid velocity (m/s)
V	Velocity (m/s)

Greek

α	Thermal diffusivity (m^2/s)
ΔP	Differential pressure loss (Pa)
ΔT	Temperature difference (K)
μ	Dynamic viscosity (Pa.s)
μ_r	Relative viscosity
ν	Kinematic viscosity (m^2/s)
ϕ	Particle volume fraction
ϕ_m	Particle mass fraction
ρ	Density (kg/m^3)

Subscript

f	Fluid
nf	Nanofluid

s Solid

w Wall

6.11 References

1. Eastman, J.A., Phillpot, S.R., Choi, S.U.S. and Keblinski, P.K., Thermal Transport in Nanofluids, *Annual Review of Material Research*, vol. 34, pp. 219-246, 2004.
2. Xuan, Y. and Li, Q., Investigation on Convective Heat Transfer and Flow Features of Nanofluids, *ASME Journal of Heat Transfer*, vol. 125, pp. 151-155, 2003.
3. Eastman, J.A., Choi, S.U.S., Li, S., Yu, W. and Thompson, L.J., Anomalously Increased Effective Thermal Conductivities of Ethylene Glycol-based Nanofluids Containing Copper Nanoparticles, *Applied Physics Letters*, vol. 78, no. 6, pp. 718-720, 2001.
4. Prasher, R., Bhattacharya, P. and Phelan, P.E., Thermal Conductivity of Nanoscale Colloidal Solutions (Nanofluids), *Physical Review Letters*, PRL 94, 025901, 2005.
5. Choi, S.U.S., Zhang, Z.G. and Keblinski, P., Nanofluids, *Encyclopedia of Nanoscience and Nanotechnology*, vol. 6, pp. 757-773, 2004.
6. Choi, S.U.S., Yu, W., Hull, J.R., Zhang, Z.G. and Lockwood, F.E., Nanofluids for Vehicle Thermal Management, *SAE 2001-01-1706*, pp. 139-144, 2001.
7. Mcquiston, F.C., Parker, J.D. and Spitler, J.D., *Heating, Ventilating, and Air Conditioning*, 6th ed., John Wiley & Sons, Inc., New York, 2005.
8. *ASHRAE Handbook, Fundamentals*, American Society of Heating, Refrigerating and Air-Conditioning Engineers Inc., Atlanta, 1985.
9. Pak, B.C. and Cho, Y.I., Hydrodynamic and Heat Transfer Study of Dispersed Fluids with Submicron Metallic Oxide Particles, *Experimental Heat Transfer*, vol. 11, pp. 151-170, 1998.
10. Li, Q. and Yimin X., Convective Heat Transfer and Flow Characteristics of Cu-water Nanofluid, *Science in China (Series E)*, vol. 45, no.4, pp 408-416, 2002.

11. Yimin X. and Li, Q., Heat Transfer Enhancement of Nanofluids, *International Journal of Heat and Fluid Flow*, Vol. 21, pp. 58-64, 2000.
12. Faulkner, D., Khotan, M. and Shekarriz R., Practical Design of a 1000 W/cm^2 Cooling System, *Proc. of IEEE SEMI-THERM Symposium*, San Jose, pp. 223-230, 2003.
13. Lee S. and Choi S.U.S., Application of Metallic Nanoparticle Suspensions in advanced Cooling Systems, *Recent Advances in Solids/Structure and Application of Metallic Materials*, ASME PVP-Vol. 342/MD-Vol. 72, pp. 227-234, 1996.
14. Yang, Y., Zhang, Z.G., Grulke, E.A., Anderson, W.B. and Wu, G., Heat Transfer Properties of nanoparticle-in-fluid dispersions (nanofluids) in Laminar Flow, *International Journal of Heat and Mass Transfer*, vol. 48, pp. 1107-1116, 2005.
15. Roy, G., Nguyen, C.T. and Lajoie, P.R., Numerical Investigation of Laminar Flow and Heat Transfer in a Radial Flow Cooling System with the Use of Nanofluids, *Superlattices and Microstructures*, vol. 35, no. 3-6, pp. 497-511, 2004.
16. Koo, J. and Kleinstreuer, C., Laminar Nanofluid Flow in Microheat-sinks, *International Journal of Heat and Mass Transfer*, vol. 48, pp. 2652-2661, 2005.
17. Kulkarni, D.P. and Das, D.K., Theoretical and Experimental Investigations on Nanofluids for Their Fluid Dynamics and Heat Transfer Behaviors, *Proc. of 39th Heat Transfer and Fluid Mechanics Institute*, Sacramento, pp. 95-109, 2006.
18. Wen, D. and Ding, Y., Experimental Investigation into Convective Heat Transfer of Nanofluids at the Entrance Region Under laminar Flow Conditions, *International Journal of Heat and Mass Transfer*, vol. 48, pp. 5181-5188, 2004.
19. Ding, Y., Alias, H., Wen, D. and Williams, R., Heat Transfer of Aqueous Suspensions of Carbon Nanotubes (CNT Nanofluids), *International Journal of Heat and Mass Transfer*, vol. 49, pp. 240-250, 2006.
20. Maiga, S.E., Nguyen C.T., Galanis, N. and Roy, G., Heat Transfer Behaviors of Nanofluids in a Uniformly Heated Tube, *Superlattices and Microstructures*, vol. 35, pp. 543-557, 2004.

21. Tseng, W.J. and Wu, C.H., Aggregation, Rheology and Electrophoretic Packing Structure of Aqueous Al_2O_3 Nanoparticle Suspensions, *Acta Materialia*, vol. 50, pp. 3757-3766, 2002.

22. Tseng, W.J. and Lin, K.C., Rheology and Colloidal Structure of Aqueous TiO_2 Nanoparticle Suspensions, *Materials Science and Engineering*, vol. A355, pp. 186-192, 2003.

23. Yang, Y., Grulke, E.A., Zhang, Z.G. and Wu, G., Rheologocal Behavior of Carbon Nanotubes and Graphite Nanoparticle Dispersions, *Journal of Nanoscience and Nanotechnology*, vol. 5, pp. 571- 579, 2005.

24. Hilding, J., Grulke, E.A., Zhang, Z.G. and Lockwood, F., Dispersion of Carbon Nanotubes in Liquids, *Journal of Dispersion Science and Technology*, vol. 24, no. 1, pp. 1-41, 2003.

25. Savarmand, S., Carreau, P.J., Betrand, F., Vidal, D.J. and Moan, M., Rheological Properties of Concentrated Aqueous Silica Suspensions: Effect of pH and Ion Content, *Journal of Rheology*, vol. 47, no. 5, pp. 1133-1149, 2003.

26. Tseng, W. and Lin, C.L., Effect of Dispersants on Rheological Behavior of $BaTiO_3$ Powders in Ethanol-Isopropanol Mixtures, *Materials Chemistry and Physics*, vol. 80, pp. 232-238, 2003.

27. Tseng, W. and Chen, C.N., Determination of Maximum Solids Concentration in Nickel Nanoparticle Suspensions, *Journal of Material Science Letters*, vol. 21, pp. 419-422, 2002.

28. Tseng, W. and Chen, C.N., Effect of Polymeric Dispersant on Rheological Behavior of Nickel-Terpineol Suspensions, *Materials Science and Engineering*, vol. A347, pp. 145-153, 2003.

29. Kulkarni, D.P., Das, D.K. and Chukwu, G.A., Temperature Dependent Rheological Property of Copper Oxide Nanoparticles Suspension (nanofluid), *Journal of Nanoscience and Nanotechnology*, vol. 6, no.4, pp. 1150-1154, 2006.

30. Buongiorno, J., Convective Transport in Nanofluids, *ASME Journal of Heat Transfer*, vol. 128, pp. 240-250, 2006.

31. Brookfield DV-II+ Programmable Viscometer Manual No. M/97-164-D1000, Brookfield Engineering Laboratories Inc, MA, USA.
32. Yaws, C.L., *Physical properties- A Guide to the Physical, Thermodynamic and Transport Property Data of Industrially Important Chemical Compounds*, McGraw-Hill, Inc., New York, 1977.
33. Bejan, A., *Heat Transfer*, John Wiley & Sons, Inc., New York, 1993.
34. Das, D.K., Kulkarni, D.P. and Silbaugh, B., A Study on Nanofluids for their Convective Heat Transfer and Hydrodynamic Characteristics, *Proc. of National Conference on Emerging Trends in Nanotechnology and Innovations in Design and Manufacturing*, National Institute of Technology, Rourkela, India, pp. 1- 23, 2006.
35. http://www.alfaaesar.com
36. White, F. M., *Viscous Fluid Flow*, McGraw Hill, Inc., New York, 1991.
37. Cheremisinoff, N.P., *Encyclopedia of Fluid Mechanics, Rheology and Non-Newtonian Flows*, vol. 7, Golf Publishing Company, Houston, 1988.
38. Hamilton, R.L. and Crosser, O.K., Thermal Conductivity of Heterogeneous Two-Component Systems, *I& EC Fundamental*, vol. 125, pp. 187-191, 1962.
39. Batchelor, G.K., The Effect of Brownian Motion on the Bulk Stress in a Suspension of Spherical Particles, *Journal of Fluid Mechanics*, vol. 83, pp. 97-117, 1977.

CHAPTER SEVEN

Application of Nanofluids in Heating or Cooling Buildings

Devdatta P. Kulkarni, Debendra K. Das*
Department of Mechanical Engineering
University of Alaska Fairbanks
P.O. Box 755905, Fairbanks, AK, 99775-5905, USA.

Abstract

This paper presents nanofluid convective heat transfer and viscosity measurements, and evaluates how they perform in heating cold climate buildings. Nanofluids contain suspended metallic nanoparticles, which increases the thermal conductivity of the base fluid by a substantial amount. The heat transfer coefficient of nanofluids increases with volume concentration. To determine how nanofluid heat transfer characteristics enhance as volume concentration is increased; experiments were performed on copper oxide, aluminum oxide and silicon dioxide nanofluids, each in an ethylene glycol and water mixture. Calculations have been carried out for conventional heat exchangers used in cold climate buildings. The analysis shows that using nanofluids in heat exchangers could reduce volumetric flow and mass flow rates, and result in an overall pumping power savings. Nanofluids necessitate smaller heating systems, which are capable of delivering the same amount of thermal energy as larger heating systems using base fluids, but are less expensive; this lowers the initial equipment cost. This will also reduce environmental pollutants because smaller heating units use less power, and the heat transfer unit has less liquid and material waste to discard at the end of its life cycle.

Under review, Building and Environment, April 2007

Key Words: Nanofluid; Heat transfer coefficient; Energy savings; HVAC; Building

*Corresponding Author:ffdkd@uaf.edu, Ph:907-474-6094, Fax: 907-474-6141

7.1 Introduction

Energy costs have escalated rapidly in the last decade and there is a tremendous need for new kinds of heating/cooling fluids, which will increase heating-system thermal efficiency and reduce overall energy consumption. Nanofluids are the new generation of heat transfer fluids for various industrial and automotive applications, because of their excellent thermal performance [1]. Nanofluids are nanometer-sized particles (<100 nm) dispersed in a base fluid such as water, ethylene glycol or propylene glycol. Addition of high thermal-conductivity metallic nanoparticles (e.g., copper, aluminum, silicon and silver) increases the thermal conductivity of such mixtures; this enhances their overall energy transport capability [2].

Eastman et al. [3] showed a 40% increase in thermal conductivity by adding 0.3% (vol.) copper nanoparticles to ethylene glycol. Recently, Prasher et al. [4] demonstrated the increase in nanofluid thermal conductivity is primarily due to the convection caused by the Brownian movement of nanoparticles. Using nanofluids in heat transfer applications will provide numerous benefits including improved heat transfer, minimal clogging, and miniaturization of heat exchangers with microchannels. Using nanofluids will conserve energy by reducing the necessary pumping power [5]. These benefits make nanofluids a future generation heat transfer fluid.

In cold climates like those found in Alaska, Canada and other circumpolar regions, heat transfer fluids regularly encounter very low temperatures on the order of -40°C. It is a common practice to use ethylene or propylene glycol mixed with water in different proportions as a heat transfer fluid [6] for automobiles, heat exchangers and

baseboard heaters in houses. Inhibited ethylene glycol and propylene glycol are used as aqueous freezing point depressants and heat transfer media in cooling systems [7]. Their main attributes are the ability to lower the freezing point of water, low volatility and relatively low corrosivity. Ethylene glycol solutions have better heat transfer properties than propylene glycol solutions, especially at low temperatures. The commonly used mixture in cold climates is 60% by weight ethylene glycol and 40% by weight water [8], and the thermal performance could be enhanced by adding copper oxide metallic nanoparticles. These nanoparticles will affect the rheology of the mixture.

Major goals of this study are: 1) investigation of the rheology of various nanofluids, 2) determination of heat transfer coefficients and pressure loss of various nanofluids and 3) application of nanofluids to building heating systems.

Since no rheological data are currently available in the literature for such nanofluids at subzero temperatures, investigating and reporting on nanofluid rheology is very important to expanding nanofluid applications in cold regions. In the present paper, the viscosity of ethylene glycol and water with up to 6% by volume of copper oxide (CuO), aluminum oxide (Al_2O_3) and silicon dioxide (SiO_2) nanoparticles has been investigated at temperatures ranging from –35°C to 50°C. Furthermore, the experimentally measured convective heat transfer coefficient and pressure loss for these nanofluids are reported herein. Finally, these values are applied in a building case study to determine the surface area reduction of the heating system, volumetric flow reduction of the heat transfer fluid and pumping power reduction by using nanofluids.

7.2 Theory

Reynolds number for nanofluid flowing through a pipe is given by:

$$\mathrm{Re} = \frac{\rho_{nf} v D}{\mu_{nf}}. \tag{1}$$

The density of nanofluid, ρ_{nf} is given by [9]

$$\rho_{nf} = \phi\rho_s + (1-\phi)\rho_f . \tag{2}$$

Where the volumetric concentration is given by:

$$\phi = \frac{1}{(100/\phi_m)(\rho_p/\rho_f)+1}(100\%)\text{; where } \phi_m \text{ is mass fraction.} \tag{3}$$

The effective specific heat of nanofluids was given by [9]:

$$C_{pnf} = (1-\phi)C_{pf} + \phi C_{ps} . \tag{4}$$

However, Buongiorno [10] asserted that the specific heat of a nanofluid should be calculated assuming the nanoparticles and base fluid are in thermal equilibrium. He presented the equation as:

$$C_{pnf} = \frac{\phi\rho_s C_{ps} + (1-\phi)\rho_f C_{pf}}{\rho_{nf}} . \tag{5}$$

Volumetric flow rate of a nanofluid in the pipe is given by:

$$\dot{V}_{nf} = A_{P,i} v . \tag{6}$$

Pumping power ($\dot{W}$) to circulate the nanofluid is given by:

$$\dot{W} = \frac{\dot{V}_{nf}\,\Delta P}{\eta_{pump}} . \tag{7}$$

Where η_{pump} is pump efficiency, assumed here as 70%.

7.3 Experimental Setup

An experimental apparatus was built to study the heat transfer and flow characteristics of a conventional ethylene glycol/water mixture and various nanofluids flowing through a tube. The experimental setup is shown in Fig. 7.1 and consists of a pump, heat transfer test section, a counterflow cooling heat exchanger, flowmeter, a flow totalizer, differential pressure transducer, bypass valve, reservoir and a datalogger.

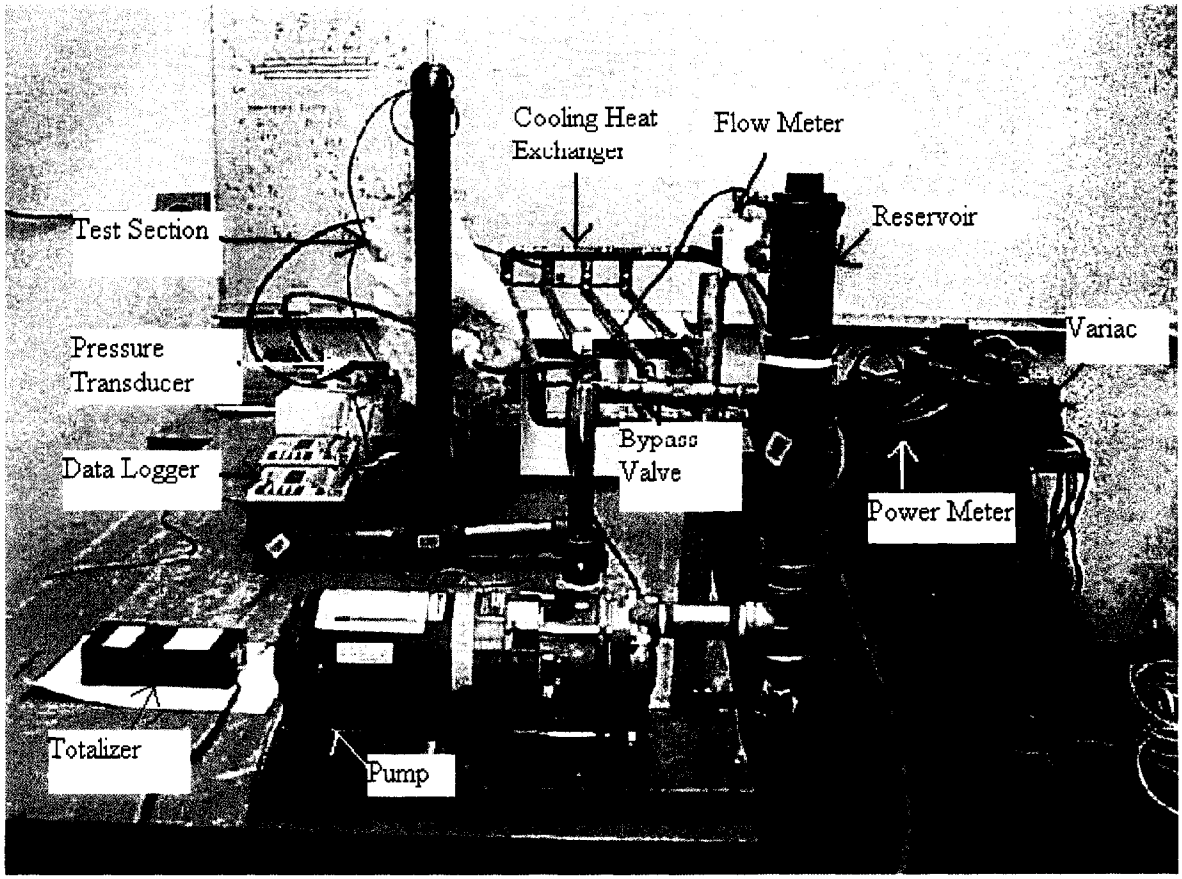

Figure 7.1. Experimental set up to investigate the convective heat transfer coefficient of nanofluids.

To hold down experimental costs, the test system was designed in such a way that a small amount of the nanofluid (approx. 2 liters) would be sufficient to investigate nanofluid heat transfer and fluid dynamic performance. The heat transfer test section is a straight copper tube with outside diameter of 4.76 mm (3/16 inch) and a length of 1 m (3.28 ft). Six type-T (copper-constantan) thermocouples mounted on the tube surface along the length measure the wall temperature. Two thermowells at the inlet and outlet of the test section measure the nanofluid's inlet and outlet temperature. Two plastic fittings at the inlet and outlet sections of the copper tube provide a thermal barrier to axial heat conduction. For turbulent flow, the hydrodynamic and thermal entry length in a tube is X/D = 10 [11]. In our experimental setup, this length is 4.76 cm beyond which all

measurements are taken to ensure that the measurements are in the fully developed regions. To attain the constant heat-flux boundary condition, the test section is heated electrically by four strip heaters capable of delivering 1 kW each. To measure the power input accurately, four power meters are connected to four variacs. To minimize the heat loss from the heat transfer test section to ambient air, the test system is insulated by 10 cm of fiber glass. A four-pass shell and tube counterflow heat exchanger cools the nanofluids to keep the inlet fluid temperature constant using shop water. A bypass valve controls the nanofluid circulation rate.

During the experiments, the tube wall temperatures, fluid inlet and outlet temperatures, volumetric flow rate of the fluid and power supplied are measured. Using these data, the convective heat transfer coefficient of the nanofluid (h_{nf}) is determined as:

$$h_{nf} = \frac{q''}{t_w - t_f} \tag{8}$$

Where t_w is the average wall temperature and t_f is the average of fluid inlet and outlet temperatures; q'' is the heat flux supplied to the test section. The heat flux provided can be equated to heat gained by fluid flowing through the test section. It is given as:

$$Q = \dot{m} C_p \Delta t_f \tag{9}$$

Before determining the nanofluid convective heat transfer coefficient, the apparatus was calibrated using deionized water. The experimental results were compared with the Dittus-Boelter equation [11] given below for fully developed turbulent flow.

$$Nu = 0.023 \mathrm{Re}^{0.8} \mathrm{Pr}^{0.4} \tag{10}$$

It was found that the experimental results and values obtained by the Dittus-Boelter equation are comparable. To ensure consistency, the test runs were repeated and the results were reproduced with similar accuracy. In the present study, the Reynolds number was varied from 3000 to 12000 due to limitations of experimental set-up.

7.4 Experimental Results

Eight to fourteen viscosity measurements were recorded at various shear rates at specific temperatures for each nanofluid volume concentration. From these results, the viscosity plot was generated (see Fig. 7.2), and it illustrates that viscosity is dependent on nanoparticle concentration. As the volume concentration increases, the nanofluid viscosity increases at a specific temperature. Also, nanofluid viscosity is very high at lower temperatures and decreases exponentially as temperature increases. This trend in viscosity was found by Kulkarni et al. [12]. For further heat transfer and pressure loss analyses, we have used these viscosity values at average fluid temperature to get more accurate results.

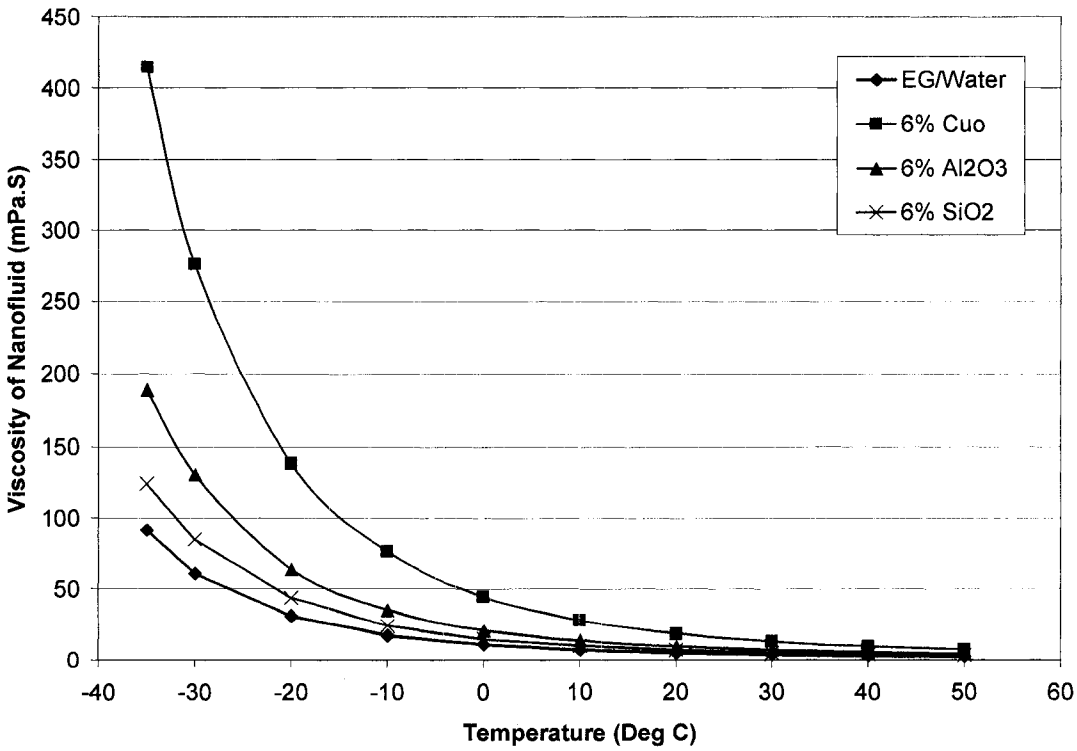

Figure 7.2. The viscosity variation of various nanofluids with respect to temperature.

Using equations (8) & (9), the heat transfer coefficient is calculated and plotted in relation to the Reynolds number (Fig. 7.3). In this analysis, we have considered the specific values for density and specific heat of nanofluids from equations (2) & (5). Fig. 7.3 depicts that as the Reynolds number increases, the heat transfer increases. For the same Reynolds number, the CuO nanofluid shows the greatest increase of the heat transfer coefficient followed by the Al_2O_3 and then by the SiO_2; all of the nanofluids have greater heat transfer coefficient than a conventional glycol/water mixture. As a typical value, at a fixed Reynolds number of 8000, copper oxide, aluminum oxide and silicon dioxide exhibit 61%, 35.4% and 18.4% enhancement in heat transfer coefficient compared with ethylene glycol/water, respectively.

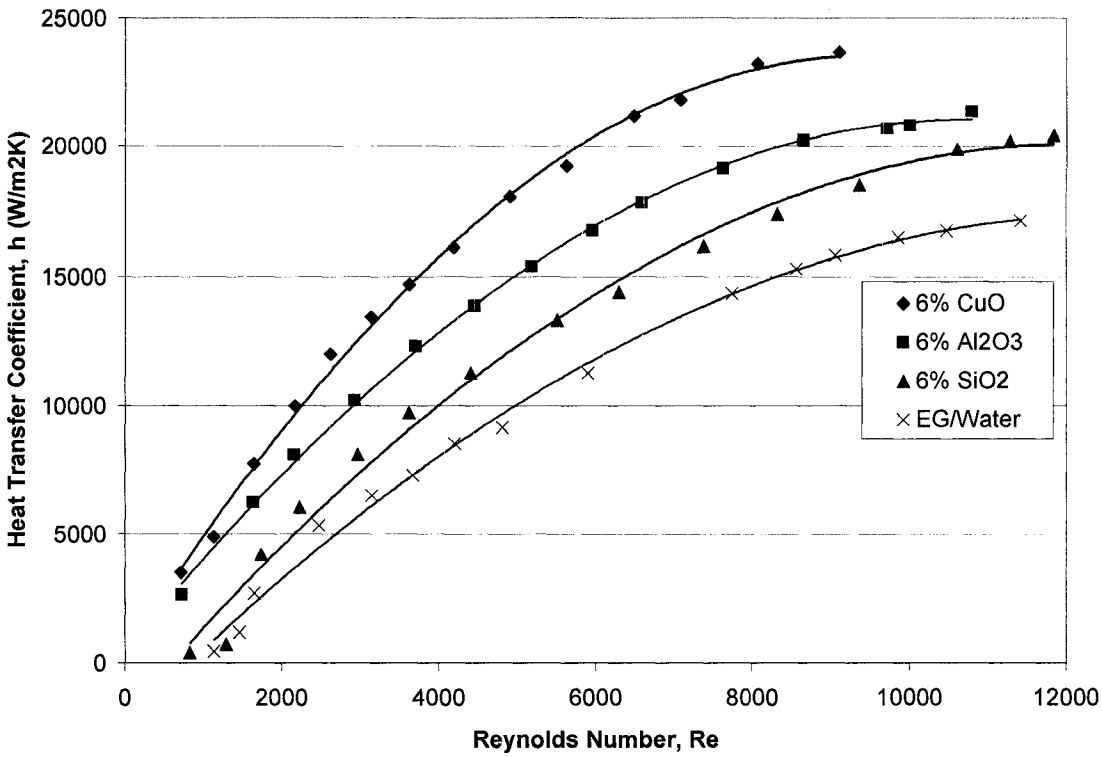

Figure 7.3. Effect of nanoparticle volume concentration on heat transfer coefficient.

For a fixed Reynolds number, as the heat transfer coefficient increases; there is also an increase in pressure loss. This increase in pressure loss is mainly attributed to an increase in the viscosity and density of the nanofluid. CuO nanofluid demonstrates the

highest viscosity and density and therefore, has the highest pressure loss at a given Reynolds number (Fig. 7.4). Nanofluid pressure loss and heat transfer performance should be carefully considered when choosing a nanofluid for a particular application.

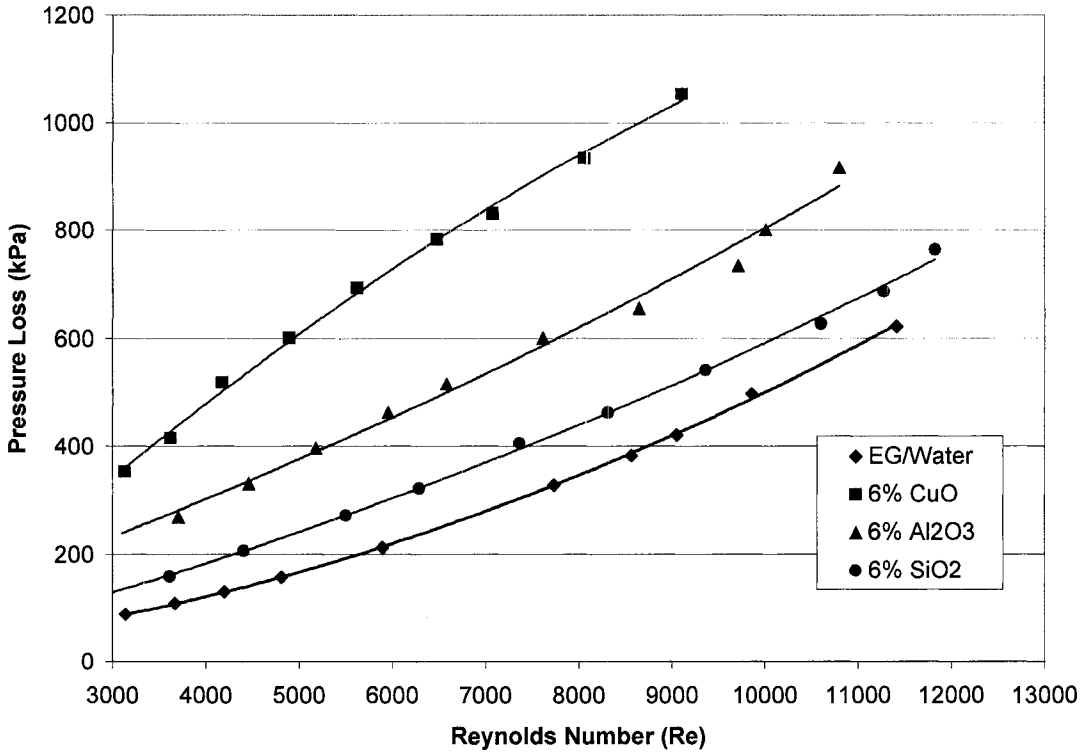

Figure 7.4. Pressure loss of various nanofluids with respect to conventional glycol/water mixture.

After characterizing different nanofluids for their heat transfer and fluid dynamic performance, we performed a detailed analysis of the energy requirement for a cold climate building. In this analysis, we held constant thermal performance (overall heat transfer coefficient) for all fluids. In other words, the inside heat transfer coefficient is maintained the same for all fluids. At a Reynolds number of 8000, the base fluid has a 14,400 W/m^2K convective heat transfer coefficient (see Fig. 7.3). Taking this as a reference, an analysis was carried out for a constant inside heat transfer coefficient of this magnitude for the other nanofluids. Based on the results from earlier experiments (Fig. 7.3), the corresponding Reynolds numbers for this heat transfer coefficient of the

different fluids was used to determine velocity, volumetric flow rate and pumping power. The results were compared with the ethylene glycol and water mixture. These calculations used the same viscosity values reported in Fig. 7.2 and were taken at the average fluid temperature. This analysis is for the test section of 4 mm I.D. and 1 m length. These results are summarized in Table 7.1.

Table 7.1. Comparison of the performance of various nanofluids with conventional 60:40 ethylene glycol/water mixture.

Type of Fluid **Parameters**	**60/40 Ethylene Glycol/Water**	**6% Copper Oxide**	**6% Aluminum Oxide**	**6% Silicon Dioxide**
Heat Transfer Coefficient (W/m^2K)	14,400	14,400	14,400	14,400
Reynolds Number (Re)	8,000	3,600	4,500	6,290
Pressure Loss (kPa)	346	430	340	322
Viscosity (mPa.s)	1.1	2.27	1.41	1.17
Density (kg/m^3)	1038	1366	1192	1116
Specific Heat (J/kgK)	3120	2339	2718	2821
Velocity (m/s)	2.12	1.5	1.33	1.65
Volumetric Flow Rate (10E+5 m^3/s)	2.66	1.89	1.67	2.07
Reduction in Volumetric Flow Rate (%)	.....	28.95	37.22	22.18
Power (W)	11.500	10.16	7.1	8.33
Power Advantage (W)	.....	1.34	4.4	3.17
Power Advantage (%)	.....	11.65	38.26	27.57
Mass Flow Rate (kg/s)	0.028	0.0258	0.0199	0.023
Reduction in Mass Flow Rate (%)	.....	6.495	27.904	16.333

Consider a loop containing a furnace and the heating coil in the duct of a building. Let $\dot{Q}$ be the heat absorbed by the fluid from the furnace and delivered into the building. To deliver the heat with nanofluid, mass flow rate ($\dot{m}$) will be lower, specific heat will be lower and therefore the temperature rise of the nanofluid as it circulates through the furnace will be higher. A lower mass of nanofluid will heat to a higher temperature. Therefore, nanofluids will run hotter than the conventional fluids in the loop. Similarly, the temperature drop of the nanofluid in the fin-tube section will also be higher; however, as the fluid exits the furnace the temperature will also be higher.

Having hotter nanofluid has two advantages: (i) The effective mean temperature difference between the fluid and the air in the fin-tube coil is higher causing more heat transfer (ii) From experiments it has been found that for nanofluids the specific heat increases (see Fig. 8.5) with temperature and the thermal conductivity increases substantially with temperature. Thus nanofluids provide better heat transfer at higher temperature. Viscosity and density diminishes at higher temperature reducing pressure loss. These characteristics of nanofluids are being taken advantage in the research at Argonne National Lab in the size reduction of radiators in heavy vehicle cooling systems for Class 7-8 truck where circulating fluid temperature is raised somewhat higher than that of the conventional coolants.

From Table 7.1, it can be observed that for same heat transfer coefficient (14,400 W/m^2K), the conventional fluid corresponds to the highest Reynolds number of 8000. Conversely, for the same heat transfer coefficient, the copper oxide nanofluid has the lowest Reynolds number of 3600, the aluminum oxide nanofluid is 4500, and the silicon dioxide nanofluid is 6290. The density (equation 2), specific heat (equation 5) and viscosity (Fig. 7.2) values of nanofluids are summarized in Table 7.1. For the same heat transfer coefficient the volumetric flow rate decreases by 29% for the CuO nanofluid, 37.2 % for the Al_2O_3 nanofluid and 22.2 % for the SiO_2 nanofluid. The volume reduction required for a heat transfer fluid will also reduce the inventory and fluid production.

Accordingly from equation (7), the pumping power savings are 11.7 % for the CuO nanofluid, 38.3 % for the Al_2O_3 nanofluid and 27.6 % for the SiO_2 nanofluid. Reducing pumping power will lead to less carbon dioxide (CO_2) release into atmosphere. Similarly, this reduces the mass flow rate by 6.5 % for the CuO nanofluid, 28 % for the Al_2O_3 nanofluid and 16.3 % for the SiO_2 nanofluid. Therefore, it turns out that Al_2O_3 nanofluid is the fluid of choice among these candidates.

7.5 Case Study: Nanofluid in Air Heat Exchanger

In this case study, we have considered the conventional method of heating a building with nanofluids by heating air in duct coils through a bank of tubes with finned surfaces. The coil consists of rectangular-plate aluminum fins bonded to copper tubes. The tubes are arranged in line in adjacent rows. The heat transfer rate ($\dot{Q}$) from a heating coil circulating nanofluid to air in a building is expressed as [8]:

$$\dot{Q} = U_o A_o \Delta t_m \ . \tag{10}$$

Rate of heat transfer from the nanofluid to the pipe is given by [8]:

$$\dot{Q} = h_i A_{P,i} (t_f - t_{P,i}) . \tag{11}$$

Rate of heat transfer through the pipe wall is given by:

$$\dot{Q} = \frac{k_P A_{P,m} (t_{P,i} - t_{P,o})}{x_P} . \tag{12}$$

Rate of heat transfer from the pipe and fin to the air is given by:

$$\dot{Q} = h_{c,o,P} A_{P,o} (t_{P,o} - t) + h_{c,o,F} A_F (t_{F,m} - t) . \tag{13}$$

Rate of heat transfer for the entire process is:

$$\dot{Q} = U_o A_o (t_f - t) . \tag{14}$$

Assuming $h_{c,o,P} = h_{c,o,F} = h_{c,o}$, we have:

$$\dot{Q} = h_{c,o} (A_{P,o} + \eta A_F)(t_{P,o} - t) . \tag{15}$$

From Eqs (11), (12), (14) and (15), we obtain:

$$U_o = \frac{1}{\frac{A_o}{A_{P,i}h_i} + \frac{A_o x_P}{A_{P,m}k_P} + \frac{1-\eta}{h_{c,o}(A_{P,o}/A_F + \eta)} + \frac{1}{h_{c,o}}} \tag{16}$$

Subscripts *i* and *o* represents inner and outer surface area. Typical value for fin efficiency for aluminum fins is about 0.75.

Typical data are given as:

$A_{P,i} = 0.03536$ m^2, $A_{P,o} = 0.03658$ m^2, $A_{P,m} = 0.0375$ m^2, $A_F = 0.948$ m^2, $A_o = 0.09845$m^2, $h_{c,o} = 57$ W/m^{2}K and fin efficiency $\eta = 0.75$.

We considered a specific Reynolds number of 4000 and read the corresponding convective heat transfer coefficients, h for all nanofluids from Fig. 7.3 which are summarized in Table 7.2. Based upon the heat exchanger geometry and Eqs. (10) through (16) our calculation yields an overall heat transfer coefficient U_o. The U_o is found to be the highest for CuO nanofluid. Maintaining a higher ΔT_f for nanofluids, reduction in heat transfer surface can be achieved.

Table 7.2. Comparison of the reduction in heat transfer surface area for various nanofluids with a conventional 60:40 ethylene glycol/water mixture.

Component	**60:40 Ethylene Glycol/Water**	**6% Copper Oxide**	**6% Aluminum Oxide**	**6% Silicon Oxide**
Reynolds Number	4000	4000	4000	4000
Inside heat transfer coefficient, h_i	3407	10,000	8,000	4,900
Inside Surface Resistance x 10^3 $R_i = A_o / A_{P,i} h_i$	8.17	2.78	3.475	5.67
Pipe Wall Resistance x 10^5 $R_P = A_o x_P / A_{P,m} k_P$	4.8	4.8	4.8	4.8
Fin Resistance x 10^3 $R_F = \frac{1}{h_{c,o}}(\frac{1-\eta}{\eta + A_{P,o}/A_F})$	6.16	6.16	6.16	6.16
Outside Surface Resistance x 10^3 $R_o = 1/h_{c,0}$	17.5	17.5	17.5	17.5
Total Resistance x 10^3 $R_t = R_i + R_P + R_F + R_o$	31.88	26.48	27.175	29.37
Overall Heat Transfer Coefficient $U_o = 1/R_t$	31.37	37.76	36.8	34.04
% Reduction in Area	.....	20.37	17.3	8.5

7.6 Conclusions

1. Nanofluid viscosity decreases exponentially as temperature increases from a subzero value. The CuO nanofluid has the highest viscosity followed by the Al_2O_3 nanofluid and then by the SiO_2 nanofluid.
2. The CuO nanofluid has the highest heat transfer coefficient followed by the Al_2O_3 nanofluid and the SiO_2 nanofluid. For example, at Re = 4000, h_{nf} is 10,000 W/m^2K for the CuO nanofluid, 8,000 W/m^2K for theAl_2O_3 nanofluid and 4,900 W/m^2K for the SiO_2 nanofluid.
3. Pressure loss is highest for the CuO nanofluid, followed by the Al_2O_3 nanofluid and the SiO_2 nanofluid.
4. Use of nanofluids can reduce the volumetric flow rate, mass flow rate and the pumping power for the same heat transfer rate at a higher fluid temperature.
5. Using nanofluids to heat buildings can reduce the size of the heat exchanger and reduce the accompanying pressure loss.
6. Similar benefits can be derived by considering nanofluids in place of chilled water in building cooling coils. An investigation similar to the one presented in this paper can quantitatively establish the benefits.
7. Using nanofluids will reduce material volume and thus reduce environmental pollution.

7.7 Acknowledgement

Financial assistance from the Arctic Region Supercomputing Center and the Dean of the Graduate School at University of Alaska Fairbanks is gratefully acknowledged. Partial funding from the UAF Department of Mechanical Engineering is greatly acknowledged.

7.8 Nomenclature

A	Area, m^2
C_p	Specific heat, J/kg K
D	Diameter of the tube, m
h	Convective heat transfer coefficient, W/m^2 K
k	Thermal conductivity, W/m K
$\dot{m}$	Mass flow rate, kg/s
Nu	Nusselt number
Pr	Prandtl number
$\dot{Q}$	Heat transfer rate, W
q''	Heat flux, W/m^2
Re	Reynolds number
Δt_m	Log mean temperature difference
v	Mean velocity, m/s
$\dot{V}$	Volumetric flow rate, m^3/s
x	Thickness, m

Greek Letters

μ	Coefficient of dynamic viscosity of the fluid, kg/m s
ϕ	Particle volume concentration
η	Efficiency
ρ	Density of the fluid, kg/m^3

Subscripts

i	Inside
f	Fluid
F	Fin
m	Mean

nf	Nanofluid
o	Outside
P	Pipe
s	Solid material
w	Wall

7.9 References

1. Eastman JA, Phillpot SR, Choi SUS, Keblinski PK. Thermal transport in nanofluids. Annual Review in Material Research. 2004; 34: 219-246.

2. Xuan Y, Li Q. Investigation on convective heat transfer and flow features of nanofluids. ASME Journal of Heat Transfer 2003; 125: 151-155.

3. Eastman JA, Choi SUS, Li S, Yu W, Thompson LJ. Anomalously increased effective thermal conductivities of ethylene glycol-based nanofluids containing copper nanoparticles. Applied Physics Letters 2001; 78(6): 718-720.

4. Prasher R, Bhattacharya P, Phelan PE. Thermal conductivity of nanoscale colloidal solutions (nanofluids). Physical Review Letters, 2005; PRL 94, 025901.

5. Choi SUS, Zhang ZG, Keblinski P. Nanofluids. Encyclopedia of Nanoscience and Nanotechnology, 2004; 6: 757-773.

6. Mcquiston FC, Parker JD, Spitler JD. Heating, ventilating, and air conditioning. New York: John Wiley & Sons Inc.; 2000.

7. ASHRAE Handbook 1985 Fundamentals, American Society of Heating, Refrigerating and Air-Conditioning Engineers Inc., Atlanta; 1985.

8. Kuehn TH, Ramsey JW, Threlkeld, JL. Thermal Environmental Engineering. New York: Prentice Hall Inc.; 1998.

9. Pak BC, Cho YI. Hydrodynamic and heat transfer study of dispersed fluids with submicron metallic oxide particles. Experimental Heat Transfer 1998; 11: 151-170.

10. Buongiorno J. Convective transport in nanofluids. ASME Journal of Heat Transfer 2006; 128: 240-250.

11. Bejan A. Heat Transfer. New York: John Wiley & Sons Inc.; 1993.

12. Kulkarni DP, Das DK, Chukwu GA. Temperature dependent rheological property of copper oxide nanoparticles suspension (nanofluid). Journal of Nanoscience and Nanotechnolgy 2006; 6: 1150-1154.

CHAPTER EIGHT

Application of Aluminum Oxide Nanofluids in a Diesel Electric Generator as Jacket Water Coolant

Devdatta P. Kulkarni, Daniel Oliva, Debendra K. Das*
Department of Mechanical Engineering
University of Alaska Fairbanks
P.O. Box 755905, Fairbanks, AK, 99775-5905, USA.

Abstract

This paper presents a study on nanofluids applications, such as a coolant in a diesel electric generator (DEG). Specific heat measurements of aluminum oxide nanofluids with various particle concentrations are presented, demonstrating a reduction in values with an increase in particle concentration and temperature. Experiments were performed on the DEG to assess the effect of nanofluids on cogeneration efficiency. The investigation shows that applying nanofluids results in a reduction of cogeneration efficiency. This is due to the decrease in specific heat, which influences the waste heat recovery from the engine. However, it was found that the efficiency of the waste heat recovery heat exchanger increases for nanofluids, due to their superior convective heat transfer coefficient.

Under review, Applied Thermal Engineering, April 2007.

Key Words: Nanofluids; Specific Heat; Cogeneration; Efficiency; Diesel Electric Generator

*Corresponding Author:ffdkd@uaf.edu, Ph:907-474-6094, Fax: 907-474-6141

8.1 Introductory Remark

The objectives of the experiments on the diesel electric generator (DEG) described in this chapter was to explore a large array of performance parameters of various nanofluids of different concentrations. One of the goals was to compare accurately the amount of heat recovery from the engine with conventional fluids and nanofluids as coolants in the load range of zero load to 30 kW in steps. At the same amount of engine load, would a nanofluid carry more heat than the regular fluid? Since the cooling system is a heat exchanger, whose cooling water flow rate we can vary, it was used to simulate radiators varying in size. Furthermore, jacket fluid temperature at emission during the start-up period for various fluids was examined as a function of time.

The scope became too large, and due to the limited time available, only a preliminary test could be completed. The test results showed us several shortcomings of the existing experimental setup. They need to be modified in the future. More precise instrumentation is necessary for the setup to obtain meaningful results. Some of the flaws observed were: the jacket fluid flow meter might be faulty, the cooling water flow rate could not be maintained constant during test runs, and the temperature sensors did not have the resolution to detect the difference in heating time between nanofluids and conventional fluids.

The results that follow may have large experimental errors and these tests should be repeated after more precise and additional instrumentation is installed. Recommended instrumentation includes temperature sensors in the engine jacket channel,

precise flow meters in the cooling water and engine coolant loops, temperature sensors and heat flux gauges on engine surfaces and an exhaust gas monitor for emission measurement.

8.2. Introduction

Cooling is one of the most important technical challenges facing numerous industries such as automobiles, electronics and manufacturing. New technological developments are increasing thermal loads and requiring faster cooling. The conventional methods in increasing the cooling rate (fins and microchannels) are already stretched to their limits. Hence, there is an urgent need for new and innovative coolants to achieve this high performance cooling [1, 2]. Thermal conductivities of traditional heat transfer fluids, such as engine coolants, lubricants and water are very low. With increasing global competition, industries have a strong need to develop energy efficient heat transfer fluids with significantly higher thermal conductivities than the available fluids. Also, government agencies like the Environmental Protection Agency (EPA) are imposing more stringent criteria for pollutant and automobile emissions. The new coolants with their higher thermal performance will reduce the overall size of heat exchangers/radiators and may decrease vehicle fuel consumption.

Nanofluids are a novel concept; heat transfer fluids containing suspended nanoparticles have been developed to meet such cooling challenges. Nanofluids are a new class of solid-liquid composites consisting of nanometer sized (<100 nm) solid particles suspended in heat transfer fluids such as water, ethylene and propylene glycol. The improvement of lubricity by adding nanoparticles to engine oil is under investigation [3].

Choi et al. [4] showed that nanofluids have the potential to be the next generation of coolants for vehicle thermal management due to their significantly higher thermal conductivities. Several researchers [5-9] showed that the convective heat transfer

coefficient increases substantially for nanofluids. The heat rejection requirements of automobiles and trucks are continually increasing, due to trends toward more powerful outputs.

Heat transfer directly affects engine performance, fuel efficiency, materials selection and emissions. Managing the heat generated during combustion is particularly important in improving engine life, oil cooling and climate control. For electric and hybrid vehicles, thermal management of advanced batteries will also be critically important. Improved thermal management systems for advanced vehicles require more compact heat exchangers, innovative heat transfer schemes and environmentally friendly fluids with improved heat transfer properties.

Nanofluids with improved properties could result in smaller, more efficient advanced vehicles. The benefits of improved heat exchangers and heat transfer devices using nanofluids are: reduced weight, which will improve fuel economy; smaller components, which take up less room under the hood and allow for greater latitude in aerodynamic styling; more effective cooling and increased component life. Additionally, mining efforts will be lower as less metal is required, minimizing the environmental impact and saving energy in metal production. By reducing the size, the solid waste disposal problem is diminished at the end of the useful life cycle of the heat transfer systems.

Utilizing nanofluids because of the benefits described above, this study focuses on evaluating the cogeneration and heat exchanger efficiency of a diesel generator with nanofluids as the coolant.

8.3 Experimental Setup for Specific Heat Measurement

Since specific heat contributes to faster and improved rates of heat transfer, accurate measurements are essential. The experimental setup for measuring the specific heat of the aluminum nanoparticles dispersed in 50:50 inhibited ethylene glycol and water mixture is shown in Figure 8.1. The apparatus consists of a plastic container, in which aluminum oxide nanofluids are tested. Aluminum oxide nanofluids are heated from 25°C to 70°C by using an electrical immersion heater (shown in Figure 8.1). Four copper–constantan thermocouples are placed at equal distances from the heating element to monitor the temperature increase of the nanofluids. These thermocouples are connected to a data logger that records the temperature data at 5-second intervals. The container is heavily insulated to eliminate the heat loss to the surroundings. A variac is used to supply constant wattage to the immersion heater and the power input into the nanofluid is monitored by a power meter.

8.3.1 Benchmark Test Case for Specific Heat Measurement:

To verify the accuracy of the specific heat measurement apparatus and the experimental procedure, the specific heat of pure water was measured.

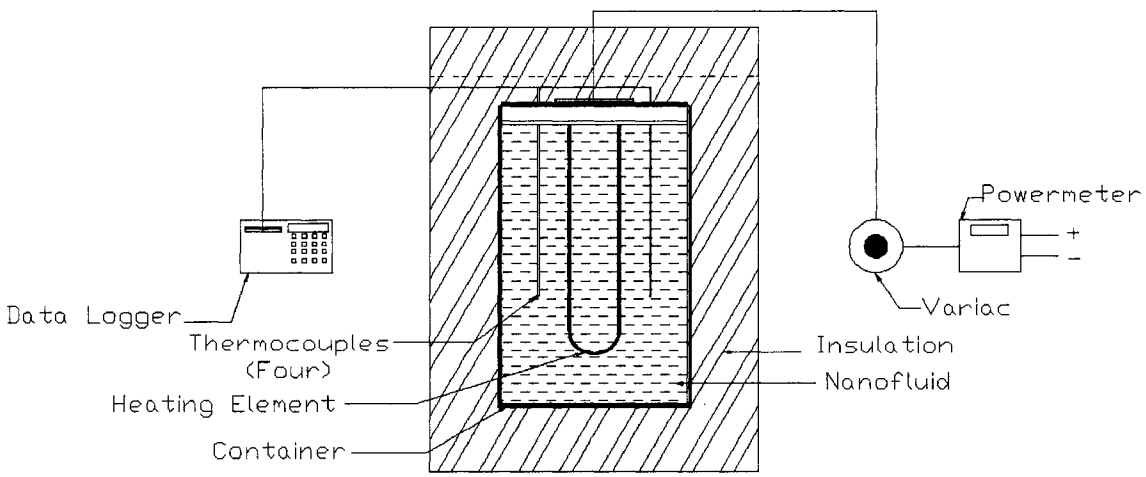

Figure 8.1. Experimental setup for specific heat measurement of aluminum oxide nanofluids.

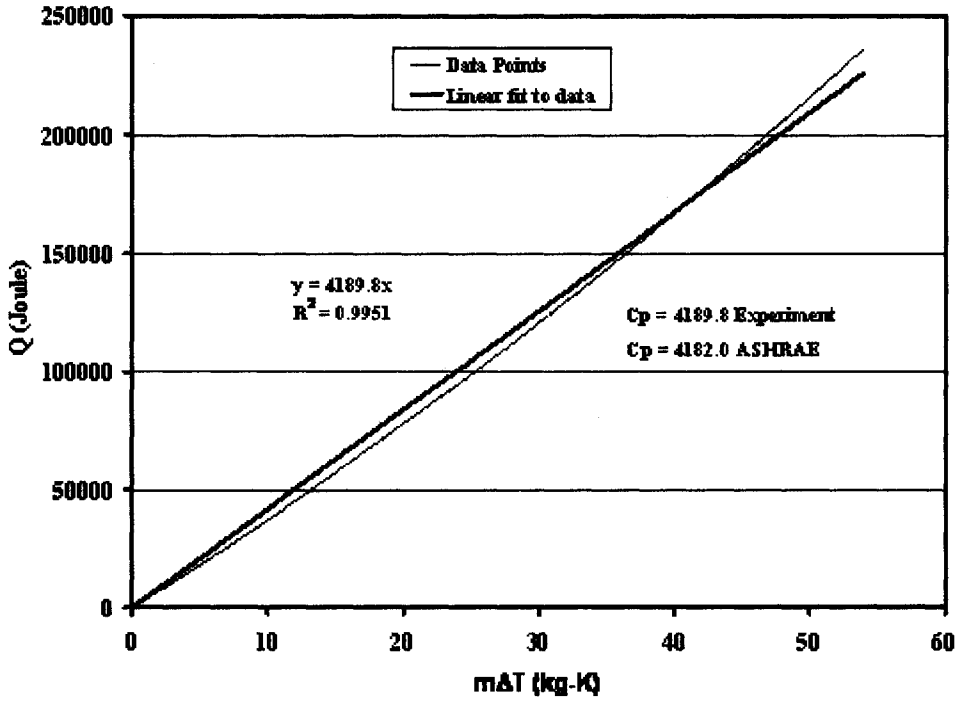

Figure 8.2. Specific heat of water obtained from the experimental setup.

Water of mass 1.25 kg at 25°C was used in the container for the specific heat measurement. A constant heat of 35.5 W was supplied to the heating element to increase the temperature of water to 70°C. The temperature change was recorded every 5 seconds using thermocouples and a data logger. The specific heat of water and each tested nanofluid was calculated from:

$$Q_s = MC_{Pnf}\Delta T \tag{1}$$

The slope of the straight line in Figure 8.2 is given by heat energy Q_s (Joule) input versus product of mass (kg), and the temperature difference (Kelvin) gives the specific heat of the fluid. The obtained specific heat of the water was then compared to the value from American Society of Heating, Refrigerating and Air Conditioning Engineers (ASHRAE) handbook [10]. The experimental value only differed by ± 0.2%, when compared with the ASHRAE value.

8.3.2 Discussion of Specific Heat Results

After confirming the readings from the specific heat measurement apparatus with water, specific heat measurements for different volume concentrations of aluminum oxide nanofluids in 50:50 ethylene glycol and water mixture were carried out.

The effective specific heat of nanofluids is given by Pak and Cho[11]:

$$C_{pnf} = (1-\phi)C_{pf} + \phi C_{ps} \tag{2}$$

However, according to Buongiorno [12], the specific heat of a nanofluid should be calculated assuming the nanoparticles and base fluid are in thermal equilibrium. He presented the equation as:

$$C_{pnf} = \frac{\phi\rho_s C_{ps} + (1-\phi)\rho_f C_{pf}}{\rho_{nf}} \tag{3}$$

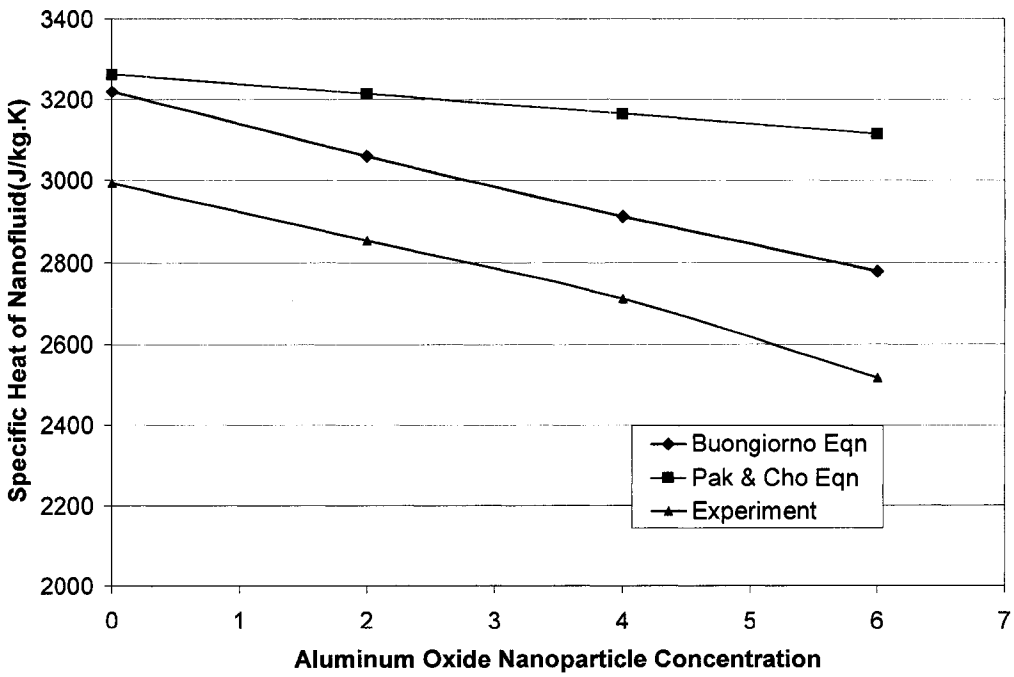

Figure 8.3. Comparison of experimental and theoretical values of specific heat for aluminum oxide nanofluids at various concentrations suspended in 50:50 ethylene glycol and water mixture at 25°C.

Figure 8.3 displays the specific heat variation for varying concentrations of aluminum oxide nanofluids. The experimental values are compared with the theoretical correlations presented in Pak & Cho [11] and Buongiorno [12]. It shows that Buongiorno's correlation is in better agreement than Pak and Cho's correlation with the experimental data. As the particle volume concentration increases, the specific heat of the aluminum nanofluids decreases. It implies for higher concentrations of aluminum nanofluid, less heat input is required to increase the temperature of the nanofluid, or with the same heat input, the time required to reach 70°C will diminish. The difference in the specific heat value (~7%) from ASHRAE [10] at 0% concentration is due to the presence of the inhibitor in commercially available fluids.

Time trend versus temperature for various nanofluids at a constant heat input of 35.5 W is shown in Figure 8.4. If the time required to heat reduces, this will be very beneficial in automobiles, especially in arctic or subarctic regions. By employing nanofluids as jacket water, the engine will heat up faster and may result in less emission to the environment. If nanofluids are successful as vehicle coolant, radiators must be sized based on nanofluid maximum flow rate using properties at operating temperatures for the most severe loading condition of the engine so that it does not overheat.

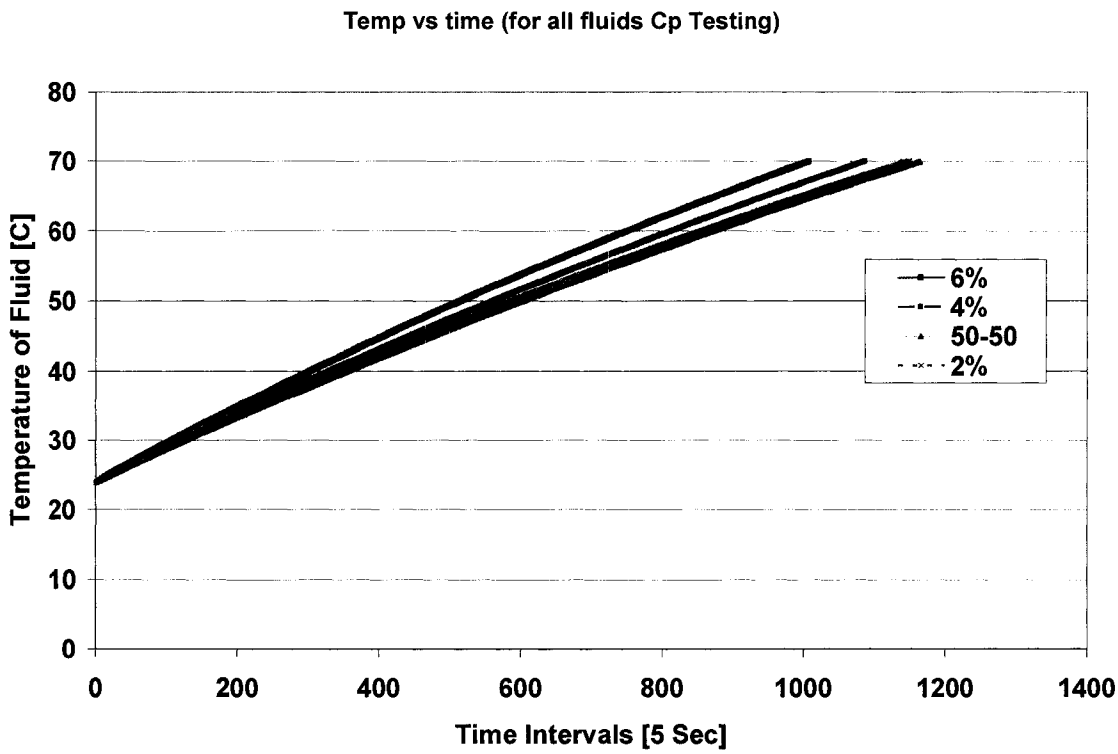

Figure 8.4. Time versus temperature to heat aluminum nanofluids with varying concentrations in 50:50 ethylene glycol and water solution.

8.3.3 Temperature Dependent Specific Heat

From the experiments, it was determined that as the temperature of the nanofluid increased, the specific heat of the nanofluids also increased (Figure 8.5). ASHRAE [10] also shows that the specific heat of glycol and water mixtures increases with temperature. This has a very profound impact: Most of the heat transfer fluids experience a temperature greater than room temperature during their operation. Therefore, there is a need to find the temperature dependency of the nanofluid specific heat. Until now, all the numerical and experimental analyses in various literatures [13-18] used a constant value of the specific heat at 20°C. This will cause substantial errors in their results.

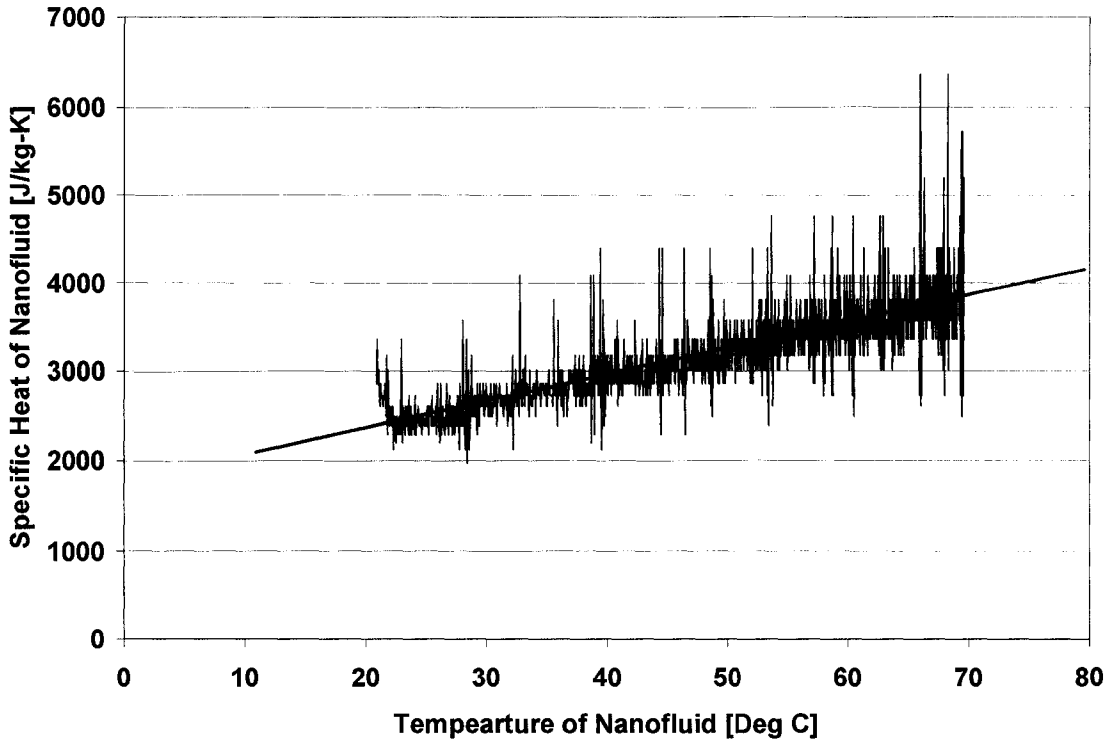

Figure 8.5. Temperature dependent specific heat of 6% aluminum oxide in ethylene glycol/water nanofluids.

8.4 Cogeneration Efficiency

In the case of a diesel generator, the efficiency is defined by the ratio of the electrical power produced and the energy rate associated with the fuel input to the generator. However, this efficiency is quite low, often in the range of 25-38%, due to the large amount of waste heat in the system. A method to increase the overall efficiency of a diesel engine is to capture some of the escaping heat energy with a heat exchanger, and utilize that energy to produce a useful deliverable. Cogeneration efficiency, η_{cogen}, is defined as follows:

$$\eta_{cogen} = (Electrical\ Power + Rate\ of\ Heat\ Recovered)/\ Fuel\ Consumption\ energy\ rate \quad (4)$$

Cogeneration efficiency can be as high as 85%. This is a substantial and very useful increase in efficiency, especially in arctic regions where the heat energy is useful to heat buildings. In warmer climates, the heat energy can be collected and used to meet other process needs such as cooling via absorption refrigeration systems.

The efficiency equations are derived by taking the ratio of the desired output to the required input and are as follows:

Heat rate from diesel fuel is given by:

$$\dot{Q}_H = \dot{V}_f \, H_V \tag{5}$$

The heating value used in this paper reflects a lower heating value since the exhaust gas temperatures were about 400°C, and condensation during combustion was not found.

Electrical efficiency is given as:

$$\eta_{el} = \frac{\dot{W}_{el}}{\dot{Q}_H} \tag{6}$$

Cogeneration efficiency is given as:

$$\eta_{cogen} = \frac{\dot{W}_{el} + \dot{Q}_{JW}}{\dot{Q}_H} \tag{7}$$

Mass flow rate of jacket water is calculated as follows:

$$\dot{m}_{JW} = \rho_{nf} \dot{V}_{JW} \tag{8}$$

Density of nanofluids is given as:

$$\rho_{nf} = (1-\phi)\rho_f + \phi\rho_s \tag{9}$$

Jacket water collects the heat from shop water. Heat transfer by shop water, $\dot{Q}_{SW}$, and the jacket water, $\dot{Q}_{JW}$, are given by:

$$\dot{Q}_{JW} = \dot{m}_{JW} C_{pJW} (T_{JW-in} - T_{JW-out}) \tag{10}$$

$$\dot{Q}_{SW} = \dot{m}_{SW} C_{pSW} (T_{SW-out} - T_{SW-in}) \tag{11}$$

8.5 Experimental Description

The test apparatus as shown in Figure 8.6 consisted of a 45 kW generator-set unit composed of a Mitsubishi diesel engine coupled with a Stamford generator unit. This is an inline-four cylinder diesel engine with turbocharger and liquid cooling. The generator set was connected to an AC system with a 3 phase, 4 wire system, with a power factor $\geq$ 0.80. A shell and tube heat exchanger was used to cool the jacket water, and the electrical loading was provided by a set of Avtron resistor load banks. A data logger was connected such that the volumetric flow rates of the jacket water and the cooling water supply (shop water) were recorded (measured via turbine flow meters). Temperatures of both jacket and shop water inlets and outlets were recorded using type-T thermocouples, as well as the exhaust gas temperature using a type-K thermocouple. Fuel consumption was logged as well via a standing reservoir style tank with a balanced series of load cells that transduce the current tank fluid mass into a volumetric measurement. The readings were taken and stored in a data logger in five-second intervals.

The selected nanofluid for this experiment was aluminum oxide with 45 nm average diameter nanoparticles mixed with 50:50 ethylene glycol and water (EG-W) mixtures with varying volume concentrations up to 6%.

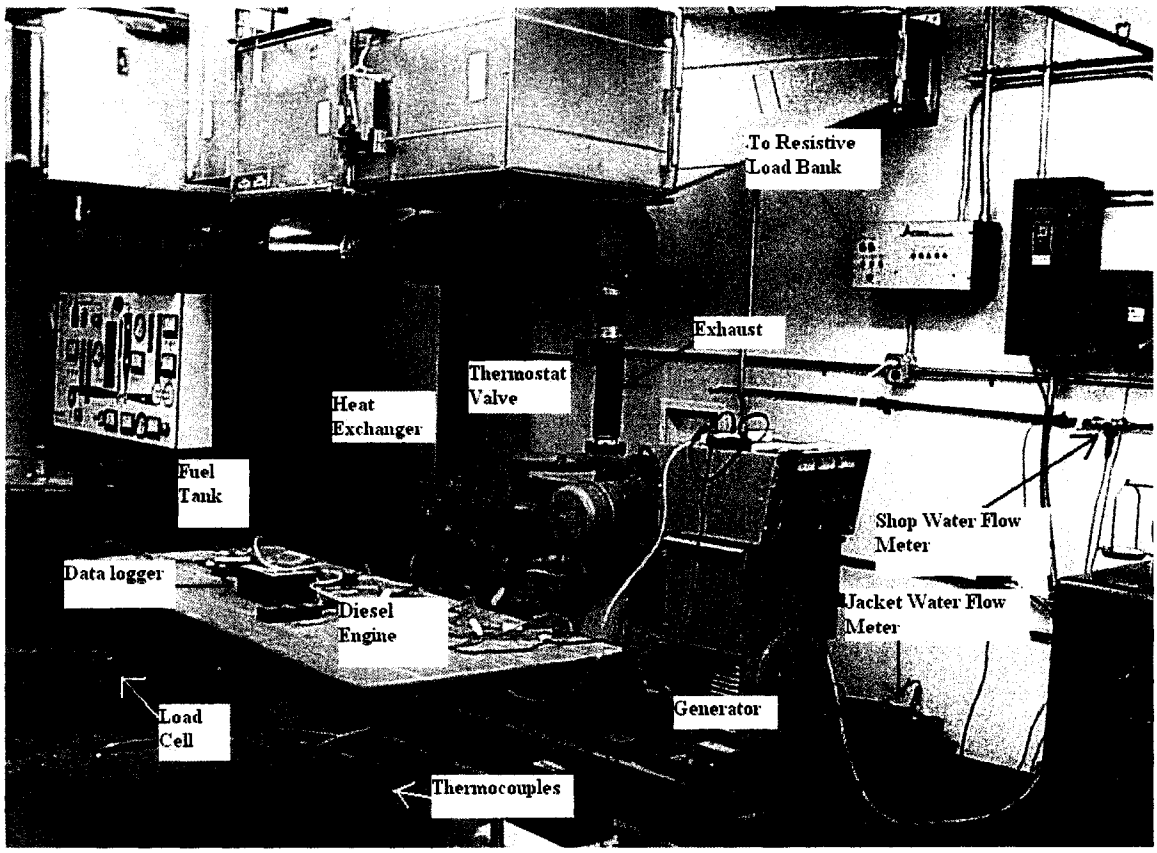

Figure 8.6 Experimental setup to measure cogeneration efficiency for a diesel engine generator.

8.6 Experimental Results

Figure 8.7 shows the electrical output of the generator versus time. For the first five minutes, the generator was running in idling condition, i.e., no electrical load was applied. When there was no obvious electrical load, a small parasitic load was observed. In 5-minute intervals, the electrical load was increased to 5 kW, 20 kW and finally to 30 kW. The same procedure was followed for all concentrations of Al_2O_3 nanofluids tested. We investigated the performance of nanofluids at 30 kW, when a steady state condition for jacket water flow rate and temperatures was reached.

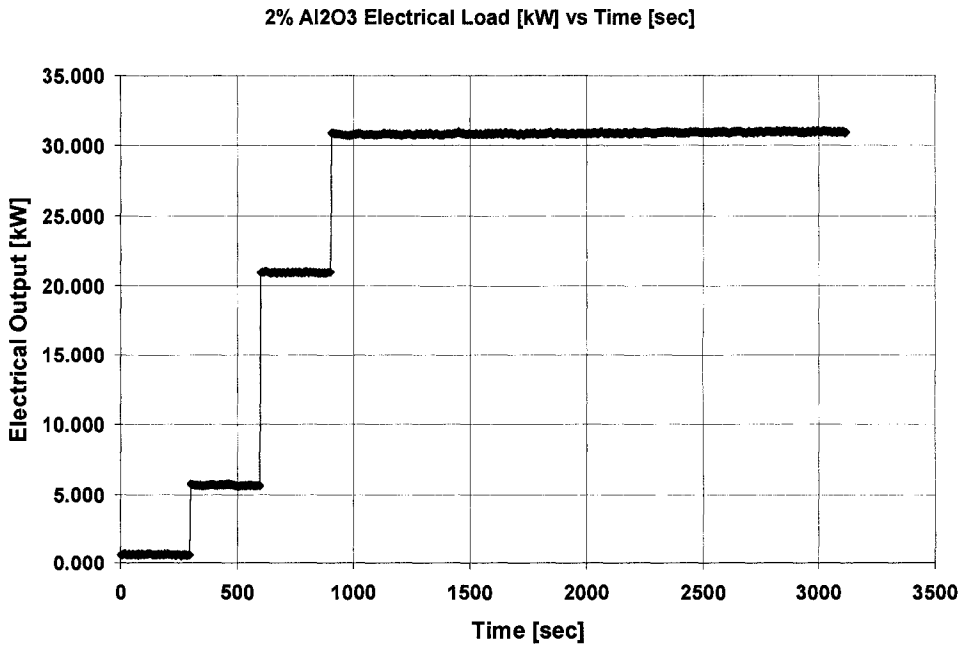

Figure 8.7. Loading profile on the diesel engine.

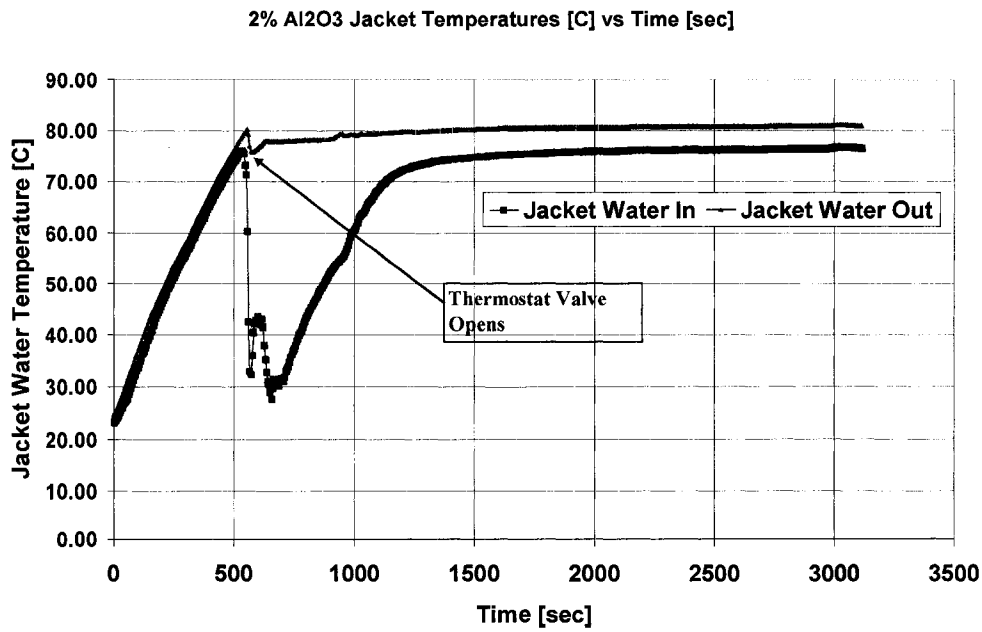

Figure 8.8. Temperature of "jacket water in" and "jacket water out" versus engine running time.

It was seen from Figure 8.8, when the engine started, the jacket water temperature was less than the set thermostatic valve temperature of 80°C. Hence, up to 6 minutes (540 seconds) the temperature of jacket water increased. As soon as the jacket water outlet temperature reached 80°C, the thermostatic valve opened and jacket water started circulating. There is a sudden decrease in jacket water inlet temperature as the cold fluid sitting in the radiator started flowing (see Figure 8.8).

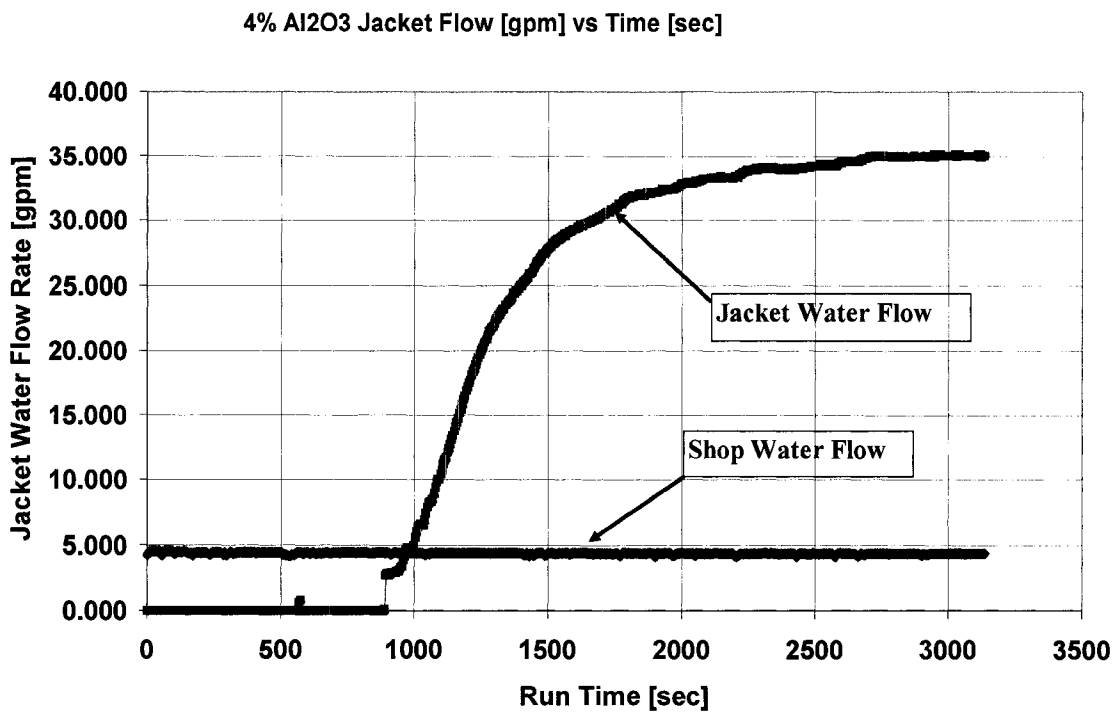

Figure 8.9. Shop water and jacket water flow rates versus time.

Figure 8.9 displays the flow rate for shop water and jacket water (nanofluids). With glycol run shop-water flow rate varied which made jacket water flow rate different. The shop water flow rate was kept constant around 4.5 GPM (2.84E-04 m^3/s). From Figure 8.9, we can see that jacket water flow rate starts around 540 sec when the flow rate is very small; the flowmeter is unable to pick up small signal. But once the flow

reaches around 3 GPM (1.89E-04 m^3/s), it picks up the signal continuously. After 2700 seconds the jacket water flow rate remains constant.

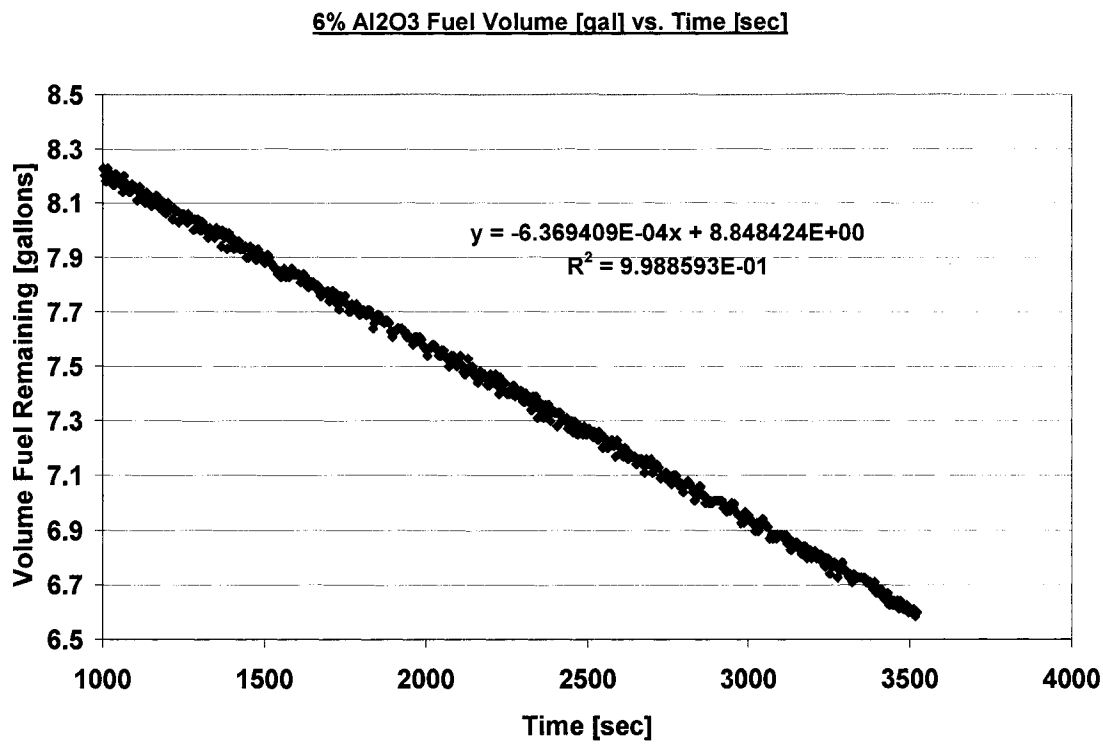

Figure 8.10. Measurement of diesel volume consumption versus time at constant electric load of 30 kW.

The mass flow rate of fuel is calculated by measuring the weight of the fuel tank using three load cells. The weight is then converted into gallons using fuel density at room temperature. Figure 8.10 displays the fuel (in gallons) remaining in the tank over a period of time when the engine was running at 30 kW. The slope of this graph represents the volumetric flow rate of the fuel consumed, from which the mass flow rate of the fuel is calculated.

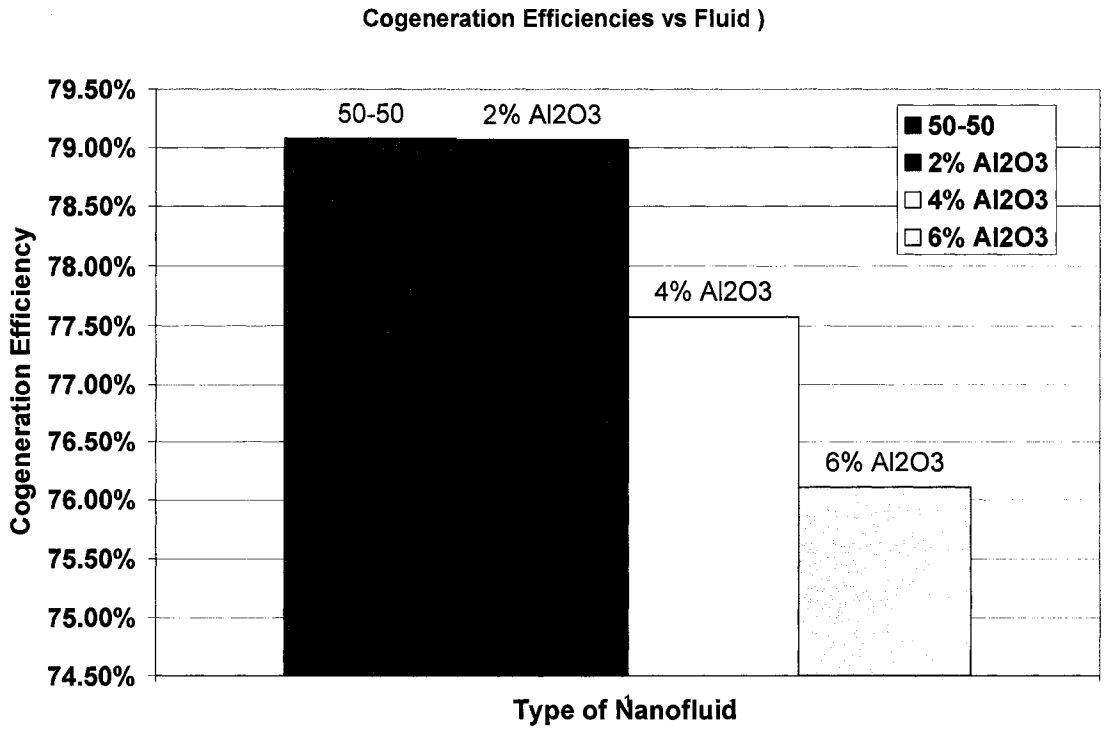

Figure 8.11. Cogeneration efficiency of various nanofluids considering jacket water heat recovery.

Knowing the flow rates of jacket water and shop water as well as the temperatures, the jacket water heat rate $\dot{Q}_{JW}$ is calculated from Eq. (10), the specific heat of nanofluids is measured from experiments and the cogeneration efficiency is calculated from Eq. (4). The cogeneration efficiency of various nanofluids is shown in Figure 8.11. From this experimental study, it has been found that with increased Al_2O_3 nanoparticle concentration, the diesel engine cogeneration efficiency decreased. This is mainly attributed to a decrease in the specific heat associated with an increase in Al_2O_3 nanoparticle concentration. As a typical value, the cogeneration efficiency of ethylene glycol-water mixture of 79.1 % dropped to 76.11% with 6% Al_2O_3 nanofluid.

The efficiency of the heat exchanger as a function of volumetric concentration of nanofluids is shown in Figure 8.12. Nanofluids flow outside the tubes and shop water flows inside the tubes in a tube and shell counter flow heat exchanger connected to the diesel engine. It is evident from Figure 8.12 that with nanofluids, the heat exchanger efficiency increased. This is due to the higher heat transfer coefficient of nanofluids compared to their base fluids. For example, the heat exchanger efficiency of an ethylene glycol-water mixture of 78.1 % increased to 81.11% for 6% Al_2O_3 nanofluid.

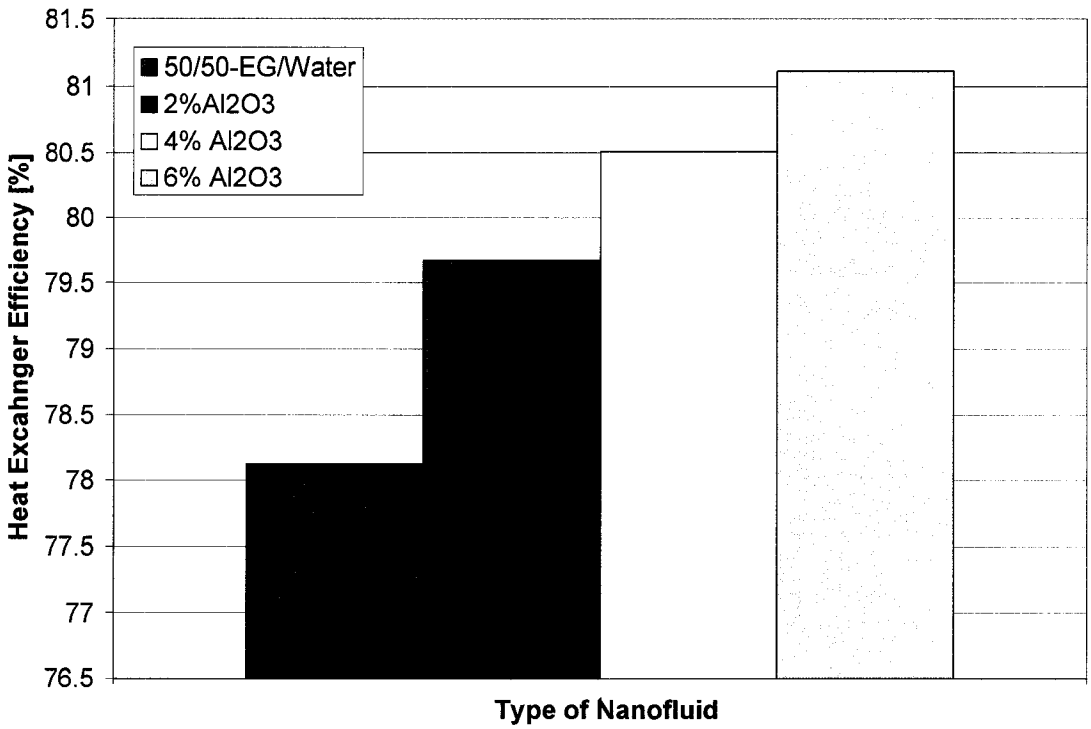

Figure 8.12. Heat exchanger efficiency of the heat recovery system with various concentrations of Al_2O_3 nanofluid.

8.7 Conclusions

1. The specific heat of nanofluids decreases as nanoparticle concentration increases. The specific heat of nanofluids increases with temperature.
2. The heating time for nanofluids decreases as nanoparticles concentration in the base fluid increases. However, when the heat rate is quite large, the time difference for heating is minimal.
3. The cogeneration efficiency of diesel generator decreases as nanoparticle concentration increases because the specific heat decreases as particle concentration increases.
4. Heat exchanger efficiency increases as particle concentration increases because of the higher heat transfer coefficients of nanofluids.

8.8 Acknowledgment

Financial assistance from the Arctic Region Supercomputing Center (ARSC) and the Dean of the Graduate School at University of Alaska Fairbanks is gratefully acknowledged.

8.9 Nomenclature

C_P	Specific heat, J/kg-K
H_v	Heating value of fuel
M	Mass of fluid, kg
$\dot{m}$	Mass flow rate, kg/s
Q_s	Heat supplied, J
$\dot{Q}_H$	Rate of heat supplied by fuel, W
$\dot{Q}_{JW}$	Rate of heat transported by jacket water, W

$\dot{Q}_{SW}$	Rate of heat transported by shop water, W
T	Temperature, °C
$\dot{V}$	Volumetric flow rate, m^3/s
$\dot{V}_f$	Volumetric flow rate of fuel, m^3/s
$\dot{W}_{el}$	Electrical output, W

Greek Letters

ρ	Density, kg/m^3
Δ	Difference
η	Efficiency
ϕ	Volumetric concentration, %

Subscripts

cogen	Cogeneration
el	Electrical
f	Fluid
in	Into the engine for JW
	Into the heat exchanger for SW
JW	Jacket water
nf	Nanofluid
out	Out of the engine for JW
	Out of the heat exchanger for SW
SW	Shop water
s	Solid

8.10 References

1. J.A. Phillpot, S.R., Choi, S.U.S. and Keblinski, P.K., 2004, Thermal Transport in Nanofluids, Annual Review of Material Research, Vol. 34, pp. 219-246.

2. Choi, S.U.S., Zhang, Z.G. and Keblinski, P., 2004, Nanofluids, Encyclopedia of Nanoscience and Nanotechnology, Vol. 6, pp. 757-773.

3. Kao, M.J., Tsung, H., Lin, H.M., 2006, The Friction of Vehicle Brake Tandem Master Cylinder, Journal of Physics: Conference Series, Vol. 48, pp. 663-666.

4. Choi, S.U.S., Yu, W., Hull, J.R., Zhang, Z.G., Lockwood, F.E., 2001, Nanofluids for Vehicle Thermal Management, Society of Automotive Engineers 2001-01-1706, pp. 139-144.

5. Li, Q., Yimin X., 2002, Convective Heat Transfer and Flow Characteristics of Cu-water Nanofluid, Science in China (Series E), Vol. 45, no.4, pp 408-416.

6. Lee, S., Choi S.U.S., 1996, Application of Metallic Nanoparticle Suspensions in advanced Cooling Systems, Recent Advances in Solids/Structure and Application of Metallic Materials, ASME PVP-Vol. 342/MD-Vol. 72, pp. 227-234.

7. Yang, Y., Zhang, Z.G., Grulke, E.A., Anderson, W.B. and Wu, G., 2005, Heat Transfer Properties of Nanoparticle-in-fluid Dispersions (Nanofluids) in Laminar Flow, International Journal of Heat and Mass Transfer, Vol. 48, pp. 1107-1116.

8. Wen, D., Ding, Y., 2004, Experimental Investigation into Convective Heat Transfer of Nanofluids at the Entrance Region Under laminar Flow Conditions, International Journal of Heat and Mass Transfer, Vol. 48, pp. 5181-5188.

9. Ding, Y., Alias, H., Wen, D. and Williams, R., 2006, Heat Transfer of Aqueous Suspensions of Carbon Nanotubes (CNT Nanofluids), International Journal of Heat and Mass Transfer, Vol. 49, pp. 240-250.

10. ASHRAE Handbook Fundamentals, American Society of Heating, Refrigerating and Air-Conditioning Engineers Inc., Atlanta, 1985.

11. Pak B.C, Cho Y.I., 1998, Hydrodynamic and Heat Transfer Study of Dispersed Fluids with Submicron Metallic Oxide Particles, Experimental Heat Transfer, Vol. 11, pp. 151-170.

12. Buongiorno J., 2006, Convective Transport in Nanofluids, ASME Journal of Heat Transfer, Vol. 128, pp. 240-250.

13. Xuan, Y., Li, Q., 2003, Investigation on Convective Heat Transfer and Flow Features of Nanofluids, ASME Journal of Heat Transfer, Vol. 125, pp. 151-155.

14. Mansour, R.B., Galanis, N., Nguyen, C.T., 2007, Effect of Uncertainties in Physical Properties on Forced Convection Heat Transfer with Nanofluids, Applied Thermal Engineering, Vol. 27, pp. 240-249.

15. Palm, S.J., Roy, G., Nguyen, C.T., 2006, Heat Transfer Enhancement with the Use of Nanofluids in Radial Flow Cooling Systems Considering Temperature Dependent Properties, Applied Thermal Engineering, Vol. 26, pp. 2209-2218.

16. Maiga, S.E.B., Palm, J., Nguyen, C.T., Roy, G., Galanis, N., 2005, Heat Transfer Enhancement by Using Nanofluids in Forced Convection Flows, International Journal of Heat and Fluid Flow, Vol. 26, pp. 530-546.

17. Heris, Z.S., Etemad, S.G., Esfahany, M.N., 2006, Experimental Investigation of Oxide Nanofluids Laminar Flow Convection Heat Transfer, International Communications in Heat and Mass Transfer, Vol. 33, pp. 529-535.

18. Heris, Z.S., Esfahany, M.N., Etemad, S.G., 2007, Experimental Investigation of Convective Heat Transfer of Al_2O_3/Water Nanofluid in Circular Tube, International Journal of Heat and Fluid Flow, Vol. 28, pp. 203-210.

CHAPTER NINE

Overall Conclusions

9.1 Conclusions for Rheology and Viscosity of Different Nanofluids

1) The experiments on copper oxide (CuO) nanofluids in water, varying in particle volume concentration from 5% to 15%, showed that these nanofluids behaved as time-independent, shear thinning, pseudoplastic fluids.
2) As a benchmark test case, the experimental viscosity values of 60:40 propylene glycol and water (PG/water) mixture and 60:40 ethylene glycol and water (EG/water) mixture agreed well with the values given in American Society of Heating Refrigeration and Air Conditioning Engineers (ASHRAE) handbook.
3) The rheological characteristics of shear stress versus shear rate of propylene glycol/water and ethylene glycol/water mixtures clearly exhibited Newtonian behavior.
4) The behavior of CuO-PG/water nanofluid up to a volume percentage of 5.9% was Newtonian in nature.
5) The deviation from Batchelor's classical equation for viscosity of nanofluids was observed to be substantial for all the tested nanofluids. Relative viscosity curves displayed higher slopes at low temperatures.
6) The viscosity was found to be an exponential function of temperature and the volumetric concentration for all the tested nanofluids. This effect is more pronounced at sub-zero temperatures. The experimental temperature range for CuO-water nanofluid was 5°C to 50°C. For CuO-PG/water mixture it was -35°C to 50°C and for all nanoparticles (CuO, Al_2O_3 and SiO_2) in EG/water mixture it was -35°C to 50°C.
7) The CuO nanofluid had the highest viscosity followed by the Al_2O_3 nanofluid and then by the SiO_2 nanofluid in EG/water mixture.

8) New correlations for viscosity of these nanofluids as a function of temperature and volumetric concentration were developed.
9) The curve-fit correlations of viscosities versus temperature agreed within ± 10% of the experimental measurements for all nanofluids.
10) As the diameter of nanoparticles decreased, the viscosity of the nanofluid increased.

9.2 Conclusions for Specific Heat Measurements of Different Nanofluids

1) An apparatus was built to measure the specific heat of various nanofluids. The measured specific heat value of water at 45°C differed by ± 0.2% when compared to thevalue from American Society of Heating, Refrigerating and Air Conditioning Engineers (ASHRAE) handbook.
2) The experimental results showed that the correlation presented by Buongiorno was in better agreement than the correlation presented by Pak and Cho.
3) As the particle volume concentration in the base fluid increased, the effective specific heat of nanofluids decreased.
4) The heating time for nanofluids decreased as nanoparticles concentration in the base fluid increased. However, when the heat rate was quite large, the time difference for the same temperature rise was minimal.
5) The specific heat of nanofluids increased with temperature. There is no correlation in the current available literature, reporting the effect of temperature on the specific heat of nanofluids.

9.3 Conclusions for Heat Transfer and Fluid Dynamic Performance of Different Nanofluids

1) The test setup was built to measure the convective heat transfer coefficient and pressure loss characteristics of various nanofluids. The experimental results for

ethylene glycol/water mixture and values obtained by the Dittus-Boelter equation were comparable.

2) Heat transfer coefficients of nanofluids increased with volume concentration. A typical enhancement of heat transfer coefficient was about 16% at a concentration of 10% with 20 nm particle diameter of SiO_2 at Re = 10,000.
3) The CuO nanofluid had the highest heat transfer coefficient followed by the Al_2O_3 nanofluid and the SiO_2 nanofluid. For example, at Re = 4000, h_{nf} was 10,000 W/m^2K for the CuO nanofluid, 8,000 W/m^2K for theAl_2O_3 nanofluid and 4,900 W/m^2K for the SiO_2 nanofluid.
4) Particle size influenced the heat transfer coefficient: the larger the particle diameter, the higher the heat transfer coefficient at a fixed Reynolds number.
5) The Prandtl number increased as particle volume concentration increased. Among the three nanofluids (CuO, Al_2O_3 and SiO_2 in EG/water mixture) analyzed, it was highest for copper oxide nanofluids and lowest for silicon dioxide nanofluids.
6) The Prandtl number also changed with particle diameter: The smaller the diameter, the higher the Prandtl number.
7) The Prandtl number increased exponentially as the nanofluid was cooled below sub zero temperatures.
8) The figure of merit (FOM) of heat transfer rates for various nanofluids was compared based on the Mouromtseff number. Results showed that for internal laminar flow, the FOM of water-based copper oxide nanofluids was much superior to that of pure water. For the CuO nanofluid, the optimal volume percentage appeared to be 5% in internal turbulent flows. Ethylene glycol based nanofluids had better FOM than propylene glycol based nanofluids.
9) Pressure loss was found to be a function of the concentration, increasing with increasing concentration. This was because the viscosity increased with concentration.
10) Pressure loss was highest for the CuO nanofluid, followed by the Al_2O_3 nanofluid and the SiO_2 nanofluid due, to higher density and viscosity.

11) No appreciable change in pressure loss was observed for different diameter nanoparticles within the range of the experiment.

9.4 Conclusions for Applications of Various Nanofluids as Heat Transfer Fluids

1) Use of various nanofluids can reduce the volumetric flow rate, mass flow rate and the pumping power for the same heat transfer rate, making it possible to heat a building at a higher fluid temperature.
2) Using nanofluids one can reduce the size of the heat exchanger and reduce the accompanying pressure loss.
3) Similar benefits can be derived by considering nanofluids in place of chilled water in building cooling coils and in condensing fluids. An investigation similar to the one presented in this study can quantitatively establish the benefits.
4) Application of nanofluids will be useful only when the thermal resistance on the nanofluids' side is the dominant resistance.
5) Nanofluids will be useful in the application of cooling microprocessor chips in electronics industry.
6) The cogeneration efficiency of diesel electric generator decreased as nanoparticle concentration increased because the specific heat decreased as particle concentration increased.
7) Heat exchanger efficiency in diesel engine increased as particle concentration increased because of the higher heat transfer coefficients of nanofluids.

9.5 Recommendations for Future Work

9.5.1. Application of Nanofluids in Electronics Cooling

To assess the application of nanofluids in electronics cooling, we performed an order of magnitude analysis for cooling microprocessor chips. The typical heat flux value to be dissipated from a chip was considered to be 20 W/cm^2. The goal of this study was to keep the chip (with surface area of 1 cm^2) at a temperature below 70°C. Hence total heat to be dissipated would be 20 W. The dissipated heat (q) can be equated to

$$q = hA\Delta T$$

where h is the heat transfer coefficient of the cooling fluid, A is surface area of a tube (5 mm O.D. and 1 cm length) and ΔT is the temperature difference between average fluid temperature (25°C) and the case temperature (70°C).

From the above equation, the heat transfer coefficient was calculated to be 2830 W/m^{2}K. By considering the cooling fluid as 60:40 ethylene glycol/water mixture, the corresponding Reynolds number was found to be 2,540 from our experimental plots. Now replacing this cooling fluid with 6% CuO nanofluid in EG/water mixture, the heat transfer coefficient of 11,694 W/m^{2}K can be read corresponding to the same Reynolds number of 2,540. With the same ΔT, now CuO nanofluids will be able to dissipate about 82.6 W/cm^2, which is about 4 times larger than the current required dissipation.

A Similar study needs to be extended to other nanofluids. Pressure loss has to be calculated to find the optimal concentration of nanoparticles and type of nanofluid.

9.5.2. Biot Number Consideration

The Biot number for a spherical particle is given by $Bi = hd/k$, where h is convective heat transfer coefficient, d is diameter of particle and k is thermal conductivity of particle material. For spherical particles to be good heat carriers, their thermal resistance must be low. For this condition the Bi << 0.1. For natural convection in liquid, a typical h value is 100 W/m^{2}K. Thermal conductivity for CuO is 40 W/mK. Therefore, the typical diameter is (hd/k =0.1) 40 mm. Therefore, all micro and nanoparticles can serve as good heat carriers.

- Thermal conductivity of nanofluids with temperature and particle size dependence should be investigated. This will be helpful in predicting the Prandtl number and heat transfer coefficients of various nanofluids.
- Correlation for specific heat should be developed which will be a function of particle concentration and temperature. This analysis will be useful for researchers exploring various benefits of nanofluids.
- The diesel electric generator set should be insulated to minimize the heat loss to the surroundings. The temperature at which the thermostatic valve opens should be very precise. This might result in increased cogeneration efficiency and in turn overall efficiency of the diesel engine.
- Nanofluids should be employed in automobiles and field tests should be performed to investigate the effect on emissions in cold regions.

Appendix A

A Study on Nanofluids for their Convective Heat Transfer and Hydrodynamic Characteristics

Debendra K. Das*, Devdatta Kulkarni, Benjamin Silbaugh
Department of Mechanical Engineering, University of Alaska Fairbanks,
Fairbanks, Alaska, 99775, USA.

Abstract

Ample bodies of data on nanofluids characteristics have appeared in the literature in recent years. Using fluid dynamic and heat transfer correlations from these literatures, this paper presents calculations on convective heat transfer coefficient and frictional head loss for a nanofluid. As an example, copper oxide nanoparticle dispersion in pure water is used and calculations are made for various volume percentages of nanoparticles. The calculations show that a volume of 1 % of copper oxide nanoparticles in water can enhance the convective heat transfer coefficient by as much as 30 %. Because of the enhanced heat transfer, the volume of nanofluid required to transfer the same amount of heat is greatly reduced. An analysis shows that in one case a pumping power reduction of about 50 % is achieved between pure fluid and a medium with 1 % copper oxide particle dispersion. Based upon such analyses, this paper also describes the design of a test apparatus to measure the convective heat transfer and friction factor. This apparatus will be capable of measuring the thermal and hydraulic characteristics of a variety of nanofluids.

Proceedings of Emerging Trends in Nanotechnology and Innovations in Design and Manufacturing, 2006, pp. 1-19.

A.1 Introduction

Recent advancements in nanotechnology have lead to the development of nanofluids. The term nanofluids refer to a stable suspension of nano-scale metallic particles in a base fluid such as water or ethylene glycol. The particles are typically made from metals or their oxides (e.g. aluminum, titanium, and copper) possessing a nominal diameter of 100-nm or less. The characteristics associated with nanofluids begin to diminish above the 100–nm diameter (Xuan and Li, 2000). The suspension is considered stable if the particles are well dispersed and do not chemically react with the base fluid. As presented by Boutin (2001), if nanoparticles are properly dispersed, the Brownian motion of the fluid molecules is sufficient to maintain particle dispersion indefinitely.

A.2 Thermal Properties

Previous research by Xuan and Li (2000) of copper-oxide nanoparticles in water has revealed that a 60% increase in the thermal conductivity can be achieved at a particle concentration of only 5% by volume. The effective thermal conductivity equation for a nanofluid presented by them is

$$k_{nf} = k_f[\frac{k_p + (n-1)k_f - (n-1)\phi(k_f - k_p)}{k_p + (n-1)k_f + \phi(k_f - k_p)}] \quad (1)$$

Pak and Cho (1998) list the following correlations for various properties of nanofluids. The effective density of nanofluids is given by

$$\rho_{nf} = (1-\phi)\rho_f + \phi\rho_s \quad (2)$$

where the volumetric concentration is given by

$$\phi = \frac{1}{(100/\phi_m)(\rho_s/\rho_f)+1} * 100(\%); \text{ where } \phi_m \text{ is mass fraction.} \quad (3)$$

The effective specific heat of nanofluids is given by

$$C_{pnf} = (1-\phi)C_{pf} + \phi C_{ps} \ . \quad (4)$$

The relative viscosity of nanofluids is given by

$$\mu_r = \frac{\mu_{nf}}{\mu_f} = 1 + 2.5\phi + 6.2\phi^2 . \quad (5)$$

The viscosity increases by 100 times for a particle volume of 10 % for γ-Al_2O_3 and water as shown by Pak and Cho (1998).

Li and Xuan (2002) present two equations for Nusselt number of nanofluids.

$$Nu_{nf} = 0.4328(1.0 + 11.285\phi^{0.754} Pe_d^{0.218}) \mathrm{Re}_{nf}^{0.333} \mathrm{Pr}_{nf}^{0.4} \quad \text{(For laminar flow)} \quad (6)$$

$$Nu_{nf} = 0.0059(1.0 + 7.6286\phi^{0.6886} Pe_d^{0.001}) \mathrm{Re}_{nf}^{0.9238} \mathrm{Pr}_{nf}^{0.4} \quad \text{(For turbulent flow)} \quad (7)$$

where $Pe_d = \frac{u_m d_p}{\alpha_{nf}}$; $\mathrm{Re}_{nf} = \frac{u_m d}{\nu_{nf}}$; $\mathrm{Pr}_{nf} = \frac{\nu_{nf}}{\alpha_{nf}}$; $\alpha_{nf} = k_{nf} / (\rho_{nf} * C_{pnf})$

Heat transfer coefficient: $h_{nf} = (Nu_{nf} k_{nf}) / d$.

Furthermore, a 60% increase in the convective heat transfer coefficient can be achieved in water-copper nanofluid at a particle concentration of only 2% by volume given by Li and Xuan (2002).

Using the convective heat transfer equations cited earlier, we have plotted the heat transfer coefficient and Reynolds number versus volumetric fraction of copper oxide nanofluids with water base. It is shown in Figure A-1.

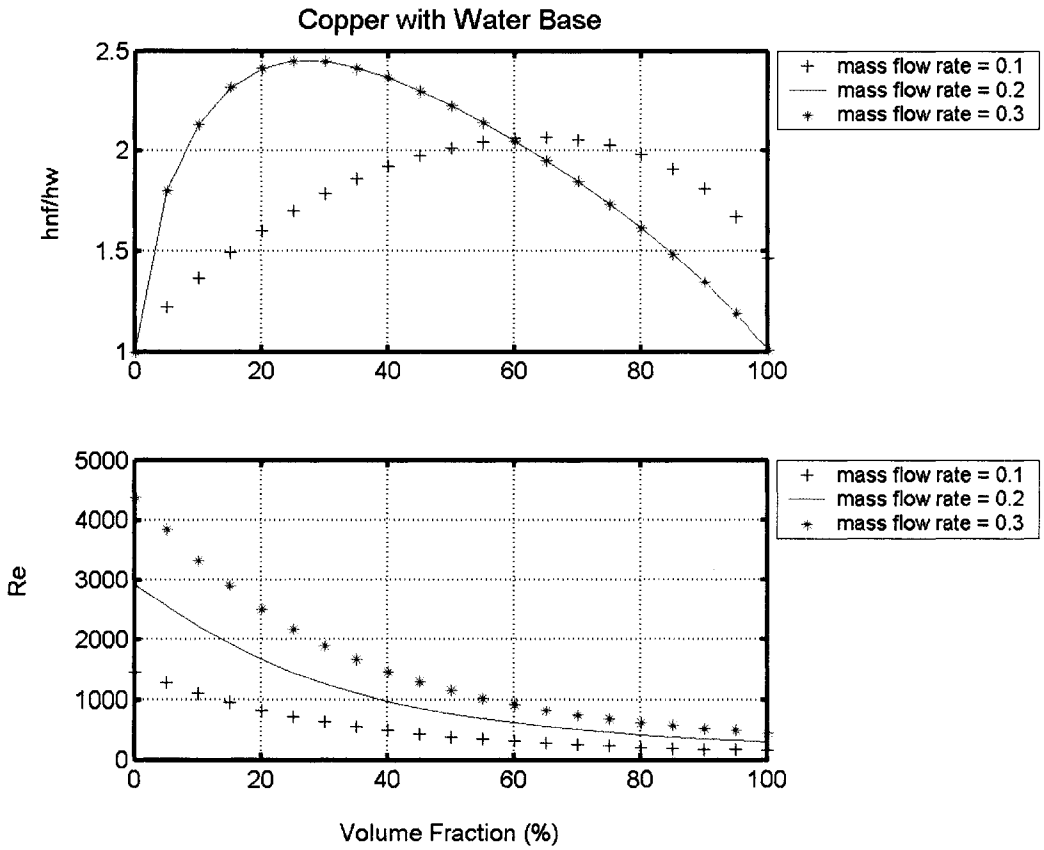

Figure A-1. Effect on heat transfer coefficient and Reynolds number due to addition of copper nanoparticles in varying percentages in water

Figure A-1 shows that theoretically the convective coefficient h_{nf} can be twice as that of water for a volume fraction of 10 % of copper oxide nanoparticles. More than this volume percentage is not recommended, as the fluid will be extremely viscous and it will loose its effectiveness. The viscosity increases with volume concentration, so the Reynolds number decreases with increase in volume concentration for a constant velocity as seen in this figure.

A.3 Saving in Pumping Power

Based on a diesel electric generator set operating in Alaska under the conditions shown in the table below, Das and Kulkarni (2005) have demonstrated the savings in pumping power by taking the example of heat recovery from the jacket water of the diesel engine.

Table A-1. Data considered from a diesel electric generator set

Generator Load	31 kW
Coolant Used	60% Ethylene Glycol & 40 % Water
Coolant Flow Rate	0.31 kg/s
Jacket Water Temperatures to Heat Exchanger	Inlet : 78.9 C and Outlet: 57.5 C
Heat Exchanger Tube Diameter	6.35 mm

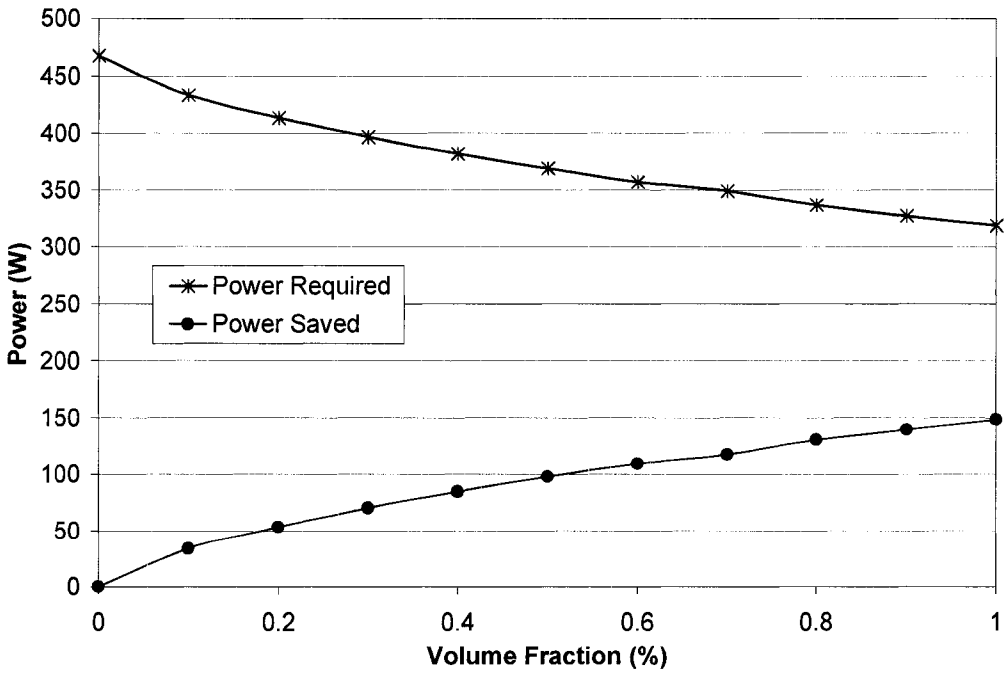

Figure A-2. Pumping power saving for a typical diesel engine generator set.

For the above generator set, the calculated pumping power is reduced from 467 W to 318.6 W (31.7%) as shown in Figure A-2 because of the diminished size of the heat exchanger due to the enhancement in heat transfer by nanofluids.

Further research performed by Boutin (2001) has also shown that the small size of the nanoparticles is such that pitting of tube surfaces does not occur. Although the addition of nanoparticles does tend to increase the viscosity of the fluid the net effect on pump power consumption is still reduced due to the dramatic increase in h for a given heat exchanger application. Furthermore, Li and Xuan (2002) show that for a concentration of up to 2% by volume of copper nanoparticles, the friction factor does not differ from that of pure water. Hence pumping power penalty does not occur for dilute nanofluids.

A.4 Nanofluids Test Apparatus

No research data on hydrodynamic and thermal characteristics of silver nanofluids has appeared in the literature thus far. The University of Alaska Fairbanks (UAF) Chemistry Department has been successful in producing this kind of nanofluid. In order to determine the fluid dynamic and heat transfer characteristics of silver nanofluids we have designed a test apparatus shown in Figure A-3. It consists of a 3/16 inch nominal diameter copper tube test section of 36 inch length in which nanofluid is heated by electric resistance strip heaters. Then the nanofluid is cooled by the laboratory water from the tap via an annular counterflow 4-passage heat exchanger. The nanofluid is circulated by a single stage regenerative turbine pump. Flow control is provided by a test loop bypass line and a throttle valve. Fluid and wall temperature measurements across the test section are obtained by type T thermocouples. Volumetric flow of nanofluids is measured by a turbine flow meter. Pressure drop measurement across the test section is achieved by a differential pressure transducer.

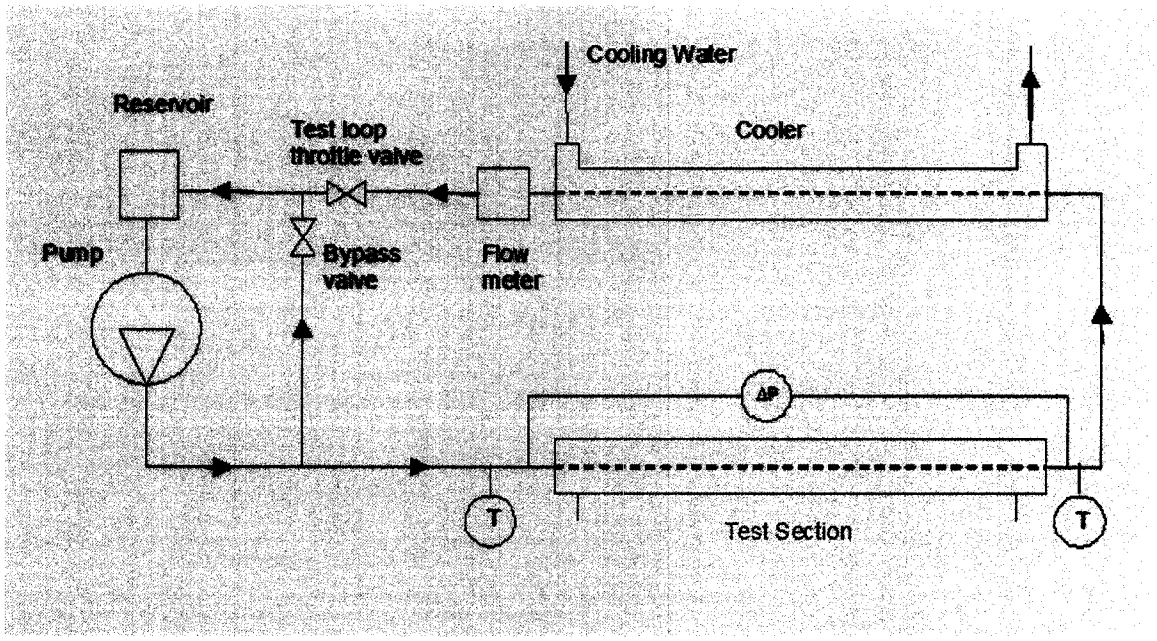

Figure A-3. A schematic diagram of the experimental apparatus, T = Thermocouples, ΔP = Differential pressure transducer.

A.4 Design Equations

A.4.1 Heat Addition Heat Exchanger

The test section is designed as a heat addition heat exchanger. The heat added to nanofluid is given by

$$q = \tfrac{1}{4}\pi d^2 \rho v c_p (T_2 - T_1). \quad (8)$$

A Reynolds number, Re = $\rho v d / \mu$, of low laminar value of less than 2300 to a turbulent value of 25,000 are considered, so that this apparatus can be used to test nanofluids in the laminar as well as turbulent regimes.

The electric heating is a constant heat flux boundary condition for the copper tube used in the test section. The Nusselt number for laminar flow is taken as Nu = 4.36 under fully developed condition. The Nusselt number for turbulent flow is given by the

Gnielinski correlation (Incropera and Dewitt, 2002). For designing this apparatus pure fluid correlations are used.

$$Nu = \frac{\left(\frac{f}{8}\right)(Re-1000)Pr}{1+12.7\sqrt{\frac{f}{8}}\left(Pr^{\frac{2}{3}}-1\right)} \tag{9}$$

The heat transfer coefficient is $h_f = Nu\ k/d$. Various commercially available copper tube sizes ranging from 1/8 to 3/8 inch OD are considered and computations using above equations with MATLAB programs are repeated to calculate the requirement for heat input. Figure A- 4 shows the heater power requirement to heat the nanofluid. From this parametric study a 3/16 inch OD tube is selected with a heating requirement of 4000 W for Re = 25,000. Four electric strip heaters of 1000 W capacity surrounding four sides of the test section are adopted.

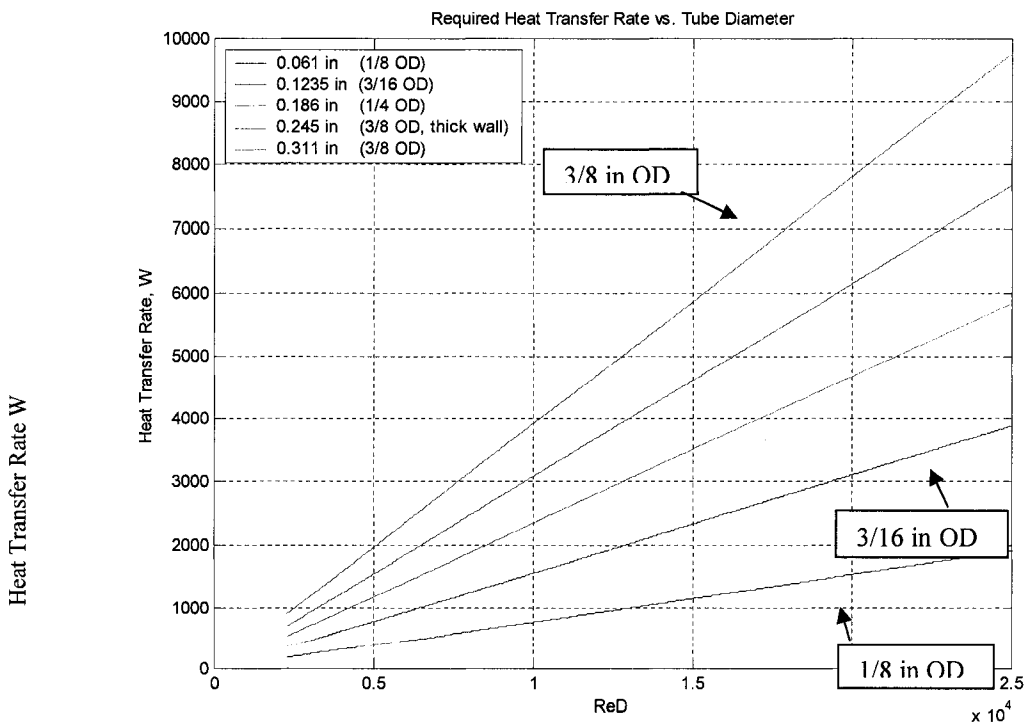

Figure A- 4. Heater power requirements for commercially available copper tubing upto a Reynolds number of 25,000. Note: All numbers in abscissa are multiplied by 10^4.

A.4.2 Pressure Loss in Test Section

For the flow in laminar regime the friction factor is

$$f = \frac{64}{\mathrm{Re}} \tag{10}$$

For turbulent flow the friction factor is calculated from the explicit formula given by Jain (1976).

$$\frac{1}{\sqrt{f}} = 1.14 - 2\log\left(\frac{\varepsilon}{d} + \frac{21.25}{\mathrm{Re}^{0.9}}\right). \tag{11}$$

Using above equations, calculations are performed for commercial copper tube sizes 1/8 inch to 3/8 inch OD. The test section pressure loss results are shown below in Figure 5. From this analysis the pressure loss of 500 kPa at Re = 25,000 for 3/16 inch OD tube is selected. As an alternate for 1/8 inch OD tube the pressure loss becomes 10 times more, which is too high. The pressure loss will be taken into account while sizing the pump.

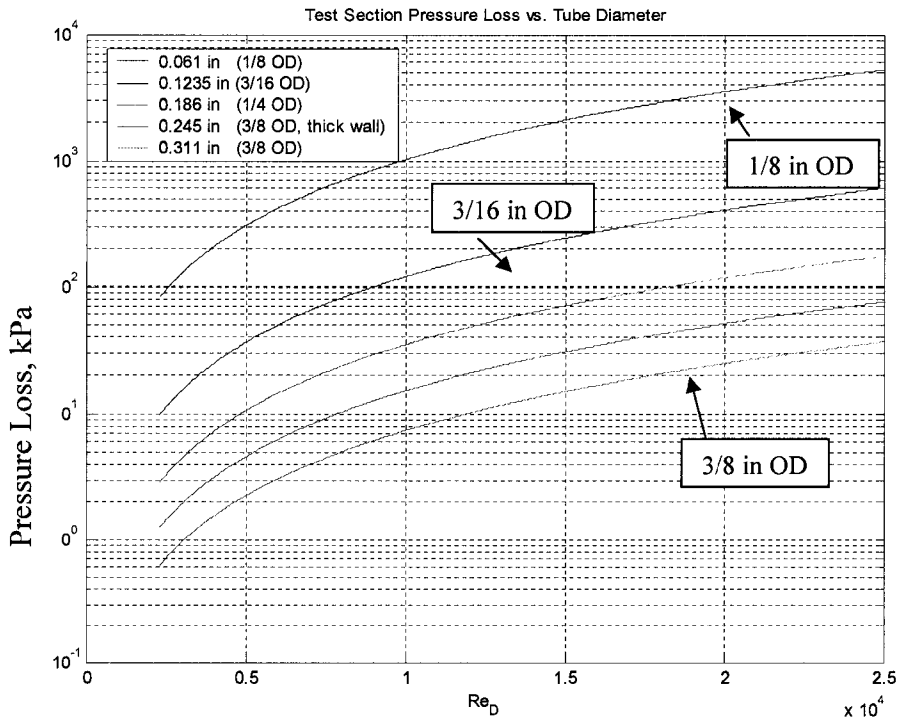

Figure A- 5. Test section pressure loss per unit length for commercially available copper tubing. Note: All numbers in abscissa are multiplied by 10^4.

A.4.3 Heat Rejection Heat Exchanger

The nanofluid is cooled in the cooling heat exchanger before reentering the test section. The cooling water requirements is determined from the equation first by calculating the heat to be removed from the nanofluid.

$$q = \dot{m}_h c_{ph}\left(T_{h1} - T_{h2}\right). \tag{12}$$

The heat rejection heat exchanger is designed as a coaxial, counterflow, double pipe heat exchanger. Nanofluids flow through the inner pipe and cooling water supplied from the laboratory water supply flows through the outer annulus.

The velocity of cooling water in the annulus is given by

$$v_c = \frac{4q}{\rho\pi c_{pc}\left(d_s^2 - d_o^2\right)\left(T_{c1} - T_{c2}\right)}. \tag{13}$$

The log mean temperature difference between the hot nanofluid and the cooling water under counter flow is

$$LMTD = \frac{\left(T_{h1} - T_{c2}\right) - \left(T_{h2} - T_{c1}\right)}{ln\left(\frac{T_{h1} - T_{c2}}{T_{h2} - T_{c1}}\right)}. \tag{14}$$

The Reynolds number for hot fluid and cold fluid are

$$\mathrm{Re}_h = \frac{\rho_h v_h d_i}{\mu_h},\ \mathrm{Re}_c = \frac{\rho_c v_c \left(D_h\right)}{\mu_c}.$$

For the annulus the hydraulic diameter D_h = (Annulus OD d_s– Annulus ID d_o).

To obtain the Nusselt number for turbulent flow in the annulus and the inner tube, equation (9) is used. Note that for the annulus the diameter is replaced by hydraulic diameter defined above.

Heat transfer coefficients for cold and hot sides are given below

$$(h_f)_c = Nu_c \frac{k_c}{D_h}; \; (h_f)_h = Nu_h \frac{k_h}{d_i}$$

The overall thermal resistance between the nanofluid and the cooling water in the heat exchanger is given by

$$R_{eq} = \frac{1}{\pi d_i L (h_f)_h} + \frac{1}{\pi d_o L (h_f)_c} + \frac{\ln(d_o / d_i)}{2\pi L k}. \quad (15)$$

The total heat transfer rate in the double pipe heat exchanger is given by

$$q = \frac{A}{R_{eq}} LMTD. \quad (16)$$

Pressure loss through the annulus is given by

$$\Delta P = \frac{1}{2} \rho_c v_c^2 f_c \frac{L}{d_s - d_o}. \quad (17)$$

Based on above equations, calculations are performed for heat transfer and pressure loss for a range of diameters for the inner tube (1/4 inch) and the outer shell of 3/4 inch National Pipe Standard (NPS) to 2 inch NPS.

Figure A- 6 shows the effect of heat exchanger shell diameter on heat exchanger length to remove approximately 4000 W of heat.

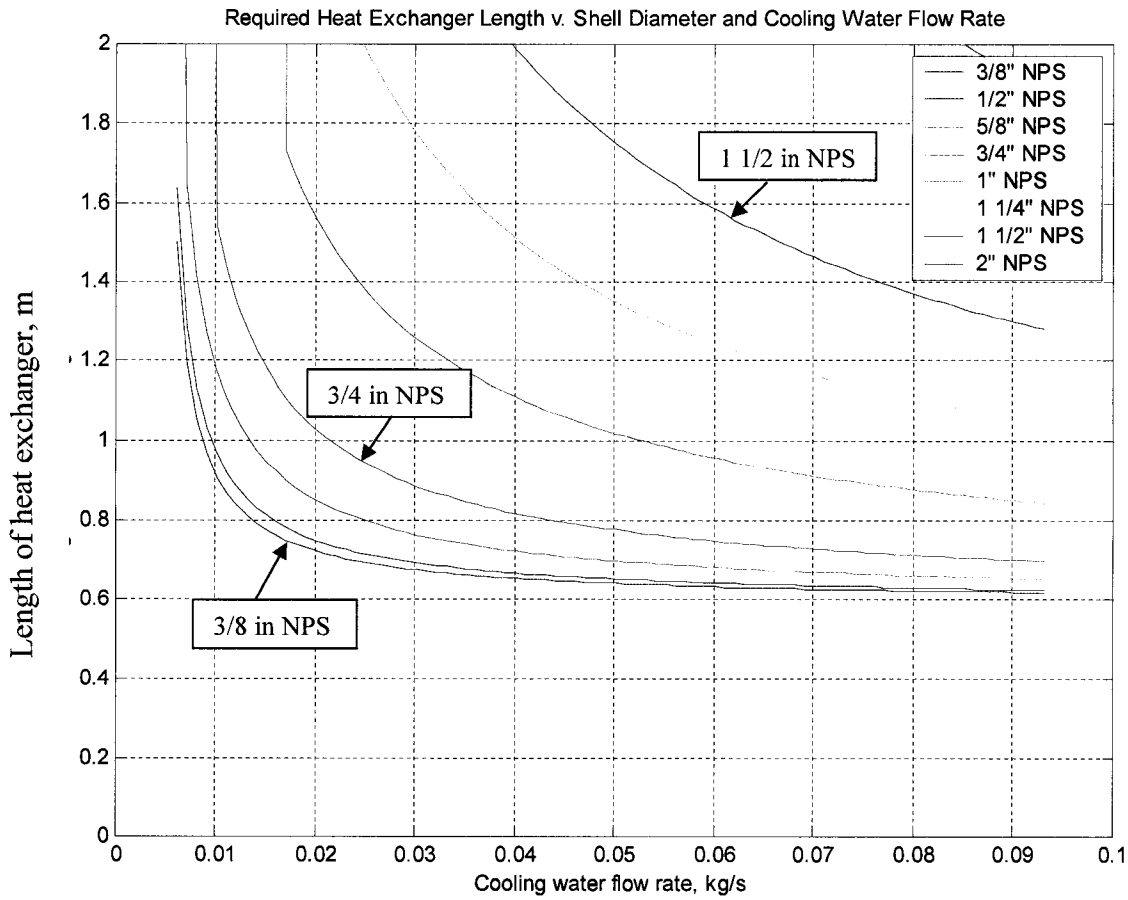

Figure A- 6. Effect of heat exchanger outer shell diameter on required heat exchanger length and cooling

From this analysis a 3/4 inch nominal diameter outer shell and 1/4 inch nominal diameter inner tube are selected for a cooling heat exchanger. Our design involves four parallel flow paths giving about 1 m length for cooling heat exchanger.

The pressure loss for unit length based on the outer shell diameter is shown in Figure 7. The discontinuity in pressure loss curve when the flow regime changes from laminar to turbulent is clearly seen. The supply water pressure in the laboratory is nearly

500 kPa (70 psia). Therefore, the pressure loss of about 1 atm in the shell side of the heat exchanger is acceptable.

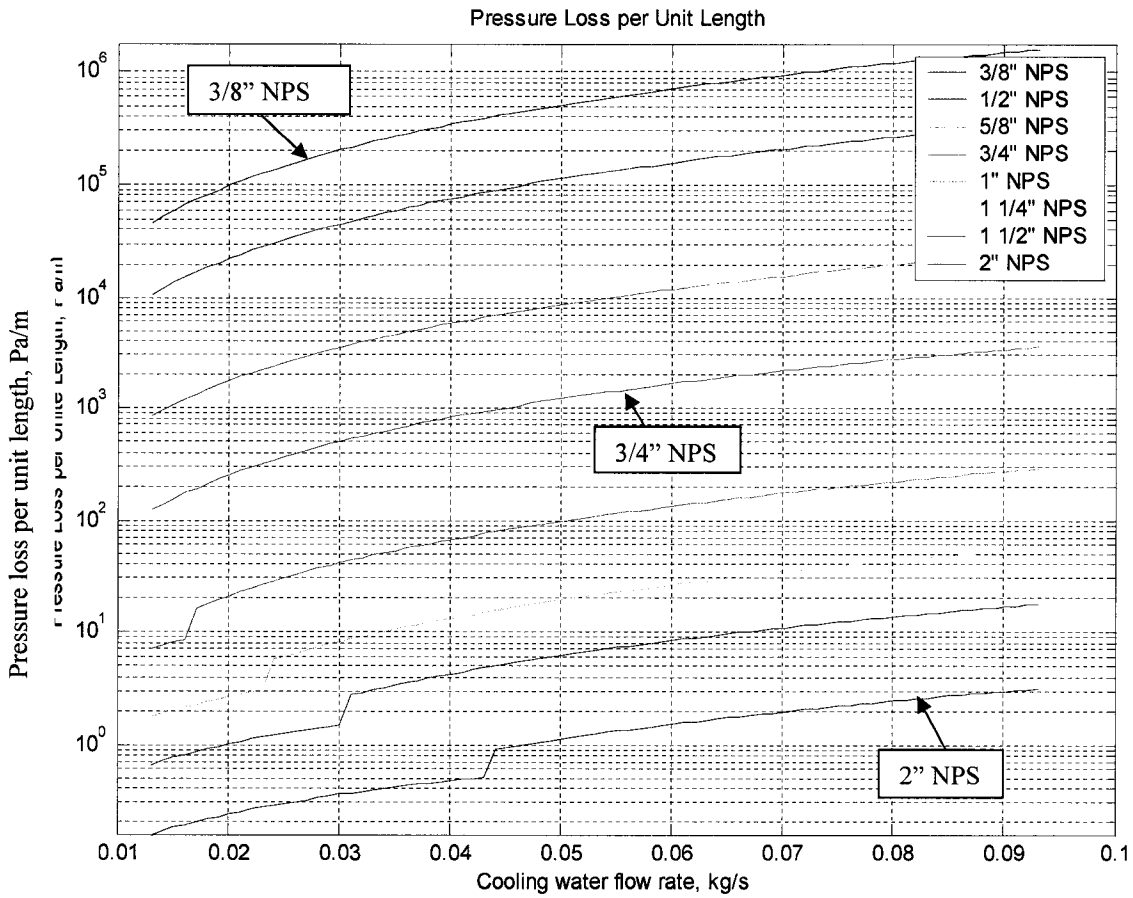

Figure A- 7. Cooling water pressure loss per unit length in the annulus.

A.4.4 Pump Selection

The pump was selected based on the volumetric flow corresponding to Reynolds number of 25,000 and head loss in the fluid circuit. The total pressure drop in the system is given by

$$\Delta p_{sys} = \frac{1}{2}\rho v^2\left(f\frac{L}{d_i} + \Sigma K\right) + \Delta p_v + \Delta p_{fm} \qquad (18)$$

Where $\Delta p_v = \frac{448.8\,\dot{V}}{(SG)C_v}$, $\dot{V}$ is the volumetric flow rate of nanofluid

$$\Delta p_{fm} \cong 448.8 \cdot 275\dot{V}^2$$

Where Δp_v is the pressure loss in the globe valve used for throttling to control the volume of flow in the test loop.

Δp_{fm} is the pressure loss in the flow meter. Both Δp_v and Δp_{fm} equations given above are obtained from manufacturers data sheet.

Figure A- 8 shows the pressure loss curve for the fluid circuit. Using the system pressure loss and the volumetric flow corresponding to Re = 25,000 gives the requirement of a 1/3 hp pump.

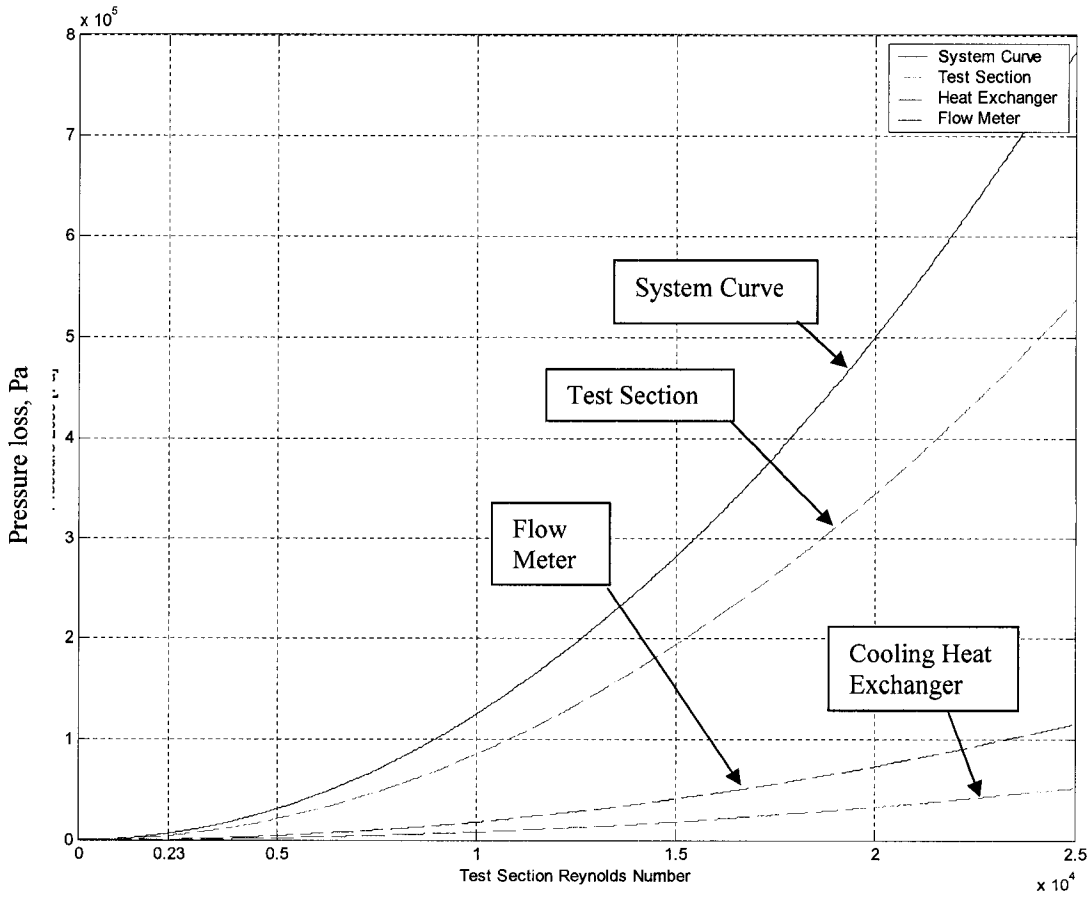

Figure A- 8. Test loop pressure loss curve as a function of test section Reynolds number

Note: All numbers in abscissa are multiplied by 10^4.

A.4.5 Conduction in the copper blocks

A finite element analysis adopting the software FEHT (Finite Element Heat Transfer) from Incropera and Dewitt (2002) is used to asses the temperatures in the heater block. Due to symmetry only 1/8 of the cross section of the block is modeled as shown in Figure A- 9. The modeling is based on a large number of nodes with inner boundary at 90 ^{0}C due to nanofluid temperature. The outer boundary is based upon a uniform heat flux generated by 1000 W. This conduction analysis is performed to ensure that not too much

temperature differential exists in the copper block. Because this will cause uneven thermal expansion and discontinuity between the thermal glue, tube and the copper block. This computation gives nodal temperature distribution as displayed in Figure 9. The temperature distribution shows that the temperatures vary only from 125 ^{0}C to 131 ^{0}C on the outer surface of the block. This small difference in temperature will cause negligible thermal differential expansion and hence the heater block design is safe.

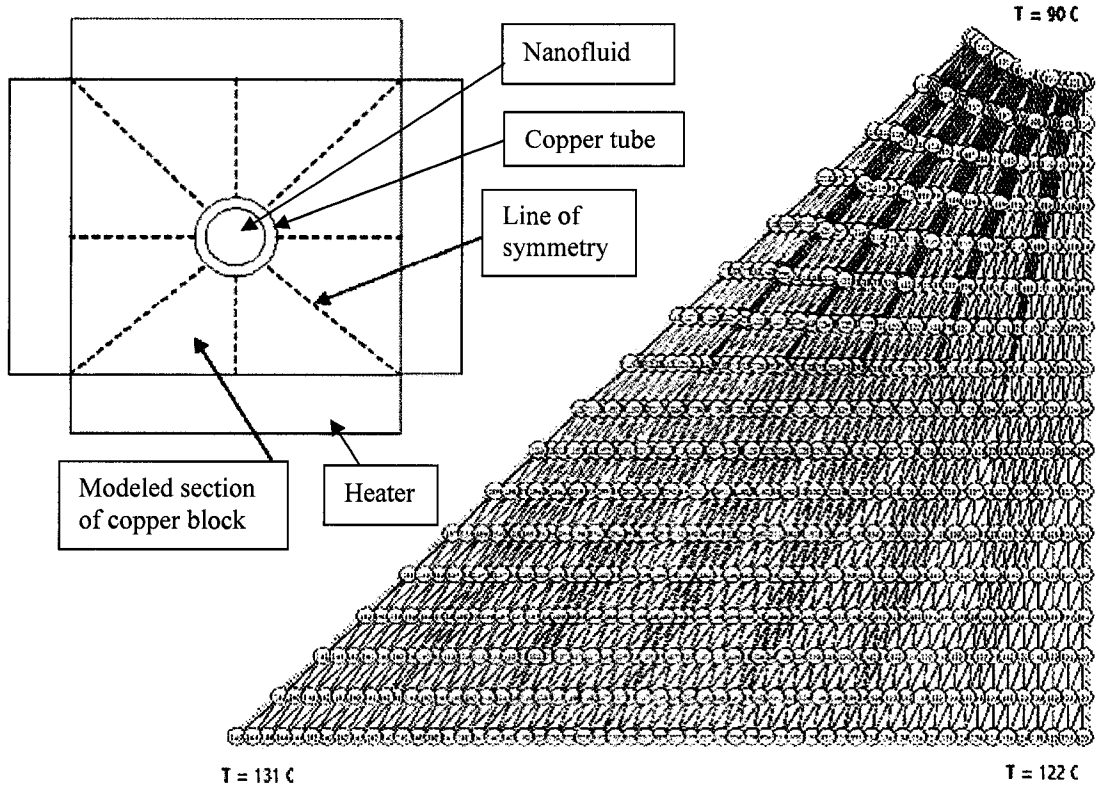

Figure A- 9. Arrangement of the heater blocks and temperature distribution in copper block

A.4.6 Test Section Convective Heat Loss

Heat loss at the test section is minimized by fiber glass insulation as shown in Figure A-10, so that all heat from strip heaters go into nanofluid.

Conductive heat transfer through the insulation is given by

$$Q_{loss} = \frac{2\pi L k_{ins}(T_h - T_s)}{\ln(1+\frac{t}{R})} \tag{19}$$

Heat transfer through convection on insulation surface is

$$Q_{loss} = 2\pi(R+t)Lh(T_s - T_\infty) \tag{20}$$

The convection coefficient in air is obtained from the natural convection on a horizontal cylinder given by Incropera and Dewitt (2002).

$$\begin{aligned} h &= \frac{k_{ins}}{2(R+t)} Nu_D \\ &= \frac{k_{ins}}{2(R+t)} \{0.60 + \frac{0.387 Ra_D^{1/6}}{[1+(0.559/\mathrm{Pr})^{9/16}]^{8/27}}\}^2 \end{aligned} \tag{21}$$

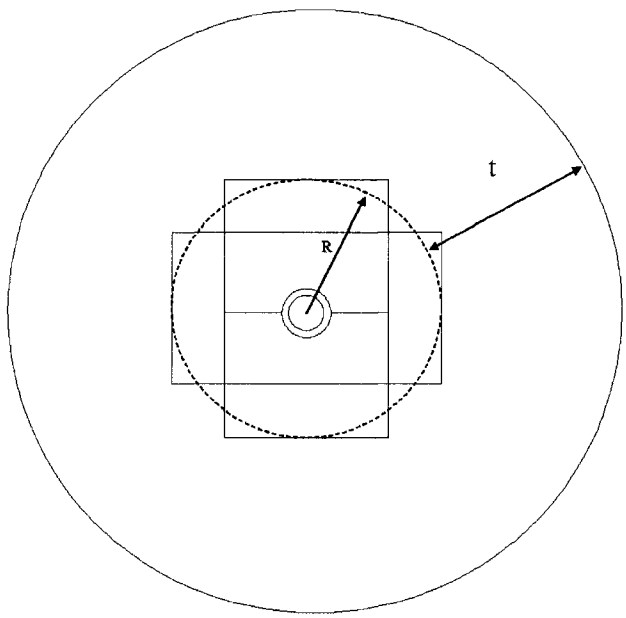

Figure A- 10. Insulated test section with mean radius R and insulation thickness t shown

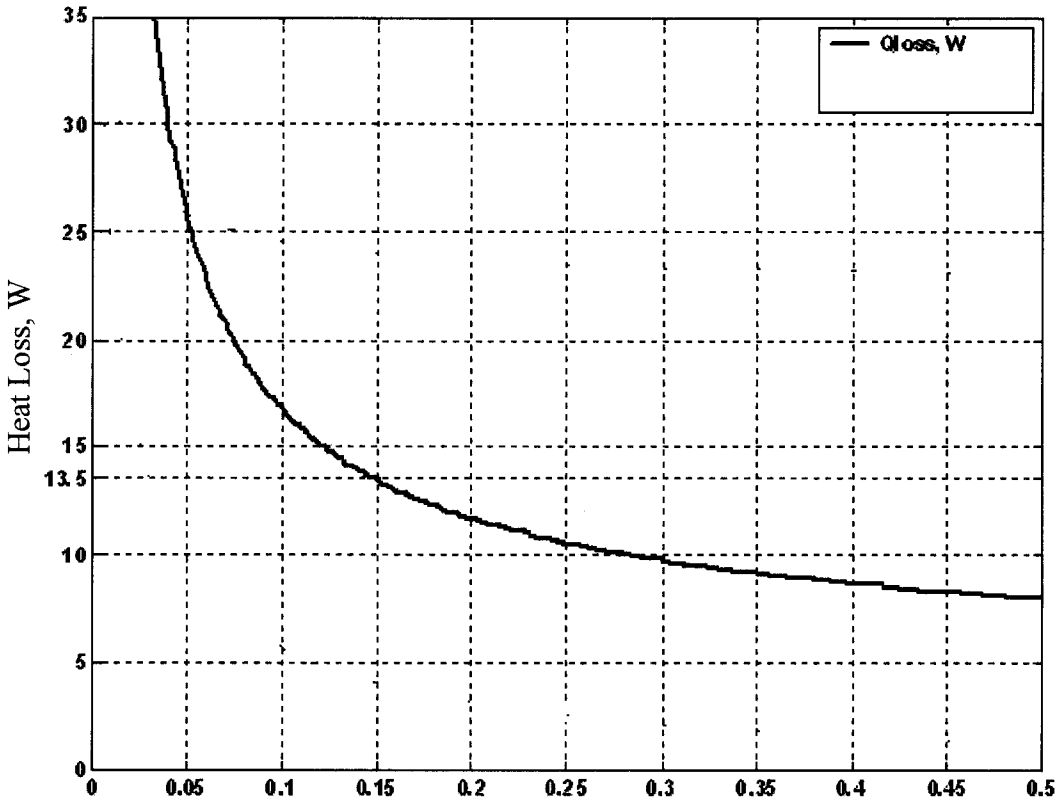

Figure A- 11. Test section heat loss as a function of insulation thickness

From calculations using above equations it is found that a 15 cm thick insulation reduce the heat loss to 13.5 W (0.3%) as shown in Figure A-11. Further increase in insulation does not reduce heat loss appreciably. So 15 cm (6 inch) fiber glass insulation is adopted in our design.

A.4.7 Reservoir Volume

A reservoir has been designed to absorb the expansion of hot nanofluid and to ensure sufficient fluid availability on the suction side of the pump. This guarantees prevention of cavitation and ease of priming the pump. The volume of reservoir is given by the equation from McQuiston et al. (2005).

$$V_{res} = \frac{V_{nf}[(\frac{v_2}{v_1} - 1) - 3\alpha\Delta T]}{P_a(\frac{1}{P_1} - \frac{1}{P_2})} . \quad (22)$$

In the above equation $\Delta T = T_1$ (Highest) – T_2 (Lowest) temperature in the loop, v_1 and v_2 are specific volumes at T_1 and T_2, P_1 and P_2 are the highest and lowest pressures in the loop, P_a is atmospheric pressure and α is coefficient of thermal expansion of copper tube. The calculation reveals that about 2 liters of nanofluid (V_{nf}) is required to conduct a test using this apparatus. As nanofluids are expensive, having this low volume needed for the test is a beneficial feature of this apparatus.

A.5 Final Test Apparatus

The device shown in Figure A- 12 consists of a fluid circuit powered by a 1/3-hp single stage regenerative turbine pump, and flow control achieved via throttle valves and a bypass line bridging the circuit. The heat supply consists of four 1,250 W (max) strip heaters that are controlled by four variable transformers (i.e. variacs). The test section is covered by fiber glass insulation of 15 cm thickness. Cooling is provided by four counter-flow heat exchangers arranged in parallel, and shop water is used as the cooling medium. All temperature measurements are performed using Type-T thermocouples, the differential pressure transducer is used to measure the pressure loss through the test section, and an Omega turbine-like flow meter is used to measure fluid flow rate through the test section. A Campbell Scientific data logger is programmed for data acquisition recording temperatures, pressures and volumetric flow rates at regular intervals of a few seconds.

The device allows an experiment to be conducted with as little at 2-Liters of fluid, and can maintain a thermally and dynamically steady flow for a test section Reynolds range from 0 to 25,000. Additionally, the heater and cooling systems have been

demonstrated to achieve and maintain a test section inlet temperature of 60°C and 70°C; even lower test section inlet temperatures and larger temperature differentials were achieved during trial runs with water. A temperature below 100^0C in the test loop is maintained to prevent steam formation and evaporative loss.

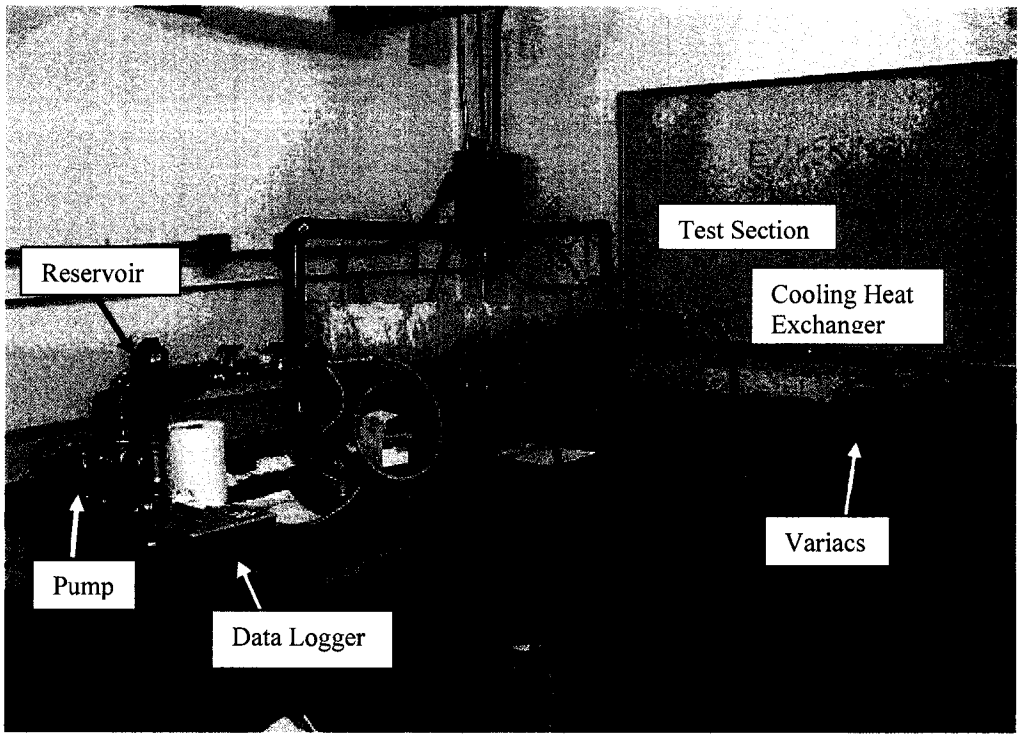

Figure A-12. Completed apparatus to investigate nanofluid thermal performance

A.6 Conclusions

Theoretical analysis is presented to show the heat transfer enhancement by using nanofluids. It is proven that pumping power is reduced. An experimental apparatus has been developed that will provide a means of measuring the convective coefficient of nanofluids. The apparatus is now ready to measure the hydrodynamic and heat transfer characteristics of various types of nanofluids including silver nanofluid. The experimental results from this apparatus will be valuable to provide test cases for calibration of new computational fluid dynamics codes that are being developed for nanofluids applications.

A.7 Acknowledgment

Financial assistance to conduct this research is provided by:

Arctic Region Supercomputing Center, University of Alaska Fairbanks (UAF),

Vice Provost of Research: Undergraduate Research Opportunities Program, UAF,
EPSCoR: Undergraduate Research Program, UAF.

A.8 Nomenclature

A	Heat exchanger surface area, m^2
c_p	Specific heat, J/kg K
d_i	Inner diameter of the pipe, m
d_p	Particle diameter, m
d_s	Annulus OD, m
d_o	Annulus ID, m
D_h	Hydraulic diameter, m
ε	Roughness of pipe, m

f	Friction factor
h_f	Frictional head loss, m
h_i	Inside convective heat transfer coefficient, W/m^2 K
h_m	Head loss in fittings, m
h_o	Outside convective heat transfer coefficient, W/m^2 K
k	Thermal conductivity, W/m k
k_f	Thermal conductivity of fluid, W/m K
k_i	Thermal conductivity of insulation, W/m K
k_p	Thermal conductivity of particle, W/m K
k_s	Thermal conductivity of solid, W/m K
L	Length of the pipes, m
$\dot{m}$	Mass flow rate of the fluid, kg/s
Nu	Nusselt number
Pr	Prandtl number
q	Heat flow rate, W
Re	Reynolds number
T_1	Nanofluid temperature at test section inlet, ^{o}C
T_2	Nanofluid temperature at test section outlet, ^{o}C
T_s	Surface temperature of insulation, ^{o}C
T_∞	Ambient air temperature, ^{o}C
u_m	Mean velocity, m/s
v	Velocity of fluid flowing through the pipe, m/s
v_c	Velocity of fluid flowing in annulus, m/s
μ	Coefficient of dynamic viscosity of the fluid, kg/m s
ρ	Density of the fluid, kg/m^3

Subscript

c	Cold
f	Fluid
h	Hot
nf	Nanofluid
m	Mean
p	Particle
s	Solid

A.9 References

Boutin, C., 2001, " Taking the heat off: Nanofluids promise efficient heat transfer," logos, Vol. 19, No. 2.

Das D.K., Kulkarni, D,P., 2005, "A Theoretical Investigation on Heat Transfer Characteristics of Nanofluids," Arctic Science Conference Proceedings, Kodiak, Alaska, USA, p. 14.

Incropera Frank P., David P. DeWitt. 2002. *Fundamentals of Heat And Mass Transfer*. Fifth Ed, John Wiley and Sons Inc, NJ.

Jain, A.K., 1976, "An accurate explicit equation for friction factor," J. Hydraulics Div. ASCE, Vol. 102, HY5.

Li, Q., Xuan, Y., 2002, "Convective heat transfer and flow characteristics of Cu-water nanofluid," Science in China (Series E), Vol. 45, No. 4, pp. 408-416.

McQuiston, F., Parker, J. and Spitler, J., 2005, *Heating, Ventilating, and Air Conditioning.* Sixth Ed, John Wiley and Sons Inc, NJ.

Pak, Bock Choon, Young I. Cho. 1998. "Hydrodynamic and heat transfer study of dispersed fluids with submicron particles." Experimental Heat Transfer. Vol. 11, pp. 151-170.

Xuan, Y., Li, Q., 2000, "Heat transfer enhancement of nanofluids." International Journal of Heat and Fluid Flow. Vol 21.pp. 58-64.

APPENDIX B

Theoretical and Experimental Investigations on Nanofluids for Their Fluid Dynamics and Heat Transfer Behaviors

Devdatta P. Kulkarni[1], Debendra K. Das[2]
[1]Graduate Student, [2]Professor, Department of Mechanical Engineering,
University of Alaska Fairbanks, Fairbanks, Alaska, 99775.

Abstract

As a first part of this paper an analytical study is presented for heat transfer by nanofluids using heat transfer correlations for laminar as well as turbulent flows available in the current literature. This study shows an increase of 50% in convective heat transfer coefficient in laminar regime and about 2.2 times in turbulent regime due to the addition of 10% copper oxide nanoparticles in water. It is also observed that in turbulent regime beyond 30% of copper oxide nanoparticles concentration, the heat transfer coefficient begins to diminish as predicted by the correlations presented in published papers. In the second part of the paper, modeling studies have been presented for two dimensional flows using the well-known computational fluid dynamics software Fluent (2005) where the nanofluid is treated as a homogeneous fluid with special thermal properties, e.g. viscosity, density, specific heat and thermal conductivity computed from new correlations available for nanofluids. These values differ substantially from the pure liquid phase and are dependent on the nanoparticle volume fraction. Fluent results show an increase of 45% in convective heat transfer coefficient in laminar regime for 10% particle concentration of copper oxide in water.

Proceedings of 39th Heat Transfer and Fluid Mechanics Institute, 2006, pp. 95-110.

Finally, to verify the theoretical studies an experimental apparatus has been built to measure the frictional head loss and the convective heat transfer coefficients of various types of nanofluids. This apparatus and its function to determine fluid dynamic and thermal characteristics of nanofluids to corroborate the theoretical findings are described in this paper.

* Corresponding Author: ffdkd @uaf.edu

B.1 Introduction

Recent advancements in nanotechnology have lead to the development of nanofluids. The term nanofluids refer to a stable suspension of nano-scale metallic particles in a base fluid such as water or ethylene glycol. The particles are typically made from metals or their oxides (e.g. aluminum, copper and titanium) possessing a nominal diameter of 100-nm or less. The suspension is considered stable if the particles are well dispersed and do not chemically react with the base fluid. As presented by Boutin (2001), if nanoparticles are properly dispersed, the Brownian motion of the fluid molecules is sufficient to maintain particle dispersion indefinitely. The characteristics of uniform dispersion associated with nanofluids begin to diminish above the 100–nm diameter (Xuan and Li, 2000).

Recent literatures on nanofluids have shown that they are capable of enhancing the convective heat transfer by a substantial amount. A 60% increase in the convective heat transfer coefficient can be achieved in water-copper oxide nanofluid at a particle concentration of only 2% by volume given by Li and Xuan (2002). Therefore, both theoretical and experimental investigations have been undertaken at the University of Alaska Fairbanks to study the behaviors of silver, copper and aluminum nanofluids to establish their abilities in enhancing convective heat transfer.

Application of nanofluids can result in reduction in sizes of equipment in industries that employ heat transfer devices, in household heating systems that conventionally employ water or glycol solutions (McQuiston et al., 2005), in high heat flux devices such as electronic equipment and in new weapon systems being developed by the Department of Defense. Reduction in pollution from internal combustion engines can be achieved by using nanofluids as coolants in internal combustion engines due to the faster warm-up during the starting of engines. Reduction in drag for ship hulls can be achieved by heating the hull using nanofluids recovering waste heat from diesel engines and gas turbines of ships thus resulting in substantial savings in fuel cost. This would also result in reducing pollution and mitigating the problem of global warming. Due to the reduction in volume for same magnitude of heat transfer, nanofluids may be attractive in NASA missions where lifting cost of payloads is high.

B.2 Theory

Previous research by Xuan and Li (2000) on copper-oxide nanoparticles in water has revealed that a 60% increase in the thermal conductivity can be achieved at a particle concentration of only 5% by volume. The effective thermal conductivity equation for a nanofluid presented by them is

$$k_{nf} = k_f\left[\frac{k_p + (n-1)k_f - (n-1)\phi(k_f - k_p)}{k_p + (n-1)k_f + \phi(k_f - k_p)}\right] \quad (1)$$

Pak and Cho (1998) list the following correlations for various properties of nanofluids. The effective density of nanofluids is given by

$$\rho_{nf} = (1-\phi)\rho_f + \phi\rho_s \quad (2)$$

where the volumetric concentration is given by

$$\phi = \frac{1}{(100/\phi_m)(\rho_s/\rho_f)+1}(100\%)\text{; where } \phi_m \text{ is mass fraction.} \quad (3)$$

The effective specific heat of nanofluids is given by

$$C_{pnf} = (1-\phi)C_{pf} + \phi C_{ps} \ . \tag{4}$$

The relative viscosity of nanofluids is given by

$$\mu_r = \frac{\mu_{nf}}{\mu_f} = 1 + 2.5\phi + 6.2\phi^2 \ . \tag{5}$$

The viscosity increases by 100 times for a particle volume of 10 % for γ-Al_2O_3 nanoparticles in water as shown by Pak and Cho (1998). The experiments conducted on rheological properties of copper oxide nanofluids by Kulkarni et al. (2006) show that the viscosity of nanofluid is about 100 cP for a 15% particle concentration whereas for pure water the value is around 1-2 cP at 298 K.

Li and Xuan (2002) present two equations for Nusselt number of nanofluids.

$$Nu_{nf} = 0.4328(1.0 + 11.285\phi^{0.754} Pe_d^{0.218}) \mathrm{Re}_{nf}^{0.333} \mathrm{Pr}_{nf}^{0.4} \quad \text{(For laminar flow)} \tag{6}$$

$$Nu_{nf} = 0.0059(1.0 + 7.6286\phi^{0.6886} Pe_d^{0.001}) \mathrm{Re}_{nf}^{0.9238} \mathrm{Pr}_{nf}^{0.4} \quad \text{(For turbulent flow)} \tag{7}$$

where $Pe_d = \frac{u_m d_p}{\alpha_{nf}}$; $\mathrm{Re}_{nf} = \frac{u_m d}{\nu_{nf}}$; $\mathrm{Pr}_{nf} = \frac{\nu_{nf}}{\alpha_{nf}}$; $\alpha_{nf} = k_{nf} / (\rho_{nf} . C_{pnf})$

Heat transfer coefficient: $h_{nf} = (Nu_{nf} . k_{nf}) / d$. (8)

B.3 Analytical Study Results

Using the available correlations in the current literature cited above, a MATLAB code was developed to compute heat transfer in nanofluids. The MATLAB code incorporated the thermal properties of nanofluids outlined in equations (1) through (5). These equations indicate volume fraction ϕ of nanoparticles directly influences properties ρ, μ, c_p, k. Therefore they affect Reynolds number which diminishes with increase in particle loading as shown in Figure 1. The density increase is modest but the viscosity increase is higher and hence the Reynolds number decreases. The results from heat transfer coefficient computations using equations (6) through (8) denoted above is

also shown in the upper section of Figure B.1. We observe that for a volume concentration of copper oxide nanoparticles of 10%, the convective heat transfer coefficient is 2.2 times that of base fluid (water). The mass flow rate of 0.1 kg/s is in laminar regime, whereas mass flow rates of 0.2 and 0.3 kg/s are in the turbulent regime. The upper plot of Figure B.1 reveals the ratio of heat transfer coefficient of nanofluid to the base fluid is strongly dependent upon volume fraction of particles and is very weakly dependent upon Reynolds number.

Figure B.2 presents the same information as presented in Figure B.1, but for higher percentages of particle loading. It is understandable that volume fraction beyond, say 30% is highly undesirable due to high viscosity and agglomeration problem. These may lead to pitting of the surface. However we wanted to explore how far the heat transfer coefficient increases before it starts diminishing with particle concentration. The results in Figure B.2 clearly indicate that beyond a particle concentration of 30% the advantage of nanofluids for heat transfer as a medium becomes less effective.

B.4 Savings in Pumping Power

Based on the specification of a diesel electric generator set operating in Lime Village, Alaska under the conditions shown in the table below, Das and Kulkarni (2005) have demonstrated the savings in pumping power by taking the example of heat recovery from the jacket water of the diesel engine.

Table B.1. Data considered from a diesel electric generator set

Generator Load	31 kW
Coolant Used	60% Ethylene Glycol & 40 % Water
Coolant Flow Rate	0.31 kg/s
Jacket Water Temperatures to Heat Exchanger	Inlet : 78.9 C and Outlet: 57.5 C
Heat Exchanger Tube Diameter	6.35 mm

For the above generator set, the calculated pumping power for jacket water is reduced from 467 W to 318.6 W (31.7%) as shown in Figure B.3 because of the diminished size of the heat exchanger due to the enhancement in heat transfer by nanofluids.

Research performed by Boutin (2001) indicates that the small size of the nanoparticles is such that pitting of tube surfaces does not occur. Although the addition of nanoparticles does tend to increase the viscosity of the fluid the net effect on pumping power is still reduced due to the dramatic increase in h resulting in lower volumetric flow for a given heat exchanger application. Furthermore, Li and Xuan (2002) show that for a concentration of up to 2% by volume of copper nanoparticles, the friction factor does not differ from that of pure water. Hence pumping power penalty does not occur for dilute nanofluids. Hence we have only considered upto 1% of particle volume concentration in Figure B.3.

B. 5 Numerical Study

To verify and improve the results obtained from the analytical study, a numerical study was performed using the computational fluid dynamics code, Fluent. The first attempt was a two-dimensional analysis of nanofluids flowing through parallel planes. The computational geometry with a domain of 5 mm wide x 915 mm long channel was created. These dimensions are adopted from the design of the test apparatus we have built which is described later in this paper. This computation used a grid having 18300 quadrilateral cells with 19236 nodes, as shown in Figure B.4. The boundary conditions are inlet velocity of 0.2 m/s, outflow boundary value is matched by mass conservation. A uniform heat flux of 147,000 W/m^2 was imposed on bottom and top walls. It was a laminar flow simulation.

To simulate nanofluids in Fluent, the mixture model, which is designed for two or more phases (fluid or particulate), is adopted. The mixture model solves the continuity

equation, the momentum equation, the energy equation for the mixture and the volume fraction equation for the secondary phase. The mixture model can also be used without relative velocities for the dispersed phases to model homogeneous multiphase flow.

B.5.1 Theory used for numerical simulation

Fluent employs the following equations for the mixture model. The continuity equation for the mixture is

$$\frac{\partial}{\partial t}(\rho_m) + \nabla.(\rho_m \bar{v}_m) = 0 \tag{9}$$

where $\bar{v}_m$ is the mass-averaged velocity:

$$\bar{v}_m = \frac{\sum_{k=1}^{n} \alpha_k \rho_k \bar{v}_k}{\rho_m} \tag{10}$$

and ρ_m is the mixture density:

$$\rho_m = \sum_{k=1}^{n} \alpha_k \rho_k \tag{11}$$

α_k is the volume fraction of phase *k*.

Momentum equation for the mixture can be obtained by summing the individual momentum equations for all phases.

$$\frac{\partial}{\partial t}(\rho_m \bar{v}_m) + \nabla.(\rho_m \bar{v}_m \bar{v}_m) = -\nabla P + \nabla.[\mu_m(\nabla \bar{v}_m + \nabla \bar{v}_m^{T})] + \rho_m \bar{g} + \bar{F} + \nabla.(\sum_{k=1}^{n} \alpha_k \rho_k \bar{v}_{dr,k} \bar{v}_{dr,k}) \tag{12}$$

where n is number of phases, $\bar{F}$ is a body force and μ_m is the viscosity of the mixture.

$$\mu_m = \sum_{k=1}^{n} \alpha_k \mu_k \tag{13}$$

The energy equation for the mixture is given as:

$$\frac{\partial}{\partial t}\sum_{k=1}^{n}(\alpha_k \rho_k E_k) + \nabla.\sum_{k=1}^{n}(\alpha_k \bar{v}_k(\rho_k E_k + p)) = \nabla.(k_{eff}\nabla T) + S_E \quad (14)$$

where k_{eff} is the effective thermal conductivity and S_E includes any other volumetric heat sources. E_k is given by:

$$E_k = h_k \qquad \text{for an incompressible phase} \quad (15)$$

where h_k is the sensible enthalpy for phase *k*.

The relative velocity is defined as the velocity of a secondary phase (p) relative to the velocity of primary phase (q). In our simulation the primary phase is water and secondary phase is particles of 50 nm.

$$\bar{v}_{pq} = \bar{v}_p - \bar{v}_q \quad (16)$$

The drift velocity and the relative velocity (v_{pq}) are connected by following correlation

$$\bar{v}_{dr,p} = \bar{v}_{pq} - \sum_{k=1}^{n} c_k \bar{v}_{qk} \quad (17)$$

The mass fraction for any phase (k) is defined as

$$c_k = \frac{\alpha_k \rho_k}{\rho_m} \quad (18)$$

From the continuity equation for secondary phase p, the volume fraction equation for secondary phase p is given as:

$$\frac{\partial}{\partial t}(\alpha_p \rho_p) + \nabla.(\alpha_p \rho_p \bar{v}_m) = -\nabla.(\alpha_p \rho_p \bar{v}_{dr,p}) \quad (19)$$

The above equations are solved in Fluent and heat transfer results are obtained in post processing.

B.5.2 Numerical results

Figure B.5 shows the numerical results obtained from the Fluent simulation. At the leading edge of the duct the convection coefficient is observed to be about 3300

W/m^2K and it approaches the thermally fully developed value of about 500 W/m^2K. The average value of heat transfer coefficient over the duct is 681 W/m^2K.

Figure B.6 displays that the average value of convective heat transfer coefficient increases with increase in the particle volume loading. The convection coefficient is higher at higher Reynolds number. The Reynolds numbers of 2487 and 3482 have exceeded the laminar regime limit of 2300 and introduce some error in our laminar simulation. We intend to repeat the computations for Reynolds numbers: 500, 1000, 1500, 2000 and 2300 in the future.

Figure B.7 shows the ratio of heat transfer coefficient of nanofluids to the base fluid. For a particle volume fraction of 10% copper oxide nanoparticles it enhances the heat transfer coefficient by 45 % over the base fluid. It is also observed that the ratio of heat transfer coefficient of nanofluid to water is practically independent of Reynolds number.

B.6 Nanofluids Test Apparatus

No research data on hydrodynamic and thermal characteristics of silver nanofluids has appeared in the literature thus far. The University of Alaska Fairbanks Chemistry Department has been successful in producing this kind of nanofluid. In order to determine the fluid dynamic and heat transfer characteristics of silver nanofluids we have designed a test apparatus shown schematically in Figure B.8. It consists of a 4.76 mm (3/16 inch) nominal diameter copper tube test section of 91.44 cm (36 inch) length in which nanofluid is heated by electric resistance strip heaters. Then the nanofluid is cooled by the laboratory water via an annular counterflow 4-pass heat exchanger. The nanofluid is circulated by a single stage regenerative turbine pump. Flow control is provided by a test loop bypass line and a throttle valve. Fluid and wall temperature measurements across the test section are obtained by type T thermocouples. Volumetric flow of nanofluids is

measured by a turbine flow meter. Pressure drop measurement across the test section is achieved by a differential pressure transducer. A detailed calculations and the principle behind the design of this test apparatus have been presented by Das et al. (2006).

The fluid circuit is equipped with a 1/3-hp single stage regenerative turbine pump as shown in Figure B.9. The heat supply consists of four 1,250 W (max) strip heaters that are controlled by four variable transformers (variacs). The test section is covered by fiberglass insulation of 15 cm thickness to minimize heat loss in the test section. All temperature measurements are performed using Type-T thermocouples. The differential pressure transducer is used to measure the pressure loss through the test section, and an Omega turbine flow meter is used to measure fluid flow rate through the test section. A Campbell Scientific data logger (Figure B.9) is programmed for data acquisition recording temperatures, pressures and volumetric flow rates at regular intervals of a few seconds.

The device allows an experiment to be conducted with as little at 2-liters of nanofluid, and can maintain a thermally and hydrodynamically fully developed steady flow for a test section Reynolds number from 0 to 25,000. Additionally, the heater and cooling systems have been designed and tested to achieve and maintain a test section inlet temperature of 60°C and outlet temperature of 70°C; even lower test section inlet temperatures and larger temperature differentials were achieved during trial runs with water. A temperature below 100°C in the test loop is maintained to prevent steam formation and evaporative loss. This apparatus is ready to be used to measure heat transfer and fluid dynamic characteristics of silver and other nanofluids.

B.7 Conclusions

Theoretical and numerical analyses are presented to show the heat transfer enhancement by using nanofluids. Analytical solutions predict a 50% increase in convective heat transfer coefficient of copper oxide nanoparticles in water. For the same condition numerical analysis predict 45% increase in convective heat transfer coefficient over the base fluid water. Analytical result show that beyond a particle concentration of 30% nanofluids loose their effectiveness and the convective heat transfer coefficient diminishes. Below 30% concentration, as the particle loading increases the heat transfer coefficient increases but the ratio of heat transfer coefficient of nanofluids to base fluid remains unaffected by the change in Reynolds number. It is proven that pumping power is reduced. An experimental apparatus was designed that would provide a means of measuring the convective coefficient of nanofluids. The apparatus is now ready to measure the hydrodynamic and heat transfer characteristics of various types of nanofluids including silver nanofluid. The experimental results from this apparatus will be valuable to provide data to validate and calibrate computational fluid dynamics results that will be employed for nanofluids applications.

B.8 Acknowledgment

Financial assistance from the Arctic Region Supercomputing Center and the Dean of the Graduate School at University of Alaska Fairbanks is gratefully acknowledged.

B.9 Nomenclature

C_p	Specific heat, J/kg K
d	Inner diameter of the tube, m
d_p	Particle diameter, m
h	Convective heat transfer coefficient, W/m^2 K
k	Thermal conductivity, W/m K
k_f	Thermal conductivity of fluid, W/m K
k_p	Thermal conductivity of particle, W/m K
Nu	Nusselt number
Pe_d	Peclet number for particle
Pr	Prandtl number
Re	Reynolds number
u_m	Mean velocity, m/s
μ	Coefficient of dynamic viscosity of the fluid, kg/m s
ρ	Density of the fluid, kg/m^3

Subscript

f	Fluid
m	Mean
nf	Nanofluid
p	Particle
w	Water

B.10 References

Boutin, C., " Taking the heat off: Nanofluids promise efficient heat transfer," logos, Vol. 19, No.2, 2001.

Das, D.K., Kulkarni, D.P., Silbaugh, B., "A Study on Nanofluids for their Convective Heat Transfer and Hydrodynamic Characteristics," Proceedings of National Conference on Emerging Trends in Nanotechnology and Innovations in Design and Manufacturing, National Institute of Technology, Rourkela, India, February 2006, pp. 1- 23.

Das D.K., Kulkarni, D,P., "A Theoretical Investigation on Heat Transfer Characteristics of Nanofluids," Arctic Science Conference Proceedings, Kodiak, Alaska, 2005, p. 14.

Fluent Inc., "Users Manual-section 24.3," Lebanon, New Hampshire, 2005.

Kulkarni, D.P., Das, D.K., Chukwu, G.A., "Temperature Dependent Rheological Property of Copper Oxide Nanoparticles Suspension (Nanofluid)," Journal of Nanoscience and Nanotechnolgy, Vol. 6, 2006, pp 1150-1154.

Li, Q., Xuan, Y., "Convective heat transfer and flow characteristics of Cu-water nanofluid," Science in China (Series E), Vol. 45, No. 4, 2002, pp. 408-416.

McQuiston, F., Parker, J. and Spitler, J., *Heating, Ventilating, and Air Conditioning.* Sixth Ed, John Wiley and Sons Inc, NJ, 2005.

Pak, Bock Choon, Young I. Cho, "Hydrodynamic and heat transfer study of dispersed fluids with submicron particles." Experimental Heat Transfer. Vol. 11, 1998, pp. 151-170.

Xuan, Y., Li, Q., "Heat transfer enhancement of nanofluids." International Journal of Heat and Fluid Flow. Vol 21., 2000, pp. 58-64.

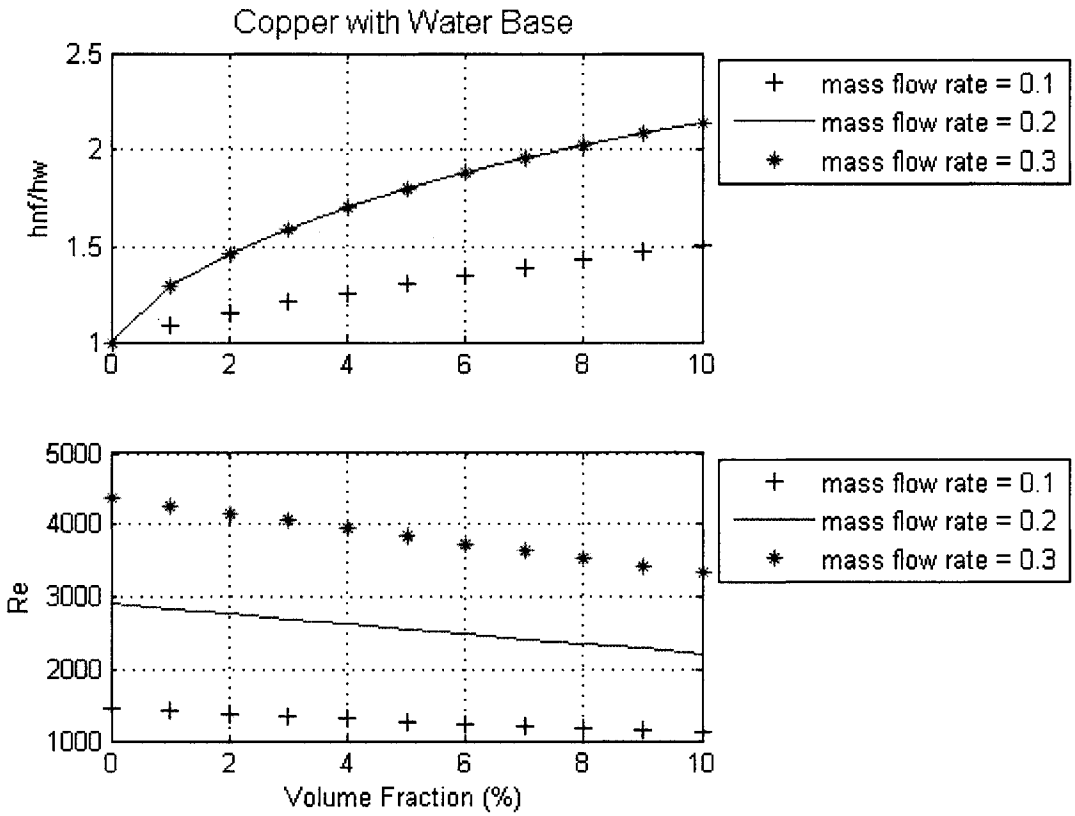

Figure B.1. Effect on heat transfer coefficient and Reynolds number due to addition of copper oxide nanoparticles in varying percentages in water.

Note: Mass flow rate is in kg/s.

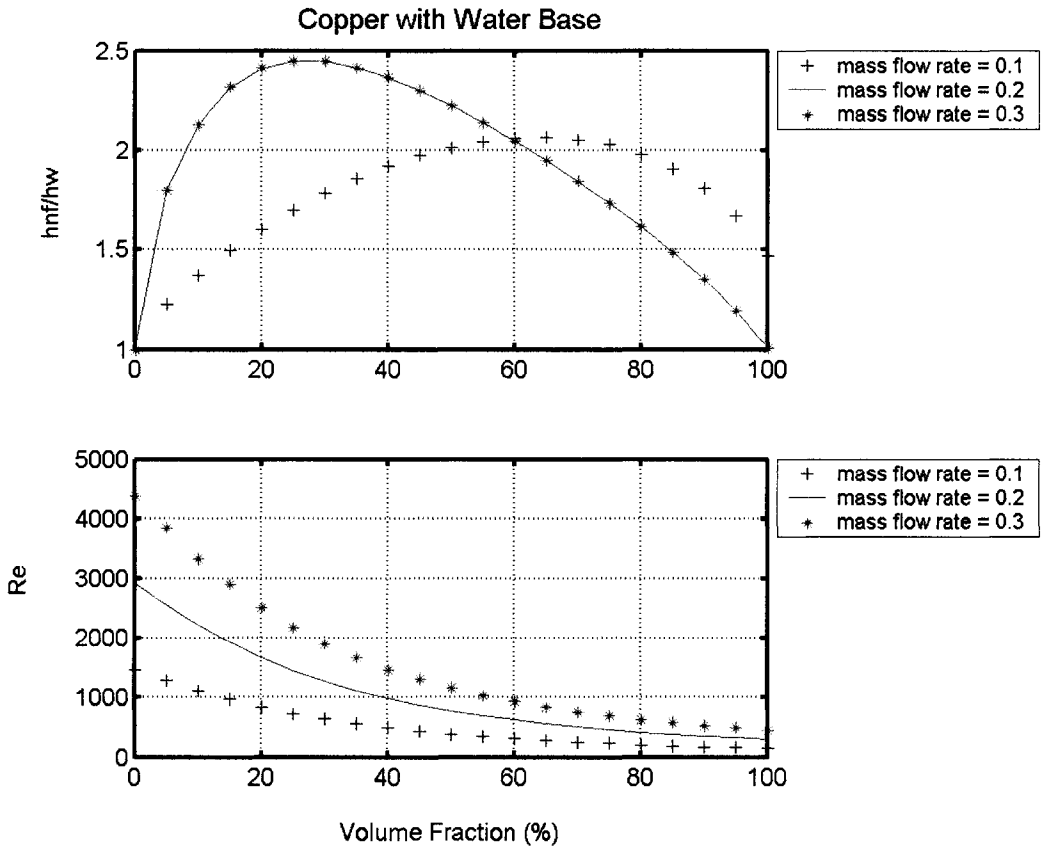

Figure B.2. Effect on heat transfer coefficient and Reynolds number due to addition of copper oxide nanoparticles in varying percentages in water.

Note: Mass flow rate is in kg/s.

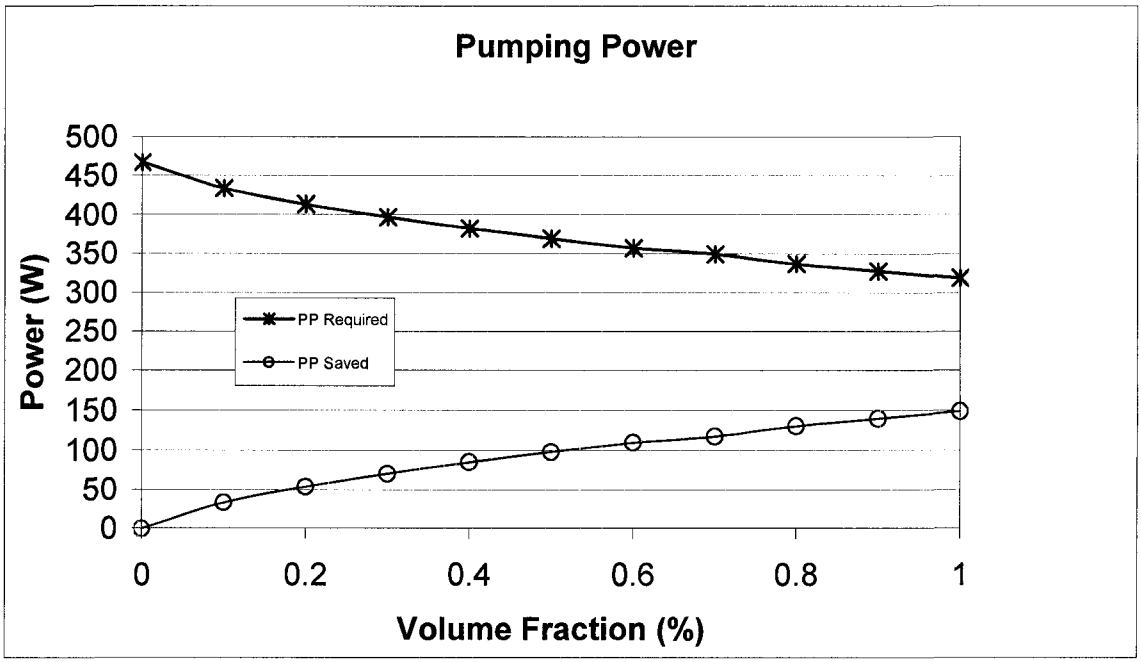

Figure B.3. Pumping power saving for a typical diesel engine generator set.

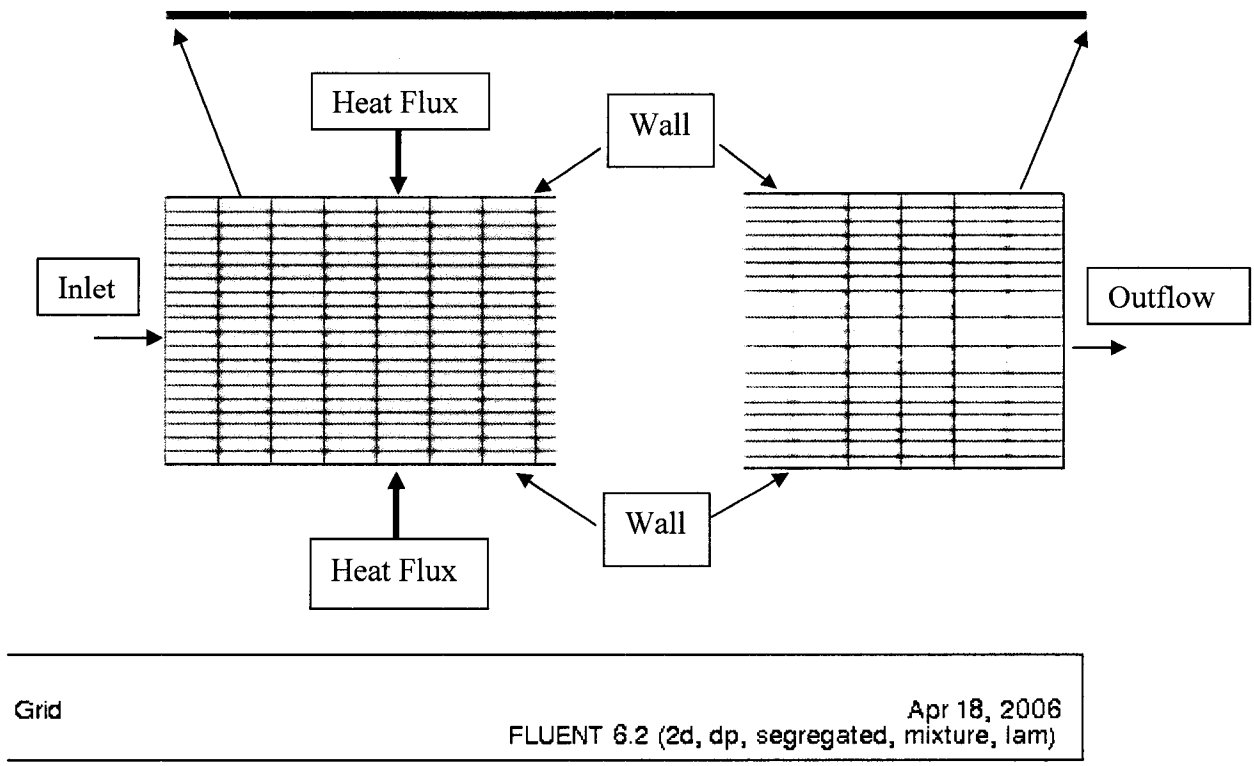

Figure B. 4. Grid geometry and boundary conditions for numerical analysis.

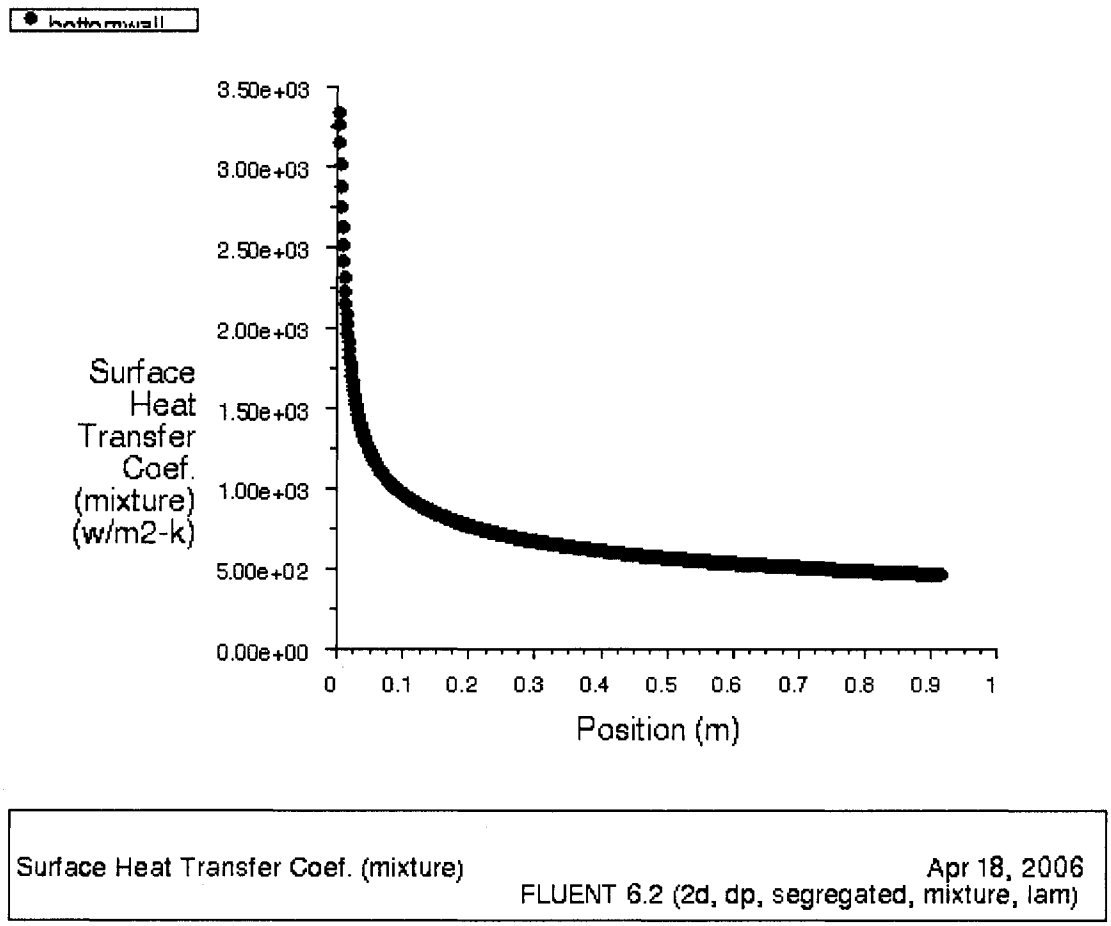

Figure B. 5. Variation in heat transfer coefficient along the bottom wall for a particle concentration of 3% (Left side is the leading edge).

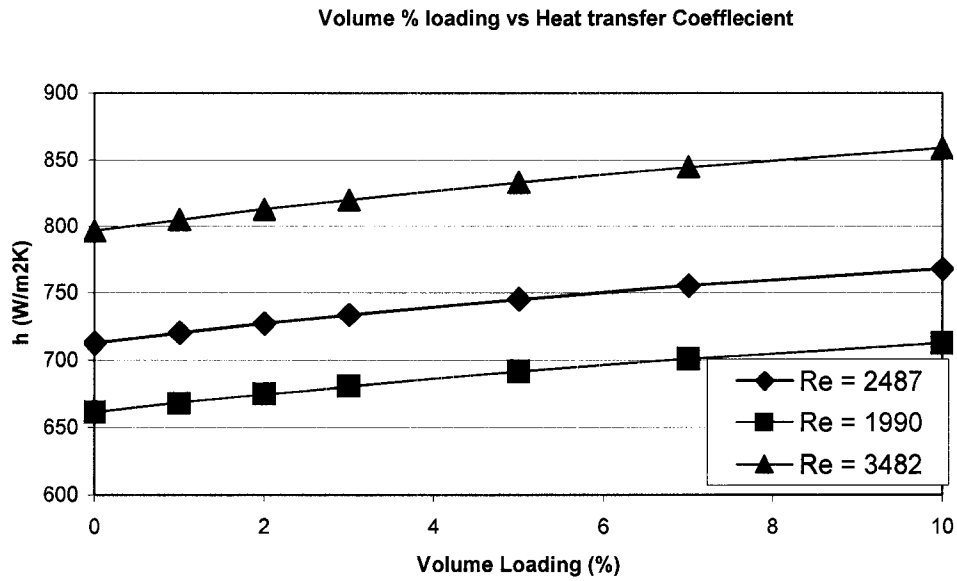

Figure B.6. Variation of heat transfer coefficient with particle volume loading for different Reynolds number.

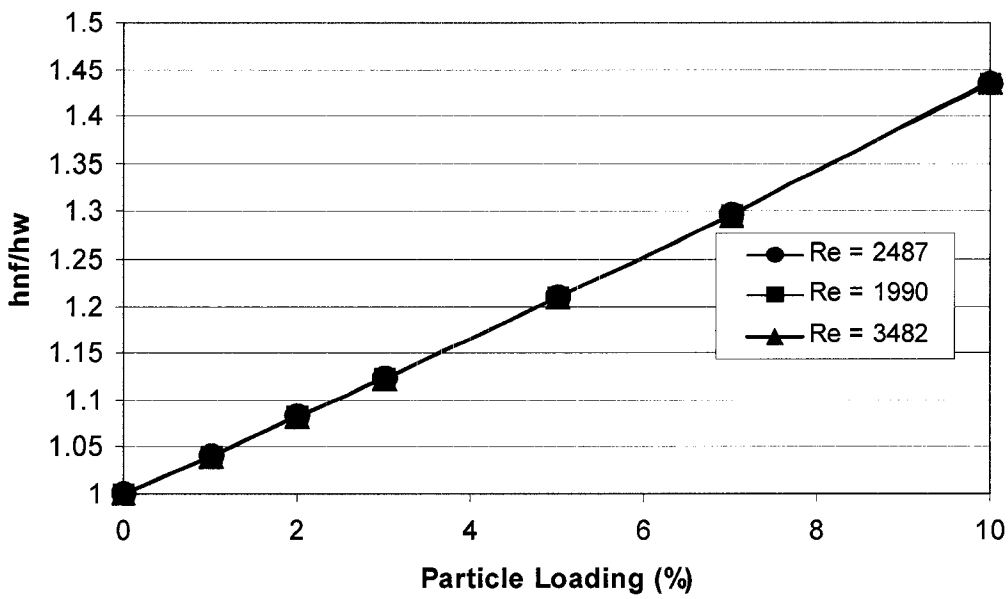

Figure B.7. Comparision of heat transfer coefficient of nanofluid versus base fluid with varying particle volume for different Reynolds number.

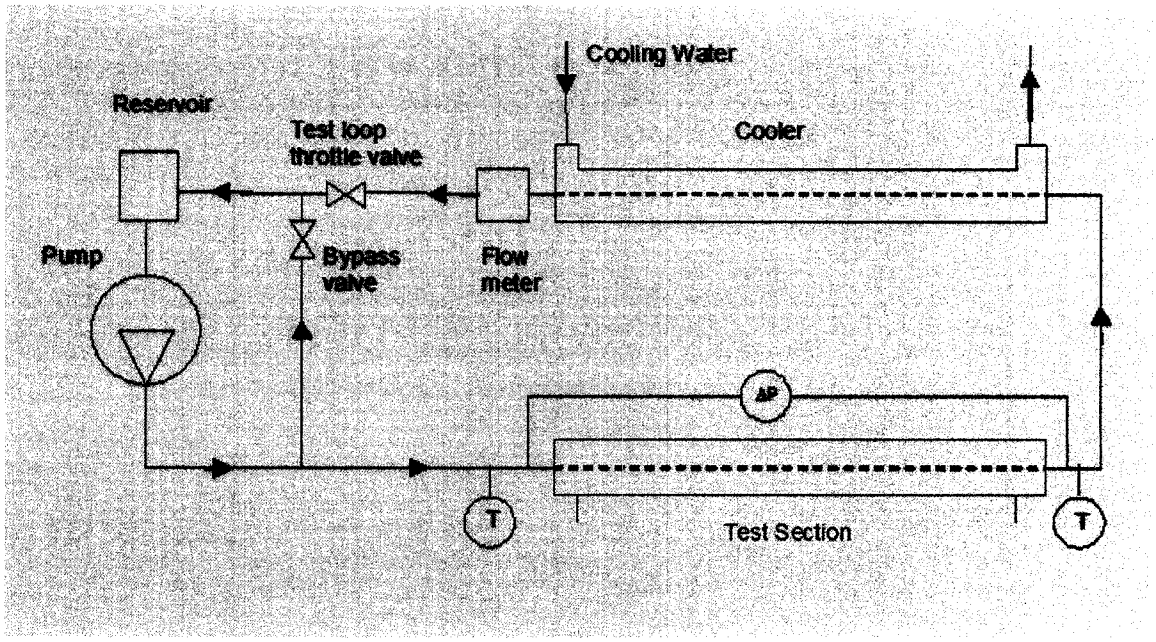

Figure B.8. A schematic diagram of the nanofluids experimental apparatus, T = Thermocouples, ΔP = Differential pressure transducer.

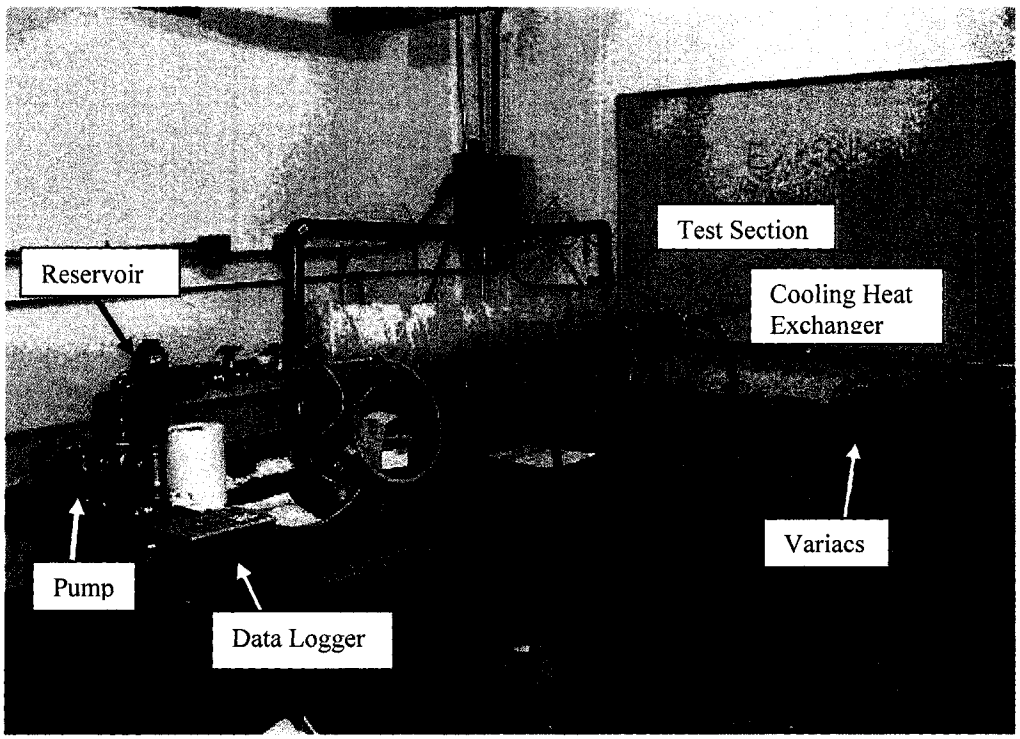

Figure B.9. Completed apparatus to investigate nanofluid thermal performance.

APPENDIX C

Viscosity of Copper Oxide Nanoparticles Dispersed in Ethylene Glycol and Water Mixture

Praveen K. Namburu[1], Devdatta P. Kulkarni[1], Debasmita Misra[2], and Debendra K. Das[1]*

[1] Department of Mechanical Engineering

[2]Department of Mining and Geological Engineering

University of Alaska, Fairbanks

P.O. Box 755905, Fairbanks, AK, 99775-5905, USA.

Abstract

Nanofluids are new kinds of fluids engineered by dispersing nanoparticles in base fluids. This paper presents an experimental investigation of rheological properties of copper oxide nanoparticles suspended in 60:40 (by weight) ethylene glycol and water mixture. Nanofluids of particle volume percentage ranging from 0% to 6.12% were tested. The experiments were carried over temperatures ranging from –35°C to 50°C to demonstrate their applicability in cold regions. For the particle volume concentrations tested, nanofluids exhibited newtonian behavior. An experimental correlation was developed based on the data, which relates viscosity with particle volume percent and the nanofluid temperature.

Accepted for Publication, Experimental Thermal and Fluid Science, May 2007

Keywords: nanofluid, ethylene glycol, viscosity, rheology, temperature dependency.

*Corresponding Author:ffdkd@uaf.edu,Ph:907-474-6094, Fax:907-474-6141.

C.1 Introduction

Nanofluids are composites consisting of solid nanoparticles with sizes varying generally from 1-100 nm dispersed in heat transfer liquids such as water, ethylene glycol, propylene glycol and so on. In the last decade, nanofluids have gained significant attention due to their enhanced thermal properties. According to Eastman et al [1], when 0.3 volume percent of copper nanoparticles are suspended in ethylene glycol, thermal conductivity of the fluid increases by 40%. Pak and Cho [2] report that the convective heat transfer coefficient increases by 75% for an Al_2O_3 particle concentration of 2.78% at a fixed Reynolds number. Results like these have motivated both the industrial and science communities to explore the heat transfer and rheological properties of nanofluids.

A great deal of energy is expended heating industrial and residential buildings in the cold regions of the world. Due to the severe winter conditions, ethylene glycol or propylene glycol mixed with water in different volume percentages are typically used to lower the aqueous freezing point of the heat transfer medium [3]. Such heat transfer fluids are used in baseboard heaters in homes, heat exchangers, automobiles and in industrial plants in cold regions. These fluids can withstand very low temperatures. At low temperatures, ethylene glycol mixtures have better heat transfer characteristics than propylene glycol mixtures [4]. A 60% ethylene glycol and 40% water by weight fluid mixture is most commonly used in the sub-arctic and arctic regions of Alaska. We have conducted experiments with this fluid mixture by adding copper oxide nanoparticles in order to explore the thermophysical properties of such nanofluids. A thorough understanding of these properties is key to testing for successful application in cold regions. Xuan and Li [5] showed that a nanofluid of low concentration increases the heat transfer coefficient substantially without much penalty in pressure loss. Therefore, copper

oxide nanoparticles dispersed in a glycol/water mixture in various volume percentages (0%, 1%, 2%, 3%, 4%, 5% and 6.12%) were tested to investigate the rheological characteristics of these nanofluids over temperatures ranging from -35°C to 50°C for their effective usage.

Determining the viscosity of the nanofluid is essential to establishing adequate pumping power as well as the convective heat transfer coefficient, as the Prandtl and Reynolds numbers (functions of viscosity) will be influenced. Until now, only a few studies have addressed the viscous properties of nanoparticles suspensions at cold temperatures. Earlier research at higher temperatures includes investigation of viscosity of carbon nanotubes [6] and graphite nanofluids [7], $BaTiO_3$ suspensions [8], nickel-terpineol suspensions [9], and TiO_2 nanoparticles in water [10]. Other investigations have focused on the rheology of aluminum nanoparticle suspensions in paraffin oil [11] and Al_2O_3 nanoparticles in water [12]. Results for copper oxide in ethylene glycol at room temperature [13] have been presented, but no data is available for subzero temperatures. Several available correlations for nanofluid viscosity are presented below.

Einstein [14] proposed a viscosity correlation for particle suspensions in base fluid when the volume concentration is lower than 5%.

$$\mu_s = \mu_f(1 + \frac{5}{2}\phi) \tag{1}$$

Here, μ_s = suspension viscosity, μ_f = viscosity of base fluid, and ϕ is volume percentage of particles in base fluid.

Bicerano et al [15] proposed a similar correlation which relates viscosity and volumetric suspensions by:

$$\mu_s = \mu_f(1 + \eta\phi + k_H\phi^2 + ...) \tag{2}$$

Here η is the virial coefficient and k_H is Huggins coefficient.

Brinkman [16] presented a viscosity correlation that extended Einstein's equation to concentrated suspensions.

$$\mu_s = \mu_f \frac{1}{(1-\phi)^{2.5}} \tag{3}$$

Notice that all three correlations, equations (1), (2) and (3) were developed to relate viscosity as a function of volume percentage only; there is no consideration of temperature dependence.

Generally fluids have higher viscosity near their freezing point and fairly low viscosity near their boiling temperature, showing that viscosity is a strong function of the temperature. White [17] presented a correlation for pure fluids between viscosity (μ_f) and temperature which is given by:

$$\ln\frac{\mu_f}{\mu_0} \approx a + b(\frac{T_0}{T}) + c(\frac{T_0}{T})^2 \tag{4}$$

Here (μ_0, T_0) are reference values and (a, b, c) given in the table by White, are dimensionless curve-fit constants. They vary from fluid to fluid; for example for water a = -2.10, b = -4.45 and c = 6.55. Kulkarni et al. [18] proposed a correlation that relates viscosity of copper oxide nanoparticles suspended in water and in the temperature range of 5°C to 50°C

$$\ln \mu_s = A(\frac{1}{T}) - B \tag{5}$$

Here A and B are the functions of volume percentage ϕ. As this is an aqueous solution, this correlation is not applicable for nanofluids in the subzero temperature range. Our investigation of the relation between temperature and nanofluid viscosity at subzero temperatures will help us develop the next generation of heat transfer fluids applicable in cold regions. A comprehensive review of heat transfer characteristics including viscosity measurements of nanofluids have been recently presented by Wang and Mujumdar [19].

C.2 Experimental Procedure

In our experiments, we used copper oxide nanoparticles with an average diameter of 29 nm and a particle density of 6.3 gm/cc (Nanopahse, Inc [20]). Nanofluids with different volume concentrations (2%, 4%, 6%, 8%, and 10%) were dispersed in a 60:40 (in weight) ethylene glycol and water mixture. Sample preparation was carried out using a very sensitive mass balance with an accuracy of 0.1 mg. The nanofluid mixture was then stirred and agitated thoroughly for 30 minutes with an ultrasonic agitator similar to the preparation of nanofluids by He et al. [21]. This ensures uniform dispersion of nanoparticles in the base fluid.

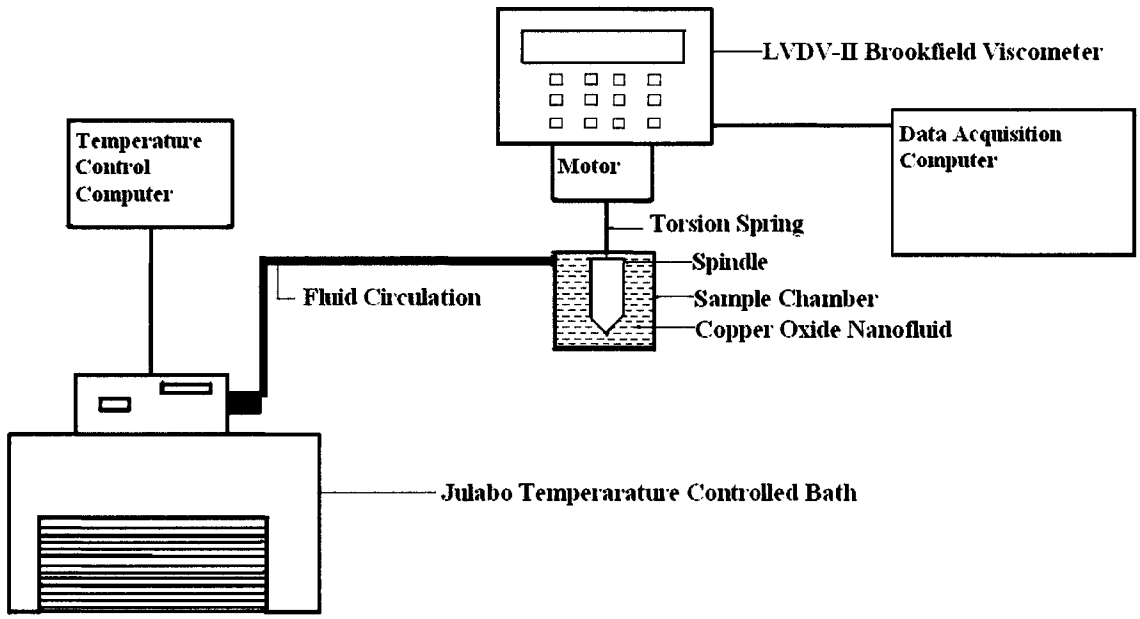

Figure C.1. Experimental setup for viscosity measurement of nanofluids.

The experimental setup for the rheological property measurements of the copper oxide nanoparticles suspended in an ethylene glycol-water mixture is shown in Figure C. 1. It consists of an LV DV-II+ Brookfield programmable Viscometer [22] and Julabo temperature- controlled bath with a computer to control temperature. The viscometer drives a spindle immersed in the test fluid. When the spindle is rotated, the

viscous drag of the fluid against the spindle is measured by the deflection of the calibrated spring. This viscometer has a viscosity measurement range of 1.5 to 30,000 mPa.s and can handle the viscosity measurement results within the temperature range of this experiment. A computer controls the temperature of this bath that is used to vary the temperature of the test sample from -35°C to 50°C. Spindle SC-18 was used in this viscometer and was calibrated by using Brookfield viscosity standard fluids. The viscometer contains a sample chamber where the fluid is tested. Temperature inside the sample chamber is carefully monitored using a RTD temperature sensor during the viscosity measurements. The spindle type and speed combinations will produce satisfactory results when the applied torque is between 10-100%; therefore spindle types and speeds are selected in such a way that the torque values lie in this prescribed range. A wide range of spindle speeds are available in this viscometer (0-200 RPM).

Viscosity measurements were started at 50°C and temperature was gradually reduced to -30°C in 10° increments, with the last reading was taken at -35°C. Because the base fluid freezes at about -45°C, the experiments were carried down to a minimum temperature of -35°C with a factor of safety of 10°C.

The viscometer is connected to another computer as shown in Figure C.1, which records the data automatically. The data collection is done by the software Wingather® [22], which collects spindle RPM, torque, viscosity, shear stress, shear rate, temperature and time. All the viscosity measurements were recorded at steady state conditions; that is, ample time (about 30 minutes) was allocated for the temperature to stabilize.

C.3 Results and Discussion

To verify the accuracy of our equipment and experimental procedure, the viscosity of the ethylene glycol and water (60:40% by weight) was measured before the addition of any copper oxide nanoparticles. The obtained readings were compared with data from the American Society of Heating, Refrigerating and Air-Conditioning Engineers (ASHRAE) handbook [4] see Figure C.2. The ASHRAE data and the experimental values match nicely (maximum difference of ± 2%) with temperatures ranging -35°C to 50°C.

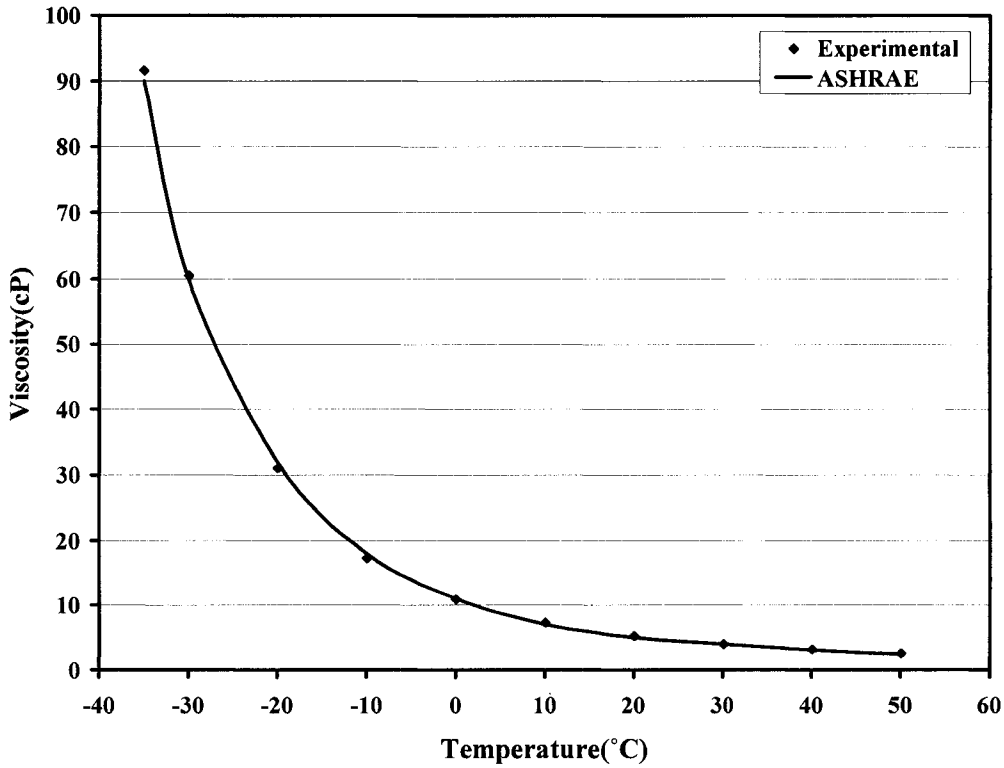

Figure C.2. Comparison of ASHRAE viscosity values of 60:40 ethylene glycol and water mixture (by weight) and experimental data. 1 cP (centipoise) = 1 mPa.s.

The next step was to verify if the nanofluid behaves in a newtonian or non-newtonian manner. The equation governing newtonian behavior of a fluid is given by

$$\tau = \mu \dot{\gamma} \tag{6}$$

Where τ is the shear stress, μ is the coefficient of viscosity and $\dot{\gamma}$ is the shear strain rate. From the ASHRAE handbook, one observes that ethylene glycol and water mixture behaves as a newtonian fluid. While deriving the viscosity values for figure C.2, it was found that 60:40 ethylene glycol and water at temperatures ranging from -35°C to 50°C, behaves as newtonian fluid.

The next step was to determine whether the fluid displays non-newtonian properties after the addition of copper oxide nanoparticles. Kulkarni et al. [18] observed that in experiments with copper oxide nanoparticles at volume concentrations of 5% to 15% in water, these mixtures became non-newtonian fluids in the temperature range of 5°C to 50°C. Figure C.3 shows shear stress versus shear strain rate for 6.12% copper oxide nanoparticles concentration in ethylene glycol/water mixture at -35°C. Despite a small intercept on the shear stress axis due to measurement uncertainty, this nanofluid clearly demonstrates newtonian behavior. We believe that since ethylene glycol water mixture exhibits newtonian behavior, it dominates the rheological property and the whole mixture behaves like a Newtonian fluid with low concentrations of nanoparticles.

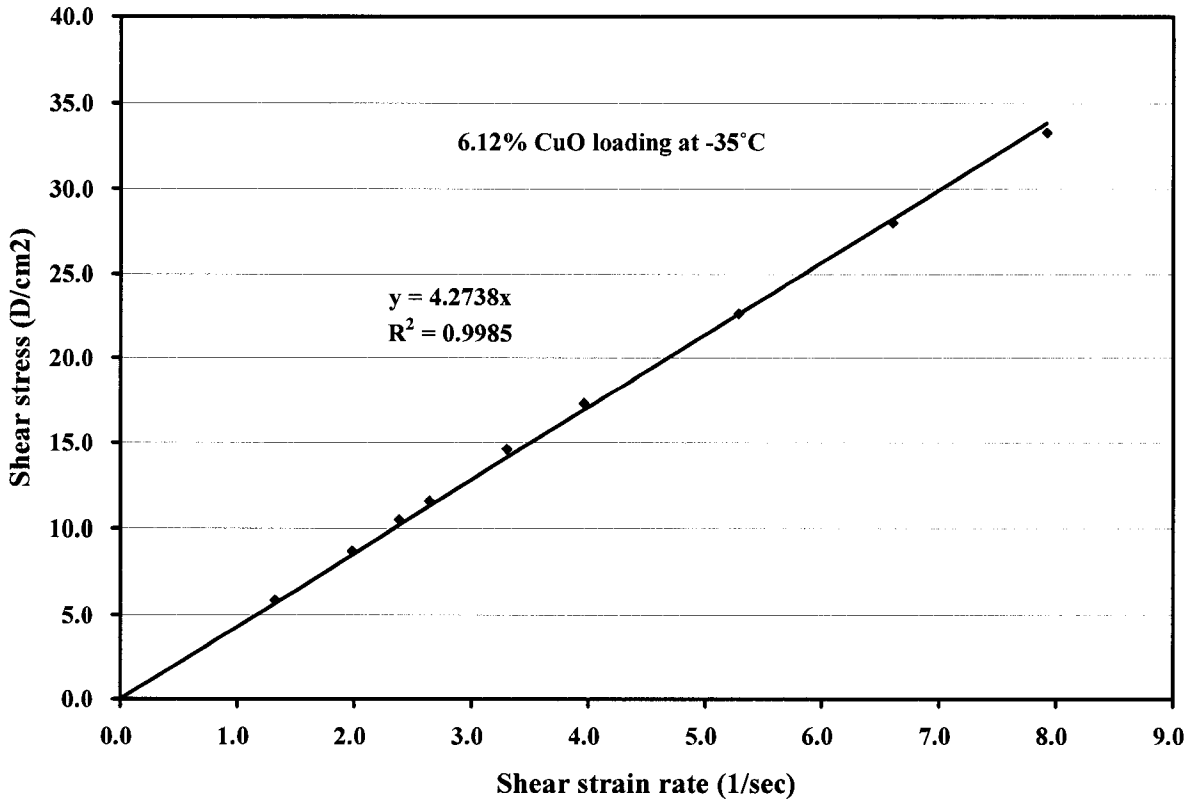

Figure C.3. Shear stress in dyne/cm^2 versus shear strain rate for 6.12% volume CuO loading at -35°C

After we performed the base case experiments, confirming that the obtained readings were correct and that the fluid was Newtonian, viscosity measurements of fluid samples with different volume concentrations were carried out with varying temperatures between -35°C to 50°C. The results of these measurements are shown in Figure C.4. Each data point in this plot was generated from the slope of a straight line given by the shear stress versus shear strain rate, similar to Figure C.3. Preliminary analysis of this data indicates viscosity diminishes exponentially with a fluid temperature increase. Higher concentrations of nanofluids possess higher viscosity. The variation trends of viscosity with temperature for all concentrations of nanofluids are similar. This indicates consistency of the trend of the experimental results.

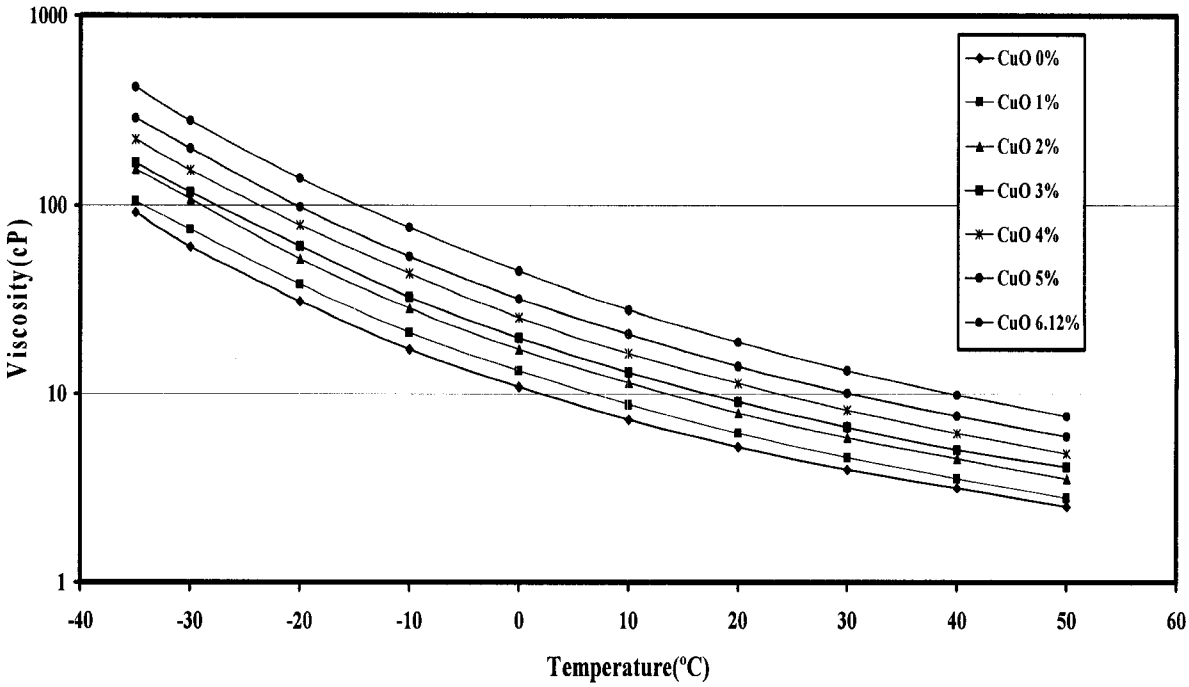

Figure C.4. Experimental values of viscosity for various volume concentrations of nanofluids with respect to temperature.

Figure C.5 illustrates the relationship between relative viscosity and temperature for varying volume concentrations of CuO nanoparticles in the mixture. Relative viscosity is a ratio of the viscosity of the nanofluid (μ_s) to the viscosity of the base fluid alone (μ_f). Figure C.5 demonstrates that relative viscosity diminishes as temperature increases at a higher rate for higher concentrations of nanoparticles. At lower concentrations, the change in relative viscosity over temperature is minimal.

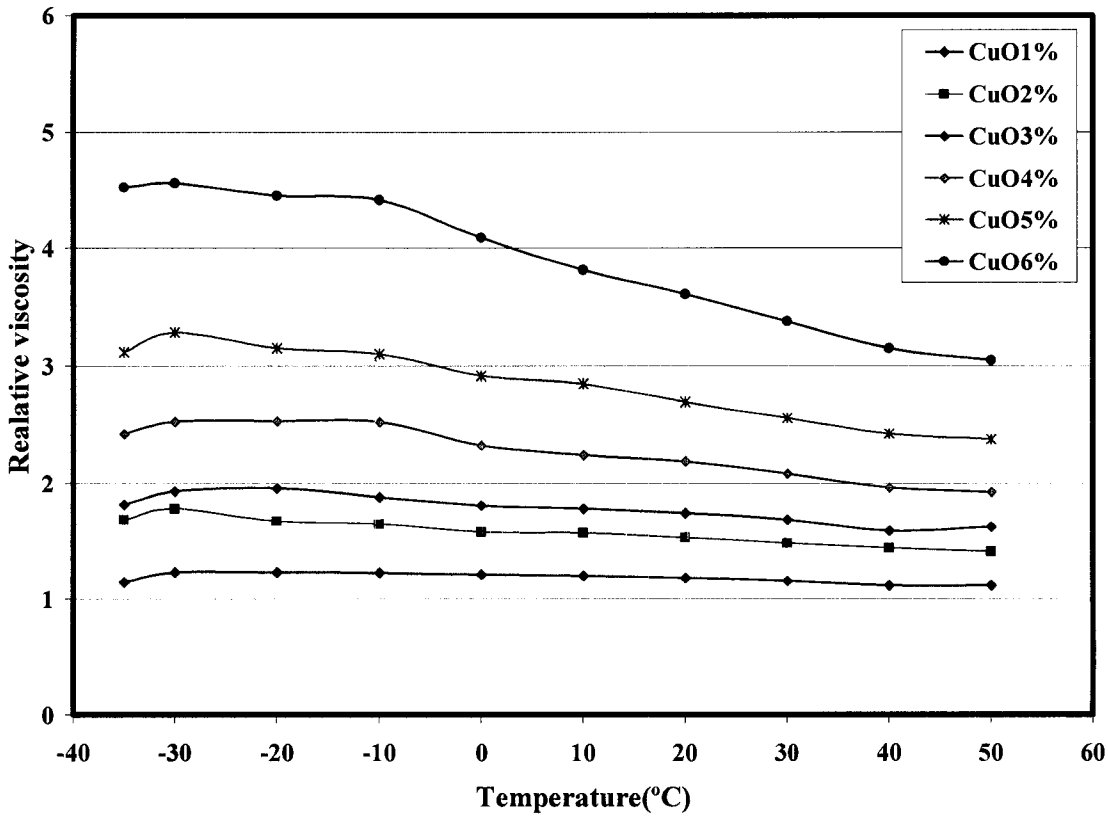

Figure C. 5. Relative viscosity and temperature relationship for various concentrations of CuO.

Different correlations were tried to fit our experimental data to correlations presented by Yaws [23], Kulkarni et al [18], Tseng [10] and White [17]. None of these correlations fit the data. Therefore, by careful statistical analyses an exponential model given by Equation (7) was derived. This equation fits the data with a correlation coefficient $R^2 > 0.99$.

$$\text{Log}\left(\mu_s\right) = Ae^{-BT} \tag{7}$$

Where μ_s is the copper oxide nanofluid viscosity in centipoise (cP), T is the temperature in K and A, B are functions of particle volume percentage (ϕ). Each volume percentage

curve in Figure 4 was fitted with Equation (7) and the corresponding values of A and B were evaluated: these appear in Table C.1 below.

Table C.1. Curve fit values of A and B with correlation factor $R^2 > 0.987$.

Volume Concentration (ϕ %)	0	1	2	3	4	5	6.12
A	162.76	139.27	121.77	86.22	75.27	63.02	55.32
B	0.0185	0.0177	0.0171	0.0154	0.0146	0.0137	0.0129

The coefficients A and B are related with volume concentration (ϕ) as

$A = 1.8375(\phi)^2 - 29.643(\phi) + 165.56$ with $R^2 = 0.9873$ (8)

$B = 4 \times 10^{-6}(\phi)^2 - 0.001(\phi) + 0.0186$ with $R^2 = 0.9881$ (9)

In the above expressions ϕ ranges from 0 to 6.12.

Figure C.6 illustrates the experimental data and the curves generated using Equation (7) for viscosity versus temperature. The maximum deviation between experimental values and curve-fit values are within ± 8.8 %. In Figure C.6, "Exp" represents experimental values of viscosity and "CF" represents the curve-fit values from the proposed correlations.

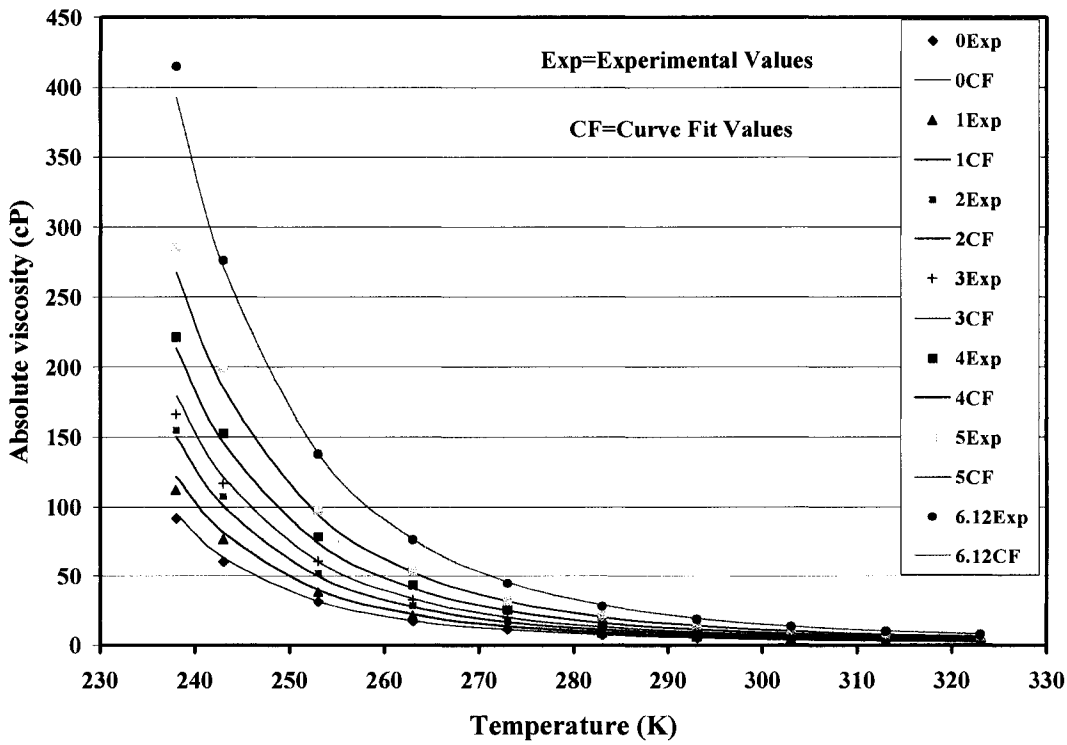

Figure C.6. Nanofluid viscosity (μ_s) versus temperature of 60:40 ethylene glycol and water mixture with different volume percentage of CuO loading.

C. 4 Conclusions

1. Copper oxide nanofluids exhibit Newtonian behavior in an ethylene glycol and water mixture for concentrations varying from 0 to 6.12% with temperatures ranging from -35°C to 50°C.
2. The viscosity of nanofluids increases when the volume concentration of nanoparticles increases. For example, the viscosity of 6.12% copper oxide volume concentration is about four times the value of the base fluid at -35°C.
3. As the temperature increases the viscosity of copper oxide nanofluids decreases exponentially.

4. The relative viscosity of copper oxide nanofluids is dependent on volume percentage and decreases substantially with temperature for higher concentrations.
5. A new empirical correlation expressed as Equation (7) for this nanofluid follows Arrhenius type expression where the coefficients A and B are functions of volume percentage ϕ.

C. 5 Acknowledgements

Financial assistance from the Arctic Region Supercomputing Center at the University of Alaska Fairbanks is gratefully acknowledged. Authors are thankful to the Institute of Northern Engineering Petroleum Development Laboratory for providing the experimental facilities to measure viscosity.

C.6 References

[1] J.A. Eastman, S.U.S. Choi, S. Li, W. Yu and L.J. Thompson, Anomalously increased effective thermal conductivities of ethylene glycol-based nanofluids containing copper nanoparticles, Applied Physics Letters 78 (6) (2001) 718-720.

[2] B.C. Pak, Y.L. Cho, Hydrodynamics and heat transfer study of dispersed fluids with submicron metallic oxide particles, Experimental Heat Transfer 11 (1998)151-170.

[3] F.C. McQuiston, J.D. Parker, J.D. Spitler, Heating Ventilating and Air conditioning, John Wiley & Sons Inc., New York (2000).

[4] ASHRAE Handbook 1985 Fundamentals, American Society of Heating, Refrigerating and Air-Conditioning Engineers Inc., Atlanta (1985).

[5] Y. Xuan, Q. Li, Investigation on convective heat transfer and flow features of nanofluids. Journal of Heat Transfer 125 (2003) 151-155.

[6] J. Hilding, E.A. Grulke, Z.G. Zhang and F. Lockwood, Dispersion of carbon nanotubes in liquids, Journal of Dispersion Science and Technology 24 (1) (2003) 1-41.

[7] Y. Yang, E.A. Grulke, Z.G. Zhang and G. Wu, Journal of Nanoscience and Nanotechnology, 5 (2005) 571-579.

[8] W. Tseng, C.L. Lin, Effect of dispersants on rheological behavior of $BaTiO_3$ powders in ethanol-isopropanol mixtures, Materials Chemistry and Physics 80, (2003) 232-238.

[9] W. Tseng and C.N. Chen, Effect of polymeric dispersant on rheological behavior of nickel–terpineol suspensions, Material Science and Engineering A 347 (1-2) (2003) 145-153.

[10] W.J. Tseng, K.C. Lin, Rheology and colloidal structure of aqueous TiO_2 nanoparticle suspensions, Materials Science and Engineering A, 355 (2003)186-192.

[11] U. Teipel, U. Barth, Rheology of nano-scale aluminum suspensions, Propellants, Explosives, Pyrotechnics 26 (2001) 268-272.

[12] W.J Tseng, C.H. Wu, Aggregation, rheology and Electrophoretic packing structure of aqueous Al2O3 nanoparticle suspensions, Acta Materialia, 50 (2002) 3757-3766.

[13] K. Kwak, C. Kim, Viscosity and thermal conductivity of copper oxide nanofluid dispersed in ethylene glycol, Korea-Australia Rheology Journal, 17(2) (2005)35-40.

[14] A. Einstein, Investigations on the Theory of the Brownian movement, Dover Publications, New York (1956).

[15] J. Bicerano, J.F. Douglas, D.A. Brune, Model for the viscosity of particle dispersions, Journal of Macromolecular Science Review C39 (1999) 561-642.

[16] H.C. Brinkman, The viscosity of concentrated suspensions and solutions, Journal Chemistry Physics 20 (1952) 571-581.

[17] F.M.White, Viscous Fluid Flow, McGraw Hill, New York (1991).

[18] D.P. Kulkarni, D.K. Das, G. A. Chukwu, Temperature dependent rheological property of copper oxide nanoparticles suspension, Journal of Nanoscience and Nanotechnology 6 (2006) 1150-1154.

[19] X.Q. Wang, A.S Mujumdar, Heat transfer characteristics of nanofluids: a review, International Journal of Thermal Sciences 46 (2007) 1-19.

[20] Nanophase Technologies, Romeoville, IL, USA. http://www.nanophase.com.

[21] Y. He, Y. Jin, H. Chen, Y. Ding, D. Cang, H. Lu, Heat transfer and flow behavior of aqueous suspensions of TiO_2 nanoparticles (nanofluids) flowing upward through a vertical pipe, International Journal of Heat and Mass Transfer 50 (2007) 2272-2281.

[22] Brookfield DV-II+ Programmable Viscometer Manual No. M/97-164-D1000, Brookfield Engineering Laboratories Inc, Massachusetts (1999).

[23] C.L.Yaws, Physical Properties-A Guide to the Physical, Thermodynamic and Transport Property Data of Industrially Important Chemical Compounds, McGraw-Hill, New York, (1977).

APPENDIX D

Experimental Investigation of Viscosity and Specific Heat of Silicon Dioxide Nanofluids

Praveen K Namburu, Devdatta P Kulkarni, Debendra K Das*
Department of Mechanical Engineering
University of Alaska, Fairbanks
P.O. Box 755905, Fairbanks, AK, 99775-5905, USA.

Abstract

This paper presents the results of an experimental investigation into the viscosity and specific heat of silicon dioxide (SiO_2) nanoparticles with various diameters (20 nm, 50 nm and 100 nm) suspended in a 60:40 (by weight) ethylene glycol and water mixture. Nanofluids with particle volume percentages ranging from 0 % to 10 % were examined. The viscosity experiments were carried out over wide temperature ranges, from –35°C to 50°C, to demonstrate their applicability in cold regions. The nanoparticle diameter effect on the rheology of the SiO_2 nanofluid is explored. Non-Newtonian behavior was observed for the particle volume concentrations of these nanofluids at sub-zero temperatures. A correlation was developed from experimental data, which related viscosity with particle volume percent and nanofluid temperature. The specific heat of the SiO_2 nanofluids for various particle volume concentrations is presented. Because of a lower specific heat, the time required to heat the nanofluids decreased in comparison with the base fluid.

Accepted for Publication, Journal of Micro and Nano Letters, June 2007.

Keywords: Silicon Dioxide Nanoparticles; Nanofluids; Rheology; Specific Heat

*Corresponding Author:ffdkd@uaf.edu,Ph:907-474-6094.

D.1 Introduction

Nanofluids are composites consisting of solid nanoparticles with sizes varying generally from 1-100 nm dispersed into effective heat-transfer liquids. Water, ethylene glycol and propylene glycol are often used for many of these applications as the base fluid in nanofluids. Nanofluids are of great significance because of their enhanced thermal properties. Eastman et al [1] found, when 0.3% (volume) of copper nanoparticles was suspended in ethylene glycol, it increased the thermal conductivity of the fluid by 40%. Pak and Cho [2] reported that at a fixed Reynolds number, the convective heat transfer coefficient increased by 75 % for a 2.78% (volume) Al_2O_3 nanofluid. Results like these have drawn much interest from the industrial and science communities to explore the heat transfer and rheological properties of nanofluids.

In the cold regions of the world, a great deal of energy is expended heating industrial and residential buildings. Due to severe winter conditions, ethylene glycol or propylene glycol mixed with water in different weight percentages are typically used to lower the aqueous freezing point of the heat transfer medium [3]. Such heat transfer fluids are used in home baseboard heaters, heat exchangers, automobiles and in industrial plants in cold regions. These fluids can withstand very low temperatures. At low temperatures, ethylene glycol mixtures have better heat transfer characteristics than propylene glycol mixtures [4]. A 60% ethylene glycol and 40% water by weight fluid mixture is most commonly used in the sub-arctic and arctic regions of Alaska. We have conducted experiments with this fluid mixture containing silicon dioxide nanoparticles with average diameters of 100 nm, 50 nm, and 20 nm in various volume percentages to

explore the thermophysical properties of these nanofluids. A thorough understanding of these properties is important for successful cold regions application.

Silicon dioxide nanoparticles are the least expensive nanoparticles and very little research has been done on their specific heat and rheological properties, making it an ideal test subject. Silicon dioxide nanoparticles with varying diameters were used to explore the diameter effect on the viscosity. These nanoparticles were dispersed in glycol/water mixtures with various volume percentages (2 %, 4 %, 6 %, 8 % and 10 %), and then were tested to investigate the rheological characteristics with temperatures ranging from -35°C to 50°C and specific heat with temperatures ranging from 20°C to 70°C.

Determining the viscosity of the nanofluid is essential to establishing accurate pumping power, Prandtl and Reynolds numbers and the convective heat transfer coefficient. Specific heat is another important thermophysical property, since Prandtl number is also a function of specific heat. Thus far very few studies have addressed the rheological properties and specific heats of silicon dioxide nanoparticles suspensions at cold temperatures.

Earlier studies done at higher temperatures include investigations of the viscosity of carbon nanotubes [5], graphite nanofluids [6], $BaTiO_3$ suspensions [7], nickel-terpineol suspensions [8], and TiO_2 nanoparticles in water [9]. Other investigations focused on the rheology of aluminum nanoparticle suspensions in paraffin oil [10] and Al_2O_3 nanoparticles in water [11]. Earlier research results for copper oxide in ethylene glycol at room temperature [12] have been presented, but no data is available for subzero temperatures. Several available correlations for nanofluid viscosity are summarized below.

Einstein [13] proposed a viscosity correlation for particle suspensions in base fluid, which is given by:

$$\mu_s = \mu_f(1+\frac{5}{2}\phi) \tag{1}$$

Where, μ_s = suspension viscosity, μ_f = viscosity of base fluid, and ϕ is volume percentage of nanoparticles in a base fluid.

Bicerano et al. [14] proposed a similar correlation which relates viscosity and volumetric suspensions by:

$$\mu_s = \mu_f(1+\eta\phi + k_H\phi^2 + ...) \tag{2}$$

Here, η is the virial coefficient, and k_H is Huggins coefficient.

Brinkman [15] presented a viscosity correlation that relates viscosity and volume percentage of nanoparticles given by:

$$\mu_s = \mu_f \frac{1}{(1-\phi)^{2.5}} \tag{3}$$

Notice that all three correlations, equations (1), (2) and (3) were developed to relate viscosity as a function of volume percentage only; there is no consideration of temperature dependence. In the present paper, we have developed a temperature depended correlation for the viscosity of silicon dioxide nanofluids

Generally fluids have higher viscosity near their freezing point and fairly low viscosity near their boiling temperature, this demonstrates that viscosity is a strong function of the temperature. White [16] presented a correlation for pure liquids between viscosity and temperature which is given by:

$$\ln\frac{\mu}{\mu_0} \approx a + b(\frac{T_0}{T}) + c(\frac{T_0}{T})^2 \tag{4}$$

Here (μ_0, T_0) are reference values and (a, b, c) are dimensionless curve-fit values.

Kulkarni et al. [17] proposed a correlation that relates viscosity of copper oxide nanoparticles suspended in water at temperatures ranging from 5°C to 50°C

$$\ln \mu_s = A(\frac{1}{T}) - B \tag{5}$$

Here A and B are the functions of volume percentage ϕ. As this is an aqueous solution, this correlation is not applicable for nanofluids in the subzero temperature range. Our investigation of the relation between temperature and nanofluid viscosity at subzero temperatures will help us develop the next generation of heat transfer fluids applicable in cold regions.

D.2 Experimental Setup for Viscosity

In our experiments, we used silicon dioxide nanoparticles with average diameters of 20 nm, 50 nm, 100 nm and a particle density of 2.33 gm/cc (Nanopahse, Inc [18]). Nanofluids with different volume concentrations (2 %, 4 %, 6 %, 8 % and 10 %) were dispersed in a 60:40 (by weight) ethylene glycol and water mixture. Sample preparation was carried out using a very sensitive mass balance with an accuracy of 0.1 mg.

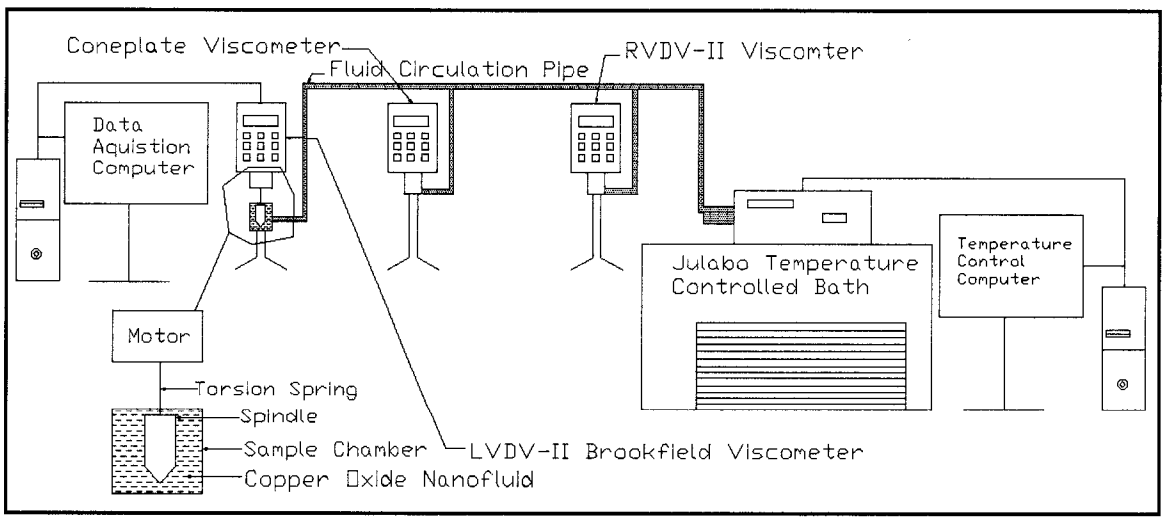

Figure D.1. Experimental setup for viscosity measurement of silicon dioxide nanofluids.

The experimental setup for the rheological property measurements of the silicon dioxide nanoparticles suspended in an ethylene glycol-water mixture is shown in Figure D.1. It consists of an LV DV-II+ Brookfield programmable Viscometer [19] and a Julabo temperature controlled bath connected to a computer to control the temperature. The viscometer drives a spindle immersed in the test fluid. As the spindle is rotated, the viscous drag of the fluid against the spindle is measured by the deflection of the calibrated spring. This viscometer has a viscosity measurement range of 1.5 to 30,000 mPa.s and can handle the viscosity measurement results within a temperature range of -35°C to 80°C. Since sub-arctic region usage of nanofluids will have temperatures in the lower range, where viscosity changes drastically, we focused on property measurement at the low range. It was observed that the change in viscosity is small between 50°C and 80°C. Therefore we have conducted the experiments at temperatures ranging from -35°C to 50°C. A computer controls the temperature of the bath to vary the temperature of the test sample from -35°C to 50°C. A SC4-18 spindle was used in this viscometer and was calibrated by using Brookfield silicon viscosity standard fluids. The viscometer contains a sample chamber where the fluid is tested. Temperature inside the sample chamber is carefully monitored using a RTD temperature sensor during the viscosity measurements. The spindle type and speed combinations will produce satisfactory results when the applied torque is between 10-100% of the maximum permissible torque. Spindle types and speeds are selected in such a way that the torque values lie in this prescribed range. A wide range of spindle speeds are available in this viscometer (0-200 RPM).

Viscosity measurements started at 50°C and temperature was gradually reduced to -30°C in 10°C decrements, with the last reading was taken at -35°C. Because the base fluid freezes at about -45°C, the experiments were carried down to a minimum temperature of -35°C with a factor of safety.

The viscometer is connected to another computer as shown in Figure D.1, which automatically records the data. The data collection is done by Wingather® software,

which collects spindle RPM, torque, viscosity, shear stress, shear rate, temperature and time. All the viscosity measurements were recorded at steady state conditions; that is, ample time (about 30 minutes) was allocated for the temperature to stabilize.

D.3 Discussion of Results

For verifying the accuracy of our equipment and experimental procedure, the viscosity of the ethylene glycol and water (60:40 by weight) was measured before the addition of any silicon dioxide nanoparticles. The obtained readings were compared with data from the American Society of Heating, Refrigerating and Air-Conditioning Engineers (ASHRAE) handbook [4] (Figure D.2). The ASHRAE data and the experimental values match closely (maximum difference of ± 2%) with temperatures ranging from -35°C to 50°C.

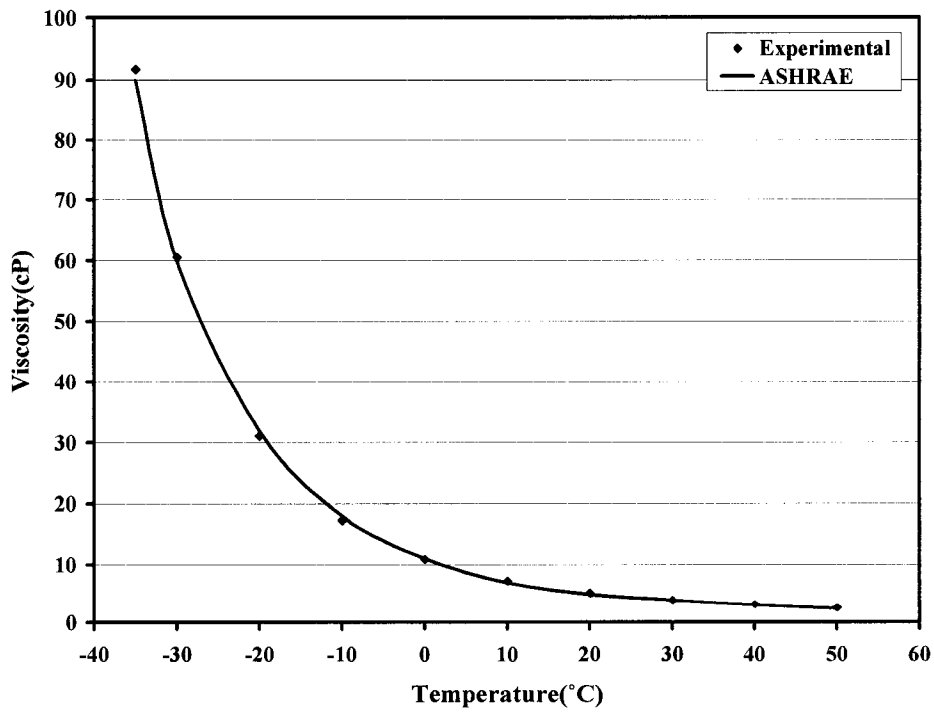

Figure D. 2. Comparison of ASHRAE viscosity values of 60:40 ethylene glycol and water mixture (by weight) and experimental data. 1 cP (centipoise) = 1 mPa.s.

Prior studies e.g. Kulkarni et al. [17] showed that adding nanoparticles changed the behavior of the base fluid to non-Newtonian. Therefore, one objective of our experiment was to verify if the nanofluid behaved in a Newtonian or a non-Newtonian manner. The equation that governs Newtonian behavior of a fluid is given by

$$\tau = \mu \dot{\gamma} \tag{6}$$

Where, τ is the shear stress, μ is the coefficient of viscosity and $\dot{\gamma}$ is the shear strain rate. ASHRAE handbook [4] shows that ethylene glycol and water mixtures behave as Newtonian fluids. While measuring the viscosity values for Figure D.2, it was observed that a 60:40 ethylene glycol and water mixture behaved as a Newtonian fluid between the temperature of -35°C to 50°C.

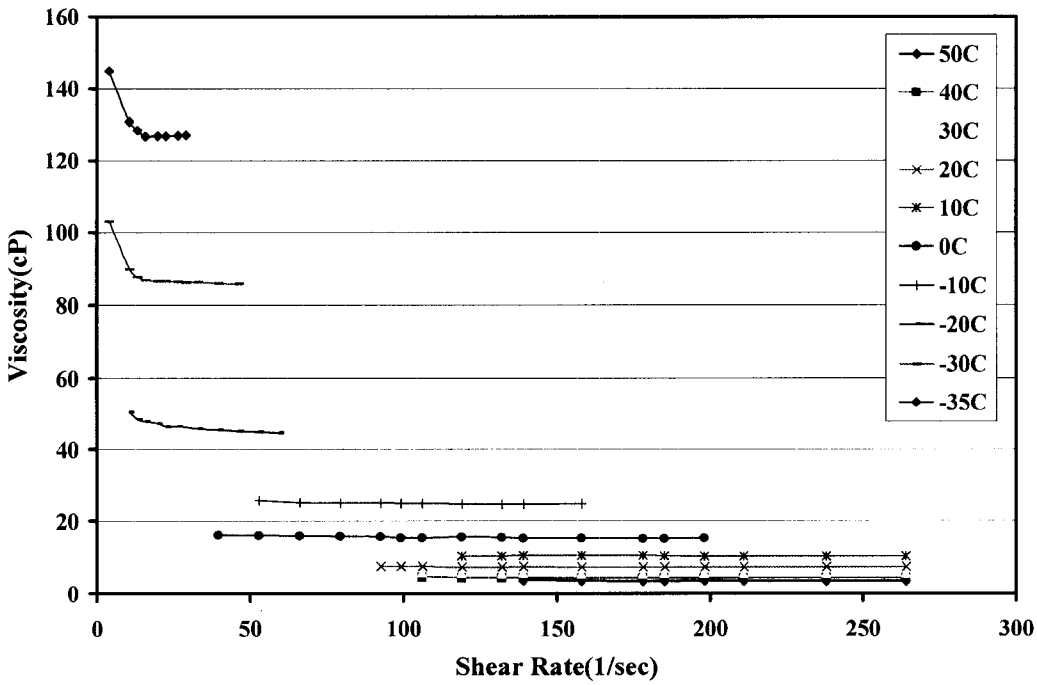

Figure D. 3. Viscosity of the silicon dioxide nanofluid (50 nm) with 6% volume concentration versus shear rate for varying temperatures from 50°C to -35°C.

Figure D. 3 illustrates viscosity versus shear rate for 6% of 50nm silicon dioxide nanoparticles in ethylene glycol and water. The curves between viscosity and shear rate are horizontal straight lines for temperatures more than -10°C; this clearly demonstrates that silicon dioxide nanofluids display Newtonian behavior. For the temperatures below -10°C, the nanofluids demonstrate non-Newtonian behavior as the curves are nonlinear and the viscosity varies with shear rate.

After performing the bench mark test case experiments and examining the behavior of the silicon dioxide nanofluids at lower temperatures, viscosity measurements were carried out for silicon dioxide nanofluids with various diameters (20 nm, 50 nm, 100 nm) and with varying particle volume concentrations (2%, 4%, 6%, 8% and 10%) between temperatures of -35°C to 50°C.

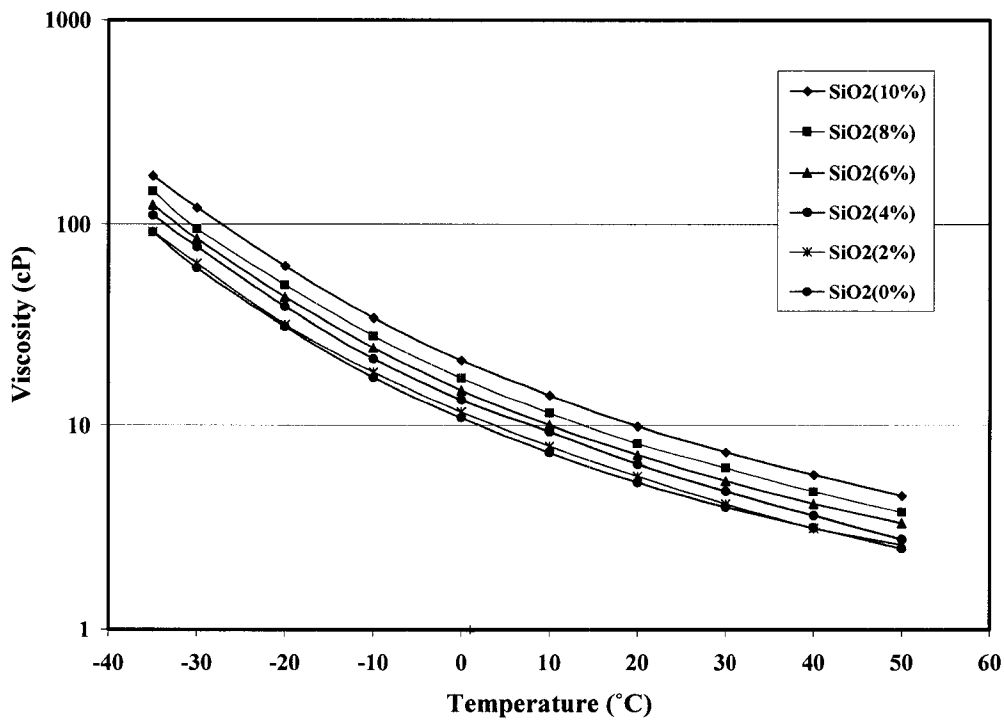

Figure D.4. Experimental values of viscosity for varying volume concentrations of silicon dioxide nanofluids (50 nm) with respect to temperature.

Figure D.4 is a semi-log plot of viscosity versus temperature. Data analysis of this figure indicates that viscosity diminishes exponentially as the sample fluid temperature increases. Furthermore, it shows that with higher nanoparticle concentrations, nanofluids possess higher viscosity. The shape of each curve for different concentrations of nanofluids in Figure D.4 is similar, which indicates consistency of trend of the experimental measurements. Similar trends were observed for viscosity measurements of silicon dioxide nanofluids with nanoparticle diameters of 20 nm and 100 nm.

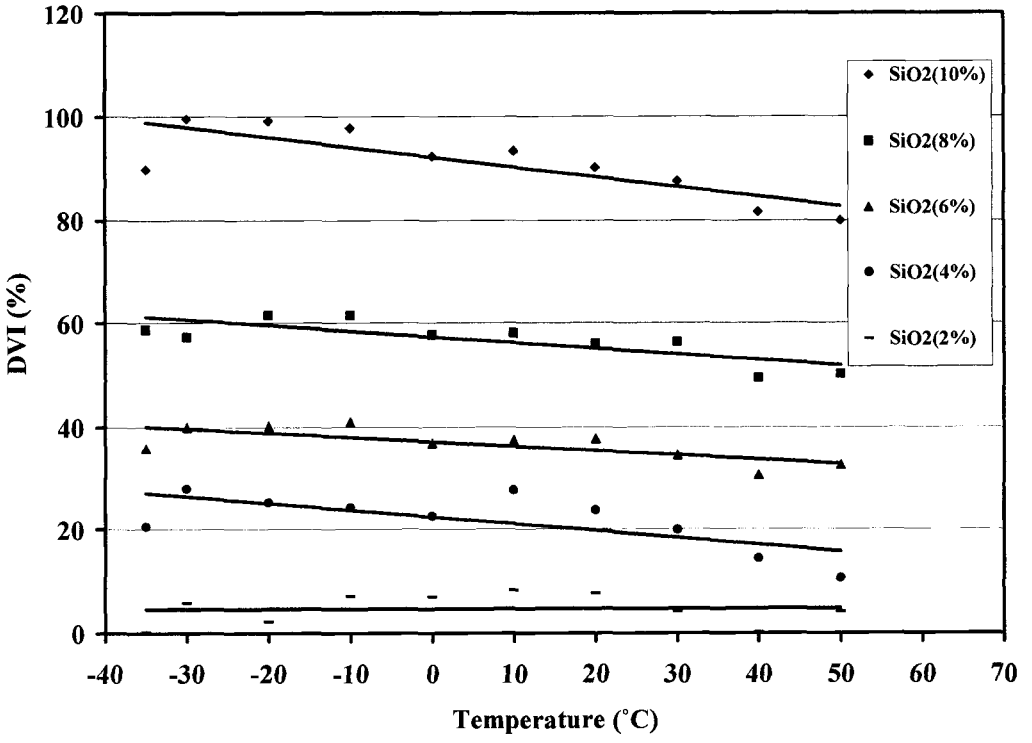

Figure D.5. Degree of viscosity increase versus temperature for varying concentrations of silicon dioxide nanofluids (50 nm).

Figure D.5 displays the degree of viscosity increase (DVI) versus the temperature for varying concentrations of silicon dioxide nanoparticles in ethylene glycol and water. The DVI is defined as the ratio the between difference of nanoparticles suspension viscosity μ_s and the viscosity of base fluid μ_f to the viscosity of base fluid.

Degree of viscosity increase (DVI) = $(\mu_s - \mu_f)/\ \mu_f$ (7)

From the Figure D.5, we infer that the DVI reduces from -35°C to 50°C for all nanofluid concentrations. If the concentration of nanoparticles is low, the DVI will be low as well. With 2 % nanofluid volume concentration, the DVI is about 5 %, whereas a 10 % volume concentration, the DVI is about 90 %.

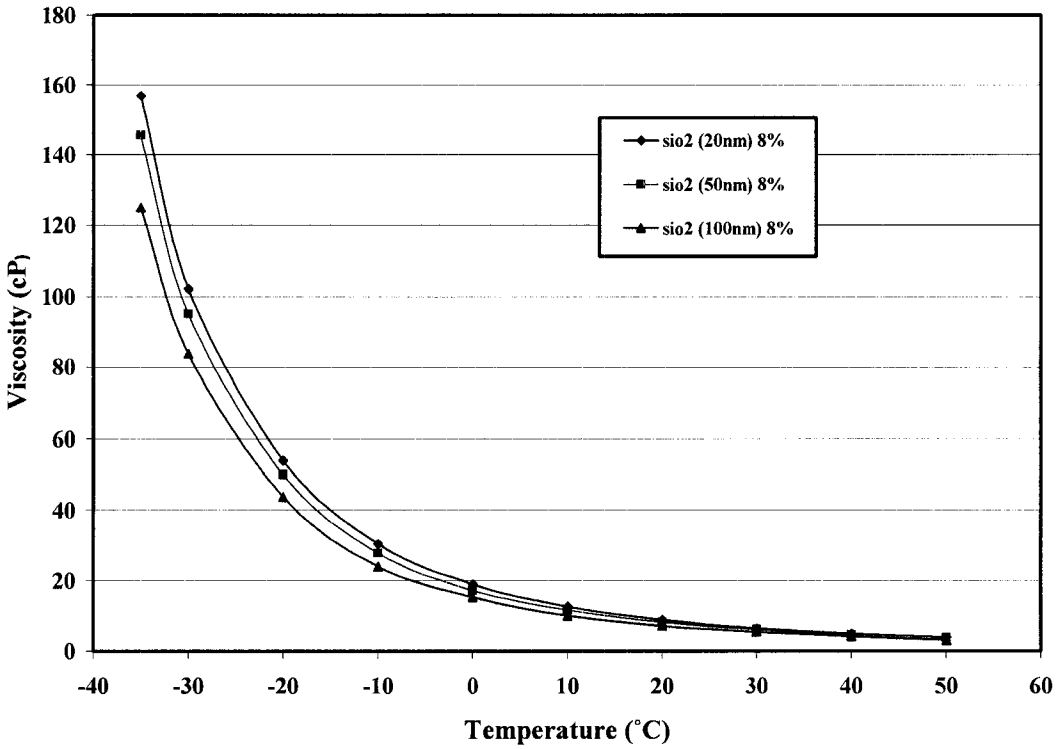

Figure D. 6. Effect of silicon dioxide nanoparticle diameter on nanofluid viscosity for varying temperature.

From Figure D.6, we infer that for the same volumetric concentration of 8%, silicon dioxide nanofluids with highest nanoparticle diameter 100 nm have the lowest viscosity. This observation is consistent with that presented by Cheremisinoff [20] for

micro particles. Similar trends of experimental results were obtained for all concentrations of silicon dioxide nanofluids.

A careful statistical analysis of experimental data revealed an exponential correlation given by Equation (3), which fits the data with a correlation factor $R^2 > 0.99$.

$$Log\ (\mu_s) = Ae^{-BT} \tag{8}$$

Here (μ_s) is the silicon dioxide nanofluid viscosity in centipoise (cP), T is the temperature in Kelvin and A and B are the functions of particle volume concentration (ϕ). Each volume percentage curve in Figure D.7 was fitted with Equation (3) and corresponding values of A and B were evaluated, which are tabulated below.

Table D.1. Curve fit values of A and B with correlation factor $R^2 > 0.99$.

Volume concentration (ϕ)	10 %	8 %	6 %	4 %	2 %
A	69.97	91.43	103.13	139.56	154.77
B	0.0145	0.0157	0.0164	0.0177	0.0183

The coefficients A and B are related to volume percentage given by:

$$A = 0.1193\ (\phi)^3 - 1.9289\ (\phi)^2 - 2.245\ (\phi) + 167.17 \text{ with } R^2 = 0.981 \tag{9}$$

$$B = -7\ E^{-6}\ (\phi)^2 - 0.0004\ (\phi) + 0.0192 \text{ with } R^2 = 0.99 \tag{10}$$

In the above expression, ϕ ranges from 2 to 10.

Equation (3) follows a logarithmic expression presented for viscosities of many liquids by Yaws [21]. The experimental values are within ± 8.4% with the curve fit values.

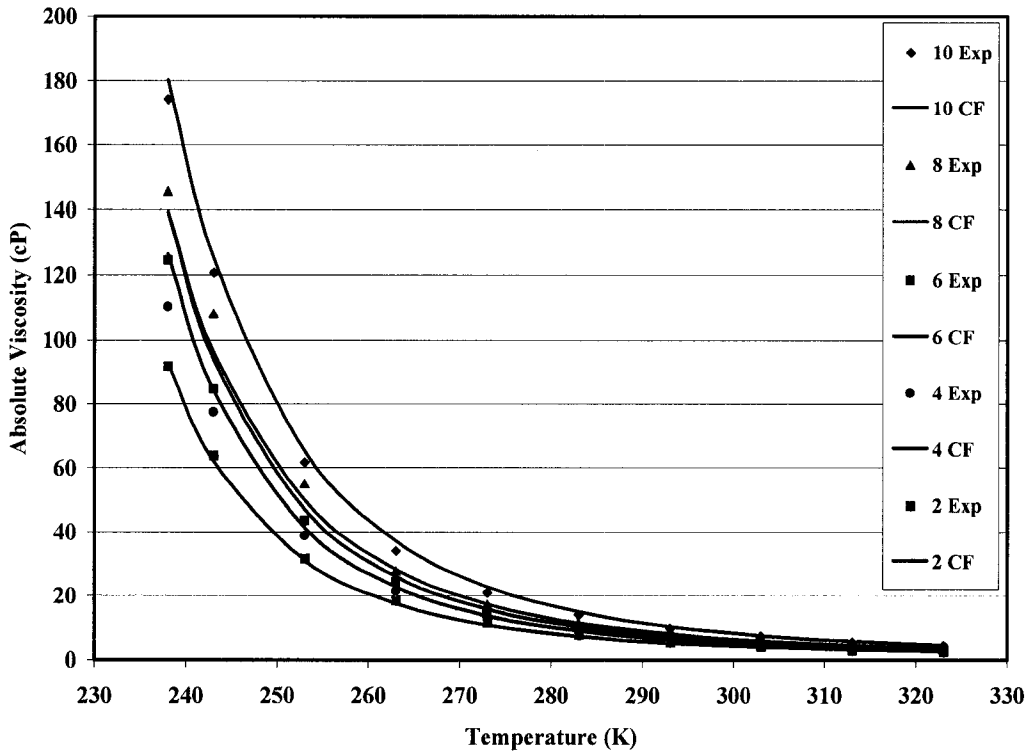

Figure D.7. Experimental values and curve fit (CF) values of absolute viscosity versus temperature for 60:40 ethylene glycol and water with different volume percentages of silicon dioxide (50 nm).

D.4 Experimental Setup for Specific Heat Measurement

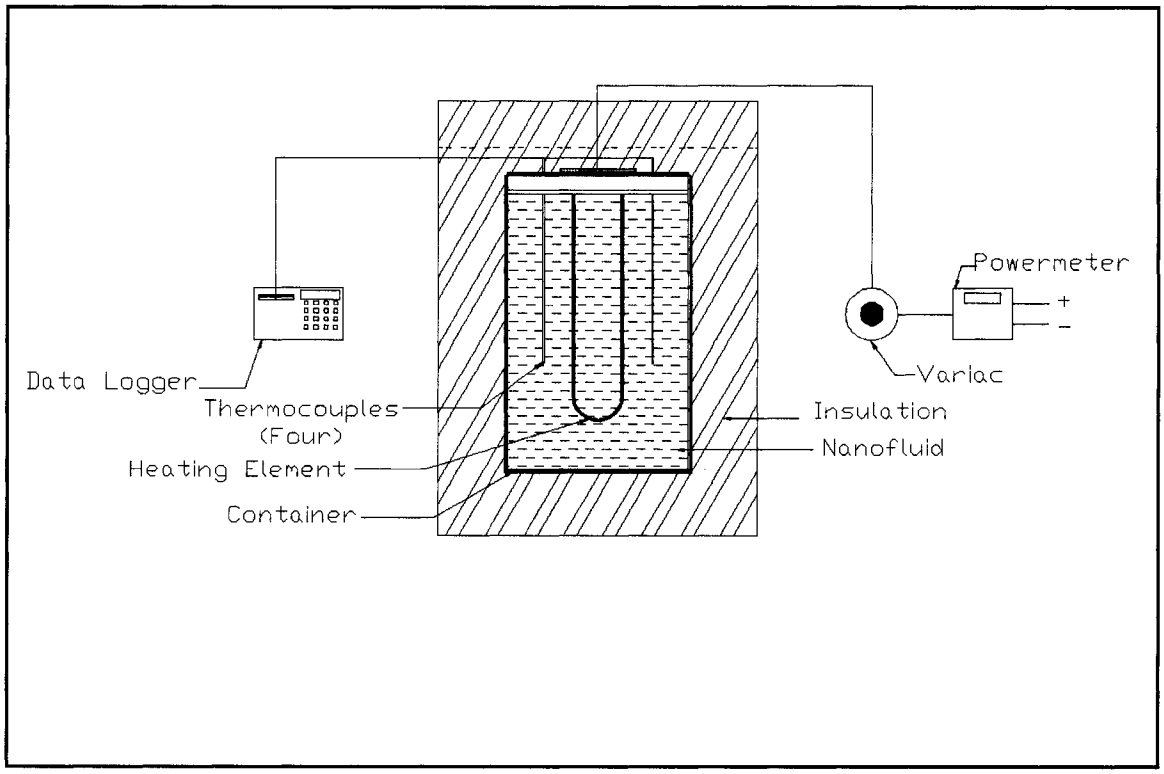

Figure D.8. Experimental setup for specific heat measurement of silicon dioxide nanofluids.

The experimental setup for measuring specific heat of silicon dioxide nanoparticles dispersed in ethylene glycol and water is shown in Figure D.8. It has a plastic container in which silicon nanofluids are stored. Silicon dioxide nanofluids are heated to 70°C by using an electrical heating element (see Figure D.8). Four copper-constantan thermocouples are placed at equal distances from the heating element to monitor the temperature increase of the silicon dioxide nanofluids. These thermocouples are attached to a data logger, which is programmed to record the temperature data in 5-second intervals. The container is well insulated to eliminate the heat transfer to the

surroundings. A variac is used to supply constant power to the heating element, which is monitored by a power meter.

D.4.1 Bench mark test case for specific heat measurement

The specific heat of pure water was measured to verify the accuracy of the specific heat measuring equipment and the experimental procedure.

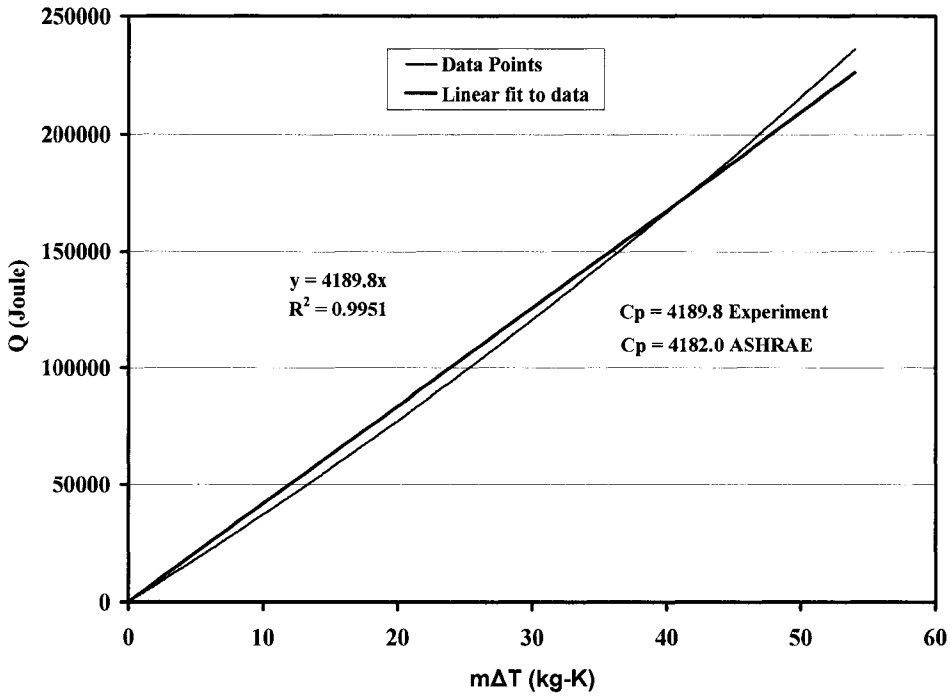

Figure D.9. Specific heat of water obtained from the experimental setup.

Water of mass 1.3 kg was used in the container for the specific heat measurement. A constant power of 40 watts is supplied to the heating element to increase the temperature of water to 70°C. The temperature change was recorded every five seconds using the data logger. Specific heat of the water is calculated from:

$$Q = m\,(Cp)\,\Delta T \tag{11}$$

Here, Q is the heat energy input in joule, m is the mass of the water (kg), Cp is the specific heat of the water (J/kg-K) and ΔT is the temperature differential (K).The slope of the straight line in Figure D.9 given by heat energy (Joule) input versus product of mass (kg) and temperature difference (Kelvin) gives the specific heat of the water. The obtained specific heat of water was then compared to the value from American Society of Heating, Refrigerating and Air-Conditioning Engineers (ASHRAE) handbook [4]. The experimental value differed by ± 0.2%, when compared with the ASHRAE value.

D.5 Discussion of Specific Heat Results

After confirming the readings from the specific heat measurement apparatus, specific heat measurements for silicon dioxide nanofluids with different volume concentrations were carried out.

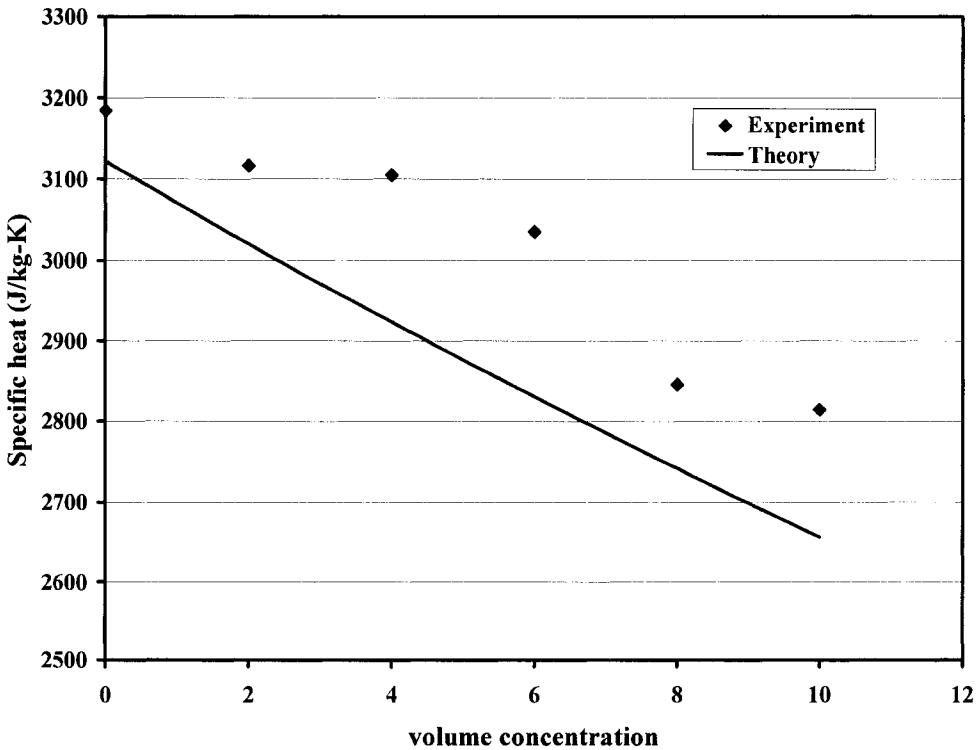

Figure D.10. Experimental values of specific heat for silicon dioxide nanofluids (20 nm) in various concentrations suspended in ethylene glycol and water solution.

Figure D.10 displays the variation of specific heat for varying concentrations of the silicon dioxide nanofluids. The experimental values are compared with the theoretical relation presented in Buongiorno [22]. As the particle volume concentration increases, the specific heat of the silicon dioxide nanofluid decreases, which implies that for higher concentrations of silicon dioxide nanofluid, less heat input is required to increase the temperature of the nanofluid.

D.5.1 Time of heating

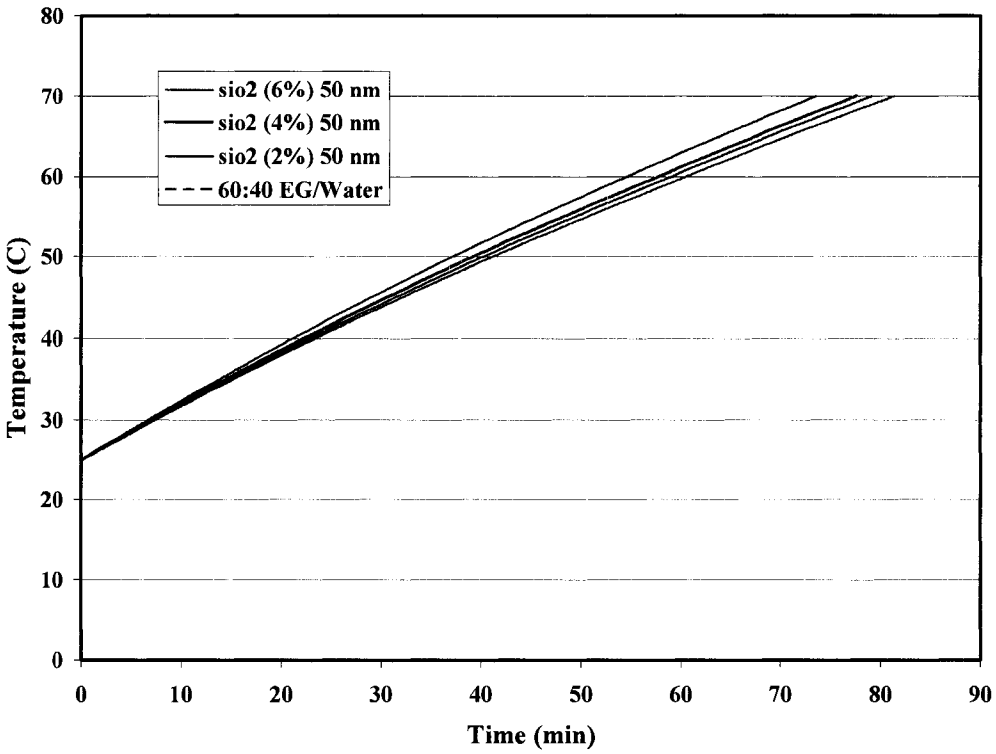

Figure D.11. Temperature versus time for various concentrations of silicon nanofluids (50 nm).

Figure D.11 displays the time required for heating the silicon dioxide nanofluids (50 nm) to increase the temperature from 25°C to 70°C. Time required for heating 1.3 kg

of silicon dioxide nanofluids (50 nm) with a volume concentration of 6 % is approximately 10 min less than that of the 60:40 ethylene glycol/water mixture.

D.6 Conclusions

1. Silicon dioxide nanofluids with ethylene glycol/water as base fluids exhibit non-Newtonian behavior at lower temperatures. At higher fluid temperatures, the viscosity and shear rate relation do not change, proving Newtonian behavior.
2. The viscosity of SiO_2 nanofluids increases as volumetric nanoparticle concentration increases. For example, the viscosity of 10 % SiO_2 particle volume concentration is about 1.8 times the viscosity of the base fluid.
3. As temperature increases, the viscosity of SiO_2 nanofluid decreases exponentially.
4. For SiO_2 nanofluids, there is a 5% increase in DVI over the base fluid with a 2 % particle volume concentration. The DVI modestly decreases as the fluid temperature increases.
5. For the same particle volume concentration, as the particle diameter increases the viscosity of SiO_2 nanofluids decreases.
6. A new empirical correlation between the viscosity, nanoparticle volume concentration and temperature of SiO_2 nanofluid has been derived in Equation (8). The maximum deviation between the curve-fit equation value and the experimental data is ± 8.4% with a correlation factor greater than 0.99.
7. The specific heat of SiO_2 nanofluid decreases as nanoparticle volume concentration increases. With a 10 % SiO_2 nanoparticle concentration, the specific heat is about 12 % lower than the base fluid.
8. From the specific heat measurements of the SiO_2 nanofluids, it is observed the temperature increases faster with SiO_2 nanofluids than with the base fluid. This property will be useful in building heating hydronic fluids and cooling baths and chillers for faster rates of heating and cooling.

D.7 Acknowledgements

Financial assistance from the Arctic Region Supercomputing Center at the University of Alaska Fairbanks is gratefully acknowledged. Authors are thankful to the Institute of Northern Engineering Petroleum Development Laboratory for providing the experimental facilities to measure viscosity.

D.8 References

[1] J.A. Eastman, S.U.S. Choi, S. Li, W. Yu and L.J. Thompson, Appl. Phys. Lett., 78:6, (2001) 718-720.

[2] B.C. Pak, Y.L. Cho, Exp Heat Transfer, 11, (1998)151-170.

[3] F.C., McQuiston, J. D. Parker, J. D., Spitler, Heating, Ventilating, and Air Conditioning, John Wiley & Sons Inc., New York (2000).

[4] ASHRAE Handbook 1985 Fundamentals, American Society of Heating, Refrigerating and Air-Conditioning Engineers Inc., Atlanta (1985).

[5] J. Hilding, E.A. Grulke, Z.G. Zhang and F. Lockwood, J. Dispersion Sci. and Tech. 24:1, 1 (2003) 1-41.

[6] Y. Yang, E.A. Grulke, Z.G. Zhang and G. Wu, J. Nanosci. Nanotechnol. 5, (2005) 571 -579.

[7] W. Tseng and C.L. Lin, Mater. Chem. and Phys. 80, (2003) 232-238.

[8] W. Tseng and C.N. Chen, Mater. Sci. Eng., A347, (2003) 145-153.

[9] W.J. Tseng and K.C. Lin, Mater. Sci. Eng., A355, (2003) 186-192.

[10] U. Teipel, U. Forter-Barth, Propellants, Explosives, Pyrotechnics, 26, (2001) 268-272.

[11] W. Tseng and C.H. Wu, Acta Materialia, 50, (2002) 3757-3766.

[12] K. Kwak, C. Kim, Korea-Australia Rheology J., 17:2, (2005) 35-40.

[13] A. Einstein, Investigations on the Theory of the Brownian Movement, Dover, New York (1906).

[14] J. Bicerano, J.F. Douglas, D.A. Brune, J. Macromolecular Sci. Rev., C39:4, (1999) 561-642.

[15] H.C. Brinkman, The viscosity of concentrated suspensions and solutions, Journal Chemistry Physics 20 (1952) 571-581.

[16] F.M.White, Viscous Fluid Flow, McGraw Hill, New York (1991).

[17] D.P. Kulkarni, D.K., Das, G. A. Chukwu, J. Nanosci. and Nanotechnol., 6, (2006) 1150-1154.

[18] Nanophase Technologies, Romeoville, IL, USA. http://www.nanophase.com

[19] Brookfield DV-II+ Programmable Viscometer Manual No. M/97-164-D1000, Brookfield Engineering Laboratories Inc, MA, USA (2000).

[20] Cheremisinoff, N.P., Encyclopedia of Fluid Mechanics, Rheology and Non Newtonian Flows, vol. 7, Golf Publishing Company, Houston (1988).

[21] C.L.Yaws, Physical Properties-A Guide to the Physical, Thermodynamic and Transport Property Data of Industrially Important Chemical Compounds, McGraw-Hill, New York, (1977).

[22] J.Buongiorno, ASME J. of Heat Transfer, 128. (2006) 240-250.